

Membrane Lipids in the Function and Organization of the Serotonin_{1A} Receptor

Thesis

Submitted for the degree of
Doctor of Philosophy

to

Jawaharlal Nehru University
New Delhi


Yamuna Devi Paila

Centre for Cellular and Molecular Biology
Hyderabad 500 007
India

April 2009

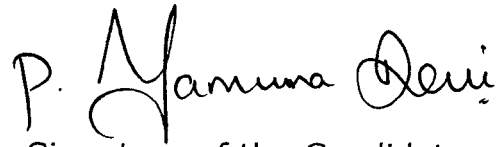
Certificate

The research work embodied in this thesis has been carried out under the guidance of Prof. Amitabha Chattopadhyay at the Centre for Cellular and Molecular Biology, Hyderabad. This work is original and has not been submitted in part or full for any other degree or diploma to any other university.



Signature of the Supervisor

(Prof. Amitabha Chattopadhyay)



Signature of the Candidate

(Yamuna Devi Paila)

Acknowledgements

I would like to express my sincere gratitude to Amit for his excellent mentorship and guidance. It has been a great privilege to work with him. I am amazed at his energy and positiveness in life in general, and science in particular. Amit encouraged me to venture into diverse areas of research which has completely changed my outlook and approach toward science. I immensely enjoyed the intellectual freedom given in his laboratory.

I am grateful to Prof. G. Krishnamoorthy (Tata Institute of Fundamental Research, Mumbai) for his help and improving my understanding of time-resolved anisotropy. I acknowledge Madhuri for her help with time-resolved anisotropy measurements. I would like to thank Dr. Probal Banerjee (College of Staten Island, City University of New York) for providing CHO and HN2 cells stably expressing the human serotonin_{1A} receptor and sharing useful information from time to time. I acknowledge Dr. Sadashiva Karnik (The Cleveland Clinic Foundation, Cleveland) for 5-HT_{1A}R-EYFP plasmid. I would like to thank Murty and Dr. Vairamani (Indian Institute of Chemical Technology, Hyderabad) for their help with GC-MS experiments. I thank Dr. Harikumar for the kind gift of coprostanol. I would like to acknowledge Sourav Ganguly for his help with FRAP experiments. I greatly appreciate Roopali's help in generating the receptor model. I acknowledge Bhairab and Aftab for their help with Western blot experiments.

I would like to thank Jafri, Sandeep, Sourav Ganguly, Pushendra, Sourav Haldar, Rajesh, Roopali and Arunima for maintaining the lab atmosphere intellectually stimulating. Special thanks to Thomas and Shanti for helping me with initial experiments and helpful discussions. I would like to thank all the past and present lab members for careful reading of my manuscripts and criticisms and suggestions for my presentations. I thank Ranga Rao and Venkatalakshmi for extending help whenever required.

I am grateful to CCMB and its staff for maintaining efficient infrastructure and excellent ambience. I acknowledge Dr. Lalji Singh for his support during my stay at CCMB and for his focus on providing the best possible equipment and facilities in CCMB. I thank Mubarak and Varalakshmi and other members at the tissue culture laboratory for their help.

I thank the Council of Scientific and Industrial Research for the Research Fellowship and the International Society for Neurochemistry for the CEAN research grant. I would like to thank Amit for providing me fellowship during the last stages of my Ph.D.

I fondly cherish my friendship with Ajuna and Abhay for making this journey much more enjoyable and memorable.

On a personal note, I would like to deeply thank my beloved parents and family for their faith and constant support. They have sailed through the highs and lows along with me throughout this journey. My Ph.D. is their dream come true.

Table of Contents

| | |
|-----------------------------------|----|
| Abbreviations | i |
| Synopsis | ii |
| List of Publications | x |
| List of Abstracts | xi |

Chapter 1. Introduction

| | | |
|-----|--|----|
| 1.1 | G-protein coupled receptors..... | 2 |
| 1.2 | Membrane cholesterol..... | 5 |
| 1.3 | Effect of membrane cholesterol on the function of GPCRs: general or specific effect ? | 9 |
| 1.4 | Cholesterol and nonannular lipids in the function of membrane proteins | 13 |
| 1.5 | Presence of specific (nonannular ?) cholesterol binding sites in the crystal structures of GPCRs | 18 |
| 1.6 | The serotonin _{1A} receptor | 24 |

Chapter 2. The cholesterol-complexing agent digitonin modulates ligand binding of the bovine hippocampal serotonin_{1A} receptor

| | | |
|------|-----------------------------|----|
| 2.1. | Introduction | 30 |
| 2.2. | Materials and methods | 32 |
| 2.3. | Results | 37 |
| 2.4. | Discussion | 47 |

Chapter 3. Signaling by the human serotonin_{1A} receptor is impaired in cellular model of the Smith-Lemli-Opitz syndrome

| | | |
|------|-----------------------------|----|
| 3.1. | Introduction | 51 |
| 3.2. | Materials and methods | 53 |
| 3.3. | Results | 60 |
| 3.4. | Discussion | 73 |

| | | |
|-------------------|---|-----|
| Chapter 4. | Metabolic depletion of sphingolipids impairs ligand binding and signaling functions of the human serotonin_{1A} receptor | |
| 4.1. | Introduction | 78 |
| 4.2. | Materials and methods | 80 |
| 4.3. | Results | 85 |
| 4.4. | Discussion | 101 |
| Chapter 5. | Oligomerization of the human serotonin_{1A} receptor in live cells: A time-resolved fluorescence anisotropy approach | |
| 5.1. | Introduction | 105 |
| 5.2. | Materials and methods | 107 |
| 5.3. | Results and Discussion | 112 |
| Chapter 6. | The human serotonin_{1A} receptor expressed in neuronal cells: Toward a native environment for neuronal receptors | |
| 6.1. | Introduction | 130 |
| 6.2. | Materials and methods | 131 |
| 6.3. | Results | 133 |
| 6.4. | Discussion | 144 |
| Chapter 7. | Conclusion and future perspectives | |
| 7.1. | Conclusion | 148 |
| 7.2. | Future perspectives | 152 |
| References | | 158 |
| Appendix | | 177 |

Abbreviations

5-HT: 5-hydroxytryptamine
5-HT_{1A} receptor: 5-hydroxytryptamine-1A receptor
5-HT_{1A}R-EYFP: 5-hydroxytryptamine-1A receptor tagged to enhanced yellow fluorescent protein
7-DHC: 7-dehydrocholesterol
7-DHCR: 3 β -hydroxy-steroid- Δ^7 -reductase
8-DHC: 8-dehydrocholesterol
8-OH-DPAT: 8-hydroxy-2(di-*N*-propylamino)tetralin
AY 9944: *trans*-1,4-*bis*(2-dichlorobenzylaminomethyl)cyclohexane dihydrochloride
BCA: bicinchoninic acid
cAMP: adenosine 3',5'-cyclic monophosphate
CCK: cholecystokinin
CCM: cholesterol consensus motif
DMPC: dimyristoyl-*sn*-glycero-3-phosphocholine
DPH: 1,6-diphenyl-1,3,5-hexatriene
EYFP: enhanced yellow fluorescent protein
FB₁: fumonisin B₁
FRAP: fluorescence recovery after photobleaching
GABA: γ -aminobutyric acid
GALR2: subtype 2 galanin receptor
GFP: green fluorescent protein
GPCR: G-protein coupled receptor
GTP- γ -S: guanosine-5'-*O*-(3-thiotriphosphate)
IBMX: 3-isobutyl-1-methylxanthine
M β CD: methyl- β -cyclodextrin
MTT: 3-(4,5-dimethyl-2-thiazolyl)-2,5-diphenyl-2H-tetrazolium bromide thiazole blue
p-MPPF: 4-(2'-methoxy)-phenyl-1-[2'-(*N*-2"-pyridinyl)-*p*-fluorobenzamido] ethyl-piperazine
p-MPPI: 4-(2'-methoxy)-phenyl-1-[2'-(*N*-2"-pyridinyl)-*p*-iodobenzamido] ethyl-piperazine
PMSF: phenylmethylsulfonyl fluoride
SLOS: Smith-Lemli-Opitz Syndrome
TMA-DPH: 1-[4-(trimethylammonio)phenyl]-6-phenyl-1,3,5-hexatriene
Tris: *tris*-(hydroxymethyl)aminomethane

Synopsis

Biological membranes are complex non-covalent assemblies of a diverse variety of lipids and proteins. They impart an identity to the cell and its organelles and provide an appropriate milieu for the function of membrane proteins involved in signaling across the membrane, cell-cell recognition, and membrane transport. Since a significant portion of integral membrane proteins remains in contact with the membrane, and functional centers in them are often buried within the membrane, the function of membrane proteins often depends on the surrounding membrane environment. Lipid-protein interactions in membranes have attracted a lot of attention in relation to the role of such interactions in assembly, stability, and function of membrane proteins. Monitoring lipid-receptor interactions is of particular importance because a cell has the ability of varying the lipid composition of its membrane in response to a variety of stress and stimuli, thus changing the environment and the activity of the receptors in its membrane. Cholesterol is a major representative lipid in higher eukaryotic cellular membranes and is crucial in the organization, dynamics, function, and sorting of membranes. Cholesterol is often found distributed nonrandomly in domains in biological and model membranes. Many of these domains (sometimes termed as 'lipid rafts') are believed to be important for the maintenance of membrane structure and function. The idea of such specialized membrane domains assumes significance in cell biology since physiologically important functions such as membrane sorting and trafficking and signal transduction processes, in addition to the entry of pathogens, have been attributed to these domains. Specifically, cholesterol is known to play a vital role in the function and organization of membrane proteins and receptors.

G-protein-coupled receptors (GPCRs) constitute a superfamily of the largest class of transmembrane proteins whose function is to transmit information across the cell membrane from the extracellular environment to the interior of cells, thereby providing a mechanism of communication between the exterior and the interior of the cell. Cellular signaling by

GPCRs involves their activation upon binding to ligands and the subsequent transduction of signals to the interior of the cell through concerted changes in their transmembrane domain structure. GPCRs are prototypical members of the family of seven transmembrane domain proteins and include >800 members which together constitute ~1-2% of the human genome. It is estimated that ~50% of clinically prescribed drugs act as either agonists or antagonists of G-protein coupled receptors which points to their immense therapeutic potential. Interestingly, although GPCRs represent 30-50% of current drug targets, only a small fraction of all GPCRs are presently targeted by drugs. For example, more than 100 out of 800 GPCRs encoded by the human genome remain 'orphan' receptors and most of these are expressed in the central nervous system. This points out the exciting possibility that the receptors those are not recognized yet could be potential drug targets for diseases which are difficult to treat with currently available drugs.

The serotonin_{1A} (5-HT_{1A}) receptor is an important neurotransmitter receptor and is the most extensively studied among the serotonin receptors. The serotonin_{1A} receptor is the first serotonin receptor to be cloned as an intronless genomic clone (G-21) of the human genome which cross-hybridized with a full length β -adrenergic receptor probe at reduced stringency. Sequence analysis of this genomic clone (later identified as the serotonin_{1A} receptor gene) showed ~43% amino acid homology with the β_2 -adrenergic receptor in the transmembrane domain.

Cholesterol plays a vital role in the function and organization of membrane proteins and receptors. The effect of cholesterol on the structure and function of integral membrane proteins and receptors has been a subject of intense investigation (reviewed in chapter 1). For example, it has been proposed that cholesterol can modulate the function of GPCRs in two ways: (i) through a direct/specific interaction with the GPCR, which could induce a conformational change in the receptor, or (ii) through an indirect way by altering the membrane physical properties in which the receptor is embedded.

The focus of the work presented in this thesis is to understand the specificity of membrane lipid interaction with proteins, which could modulate the function of membrane proteins. In this regard, the function, organization and dynamics of the serotonin_{1A} receptor, an important neurotransmitter G-protein coupled receptor, have been explored upon modulation of membrane lipids such as cholesterol and sphingolipids. In addition, the oligomerization status of the serotonin_{1A} receptor was investigated under various conditions such as ligand stimulation and membrane lipid alteration, using time-resolved fluorescence anisotropy measurements in live cells. This synopsis provides a brief outline of these studies.

The cholesterol-complexing agent digitonin modulates ligand binding of the bovine hippocampal serotonin_{1A} receptor

Previous work from our laboratory has shown the requirement of membrane cholesterol for the function of the serotonin_{1A} receptor from the bovine hippocampus. This was achieved by the use of methyl- β -cyclodextrin (M β CD) which physically depletes cholesterol from membranes. If cholesterol is necessary for ligand binding of the serotonin_{1A} receptor, modulating cholesterol availability by other means could lead to similar effects on the serotonin_{1A} receptor function. This proposal was tested by treating membranes with the sterol-complexing agent digitonin which does not physically deplete membrane cholesterol, yet would effectively reduce cholesterol-receptor interactions in the membrane due to complexation and the results are described in chapter 2. Digitonin is a plant glycoalkaloid saponin detergent obtained from *Digitalis purpurea*. It forms water-insoluble 1:1 complexes (termed 'digitonides') with cholesterol and other steroids, which possess a planar sterol nucleus, a 3 β -hydroxy- Δ^5 configuration and a hydrophobic side chain at C₁₇.

The serotonin_{1A} receptor is an important member of the superfamily of seven transmembrane domain G-protein coupled receptors. Serotonergic signaling is involved in the generation and modulation of various cognitive, behavioral and developmental functions (reviewed in chapter 1). The modulatory role of cholesterol on ligand binding of the bovine

hippocampal serotonin_{1A} receptor was examined by cholesterol complexation in native membranes using digitonin. Complexation of cholesterol from bovine hippocampal membranes using digitonin results in a concentration-dependent reduction in specific binding of the agonist 8-OH-DPAT and antagonist *p*-MPPF to serotonin_{1A} receptors. The corresponding changes in membrane order were monitored by analysis of fluorescence polarization data of the membrane depth-specific probes, DPH and TMA-DPH. These results point out the important role of membrane cholesterol in maintaining the function of the serotonin_{1A} receptor. An important aspect of these results is that non-availability of free cholesterol in the membrane due to complexation with digitonin, rather than physical depletion is sufficient to significantly reduce the serotonin_{1A} receptor function. These results provide a comprehensive understanding of the effects of the sterol-complexing agent digitonin in particular, and the role of membrane cholesterol in general, on the serotonin_{1A} receptor function.

Signaling by the human serotonin_{1A} receptor is impaired in cellular model of the Smith-Lemli-Opitz syndrome

The Smith-Lemli-Opitz Syndrome (SLOS) is a congenital and developmental malformation syndrome associated with defective cholesterol biosynthesis. SLOS is clinically diagnosed by reduced plasma levels of cholesterol along with elevated levels of 7-dehydrocholesterol (and its positional isomer 8-dehydrocholesterol) and the ratio of their concentrations to that of cholesterol. Since SLOS is associated with neurological deformities and malfunction, exploring the function of neuronal receptors and their interaction with membrane cholesterol under these conditions assumes significance. Chapter 3 describes the work in which a cellular model of SLOS was generated using CHO cells stably expressing the human serotonin_{1A} receptor. This was achieved by metabolically inhibiting the biosynthesis of cholesterol, utilizing a specific inhibitor (AY 9944) of the enzyme required in the final step of cholesterol biosynthesis. We utilized this cellular model to monitor the

function of the human serotonin_{1A} receptor under SLOS-like condition. Our results show that ligand binding activity, G-protein coupling and downstream signaling of serotonin_{1A} receptors are impaired in SLOS-like condition, although the membrane receptor level does not exhibit any reduction. Importantly, metabolic replenishment of cholesterol using serum partially restored the ligand binding activity of the serotonin_{1A} receptor. These results are potentially useful in developing strategies for the future treatment of the disease since intake of dietary cholesterol is the only feasible treatment for SLOS patients.

Metabolic depletion of sphingolipids impairs ligand binding and signaling functions of the human serotonin_{1A} receptor

Sphingolipids are essential and indispensable components of eukaryotic cell membranes and constitute 10-20% of the total membrane lipids. Sphingolipids are thought to be involved in the regulation of cell growth, differentiation, and neoplastic transformation through participation in cell-cell communication, and possible interaction with receptors and signaling systems. Sphingolipids such as sphingomyelin are regarded as reservoirs for second messengers such as sphingosine, ceramide and sphingosine 1-phosphate. Sphingolipids are abundant in the plasma membrane compared to intracellular membranes. Their distribution in the bilayer appears to be heterogeneous, and it has been postulated that sphingolipids and cholesterol occur in laterally segregated lipid domains. Chapter 4 describes the work in which sphingolipid levels in CHO cells stably expressing the human serotonin_{1A} receptor (CHO-5-HT_{1A}R) were modulated by metabolically inhibiting the biosynthesis of sphingolipids. In order to achieve this, FB₁ (a specific metabolic inhibitor of ceramide synthase) was utilized. FB₁ treatment results in reduction of sphingomyelin levels. The function of the human serotonin_{1A} receptor under these conditions was explored by monitoring ligand binding, G-protein coupling and downstream signaling of the receptor along with lateral mobility measurements using Fluorescence Recovery After Photobleaching (FRAP). Results show that the function of the serotonin_{1A} receptor is impaired upon

metabolic depletion of sphingomyelin. These results are significant since FB₁ induces a number of diseases and could possibly even impair neurotransmission. Importantly, our results provide novel evidence that sphingolipids are necessary for ligand binding and downstream signaling of the human serotonin_{1A} receptor. In addition, these results demonstrate that the effect of sphingomyelin on the ligand binding function of the serotonin_{1A} receptor caused by the metabolic depletion of sphingolipids is reversible.

Oligomerization of the human serotonin_{1A} receptor in live cells: A time-resolved fluorescence anisotropy approach

A number of studies have demonstrated the capability of a variety of GPCRs to interact and form functional homo-dimers or oligomers. Such oligomerization has been assumed to be involved in the proper folding of receptors, thereby providing the framework for efficient and controlled signal transduction. Importantly, recent structural data available for GPCRs suggest that the surface area of GPCR monomer facing the cytosol is too small to support for simultaneous interaction of α and β/γ subunits of G-proteins. Based on this consideration, it was suggested that one molecule of the G-protein trimer could be interfaced with a homo-dimer in case of rhodopsin. In addition, it was reported that one G-protein trimer binds the homo-dimer in case of the leukotriene B₄ receptor. Yet, there is another school of thought which envisages that the functional unit of GPCR could be a monomer. For example, it has been argued that only one receptor molecule is capable of activating its cognate G-protein in case of rhodopsin and the β_2 -adrenergic receptor. In spite of the wealth of information accumulated for GPCR signaling and function, there appears to be no consensus on their oligomeric status. In addition, it appears that it is not clear whether the minimum signaling unit of GPCRs is a monomer or oligomer. Prefomed oligomers of certain GPCRs could serve as signaling platforms and may retain its multimeric status throughout signaling. Other GPCRs could cycle through monomeric and multimeric states in a ligand-regulated fashion.

The serotonin_{1A} receptor is an important G-protein coupled neurotransmitter receptor which is a central player in a multitude of physiological processes, and serves as an important target in the development of therapeutic agents for neuropsychiatric disorders. However, the oligomerization status of this receptor is only beginning to be addressed. FRET (Fluorescence Resonance Energy Transfer) is a widely used approach to address the oligomerization status of GPCRs in cells. HomoFRET (*i.e.*, FRET between same fluorophores) represents a useful approach to monitor aggregation of membrane-bound molecules in general. HomoFRET can be monitored by change in fluorescence anisotropy. Chapter 5 describes the results of experiments performed to address the issue of the oligomerization status of the serotonin_{1A} receptor tagged to Enhanced Yellow Fluorescent Protein (EYFP) in live cells under various conditions such as ligand stimulation and membrane lipid modulation, utilizing time-resolved fluorescence anisotropy measurements on cells under a fluorescence microscope. These measurements were performed upon acute and metabolic deprivation of cholesterol and modulation of sphingolipid levels. The anisotropy decay of the receptor stimulated by ligands was analyzed with the aim of identifying and quantifying homo-FRET among receptor clusters. The anisotropy decay of EYFP tagged to the human serotonin_{1A} receptor upon conditions of acute and metabolic cholesterol deprivation was monitored. Importantly, reduction in initial anisotropy (r_m) compared to that of control conditions, was observed upon acute cholesterol depletion, implying that serotonin_{1A} receptors reorganize into higher oligomers upon acute cholesterol depletion. These results are in overall agreement with previous results from our laboratory. Interestingly, our results show that limiting anisotropy (r_0) value in cells is significantly low compared to the corresponding value in glycerol. This reduction could be attributed to rapid and unresolved homo-FRET. A possible explanation for this could be homo-FRET in preexisting constitutive oligomers of the receptor. These results could be useful in understanding the effect of membrane lipid modulations and ligand stimulation on serotonergic signaling mediated through this receptor.

The human serotonin_{1A} receptor expressed in neuronal cells: Toward a native environment for neuronal receptors

The pharmacological and functional characterization of the human serotonin_{1A} receptor stably expressed in HN2 cell line, which is a hybrid cell line between hippocampal cells and mouse neuroblastoma, is described in chapter 6. These cells are referred to as HN2-5-HT_{1A}R cells. Our results show that serotonin_{1A} receptors in HN2-5-HT_{1A}R cells display ligand binding properties that closely mimic binding properties observed with native receptors. We further demonstrate that the differential discrimination of G-protein coupling by the specific agonist and antagonist, a hallmark of the native receptor, is maintained for the receptor in HN2-5-HT_{1A}R cells. Importantly, the serotonin_{1A} receptor in HN2-5-HT_{1A}R cells shows efficient downstream signaling by reducing cellular cyclic AMP levels. These results show that serotonin_{1A} receptors expressed in HN2-5-HT_{1A}R cells represent a useful model system to study serotonin_{1A} receptor biology, and is a potential system for solubilization and purification of the receptor in native-like membrane environment.

List of Publications

1. **Paila, Y.D.**, Pucadyil, T.J. and Chattopadhyay, A. (2005) The Cholesterol-Complexing Agent Digitonin Modulates Ligand Binding of the Bovine Hippocampal Serotonin_{1A} Receptor. *Mol. Membr. Biol.* **22**: 241-249.
2. **Paila, Y.D.** and Chattopadhyay, A. (2006) The Human Serotonin_{1A} Receptor Expressed in Neuronal Cells: Toward a Native Environment for Neuronal Receptors. *Cell. Mol. Neurobiol.* **26**: 925-942.
3. Chattopadhyay, A. and **Paila, Y.D.** (2007) Lipid-protein Interactions, Regulation and Dysfunction of Brain Cholesterol. *Biochem. Biophys. Res. Commun.* **354**: 627-633.
- *4. Singh, P., **Paila, Y.D.** and Chattopadhyay, A. (2007) Differential Effects of Cholesterol by 7-Dehydrocholesterol on the Ligand-Binding Activity of the Serotonin_{1A} Receptor: Implications in SLOS. *Biochem. Biophys. Res. Commun.* **358**: 495-499.
- *5. Chattopadhyay, A., **Paila, Y.D.**, Jafurulla, Md., Chaudhuri, A., Singh, P., Murty, M.R.V.S. and Vairamani, M. (2007) Differential Effects of Cholesterol and 7-Dehydrocholesterol on Ligand Binding of Solubilized Hippocampal Serotonin_{1A} Receptors: Implications in SLOS. *Biochem. Biophys. Res. Commun.* **363**: 800-805.
6. **Paila, Y.D.**, Murty, M.R.V.S., Vairamani, M. and Chattopadhyay, A. (2008) Signaling by the Human Serotonin_{1A} Receptor is Impaired in Cellular Model of Smith-Lemli-Opitz Syndrome. *Biochim. Biophys. Acta-Biomembranes* **1778**: 1508-1516.
- *7. Shrivastava, S., **Paila, Y.D.**, Dutta, A. and Chattopadhyay, A. (2008) Differential Effects of Cholesterol and its Immediate Biosynthetic Precursors on Membrane Organization. *Biochemistry* **47**: 5668-5677.
8. **Paila, Y.D.**, Tiwari, S. and Chattopadhyay, A. (2009) Are Specific Cholesterol Binding Sites Present in G-protein Coupled Receptors ? *Biochim. Biophys. Acta-Biomembranes* **1778**: 295-302.
9. **Paila, Y.D.** and Chattopadhyay, A. (2009) The Function of the G-protein Coupled Receptor and Membrane Cholesterol: Specific or General Interaction ? *Glycoconj. J.* (doi 10.1007/s10719-008-9218-5).
10. **Paila, Y.D.**, Ganguly, S. and Chattopadhyay, A. (2009) Metabolic Depletion of Sphingolipids Affects Ligand Binding and Signaling Functions of the Human Serotonin_{1A} Receptor (manuscript under revision).

(* not described in the thesis)

List of Abstracts

1. **Paila, Y.D.** Pucadyil, T.J., and Chattopadhyay, A. (2004) Effect of the Cholesterol Complexing Agent Digitonin on Bovine Hippocampal Serotonin_{1A} Receptor Function and Membrane Dynamics at the "*International Neuroscience Conference*", University of Hyderabad, Hyderabad, India, Abstract No. PP-12, p. 78.
2. **Paila, Y.D.** and Chattopadhyay, A. (2006) Metabolic Depletion of Sphingolipids affects Ligand Binding and Signaling Functions of the Human Serotonin_{1A} receptor at the "*XXIX All India Cell Biology Conference & Symposium on Gene to Genome: Environment & Chemical Interaction*", Industrial Toxicology Research Centre, Lucknow, India, Abstract No. PP-18, p. 48.
3. **Paila, Y.D.**, Murthy, M.R.V.S., Vairamani, M. and Chattopadhyay, A. (2006) Modulation of the Human Serotonin_{1A} Receptor Function in Smith-Lemli-Opitz Syndrome-like Condition at the "*FEBS Special Meeting European Lipidomics Initiative – New Concepts in Lipidology: from Lipidomics to Disease*", Noordwijkherhout, The Netherlands.
4. **Paila, Y.D.** and Chattopadhyay, A. (2006) Membrane Lipid Interactions of the Serotonin_{1A} Receptor: Implications in health and Disease at the "*National Symposium on Trends & Techniques in Molecular Endocrinology*", University of Hyderabad, India. pp12-13.
5. **Paila, Y.D.**, Murty, M.R.V.S., Vairamani, M. and Chattopadhyay, A. (2006) Modulation of the Human Serotonin_{1A} Receptor Function in Smith-Lemli-Opitz Syndrome-like Condition at the "*75th Annual Meeting of Society of Biological Chemists, (India) on Metabolism to Metabolome*", Jawaharlal Nehru University, New Delhi, India, p. 35.
6. Singh, P., **Paila, Y.D.** and Chattopadhyay, A. (2006) Effect of Replacement of Membrane Cholesterol by 7-Dehydrocholesterol on the Ligand-binding Activity of the Serotonin_{1A} Receptor: Implications in SLOS. "*75th Annual Meeting of Society of Biological Chemists, (India) on Metabolism to Metabolome*", Jawaharlal Nehru University, New Delhi, India, pp. 172-173.
7. **Paila, Y.D.**, Murty, M.R.V.S., Vairamani, M. and Chattopadhyay, A. (2007) The human Serotonin_{1A} Receptor Function is Altered in Smith-Lemli-Opitz-like Condition" seminar at the "*3rd International Symposium on Neurodegeneration & Neuroprotection*" and Society for Neurochemistry (India) Meeting", Indian Institute of Chemical Biology, Kolkata, India, Abstract No. SY-7, p. 30.

8. Srinivas, G., Chaturvedi, P., Parnaik, V., **Paila, Y.D.** and Chattopadhyay, A. (2007) GFP Cell Sorting and Applications. "*The Cytometry Meet 2007*", Sanjay Gandhi Postgraduate Institute of Medical Sciences, Lucknow, India, Abstract No. P-4, p. 32.
9. **Paila, Y.D.**, Saha, B. and Chattopadhyay, A. (2008) Host Membrane Cholesterol: A Crucial Determinant for Visceral Leishmaniasis at the "*8th International Symposium on Eukaryotic Cell Surface Macromolecules*", Centre for Cellular and Molecular Biology, Hyderabad, India, Abstract No. P-13, p. 73.
10. **Paila, Y.D.**, Kombrabail, M., Krishnamoorthy, G. and Chattopadhyay, A. (2008) Oligomerization of the Human Serotonin_{1A} Receptor in live Cells: a Time-Resolved Fluorescence Anisotropy Study at the "*8th International Symposium on Eukaryotic Cell Surface Macromolecules*", Centre for Cellular and Molecular Biology, Hyderabad, India, Abstract No. P-14, p. 74.
11. Singh, P., **Paila, Y.D.** and Chattopadhyay, A. (2008) Effect of Metabolic Depletion of Glycosphingolipids on the Function of the Human Serotonin_{1A} Receptor at the "*8th International Symposium on Eukaryotic Cell Surface Macromolecules*", Centre for Cellular and Molecular Biology, Hyderabad, India, Abstract No. P-19, p. 79.
12. **Paila, Y.D.**, Murty, M.R.V.S., Vairamani, M. and Chattopadhyay, A. (2008) Signaling by the Human Serotonin_{1A} Receptor is Impaired in Cellular Model of Smith-Lemli-Opitz Syndrome at the "*2nd Singapore Lipid Symposium*", Centre for Life Sciences, National University of Singapore, Singapore.
13. **Paila, Y.D.** and Chattopadhyay, A. (2008) Role of Cholesterol and Serotonergic Signaling in Early Embryonic Development: Implications in Smith-Lemli-Opitz Syndrome at the "*XXXII Conference of Indian Society of Cell Biology (ISCB) & Symposium on Stem Cells and Pattern Formation*", MACS-Agharkar Research Institute, Pune, India, p. 32.
14. Prasad, R., **Paila, Y.D.** and Chattopadhyay, A. (2008) Effect of Sterol Enrichment on the Ligand Binding Function of the Human Serotonin_{1A} Receptor at the "*XXXII Conference of Indian Society of Cell Biology (ISCB) & Symposium on Stem Cells and Pattern Formation*", MACS-Agharkar Research Institute, Pune, India, Abstract No. P-38, p. 100.
15. **Paila, Y.D.**, Kombrabail, M., Krishnamoorthy, G. and Chattopadhyay, A. (2009) Oligomerization of the Human Serotonin_{1A} Receptor in live Cells: A Time-Resolved Fluorescence Anisotropy Study at the "*National Symposium on Cellular and Molecular Biophysics*", Centre for Cellular and Molecular Biology, Hyderabad, India, Abstract No. O-24, p. 43.

16. **Paila, Y.D.**, Kombrabail, M., Krishnamoorthy, G. and Chattopadhyay, A. (2009) Oligomerization of the Human Serotonin_{1A} Receptor in live Cells: a Time-Resolved Fluorescence Anisotropy Study at the "*Fluorescence in Biology: An International Conference*", Tata Institute of Fundamental Research, Mumbai, India, Abstract No. P-82, pp. 79-80.

Chapter 1

Introduction

1.1. G-protein coupled receptors (GPCRs)

G-protein-coupled receptors (GPCRs) constitute a superfamily of the largest class of transmembrane proteins whose function is to transmit information across the cell membrane from the extracellular environment to the interior of cells, thereby providing a mechanism of communication between the exterior and the interior of the cell (Pierce *et al.*, 2002; Kroeze *et al.*, 2003; Perez, 2003). Cellular signaling by GPCRs involves their activation upon binding to ligands and the subsequent transduction of signals to the interior of the cell through concerted changes in their transmembrane domain structure (Gether, 2000). GPCRs are prototypical members of the family of seven transmembrane domain proteins and include >800 members which together constitute ~1-2% of the human genome (Fredriksson and Schiöth, 2005). They are involved in the generation of cellular responses to a diverse array of stimuli that include biogenic amines, peptides, glycoproteins, lipids, nucleotides, and even photons. As a consequence, these receptors mediate multiple physiological processes such as neurotransmission, cellular metabolism, secretion, cellular differentiation, growth, inflammatory and immune responses. GPCRs have therefore emerged as major targets for the development of novel drug candidates in all clinical areas (Schlyer and Horuk, 2006; Jacoby *et al.*, 2006; Insel *et al.*, 2007). It is estimated that ~50% of clinically prescribed drugs act as either agonists or antagonists of GPCRs which points to their immense therapeutic potential (Karnik *et al.*, 2003). Interestingly, although GPCRs represent 30-50% of current drug targets, only a small fraction of all GPCRs are presently targeted by drugs (Lin and Civelli, 2004). For example, more than 100 out of 800 GPCRs encoded by the human genome remain 'orphan' receptors and most of these are expressed in the central nervous system (Huber *et al.*, 2008). This points out the exciting possibility that the receptors those are not recognized yet could be potential drug targets for diseases which are difficult to treat by currently available drugs.

Analysis of the entire superfamily of GPCRs in the human genome indicates the presence of five main families, namely the glutamate, rhodopsin, adhesion, frizzled/taste2, and secretin families (collectively referred to as the GRAFS classification system) with the members of each family displaying a common evolutionary origin (Fredriksson and Schiöth, 2005). The GRAFS classification system is more representative of the entire repertoire of GPCRs coded by a single mammalian species than the previously used A-E classification system which analyzed GPCRs based on the occurrence of seven transmembrane receptors from several species (Kolakowski, 1994; Karnik *et al.*, 2003). The rhodopsin family constitutes the largest number of GPCRs with 701 receptors of the total of ~800 GPCRs present in the human genome. The members of this family possess several characteristics such as the Asn-Ser-X-X-Asn-Pro-X-X-Tyr motif in the transmembrane domain VII of the receptor. This motif is involved in maintaining receptors in an inactive conformation through hydrogen bonding interactions with residues in the transmembrane domains I, II and III of the receptor. These receptors also possess the Asp/Glu-Arg-Tyr/Phe motif at the interface of transmembrane domain III and the second intracellular loop that is involved in activation of G-proteins. The ligands for most of the rhodopsin family of receptors bind in a cavity within the transmembrane region (Baldwin, 1994). These include odorants, prostaglandins, and small biogenic amines such as serotonin and melatonin. The glutamate family comprises of 15 members that includes the metabotropic glutamate and GABA receptors. The ligand recognition domain in the metabotropic glutamate is found in the extracellular N-terminus domain. The frizzled/taste 2 group contains 24 members. This group includes two distinct clusters, the frizzled receptors and taste 2 receptors. The frizzled receptors bind the glycoprotein Wnt and control cell fate, proliferation, and polarity during vertebrate development. The taste 2 receptors clearly show the presence of seven hydrophobic regions in a hydrophobicity plot but have a very short N-terminus that is unlikely to contain a ligand-binding domain. The secretin family comprises of 15

members and bind large homologous peptides that most often act in a paracrine manner. The adhesion receptor family consists of 24 members that contain GPCR-like transmembrane-spanning regions fused together with one or several functional domains with adhesion-like motifs in the N-terminus, such as EGF-like repeats, mucin-like regions, and conserved cysteine-rich motifs (Pucadyil and Chattopadhyay, 2006).[¶]

GPCRs primarily transmit signals across the plasma membrane *via* their interactions with heterotrimeric G-proteins present on the cytoplasmic side of the cell membrane (Neer, 1995; Hamm, 2001). Heterotrimeric G-proteins are composed of α , β and γ subunits, with molecular masses of ~39-45, 35-39, and 6-8 kDa, respectively. To date, at least 28 distinct G-protein α subunits, 5 different β , and 12 different γ subunits have been described (Cabrera-Vera *et al.*, 2003). Heterotrimeric G-proteins can be divided into four families based on the degree of primary sequence similarities of their α subunits: G_s (G_s and G_{olf}), G_i (G_{ir} , G_{tc} , G_g , G_{i1-3} , G_o , and G_z), G_q (G_q , G_{11} , G_{14} , and $G_{15/16}$), and G_{12} (G_{12} and G_{13}). These heterotrimeric G-proteins follow the same scheme of activation/inactivation cycle allowing reversible and specific transmission of signals into cells. The G-protein heterotrimer is maintained in an inactive state by mutual association in a complex, with the α subunit bound to a GDP moiety. Although a GDP-bound α subunit is able to bind to the receptor without $\beta\gamma$, its association with the receptor is greatly enhanced by the presence of $\beta\gamma$. Upon binding to the agonist, the receptor undergoes a conformational change resulting in increased affinity for the G-protein. The conformational change in the receptor acts as a switch to release GDP from the $G\alpha$ subunit. Since the concentration of GTP is much higher than GDP under physiological conditions, GTP immediately replaces GDP. The activated state lasts until GTP is hydrolyzed to GDP by the intrinsic GTPase activity of $G\alpha$ subunits. Exchange of GDP for GTP on the α subunit leads to dissociation/reorganization (Frank *et al.*, 2005) of the heterotrimeric G-protein complex that facilitates transduction of signals to effector molecules such as adenylyl cyclase, phospholipases, and ion channels (Pierce *et*

al., 2002). The multiple components of GPCR signal transduction such as different types of receptors and G-protein subunits provide cells with enough flexibility to customize their responses to a diverse array of ligands such as hormones, neurotransmitters, and pharmacological agonists. In addition, recent evidence suggests that GPCRs are capable of transducing signals across the plasma membrane through alternative mechanisms such as by activating Jak2 kinase, phospholipase C γ , or protein kinase C *via* direct interaction with the receptor (Ji *et al.*, 1998; Hall *et al.*, 1999).

The membrane organization of GPCRs assumes significance in the light of their role in health and disease. Interestingly, the efficiency of signal transduction processes carried out by GPCRs appears to be influenced by the local composition and organization of lipids within the plasma membrane (Ostrom and Insel, 2004). It has been proposed that the G-protein coupled receptors are not uniformly present on the plasma membrane but are concentrated in specific membrane microdomains (Ostrom *et al.*, 2000; Ostrom, 2002). It has been shown that some of these domains are enriched in cholesterol (Ostrom and Insel, 2004). For example, it has been reported that serotonin_{2A} receptors are localized in cholesterol-enriched membrane microdomains (caveolae) and serotonergic signaling induced by serotonin_{2A} receptors depends on the membrane cholesterol content (Dreja *et al.*, 2002) and on caveolin-1, a scaffolding protein found in caveolae (Bhatnagar *et al.*, 2004). Localization of GPCRs into domains has given rise to new challenges and complexities in receptor signaling since signaling has to be understood in context of the three dimensional organization of various signal transduction components which include receptors and G-proteins (Ostrom *et al.*, 2000).

1.2. Membrane cholesterol

Biological membranes are complex non-covalent assemblies of a diverse variety of lipids and proteins that allow cellular compartmentalization thereby imparting an identity to the cell and its organelles. Since a significant portion of integral membrane proteins remains in contact with the membrane bilayer (Lee, 2003), and reaction centers in them are often buried within the membrane, the structure and function of membrane proteins often depend on their interactions with surrounding lipids (Palsdottir and Hunte, 2004; Lee, 2004). Cholesterol is a major representative lipid in higher eukaryotic cellular membranes and is crucial in the organization, dynamics, function, and sorting of membranes (Liscum and Underwood, 1995; Simons and Ikonen, 2000). Cholesterol is a predominantly hydrophobic molecule comprising a near planar tetracyclic fused steroid ring and a flexible isooctyl hydrocarbon tail (see Figure 1.1a). The 3 β -hydroxyl moiety provides cholesterol its amphiphilic character, thereby orienting it in the membrane bilayer with its long axis perpendicular to the plane of the membrane (see Figure 1.1b). Interestingly, it has been reported that tail-to-tail cholesterol dimers spanning the two leaflets of the membrane bilayer can be formed under certain conditions (Harris *et al.*, 1995; Mukherjee and Chattopadhyay, 1996; Loura and Prieto, 1997; Tulenko *et al.*, 1998; Rukmini *et al.*, 2001; Mason *et al.*, 2003). Cholesterol is often found distributed nonrandomly in domains in biological and model membranes (Liscum and Underwood, 1995; Simons and Ikonen, 1997, 2000; Schroeder *et al.*, 1995; Xu and London, 2000; Mukherjee and Maxfield, 2004). Many of these domains (sometimes termed as ‘lipid rafts’) are believed to be important for the maintenance of membrane structure and function. The idea of such specialized membrane domains assumes significance in cell biology since physiologically important functions such as membrane sorting and trafficking (Simons and van Meer, 1988) and signal transduction processes (Simons and Toomre, 2000), in addition to the entry of pathogens (Simons and Ehehalt, 2002; Pucadyil and Chattopadhyay, 2007a), have been attributed to these domains. Specifically, cholesterol is known to play a vital role in the function and organization of

membrane proteins and receptors (Burger *et al.*, 2000; Pucadyil and Chattopadhyay, 2006).

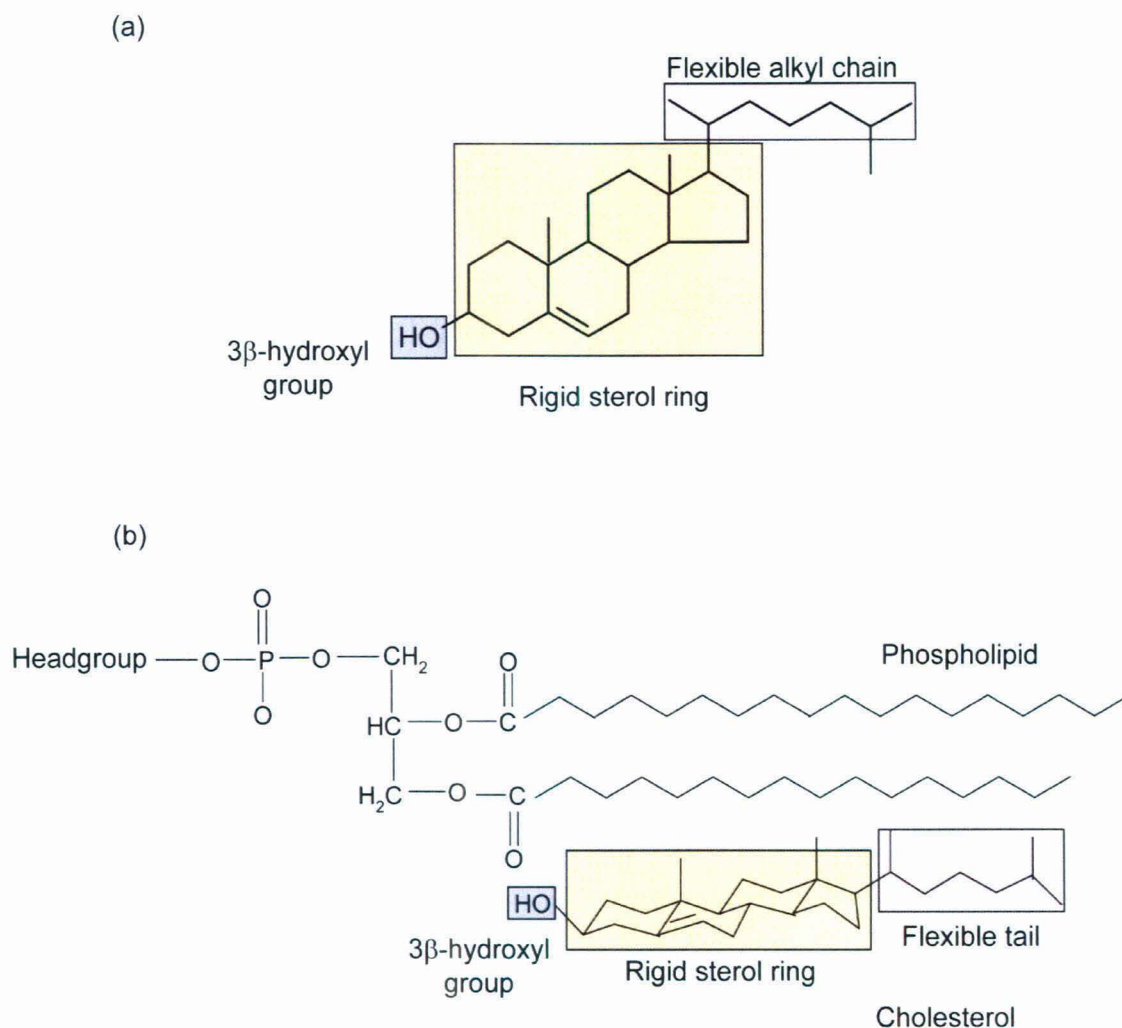


Figure 1.1. Chemical structure and membrane orientation of cholesterol. Three structurally distinct regions are shown as shaded boxes in panel (a): the 3 β -hydroxyl group, the rigid steroid ring, and the flexible alkyl chain. The 3 β -hydroxyl moiety is the only polar group in cholesterol thereby contributing to its amphiphilic character and helps to orient and anchor it in the membrane. Panel (b) shows the schematic orientation of cholesterol in relation to a phospholipid molecule in a lipid bilayer. The rigid and near planar steroid ring contributes to the ordering effect of cholesterol in phospholipid bilayers due to the restriction in motion imposed by it to adjacent phospholipid fatty acyl chains. The flexible alkyl chains extend into the hydrophobic core of the membrane. Reproduced from Chattopadhyay and Paila, 2007.

Interestingly, a strong asymmetry exists even in the manner cholesterol is distributed among various organs in the body of higher eukaryotes. For example, the central nervous system which accounts for only 2% of the body mass contains ~25% of free cholesterol present in the whole body (Dietschy and Turley, 2001). Although the brain is highly enriched in cholesterol and important neuronal processes such as synaptogenesis require cholesterol (Mauch *et al.*, 2001), the organization and dynamics of brain cholesterol is still poorly understood (Wood *et al.*, 1999). Brain cholesterol is synthesized *in situ* (Kabara, 1973) and is developmentally regulated (Turley *et al.*, 1998). The organization, traffic, and dynamics of brain cholesterol are stringently controlled since the input of cholesterol into the central nervous system is almost exclusively from *in situ* synthesis as there is no evidence for the transfer of cholesterol from blood plasma to brain (Dietschy and Turley, 2001). As a result, a number of neurological diseases share a common etiology of defective cholesterol metabolism in the brain (Porter, 2002; Chattopadhyay and Paila, 2007). The recent increase in the number of studies in understanding the mechanisms by which cholesterol metabolism in the brain is regulated could be attributed to the fact that defects in cholesterol homeostasis in the brain have been linked to development of several neurological disorders such as Alzheimer's disease, Niemann-Pick type C disease and the Smith-Lemli-Opitz syndrome (Vance *et al.*, 2005). In the Smith-Lemli-Opitz syndrome, for example, the marked abnormalities in brain development and function leading to serious neurological and mental dysfunctions have their origin in the fact that the major input of brain cholesterol comes from the *in situ* synthesis and such synthesis is defective in this syndrome (Waterham and Wanders, 2000). In view of the importance of cholesterol in relation to membrane domains (Rukmini *et al.*, 2001; Liscum and Underwood, 1995; Simons and Ikonen, 1997, 2000; Schroeder *et al.*, 1995; Xu and London, 2000; Mukherjee and Maxfield, 2004), the effect of alteration in the cholesterol content of neuronal membranes on membrane dynamics and receptor function represents an

important determinant in the analysis of neurogenesis and several neuropathologies. The interaction between cholesterol and other membrane components (such as receptors) in the brain therefore assumes relevance for a comprehensive understanding of brain function.

1.3. Effect of membrane cholesterol on the function of GPCRs: general or specific effect ?

Membrane cholesterol has been shown to modulate the function of a number of GPCRs. From the available data on the role of cholesterol on GPCR function (see Table 1.1), it appears that there is a lack of consensus in the manner in which cholesterol modulates receptor function. For example, while cholesterol is found to be essential for the proper function of several GPCRs, the function of rhodopsin has been shown to be inhibited by the presence of cholesterol. This brings out the necessity for a detailed mechanistic analysis of the effects of cholesterol on the specific receptor system. A critical analysis of some of the available literature on the role of membrane cholesterol in GPCR function, with an overall objective to distinguish specific and general effects, is provided below.

Cholesterol plays a vital role in the function and organization of membrane proteins and receptors (Burger *et al.*, 2000; Pucadyil and Chattopadhyay, 2006). The effect of cholesterol on the structure and function of integral membrane proteins and receptors has been a subject of intense investigation (Burger *et al.*, 2000; Pucadyil and Chattopadhyay, 2006). For example, it has been proposed that cholesterol can modulate the function of GPCRs in two ways: (i) through a direct/specific interaction with the GPCR, which could induce a conformational change in the receptor (Gimpl *et al.*, 2002a,b), or (ii) through an indirect way by altering the membrane physical properties in which the receptor is embedded (Ohvo-Rekilä *et al.*, 2002; Lee, 2004) or due to a

Table 1.1
Effect of membrane cholesterol on the function of GPCRs

| GPCR | References |
|---|--|
| Rhodopsin | (Straume and Litman, 1988; Mitchell <i>et al.</i> , 1990; Albert and Boesze-Battaglia, 2005) |
| Cholecystokinin (CCK) | (Gimpl <i>et al.</i> , 1997; Burger <i>et al.</i> , 2000; Harikumar <i>et al.</i> , 2005) |
| Galanin (GAL2) | (Pang <i>et al.</i> , 1999) |
| Serotonin _{1A} (5-HT _{1A}) | (Pucadyil and Chattopadhyay, 2004a, 2005, 2006; Paila <i>et al.</i> , 2005, 2008) |
| Serotonin ₇ (5-HT ₇) | (Sjögren <i>et al.</i> , 2006) |
| Metabotropic glutamate ^a | (Eroglu <i>et al.</i> , 2002, 2003) |
| δ Opioid | (Huang <i>et al.</i> , 2007) |
| κ Opioid | (Xu <i>et al.</i> , 2006) |
| μ Opioid | (Lagane <i>et al.</i> , 2000) |
| Oxytocin | (Gimpl <i>et al.</i> , 1995, 1997, 2002b; Fahrenholz <i>et al.</i> , 1995; Klein <i>et al.</i> , 1995) |
| β ₂ -adrenergic | (Kirilovsky and Schramm, 1983; Kirilovsky <i>et al.</i> , 1987; Ben-Arie <i>et al.</i> , 1988) |
| Chemokine (CXCR4, CCR5) | (Nguyen and Taub, 2002a,b, 2003) |
| Neurokinin (NK1) | (Monastyrskaya <i>et al.</i> , 2005; Meyer <i>et al.</i> , 2006) |
| Cannabinoid (CB1) | (Bari <i>et al.</i> , 2005a,b) |
| M ₂ Muscarinic | (Colozo <i>et al.</i> , 2007) |

^aThese studies were carried out in the *Drosophila* eye where the major sterol present is ergosterol

combination of both factors. There could be yet another manner in which membrane cholesterol could affect structure and function of membrane proteins. For example, it has been reported that for the nicotinic acetylcholine receptor (which requires cholesterol for its function), cholesterol is proposed to be present at the 'nonannular' sites around the receptor (Jones and McNamee, 1988). These nonannular sites, initially postulated for $\text{Ca}^{2+}/\text{Mg}^{2+}$ -ATPase (Lee *et al.*, 1982; Simmonds *et al.*, 1982), are characterized by occlusion of phospholipids. It has been suggested that the possible locations for the nonannular sites could be either inter- or intramolecular protein interfaces (Simmonds *et al.*, 1982). In the context of GPCRs, it is interesting to note that many GPCRs are believed to function as oligomers (Park *et al.*, 2004).

GPCRs such as oxytocin and cholecystokinin (CCK) receptors have been shown to require membrane cholesterol for their function (Gimpl *et al.*, 1995, 1997, 2002a,b; Harikumar *et al.*, 2005; Fahrenholz *et al.*, 1995; Klein *et al.*, 1995). Interestingly, while the interaction between the oxytocin receptor and cholesterol is believed to be specific, the function of the CCK receptor appears to be dependent on the physical properties of membranes which are a function of cholesterol content. This is demonstrated by the fact that these receptors displayed different types of correlation, when fluorescence anisotropy of the popular membrane probe DPH was correlated with the ligand binding activity. In case of the CCK receptor, ligand binding showed linear increase with measured anisotropy values (Gimpl *et al.*, 1997). In contrast to this, the ligand binding activity of the oxytocin receptor showed a slight reduction with cholesterol depletion followed by a sharp decline when the membrane cholesterol content reached a certain critical level (~57% of the original cholesterol content). This shows that membrane cholesterol could affect the ligand binding activity of the oxytocin receptor by a cooperative mechanism. Hill analysis of cholesterol content vs. ligand binding revealed that the oxytocin receptor binds several molecules of cholesterol ($n \geq 6$) in a positive cooperative manner (Burger *et al.*, 2000; Gimpl *et al.*, 2002b). These conclusions are

further supported by structure-activity analysis of the oxytocin and cholecystokinin receptor using a variety of cholesterol analogues substituting for membrane cholesterol (Gimpl *et al.*, 1997). In order to assess the specific structural features of cholesterol that are required to maintain the high-affinity state of the oxytocin receptor, cyclodextrins were used to replenish cholesterol-depleted membranes with a broad range of cholesterol analogues that were subtly different from cholesterol either in the headgroup, the steroid ring, or in the hydrocarbon tail. Interestingly, ligand binding of the oxytocin receptor could be restored only with certain analogues, thereby indicating a specific structural feature in cholesterol to support receptor function. Although cholesterol depletion reduces ligand binding to the cholecystokinin receptor, this effect could be reversed with most analogues of cholesterol that could restore membrane order. The ligand binding of the CCK receptor therefore was supported by each of the cholesterol analogue and was well correlated with the corresponding fluorescence anisotropy values. Similar effects on the oxytocin receptor could be demonstrated only with certain analogues that structurally resembled cholesterol in some critical features. Taken together, this data provide support for a specific molecular interaction between the oxytocin receptor and cholesterol. Further, molecular modeling studies have indicated a putative docking site (involving residues on the surface of transmembrane segments V and VI) for cholesterol in the oxytocin receptor that is absent in the CCK receptor (Politowska *et al.*, 2001). In addition, it has been reported that cholesterol stabilizes the oxytocin receptor against thermal inactivation and protects the receptor from proteolytic degradation (Gimpl and Fahrenholz, 2002). It has also recently been shown that cholesterol promotes cooperativity in the binding of ligands to the M₂ muscarinic receptor (Colozo *et al.*, 2007).

Pang *et al.* (1999) have shown that membrane cholesterol is required for ligand binding of the subtype 2 galanin receptor (GalR2) and intracellular signaling of the receptor. The role of membrane cholesterol in modulating ligand binding to the galanin

receptor was examined by treating membranes with M β CD or by culturing cells expressing the receptor in lipoprotein-deficient serum. These studies revealed a marked reduction in galanin binding to the receptor in cholesterol-deficient membranes. Importantly, replenishment of cholesterol to cholesterol-depleted membranes restored galanin binding to normal levels. This interaction appears to be specific to cholesterol, as only a limited number of cholesterol analogues were able to rescue galanin binding. In addition, treatment of membranes with filipin, a cholesterol-binding agent, or with cholesterol oxidase markedly reduced galanin binding. Hill analysis suggested that several molecules of cholesterol ($n \geq 3$) could bind in a positively cooperative manner to GalR2 (Pang *et al.*, 1999).

1.4. Cholesterol and nonannular lipids in the function of membrane proteins

The role of dynamic lipid-protein interactions in regulating the structure and functional activity of membrane proteins has been extensively studied using a variety of spectroscopic approaches (Devaux and Seigneuret, 1985). Integral membrane proteins are surrounded by a shell or annulus of lipid molecules which mimics the immediate layer of solvent surrounding soluble proteins (Jost *et al.*, 1973; Lee, 2003). These are termed ‘annular’ lipid around the membrane protein. After several years of moderate controversy surrounding the interpretation of spectroscopic data, it later became clear that the annular lipids are exchangeable with bulk lipids (Figure 1.2; Devaux and Seigneuret, 1985). The rate of exchange of lipids between the annular lipid shell and the bulk lipid phase was shown to be approximately an order of magnitude slow than the rate of exchange of bulk lipids resulting from translational diffusion of lipids in the plane of the membrane. It therefore appears that exchange between annular and bulk lipids is slightly slower since lipid-protein interaction is favorable compared to lipid-lipid interaction. However, the difference in interaction energy is modest, consistent

with the observation that lipid-protein binding constants (affinity) depend weakly on lipid structure (Lee, 2003). Interestingly, the two different types of lipid environments (annular and bulk) can be readily detected using electron spin resonance (ESR) spectroscopy (Marsh, 1990). In addition to the annular lipids, there is evidence for other lipid molecules in the immediate vicinity of integral membrane proteins. These are termed as ‘nonannular’ lipids (Figure 1.2). Nonannular sites are characterized by lack of accessibility to the annular lipids, *i.e.*, these sites cannot be displaced by competition with annular lipids. This is evident from analysis of fluorescence quenching of intrinsic tryptophans of membrane proteins by phospholipid or cholesterol covalently labeled with bromine (Jones and McNamee, 1988; Simmonds *et al.*, 1982), which acts as a quencher due to the presence of the heavy bromine atom (Chattopadhyay, 1992). These results signify that nonannular lipid binding sites remain vacant even in the presence of annular lipids around the protein (Marius *et al.*, 2008). Although not shown experimentally yet, the exchange of lipid molecules between nonannular sites and bulk lipids would be relatively slow compared to the exchange between annular sites and bulk lipids, and binding to the nonannular sites is considered to be more specific compared to annular binding sites (Lee, 2003).

The location of the postulated nonannular sites represents an intriguing question. It has been suggested that the possible locations for the nonannular sites could be either inter or intramolecular (interhelical) protein interfaces (Figure 1.2), characterized as deep clefts (or cavities) on the protein surface (Simmonds *et al.*, 1982; Marius *et al.*, 2008). For example, in the crystal structure of the potassium channel KcsA from *S. lividans*, one of the best understood ion channels, a negatively charged lipid molecule was found to be bound as ‘anionic nonannular’ lipid at each of the protein-protein interface in the homotetrameric structure (Marius *et al.*, 2005). These nonannular sites show high selectivity for anionic lipids over zwitterionic lipids, and it has been proposed that the change in the nature of the nonannular lipid results in a change in packing at the

Table 1.2. Number of annular and nonannular lipid molecules associated with membrane proteins

| Membrane protein | Annular lipids | Nonannular lipids | | Reference |
|--|--------------------------|-------------------|------------------|--|
| | | Intraprotein | Interprotein | |
| (a) G-protein coupled receptors | | | | |
| ^a Rhodopsin | 24 | | | Watts <i>et al.</i> , 1979 |
| ^d Metarhodopsin I | | 1 (nonannular ?) | | Ruprecht <i>et al.</i> , 2004 |
| ^d β_2 -adrenergic receptor | | 2 (nonannular ?) | 6 (nonannular ?) | Cherezov <i>et al.</i> , 2007; Hanson <i>et al.</i> , 2008 |
| (b) Other proteins | | | | |
| ^a Ca ²⁺ /Mg ⁺² ATPase | 32 at 0 °C (22 at 37 °C) | | | East <i>et al.</i> , 1985 |
| ^{a,c} Nicotinic acetylcholine receptor (pentamer) | 45 | 10 | | Ellena <i>et al.</i> , 1983; Jones <i>et al.</i> , 1988; Jones & McNamee, 1988 |
| ^a Gramicidin A (monomer) | 3-4 | | | Kóta <i>et al.</i> , 2004 |
| ^c Potassium channel KcsA (homotetramer) | | | 3 | Marius <i>et al.</i> , 2005, 2008 |
| ^a MscL from <i>Mycobacterium tuberculosis</i> | 30 | | | Powl <i>et al.</i> , 2007 |

Chapter 1. Introduction

| | | | | |
|--|----|---|---|----------------------------------|
| ^a Na ⁺ /K ⁺ -ATPase from <i>Squalus acanthus</i> (dimer) | 66 | | | Esmann <i>et al.</i> , 1985 |
| ^a Yeast cytochrome oxidase | 55 | | | Knowles <i>et al.</i> , 1979 |
| ^b Human erythrocyte glycophorin | 29 | | | Yeagle, 1982 |
| ^d Bacteriorhodopsin | 6 | 2 | | Lee, 2004 |
| ^d Aquaporin-0 (per monomer) | 7 | 2 | | Hite <i>et al.</i> , 2008 |
| ^d Yeast cytochrome <i>bc₁</i> complex | | 1 | 4 | Lange <i>et al.</i> , 2001 |
| ^d Cytochrome oxidase from <i>Paracoccus denitrificans</i> | | 1 | 1 | Lee, 2004 |
| ^d <i>E. coli</i> succinate dehydrogenase | 1 | | 1 | Yankovskaya <i>et al.</i> , 2003 |
| ^d Photosynthetic reaction center from <i>Thermochromatium tepidum</i> | | | 1 | Nogi <i>et al.</i> , 2000 |
| ^d ADP/ATP carrier from mitochondria | 7 | | | Lee, 2004 |

^afrom ESR

^bfrom ³¹P NMR

^cfrom fluorescence quenching

^dfrom electron crystallography

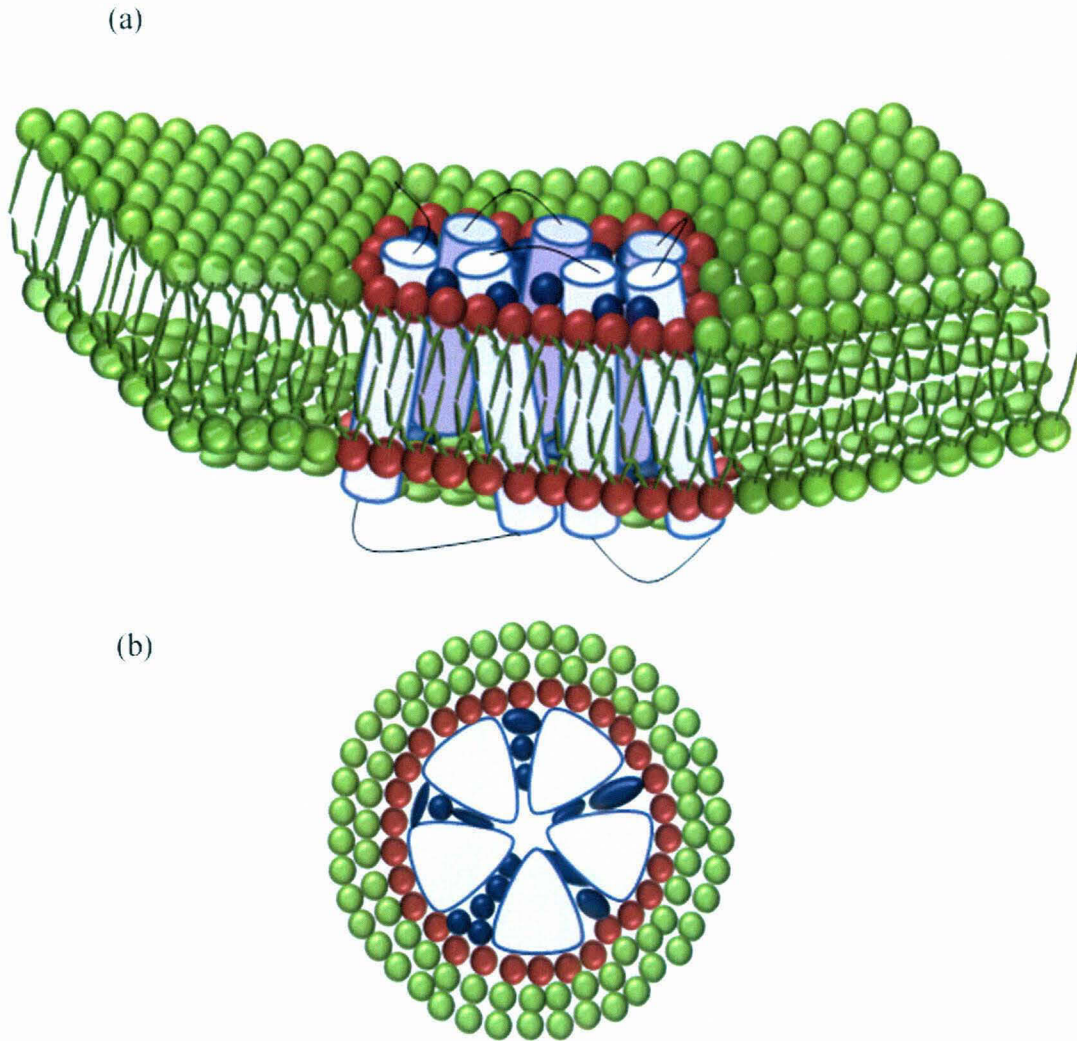


Figure 1.2. A schematic representation of (a) a membrane embedded seven transmembrane domain protein, (b) the top view of a multisubunit (or oligomeric) integral membrane protein, showing various classes of lipids in the vicinity of the protein. Annular lipids (shown in red) represent the shell (or annulus) of lipid molecules which mimics the immediate layer of solvent surrounding soluble proteins. The annular lipids are in dynamic equilibrium (exchangeable) with bulk lipids (shown in green). The rate of exchange of lipids between the annular lipid shell and the bulk lipid phase is approximately an order of magnitude slow than the rate of exchange of bulk lipids. Annular and bulk lipids can be readily detected using Electron Spin Resonance (ESR) spectroscopy. Nonannular lipids (shown in blue) are characterized by lack of accessibility to annular lipids. Nonannular lipids can be distinguished from annular lipids by analysis of fluorescence quenching measurements of intrinsic tryptophans in membrane proteins by phospholipid or cholesterol covalently labeled with bromine. Interestingly, lipid molecules resolved in high resolution crystal structures of membrane proteins are likely to be nonannular lipids (Lee, 2004). It has been implicated from the recently reported crystal structure of the β_2 -adrenergic receptor (a representative member of the G-protein coupled receptor superfamily) that cholesterol molecules located at the interhelical/interprotein regions of the receptor could represent nonannular lipids (Paila et al., 2009). See text for details.

protein-protein interface which modulates the open channel probability and its conductance. Interestingly, the relationship between open channel probability of KcsA and negative phospholipid content exhibits cooperativity. This is consistent with a model in which the nonannular sites in the KcsA homotetramer have to be occupied by anionic lipids for the channel to remain open (Marius *et al.*, 2008). This example demonstrates the crucial requirement of nonannular lipids in the function of membrane proteins and the stringency associated with regard to specificity of nonannular lipids. In addition to nonannular lipids, another class of lipids have been suggested to reside within a membrane protein complex and these lipids could have an important role in proper folding and assembly of membrane proteins. These lipids are termed integral protein lipids. For example, phosphatidylinositol was observed as an integral protein lipid in the crystal structure of the yeast cytochrome *bc₁* complex (Palsdottir and Hunte, 2004). However, the distinction between the above definition of nonannular lipids and integral protein lipids is somewhat arbitrary.

1.5. Presence of specific (nonannular ?) cholesterol binding sites in the crystal structures of GPCRs

(i) Rhodopsin

Rhodopsin, the photoreceptor of retinal rod cells, undergoes a series of conformational changes upon exposure to light. The light activated receptor exists in equilibrium with various intermediates collectively called metarhodopsins. The state of equilibrium is sensitive to the presence of cholesterol in the membrane (Straume and Litman, 1988; Mitchell *et al.*, 1990; Bennet and Mitchell, 2008). An increase in the amount of cholesterol in the membrane shifts this equilibrium toward the inactive

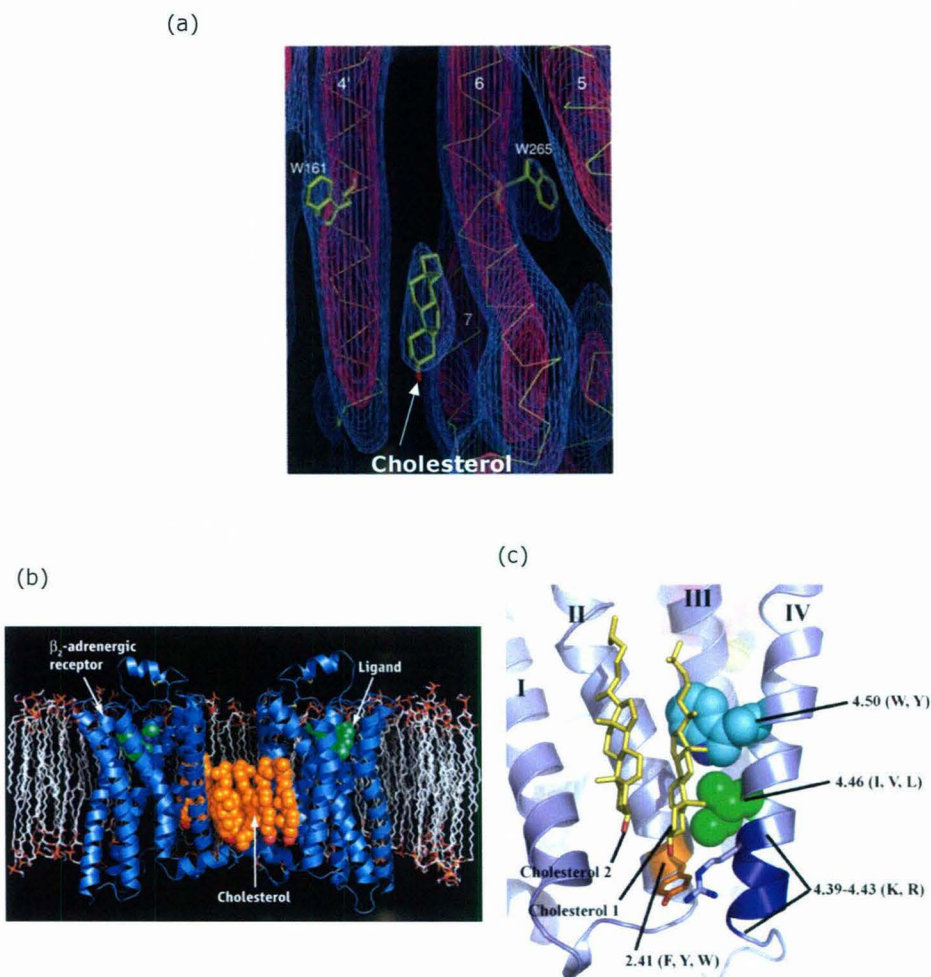


Figure 1.3. Presence of tightly bound cholesterol molecules in the transmembrane regions in the recently reported crystal structures of metarhodopsin I (panel a) and human β_2 -adrenergic receptor (panels b and c). Panel (a) shows side view of metarhodopsin I showing cholesterol between transmembrane helices. Notice the close proximity of tryptophan residues (W161 and W265) to cholesterol, independently confirmed by FRET studies (see text for more details). Reproduced from Ruprecht *et al.*, 2004. Panel (b) depicts the structure of the human β_2 -adrenergic receptor (shown in blue) bound to the partial inverse agonist carazolol (in green) embedded in a lipid bilayer. Cholesterol molecules between two receptor molecules are shown in orange (reproduced from Cherezov *et al.*, 2004). Panel (c) shows the Cholesterol Consensus Motif (CCM) in the β_2 -adrenergic receptor (bound to the partial inverse agonist timolol) crystal structure. The side chain positions of the β_2 -adrenergic receptor and two bound cholesterol molecules are shown. Residues at positions 4.39-4.43 fulfill the CCM requirement (if one or more of these positions contains an arginine or lysine residue) and constitute site 1 (shown in blue) toward the cytoplasmic end of transmembrane helix IV. Site 2 (in cyan) represents the most important site at position 4.50 on transmembrane helix IV since it is the most conserved site with tryptophan occupying this position in 94% of class A GPCRs. The other choice of amino acid for this site is tyrosine. Site 3 (in green) at position 4.46 on transmembrane helix IV satisfies the CCM requirement if isoleucine, valine, or leucine occupy the position. Site 4 (in orange) on transmembrane helix II is at position 2.41 and can be either phenylalanine or tyrosine (reproduced from Hanson *et al.*, 2008).

conformation of the protein. Direct interaction between rhodopsin and cholesterol has been monitored utilizing fluorescence resonance energy transfer (FRET) between tryptophan residues of rhodopsin (donor) and a fluorescent cholesterol analogue, cholestatrienol (acceptor) (Albert *et al.*, 1996). In this work, replenishment of cholesterol or ergosterol into cholesterol-depleted rod outer segment disk membranes was carried out and their ability to inhibit the quenching of donor tryptophan fluorescence was monitored. Interestingly, cholesterol was able to inhibit tryptophan quenching, whereas in presence of ergosterol, quenching was observed due to energy transfer between tryptophan residues of rhodopsin and cholestatrienol, indicating a specific interaction between rhodopsin and cholesterol. In addition, it was postulated that one cholesterol molecule per rhodopsin monomer would be present at the lipid-protein interface (Albert *et al.*, 1996). This was supported by the crystal structure of a photo-stationary state, highly enriched in metarhodopsin I, which shows a cholesterol molecule between two rhodopsin monomers, which could possibly represent a nonannular site for cholesterol binding (Ruprecht *et al.*, 2004, see Figure 1.3a). In addition, cholesterol was reported to improve the reliability and yield of crystallization. In this structure, cholesterol is shown to be oriented with its tetracyclic ring aligned normal to the membrane bilayer. Interestingly, these authors proposed that some of the tryptophans in transmembrane helices would be able to interact with the cholesterol tetracyclic ring. Recently reported crystallographic structures of the β_2 -adrenergic receptor have shown similar interactions.

(ii) β_2 -adrenergic receptor

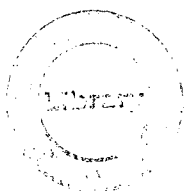
In general, lipid molecules that are resolved in crystal structures of membrane proteins are tightly bound. These lipid molecules, which are preserved even in the crystal structure, are often localized at protein-protein interfaces in multimeric proteins and belong to the class of nonannular (sometimes termed as ‘co-factor’) lipids (Lee, 2003, 2005). Cholesterol has been shown to improve stability of GPCRs such as the β_2 -adrenergic receptor (Yao and Kobilka, 2005), and appears to be a necessary component for crystallization of the receptor since it is believed to facilitate receptor-receptor interaction and consequent oligomerization (Cherezov *et al.*, 2007). The cholesterol analogue, cholesterol hemisuccinate, has recently been shown to stabilize the β_2 -adrenergic receptor against thermal inactivation (Hanson *et al.*, 2008). Since a possible location of the nonannular sites is interprotein interfaces (Simmonds *et al.*, 1982; Jones and McNamee, 1988), it is possible that cholesterol molecules located between individual receptor molecules (Figure 1.3b) occupy nonannular sites and modulate receptor structure and function. Importantly, the recent crystal structure of the β_2 -adrenergic receptor has revealed structural evidence of a specific cholesterol binding site (Figure 1.3c, Hanson *et al.*, 2008). The crystal structure shows a cholesterol binding site between transmembrane helices I, II, III and IV with two cholesterol molecules bound per receptor monomer. The cholesterol binding site appears to be characterized by the presence of a cleft located at the membrane interfacial region. Both cholesterol molecules bind in a shallow surface groove formed by segments of the above mentioned helices (I, II, III and IV), thereby providing an increase in the intramolecular occluded surface area, a parameter often correlated to the enhanced thermal stability of proteins (DeDecker *et al.*, 1996). Calculation of packing values of various helices in the β_2 -adrenergic receptor which are involved in the cholesterol interacting site showed that the packing of transmembrane helices IV and II

TH-16514

572,696

P154

Me



increases upon cholesterol binding, which would restrict their mobility rendering greater thermal stability to the protein (Hanson *et al.*, 2008).

It has been recently proposed that cholesterol binding sequence or motif should contain at least one aromatic amino acid which could interact with ring D of cholesterol (Hanson *et al.*, 2008) and a positively charged residue (Epanand *et al.*, 2006; Jamin *et al.*, 2005) capable of participating in electrostatic interactions with the 3 β -hydroxyl group. In the crystal structure of the β_2 -adrenergic receptor, three amino acids in transmembrane helix IV, along with an amino acid in transmembrane helix II, have been shown to constitute a cholesterol consensus motif (CCM, see Figure 1.3c). The aromatic Trp 158^{4.50} (according to the Ballesteros-Weinstein numbering system (Ballesteros and Weinstein, 1995) is conserved to a high degree (~94%) among rhodopsin family GPCRs and appears to contribute the most significant interaction with ring D of cholesterol (Hanson *et al.*, 2008). In this structure, the hydrophobic residue Ile154^{4.46} would interact with rings A and B of cholesterol and is largely conserved (~60%) in rhodopsin family GPCRs. The aromatic residue Tyr70^{2.41} in transmembrane helix II could interact with ring A of cholesterol and with Arg151^{4.43} of transmembrane helix IV through hydrogen bonding. The criterion of specific residues in CCM (as described above) could be somewhat broadened by conservative substitutions of amino acids.

The above description of CCM in the recently reported crystal structure of the β_2 -adrenergic receptor raises the interesting possibility of the presence of putative nonannular binding sites in transmembrane interhelical locations in GPCRs. Interestingly, it was previously proposed from quenching analysis of intrinsic tryptophan fluorescence in the nicotinic acetylcholine receptor by brominated lipids and cholesterol analogues, that there could be 5-10 nonannular sites per ~250,000 dalton monomer of the receptor (Jones and

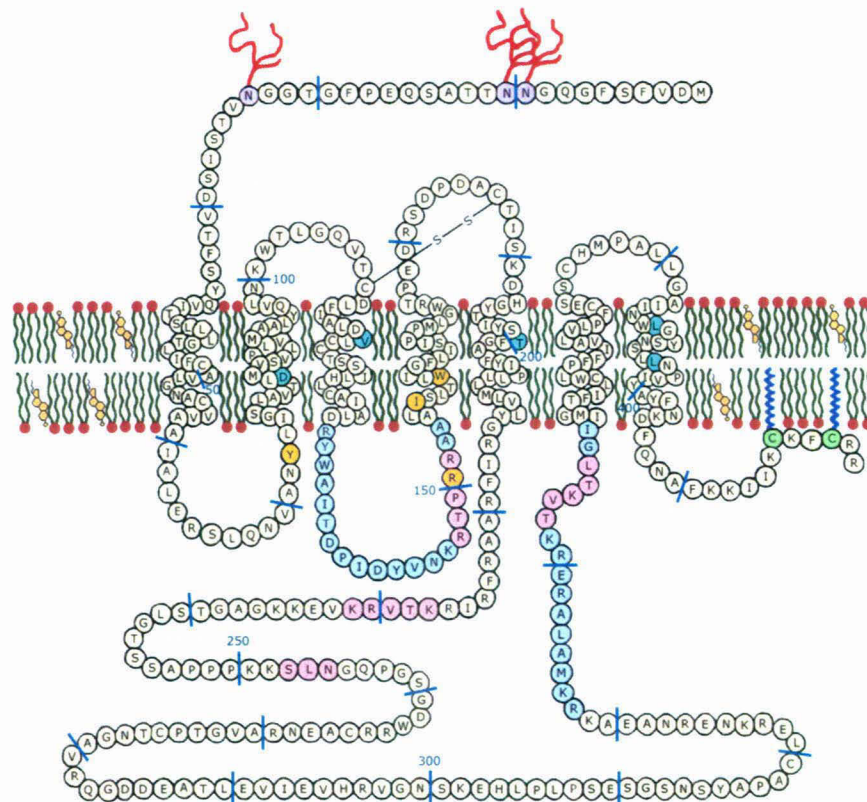


Figure 1.4. A schematic representation of the membrane embedded human serotonin_{1A} receptor showing its topological and other structural features. The membrane is shown as a bilayer of phospholipids and cholesterol, representing typical eukaryotic membranes. The transmembrane helices of the receptor were predicted using TMHMM2. The predictions were confirmed by other programs such as MEMSTAT, SPLIT4 and HMMTOP2 (it has been earlier reported that these four programs were among the best and perform equally well in predicting transmembrane helices (Cuthbertson *et al.*, 2005)). Seven transmembrane stretches, each composed of ~22 amino acids, are depicted as putative α -helices. The exact boundary between the membrane and the aqueous phase is not known and therefore the location of the residues relative to the membrane bilayer is putative. The amino acids in the receptor sequence are shown as circles and are marked for convenience. The potential sites (shown in lavender) for N-linked glycosylation (depicted as branching trees in red) on the amino terminus are shown. A putative disulfide bond between Cys¹⁰⁹ and Cys¹⁸⁷ is shown. The transmembrane domains contain residues (shown in cyan) that are important for ligand binding. The putative cholesterol binding site (see text) is highlighted (in orange). The receptor is stably palmitoylated (shown in blue) at residues Cys⁴¹⁷ and/or Cys⁴²⁰ (shown in green). Light blue circles represent contact sites for G-proteins. Light pink circles represent sites for protein kinase mediated phosphorylation. Further structural details of the receptor are available in (Pucadyil *et al.*, 2005a) and (Pucadyil and Chattopadhyay, 2006). It is probable, based on comparison with known crystal structures of similar GPCRs such as rhodopsin and β_2 -adrenergic receptor, that there are motionally restricted water molecules that could be important in inducing conformational transitions in the transmembrane portion of the receptor. Reproduced from Paila *et al.* (2009).

McNamee, 1988). This is consistent with the above proposal of two putative nonannular sites per ~50,000 dalton monomer of the β_2 -adrenergic receptor.

1.6. The serotonin_{1A} receptor

The serotonin_{1A} receptor is an important neurotransmitter receptor and is the most extensively studied of the serotonin receptors for a number of reasons (Pucadyil *et al.*, 2005a; Kalipatnapu and Chattopadhyay, 2007a). One of the main reasons is the availability of a selective ligand 8-OH-DPAT that allows extensive biochemical, physiological, and pharmacological characterization of the receptor (Arvidsson *et al.*, 1981; Gozlan *et al.*, 1983). Serotonin receptors have been classified into at least 14 subtypes on the basis of their pharmacological responses to specific ligands, sequence similarities at the gene and amino acid levels, gene organization, and second messenger coupling pathways (Hoyer *et al.*, 2002). The serotonin_{1A} receptor is the first among all the types of serotonin receptors to be cloned as an intronless genomic clone (G-21) of the human genome which cross-hybridized with a full length β -adrenergic receptor probe at reduced stringency (Pucadyil *et al.*, 2005a; Kobilka *et al.*, 1987). Sequence analysis of this genomic clone (later identified as the serotonin_{1A} receptor gene) showed ~43% amino acid homology with the β_2 -adrenergic receptor in the transmembrane domain (Paila *et al.*, 2009). The serotonin_{1A} receptor was therefore initially discovered as an 'orphan' receptor and was identified ('deorphanized') later (Fargin *et al.*, 1988). While the gene was shown to be localized in chromosome 5 of the human genome and speculated to code for a potential member of the GPCR superfamily (Kobilka *et al.*, 1987), its identity as a serotonin receptor was discovered only later (Fargin *et al.*, 1988). Membranes prepared

from COS-1 cells transiently transfected with G-21 showed typical ligand binding characteristics of the serotonin_{1A} receptor. Subsequently, genes for the rat and mouse serotonin_{1A} receptors have been cloned, and their amino acid sequences deduced (Albert *et al.*, 1990; Charest *et al.*, 1993). These developments facilitated stable expression and characterization of the receptor in a number of neural and non-neural cell lines (Banerjee *et al.*, 1993; Newman-Tancredi *et al.*, 1997; Kalipatnapu *et al.*, 2004a; Paila and Chattopadhyay, 2006). Furthermore, it was the first serotonin receptor for which polyclonal antibodies were obtained (Fargin *et al.*, 1988; Pucadyil *et al.*, 2005a) allowing their visualization at the subcellular level in various regions of the brain.

The human serotonin_{1A} receptor is composed of 422 amino acids with a core molecular weight of ~46,000 (Raymond *et al.*, 1999; Pucadyil *et al.*, 2005a; Paila and Chattopadhyay, 2009). Considering the presence of three consensus sequences for N-linked glycosylation on the amino terminus, and the homology of the receptor with β -adrenergic receptor, it is predicted that the receptor is oriented in the plasma membrane with the amino terminus facing the extracellular region and the carboxy terminus facing the intracellular cytoplasmic region (Raymond *et al.*, 1999; Pucadyil *et al.*, 2005a; Paila and Chattopadhyay, 2009; see Figure 1.4). The transmembrane domains (TM1-TM7) of the receptor are connected by hydrophilic sequences of three extracellular loops (EC1, EC2, EC3) and three intracellular loops (IC1, IC2, IC3). Such an arrangement is typical of the G-protein coupled receptor superfamily (Gether and Kobilka 1998). Although the structure of the serotonin_{1A} receptor has not yet been experimentally determined, mutagenesis studies have helped in identifying amino acid residues important for ligand binding and G-protein coupling of the serotonin_{1A} receptor (reviewed in Pucadyil *et al.*, 2005a). Among the predicted structural features of the serotonin_{1A} receptor, palmitoylation status of the receptor has been confirmed in a recent report (Papoucheva *et al.*, 2004).

Palmitoylation of Cys-417 and Cys-420 of the heterologously expressed rat serotonin_{1A} receptor, and its requirement in G-protein coupling and signaling of the serotonin_{1A} receptor have been demonstrated in this report. An interesting aspect of this study is that palmitoylation of the serotonin_{1A} receptor was found to be stable and independent of stimulation by the agonist. This is unusual for GPCRs which undergo repeated cycles of palmitoylation and depalmitoylation (Milligan *et al.*, 1995). It has therefore been proposed that stable palmitoylation of the receptor could play an important role in maintaining the receptor structure (Papoucheva *et al.*, 2004).

The serotonin_{1A} receptor has recently been shown to have a role in neural development (del Olmo *et al.*, 1998; Gaspar *et al.*, 2003), and protection of stressed neuronal cells undergoing degeneration and apoptosis (Singh *et al.*, 1996a). Treatment using agonists for the serotonin_{1A} receptor constitutes a potentially useful approach in case of children with developmental disorders (Azmitia, 2001). The serotonin_{1A} receptor agonists and antagonists have been shown to possess potential therapeutic effects in anxiety-or stress-related disorders (Pucadyil *et al.*, 2005a). As a result, the serotonin_{1A} receptor serves as an important target in the development of therapeutic agents for neuropsychiatric disorders such as anxiety and depression. Interestingly, mutant (knockout) mice lacking the serotonin_{1A} receptor generated a few years back exhibit enhanced anxiety-related behavior (described in Julius, 1998), and represent an important animal model for the analysis of complex traits such as anxiety disorders and aggression in higher animals (Gingrich and Hen, 2001; Toth, 2003). On the clinical front, serotonin_{1A} receptor levels have been shown to be altered in schizophrenia, and in patients suffering from major depression (Pucadyil *et al.*, 2005a). Interestingly, a recent observation has associated genetic polymorphisms at the upstream repressor region of the serotonin_{1A} receptor gene to major depression and suicide in humans (Lemonde *et al.*, 2003) linking its

expression status to these clinical syndromes. The selective serotonin_{1A} receptor agonist 8-OH-DPAT has recently been shown to inhibit growth of *Plasmodium falciparum* (reviewed in Chattopadhyay and Kalipatnapu, 2004) opening novel possibilities in antimalarial drug research. Besides, serotonin_{1A} receptors are implicated in feeding, regulation of blood pressure, temperature, and working memory (Pucadyil *et al.*, 2005a). Taken together, the serotonin_{1A} receptor is a central player in a multitude of physiological processes, and an important drug target.

Previous work from our laboratory has shown the requirement of membrane cholesterol for the function of the serotonin_{1A} receptor from the bovine hippocampus (Pucadyil and Chattopadhyay, 2004a). This was achieved by the use of methyl- β -cyclodextrin (M β CD) which physically depletes cholesterol from membranes. Based on these results, it was proposed that if cholesterol is necessary for function of the serotonin_{1A} receptor, modulating cholesterol availability by other means could lead to similar effects on the serotonin_{1A} receptor function. This proposal was tested in the first part of the thesis, by treating membranes with the sterol-complexing agent digitonin which does not physically deplete membrane cholesterol, yet would effectively reduce cholesterol-receptor interactions in the membrane due to complexation. This work is followed by addressing the issue of membrane cholesterol specificity for the function of the serotonin_{1A} receptor. Toward this direction, a cellular model of the Smith-Lemli-Opitz Syndrome (SLOS) was generated. SLOS serves as an appropriate condition to ensure the specific effect of membrane cholesterol in the function of the serotonin_{1A} receptor, since the two aberrant sterols that get accumulated in SLOS, *i.e.*, 7-dehydrocholesterol (7-DHC) and 8-DHC, differ with cholesterol only in a double bond. Furthermore, sphingolipid levels in CHO cells stably expressing the human serotonin_{1A} receptor were modulated using FB₁, which metabolically inhibits the biosynthesis of sphingolipids. In addition, the pharmacological

and functional characterization of the human serotonin_{1A} receptor stably expressed in hippocampal neuronal cell line (HN2) was carried out. The oligomerization state of the serotonin_{1A} receptor under various conditions such as ligand stimulation, cholesterol and sphingolipid depletion was monitored utilizing time-resolved fluorescence anisotropy measurements in live cells. These results are discussed in the later part of the thesis.

Chapter 2

The cholesterol-complexing agent digitonin modulates ligand binding of the bovine hippocampal serotonin_{1A} receptor

2.1. Introduction

Cholesterol is an essential and representative lipid component of eukaryotic membranes and plays a crucial role in membrane organization, dynamics, function, and sorting (Liscum and Underwood, 1995; Simons and Ikonen, 2000). Cholesterol in the plasma membrane plays a key role in regulating the activity of membrane proteins including receptors (Burger *et al.*, 2000; recently reviewed in Pucadyil and Chattopadhyay, 2006). The interaction between cholesterol and other membrane components (such as receptors) in the brain therefore assumes relevance for a comprehensive understanding of brain function.

Serotonin receptors represent one of the largest, evolutionarily ancient, and highly conserved families of G-protein-coupled receptors (Peroutka and Howell, 1994). Serotonin exerts its diverse actions by binding to distinct cell surface receptors which have been classified into many groups (Hoyer *et al.*, 2002). Serotonin receptors are members of a superfamily of seven transmembrane domain receptors (Pierce *et al.*, 2002) that couple to and transduce signals *via* GTP-binding regulatory proteins (G-proteins) (Clapham, 1996). Among the 14 subtypes of serotonin receptors, the G-protein coupled serotonin_{1A} (5-HT_{1A}) receptor is the best characterized for a variety of reasons (Pucadyil *et al.*, 2005a). We have earlier partially purified and solubilized serotonin_{1A} receptors from bovine hippocampus in a functionally active form (Chattopadhyay *et al.*, 2002, 2005).

Previous work from our laboratory has shown the requirement of membrane cholesterol in modulating ligand binding activity of the serotonin_{1A} receptor from the bovine hippocampus (Pucadyil and Chattopadhyay, 2004a). This was achieved by the use of methyl- β -cyclodextrin which physically depletes cholesterol from membranes. Treatment of bovine hippocampal membranes with methyl- β -cyclodextrin therefore resulted in specific removal of membrane cholesterol without any change in phospholipid content. Removal of cholesterol from bovine hippocampal membranes in this manner resulted in a reduction in ligand binding and G-protein coupling to the serotonin_{1A} receptor (Pucadyil and

Chattopadhyay, 2004a). If cholesterol is necessary for ligand binding of the serotonin_{1A} receptor, modulating cholesterol availability by other means could lead to similar effects on the serotonin_{1A} receptor function. This proposal was tested by treating membranes with the sterol-complexing agent digitorin which does not physically deplete membrane cholesterol, yet would effectively reduce cholesterol-receptor interactions in the membrane due to complexation (Elias *et al.*, 1978; Nishikawa *et al.*, 1984). Digitorin is a plant glycoalkaloid saponin detergent (see Figure 2.1) obtained from *Digitalis purpurea*. It forms water-insoluble 1:1 complexes (termed 'digitorinides') with cholesterol and other steroids, which possess a planar sterol nucleus, a 3 β -hydroxy- Δ^5 configuration and a hydrophobic side chain at C₁₇ (Severs and Robenek, 1983).

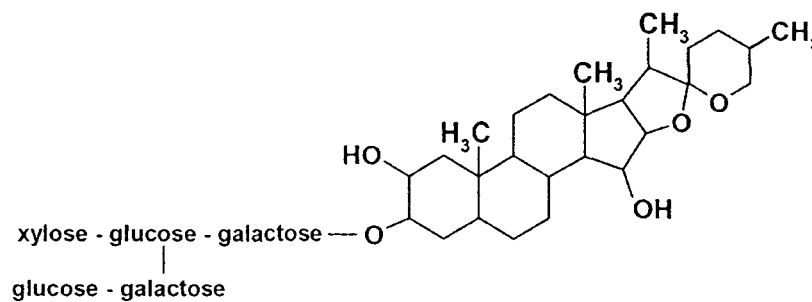


Figure 2.1. Chemical structure of digitorin

Digitorin treatment has been shown to result in the formation of cholesterol-digitorin rich domains in the membrane (Akiyama *et al.*, 1980), thereby reducing the freely available cholesterol capable of interacting with other membrane constituents such as receptors. This property of digitorin has resulted in its use as an agent to distinguish between cholesterol-rich and -poor membranes in the ultrastructure analysis of cell membranes (Dontchev *et al.*, 1994). The modulatory role of cholesterol on the function (specific agonist and antagonist binding) of the bovine hippocampal serotonin_{1A} receptor by cholesterol complexation in native membranes was examined using digitorin. The

corresponding changes in membrane dynamics were monitored by analysis of fluorescence polarization data of the membrane depth-specific probes, DPH and TMA-DPH.

2.2. Materials and methods

Materials

BCA, DMPC, DPH, EDTA, EGTA, MgCl₂, MnCl₂, Na₂HPO₄, *p*-MPPI, PMSF, TMA-DPH, Tris, iodoacetamide, polyethylenimine, serotonin, sodium azide, and sucrose were obtained from Sigma Chemical Co. (St. Louis, MO). Digitonin was from Research Organics (Cleveland, OH). Amplex Red cholesterol assay kit was from Molecular Probes (Eugene, OR). GTP- γ -S was from Roche Applied Science (Mannheim, Germany). [³H]8-OH-DPAT (specific activity = 135.0 Ci/mmol) and [³H]*p*-MPPF (specific activity = 70.5 Ci/mmol) were purchased from DuPont New England Nuclear (Boston, MA). BCA reagent for protein estimation was obtained from Pierce (Rockford, IL). All other chemicals used were of the highest available quality. GF/B glass microfiber filters were from Whatman International (Kent, U.K.). Pre-coated silica gel 60 thin-layer chromatography plates were from Merck (Merck KGaA, Germany). All solvents were of analytical grade. Water was purified through a Millipore (Bedford, MA) Milli-Q system and used throughout. Fresh bovine brains were obtained from a local slaughterhouse within 10 min of death and the hippocampal region was carefully dissected out. The hippocampi were immediately flash frozen in liquid nitrogen and stored at -70 °C till further use.

Preparation of native hippocampal membranes

Native hippocampal membranes were prepared as described earlier (Harikumar and Chattopadhyay, 1998). Bovine hippocampal tissue (~100 g) was homogenized as 10% (w/v) in a polytron homogenizer in buffer A (2.5 mM Tris, 0.32 M sucrose, 5 mM EDTA, 5 mM

EGTA, 0.02% sodium azide, 0.24 mM PMSF, 10 mM iodoacetamide, pH 7.4). The homogenate was centrifuged at 900g for 10 min at 4 °C. The supernatant was filtered through four layers of cheesecloth and the pellet was discarded. The supernatant was further centrifuged at 50,000g for 20 min at 4 °C. The resulting pellet was suspended in 10 vol. of buffer B (50 mM Tris, 1 mM EDTA, 0.24 mM PMSF, 10 mM iodoacetamide, pH 7.4) using a hand-held Dounce homogenizer and centrifuged at 50,000g for 20 min at 4 °C. This procedure was repeated until the supernatant was clear. The final pellet (native membranes) was resuspended in a minimum volume of buffer C (50 mM Tris, pH 7.4), homogenized using a hand-held Dounce homogenizer, flash frozen in liquid nitrogen and stored at -70 °C. Protein concentration was determined using the BCA reagent with bovine serum albumin as a standard (Smith *et al.*, 1985).

Preparation of digitonin stock solutions and treatment of hippocampal membranes

Stock solutions of digitonin in water were prepared as described previously (Winter, 1974). Briefly, digitonin was dissolved in ethanol by mild shaking in a water bath at 37 °C and the solution was evaporated to dryness under a gentle stream of N₂. This procedure results in the deposition of a fine film of digitonin on the walls of the glass tube that dissolves instantly upon addition of water. Aliquots of this aqueous stock solution were immediately added to hippocampal membranes at a total protein concentration of 0.5 mg/ml in 50 mM Tris, pH 7.4 buffer and incubated for 1 hr at 25 °C with constant shaking.

Membrane solubilization mediated by digitonin was assayed as described previously (Pucadyil and Chattopadhyay, 2004b). Briefly, membrane samples treated with increasing concentrations of digitonin for 1 hr at 25 °C were spun down at 100,000g for 45 min at 4 °C. The lipid phosphate and cholesterol content of the membrane pellet dissolved in 50 mM Tris, pH 7.4 buffer was assayed as described below.

Estimation of inorganic phosphate and cholesterol

The concentration of lipid phosphate was determined subsequent to total digestion by perchloric acid (McClare, 1971) using Na₂HPO₄ as standard. DMPC was used as an internal standard to assess lipid digestion. Samples without perchloric acid digestion produced negligible readings. Membrane cholesterol was estimated using the Amplex Red cholesterol assay kit (Amundson and Zhou, 1999).

Thin-layer chromatography of lipids extracted from native membranes

Lipid extraction was carried out according to Bligh and Dyer (Bligh and Dyer, 1959). The extracts were dried under a stream of nitrogen at 45 °C. The dried extracts were resuspended in a mixture of chloroform-methanol (1:1, v/v). Thin-layer chromatography of the extracted lipids was carried out using chloroform/methanol/water (65:25:4, v/v). The separated lipids were visualized by charring with a solution containing cupric sulfate (10% w/v) and phosphoric acid (8% v/v) at 150 °C. The TLC plates were scanned and lipids band intensities were analyzed using the Adobe Photoshop software version 5.0 (Adobe Systems Inc., San Jose, CA).

Radioligand binding assays

Receptor binding assays were carried out in presence of increasing concentrations of digitonin. Tubes in duplicate containing 0.5 mg total protein in a volume of 1 ml of buffer D (50 mM Tris, 1 mM EDTA, 10 mM MgCl₂, 5 mM MnCl₂, pH 7.4) for agonist binding or in 1 ml of buffer E (50 mM Tris, 1 mM EDTA, pH 7.4) for antagonist binding assays were used. Tubes were incubated with the radiolabeled agonist [³H]8-OH-DPAT (final concentration in assay tube being 0.29 nM) or antagonist [³H]*p*-MPPF (final concentration in assay tube 0.5 nM) for 1 hr at 23 °C in presence of increasing concentrations of digitonin. Non-specific binding was determined by performing the assay either in the presence of 10 μM serotonin (for agonist binding assays) or in the presence of 10 μM *p*-MPPI (for antagonist binding assays). The binding reaction was terminated by rapid filtration under

vacuum in a Millipore multiport filtration apparatus through Whatman GF/B 2.5 cm diameter glass microfiber filters (1.0 μm pore size), which were presoaked in 0.15% (w/v) polyethylenimine for 1 hr (Bruns *et al.*, 1983). The filters were then washed three times with 3 ml cold water (4 °C), dried and the retained radioactivity was measured in a Packard Tri-Carb 1500 liquid scintillation counter using 5 ml of scintillation fluid.

GTP-γ-S sensitivity assay

In experiments with GTP-γ-S, agonist binding assays were carried out as described above in the presence of a range of concentrations of GTP-γ-S as described previously (Harikumar and Chattopadhyay, 1999). The concentrations of GTP-γ-S leading to 50% inhibition of specific agonist binding (IC₅₀) were calculated by non-linear regression fitting of the data to a four parameter logistic function (Higashijima *et al.*, 1987):

$$B = [a/(1+(x/I)^s)] + b \quad (1)$$

where B is the specific binding of the agonist normalized to control binding (in absence of GTP-γ-S), x is the concentration of GTP-γ-S, a is the range ($y_{\max}-y_{\min}$) of the fitted curve on the ordinate (y-axis), I is the IC₅₀ concentration, b is the background of the fitted curve (y_{\min}) and s is the slope factor.

Fluorescence polarization measurements

Fluorescence polarization experiments were carried out with membranes containing 50 nmol of total phospholipids suspended in 1.5 ml of 50 mM Tris, pH 7.4 buffer with increasing concentrations of digitonin. Stock solutions of the fluorescent probes (DPH and TMA-DPH) were prepared in methanol. The amount of probe added was such that the final probe concentration was 1 mol% with respect to the total phospholipid content. This ensures optimal fluorescence intensity with negligible membrane perturbation. Membranes

were vortexed for 1 min after addition of the probe and kept in the dark for 1 hr before measurements. Background samples were prepared the same way except that the probe was omitted. The final probe concentration was 0.33 μM in all cases and the methanol content was low (0.03% v/v). Control experiments showed that at this concentration of methanol, the ligand binding properties of the receptor are not altered.

Steady state fluorescence was measured in a Hitachi F-4010 spectrofluorometer using 1 cm path length quartz cuvettes at room temperature (23 °C). Excitation and emission wavelengths were set at 358 and 430 nm. Excitation and emission slits with nominal bandpasses of 1.5 nm and 20 nm were used. The excitation slit was kept low to avoid any photoisomerization of DPH and TMA-DPH. In addition, fluorescence was measured with a 30 sec interval between successive openings of the excitation shutter (when the sample was in the dark in the fluorimeter) to reverse any photoisomerization of DPH and TMA-DPH (Chattopadhyay and London, 1984). Fluorescence polarization experiments were performed using a Hitachi polarization accessory. Polarization values were calculated from the equation (Lakowicz, 2006):

$$P = \frac{I_{VV} - GI_{VH}}{I_{VV} + GI_{VH}} \quad (2)$$

where I_{VV} and I_{VH} are the measured fluorescence intensities (after appropriate background subtraction) with the excitation polarizer vertically oriented and the emission polarizer vertically and horizontally oriented, respectively. G is the instrumental correction factor and is the ratio of the efficiencies of the detection system for vertically and horizontally polarized light and is equal to I_{HV}/I_{HH} . The optical density (measured with a Hitachi U-2000 spectrophotometer using 1 cm path length quartz cuvettes) of the membrane samples in the absence of digitonin measured at 358 nm was ~ 0.2 which increased in presence of digitonin. To avoid any scattering artifacts due to the presence of digitonin, the fluorescence

polarization values reported in Figure 8 were corrected for scattering by diluting the samples with 50 mM Tris, pH 7.4 buffer as described earlier (Lentz *et al.*, 1979). Fluorescence polarization values of samples (control and digitonin-treated, undiluted and diluted with the same buffer) were plotted against their corresponding optical densities as shown in Figure 2.8. The intercept on the ordinate (y-axis) from linear fits of this data was considered as the corrected fluorescence polarization value.

2.3. Results

Digitonin complexes membrane cholesterol without altering the cholesterol and phospholipid contents of hippocampal membranes

Digitonin is a widely used detergent and has been used to solubilize specific membrane components such as receptors (Bahouth and Malbon, 1987). It is therefore important to choose a range of concentration where digitonin would be present predominantly as a monomer and exert its cholesterol-complexing activity without causing any significant loss of membrane lipids (cholesterol and/or phospholipids). We estimated the loss of membrane lipids in the presence of digitonin by assaying the amount of total cholesterol and phospholipids present in the insoluble pellet obtained by high speed centrifugation following digitonin treatment (Pucadyil and Chattopadhyay, 2004b). The total cholesterol content was analyzed by thin-layer chromatography of lipids extracted from digitonin-treated membranes. Figure 2.2.a is a thin-layer chromatogram of lipids extracted from native membranes, and membranes treated with 0.6 and 1.0 mM of digitonin. Quantitative densitometric analysis of the cholesterol content (Figure 2.2b) indicates that the treatment with digitonin does not deplete membrane cholesterol. However, analysis of the cholesterol content of digitonin-treated membranes using the cholesterol oxidase

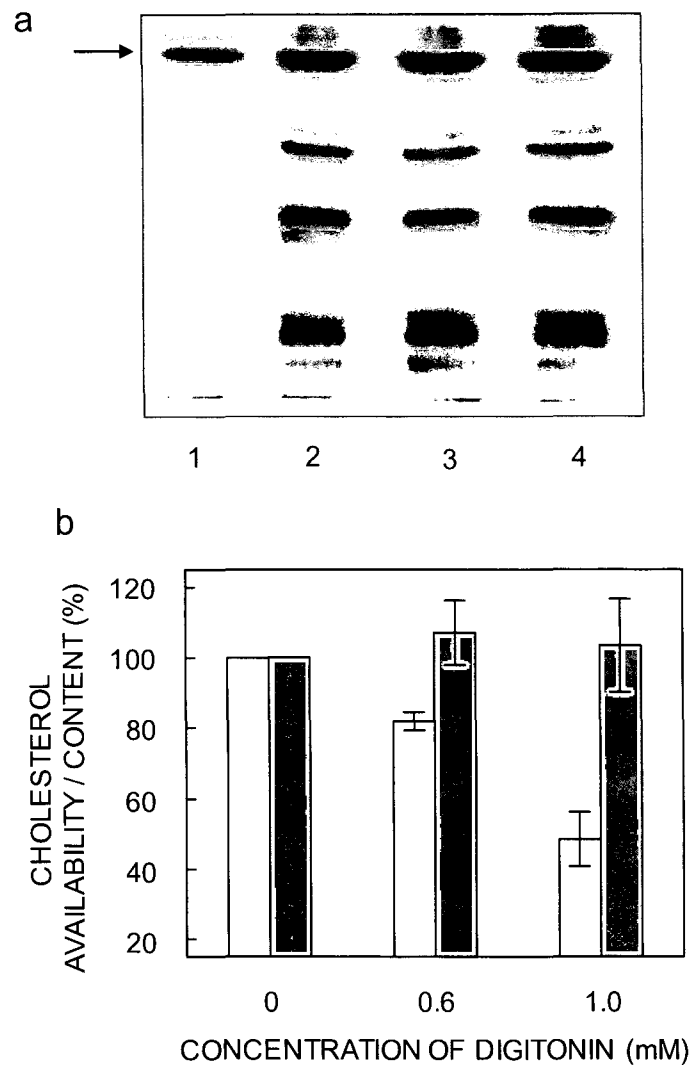


Figure 2.2. Cholesterol-complexing effect of digitonin. Total lipids extracted from digitonin-treated membranes were separated by thin-layer chromatography, as shown in (a). The lanes represent lipids extracted from native membranes (lane 2), and membranes treated with 0.6 mM (lane 3) and 1 mM (lane 4) digitonin. The arrow represents position of cholesterol on the thin-layer chromatogram identified using a standard in lane 1. The total and freely available cholesterol content in digitonin-treated membranes were distinguished as shown in (b). The total cholesterol content (grey bars) in the lipid extract was determined by a densitometric analysis of the thin-layer chromatogram. Values are expressed as a percentage of the cholesterol content in native membranes in the absence of digitonin. The amount of freely available cholesterol content (white bars) in membranes treated with digitonin was determined by the Amplex Red cholesterol assay kit. Values are expressed as a percentage of available cholesterol in native membranes in the absence of digitonin. Data represents the mean \pm SD of two independent experiments. See section 2.2 for further details.

enzyme based Amplex Red cholesterol assay kit (Amundson and Zhou, 1999) reveals an apparent reduction in the cholesterol content (Figure 2.2b). Thus, treatment of membranes with 1 mM digitonin reduces the available cholesterol content by ~50%. These results suggest that the presence of digitonin reduces the ability of the enzyme cholesterol oxidase to catalyze the oxidation of cholesterol thereby demonstrating the cholesterol-complexing ability of digitonin. Importantly, Figure 2.3 shows that in the concentration range of digitonin used (up to 1 mM), there is minimal loss of phospholipid content. All experiments were therefore carried out with this range (upto 1 mM) of digitonin concentration that complexes membrane cholesterol to a significant extent without physically depleting membrane lipids.

Ligand binding to serotonin_{1A} receptors is differentially affected in presence of digitonin

Figure 2.4 shows the reduction in the specific binding of the selective serotonin_{1A} receptor agonist [³H]8-OH-DPAT with increasing concentrations of digitonin, which results in progressive complexation of membrane cholesterol. This shows that complexation of cholesterol from hippocampal membranes results in loss of specific agonist binding to the serotonin_{1A} receptor. Thus, the specific agonist binding reduces by 86% in the presence of 1 mM digitonin. To the best of our knowledge, this result represents the first observation of reduction in specific ligand binding to the serotonin_{1A} receptor due to complexation of membrane cholesterol by digitonin. Although selective serotonin_{1A} agonists such as 8-OH-DPAT were discovered long back (Gozlan *et al.*, 1983), the development of selective serotonin_{1A} antagonists has been relatively slow and less successful. Two specific antagonists for the serotonin_{1A} receptor, *p*-MPPI and *p*-MPPF, were introduced later (Zhuang *et al.*, 1994; Thielen and Frazer, 1995). These compounds bind specifically to the serotonin_{1A} receptor with high affinity which is equivalent to the affinity displayed by the specific agonist 8-OH-DPAT.

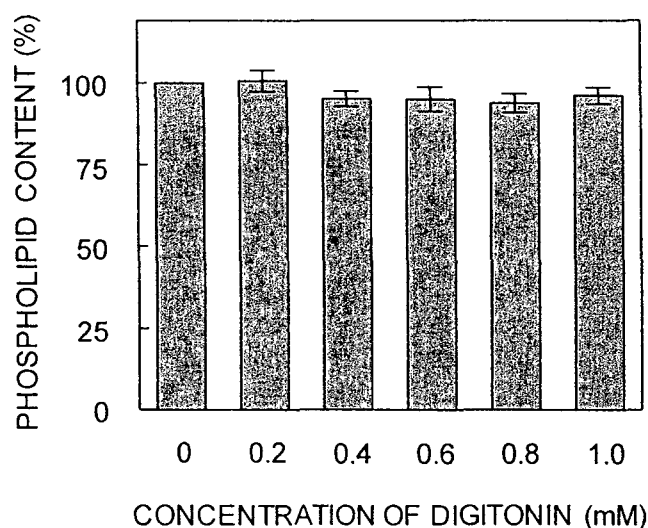


Figure 2.3. Effect of increasing concentrations of digitonin on the phospholipid content of bovine hippocampal membranes. Phospholipid contents were assayed as described in section 2.2. Values are expressed as a percentage of the phospholipid content in native membranes in the absence of digitonin. Data represent the means \pm SE of three independent experiments.

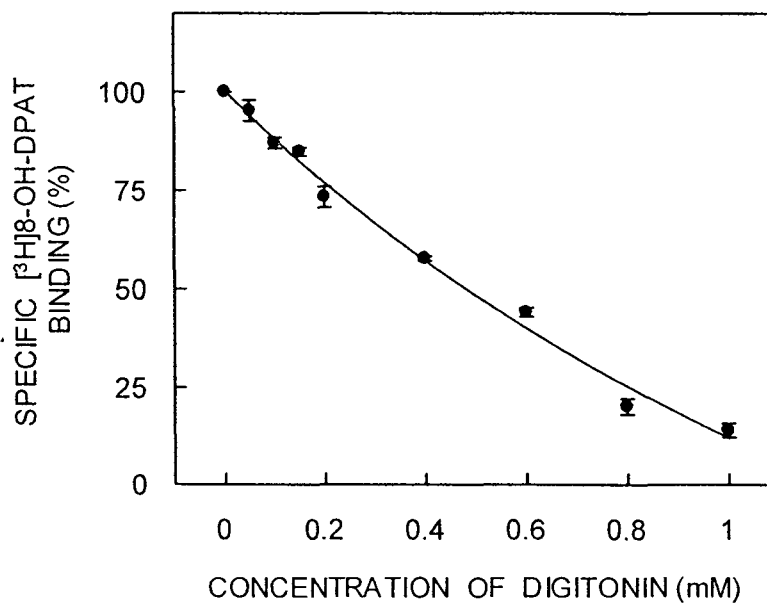


Figure 2.4. Effect of increasing concentrations of digitonin on specific [³H]8-OH-DPAT binding to the serotonin_{1A} receptor in hippocampal membranes. Values are expressed as a percentage of specific binding for native membranes in the absence of digitonin. Data shown are the means \pm SE of at least three independent experiments. See section 2.2 for other details.

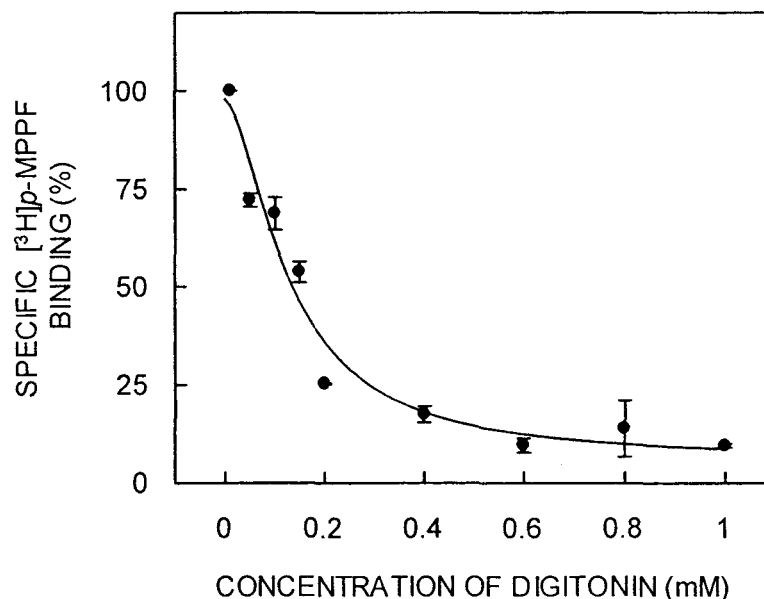


Figure 2.5. Effect of increasing concentrations of digonin on specific [³H]p-MPPF binding to the serotonin_{1A} receptor in hippocampal membranes. Values are expressed as a percentage of specific binding for native membranes in the absence of digonin. Data shown are the means \pm SE of at least three independent experiments. See section 2.2 for other details.

Figure 2.5 shows the decrease in specific binding of the serotonin_{1A} selective antagonist [³H]p-MPPF in the presence of increasing concentrations of digonin. In contrast to the observed reduction in specific agonist binding (Figure 2.4), the reduction in specific antagonist binding appears to be more drastic at lower digonin concentrations used. For example, the reduction in specific antagonist binding is ~83% in the presence of 0.4 mM digonin. The corresponding reduction in specific agonist binding is ~42% (see Figure 2.4). Taken together, these results show that the complexation of free membrane cholesterol in hippocampal membranes results in the loss of the serotonin_{1A} receptor ligand binding ability. The present results constitute the first observation where the availability of free cholesterol rather than its mere physical presence in the membrane is essential for the receptor function.

Digitonin alters the interaction of the receptor with G-proteins

G-protein-coupled receptors transduce signals from the extracellular milieu to the inside of the cell *via* their interaction with their cognate G-proteins located on the cytoplasmic face of the cell. The hippocampal serotonin_{1A} receptor is negatively coupled to the adenylate cyclase system through pertussis toxin-sensitive G-proteins (G_i/G_o) (Emerit *et al.*, 1990). We previously showed that the specific binding of the agonist [³H]8-OH-DPAT to bovine hippocampal serotonin_{1A} receptors is sensitive to guanine nucleotides and is inhibited with increasing concentrations of GTP- γ -S, a non-hydrolyzable GTP analogue which blocks the G-protein cycle (Harikumar and Chattopadhyay, 1999). Thus, the presence of GTP- γ -S induces transition of the receptor from a high affinity G-protein coupled state to a low affinity G-protein uncoupled state. Figure 2.6 shows the representative inhibition of specific [³H]8-OH-DPAT binding to the serotonin_{1A} receptor in the presence of GTP- γ -S in a characteristic concentration-dependent manner in control and digitonin-treated membranes. The half maximal inhibition concentration (IC₅₀) value for inhibition of [³H]8-OH-DPAT binding by GTP- γ -S is found to be 58.6 nM for native membranes. The inhibition curve for digitonin-treated membranes, however, exhibits a significant ($p < 0.05$) ~2.0 fold shift toward higher concentration of GTP- γ -S with an increased IC₅₀ value of 122 nM. This implies that the agonist binding to the serotonin_{1A} receptor in digitonin-treated membranes is less sensitive to GTP- γ -S indicating that G-protein coupling of the receptor is drastically reduced. This points out to a possible perturbation of receptor/G-protein interaction due to non-availability of membrane cholesterol because of complexation with digitonin.

Change in hippocampal membrane dynamics due to digitonin treatment

The overall membrane order and dynamics could be an important determinant for the function of a transmembrane receptor, a large portion of which remains in contact with the membrane lipids. In order to explore the possible changes in membrane order induced

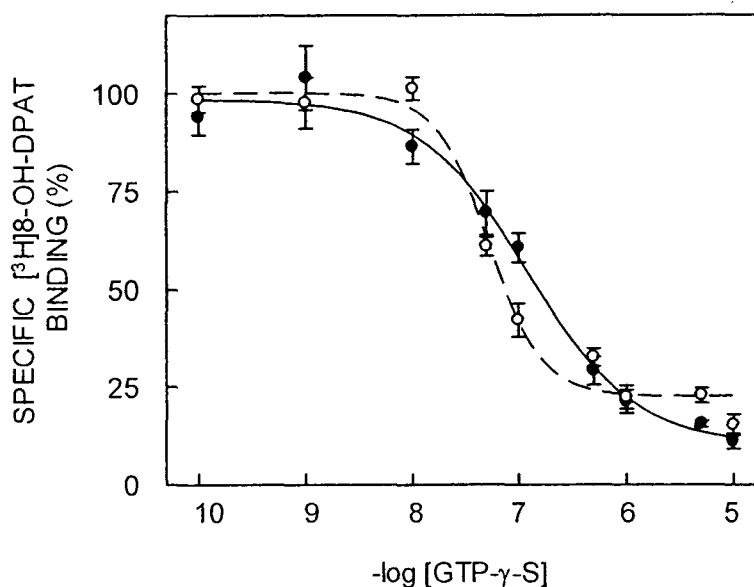


Figure 2.6. Sensitivity of specific [³H]8-OH-DPAT binding to GTP- γ -S in native and digitonin-treated membranes. Values are expressed as a percentage of specific binding for membranes in the absence of GTP- γ -S. Plot shows the effect of increasing concentrations of GTP- γ -S on specific [³H]8-OH-DPAT binding to control (----O----) membranes and membranes treated with 0.4 mM digitonin (—●—). The inhibition curves are non-linear regression fits to the experimental data using the four parameter logistic function (equation 1). The values represent the means \pm SE of four independent experiments. See section 2.2 for other details.

Table 2.1

Effect of cholesterol-complexing agent digitonin on specific [³H]8-OH-DPAT binding sensitivity to GTP- γ -S^a

| Treatment | IC ₅₀ (nM) |
|------------------|-----------------------|
| Control | 58.6 \pm 10 |
| 0.4 mM digitonin | 122 \pm 15 |

^aSensitivity of specific [³H]8-OH-DPAT binding to GTP- γ -S in the assay was measured by calculating the IC₅₀ for inhibition of [³H]8-OH-DPAT binding in presence of a range of concentrations of GTP- γ -S. The data represent the means \pm SE of four independent experiments. See section 2.2 for other details.

by digitonin treatment, we measured the fluorescence polarization of membrane depth-specific fluorescence probes DPH and TMA-DPH (see Figure 2.7). In general, fluorescence polarization is correlated to the rotational diffusion (Lakowicz, 2006) of membrane embedded probes, which is sensitive to the packing of fatty acyl chains and cholesterol. Since membranes display a considerable degree of anisotropy in terms of motional properties of constituent lipids and proteins (Chattopadhyay, 2003), a comprehensive understanding of membrane dynamics can be achieved by the use of more than one probe which localize at different depths in the membrane. DPH and its derivatives represent

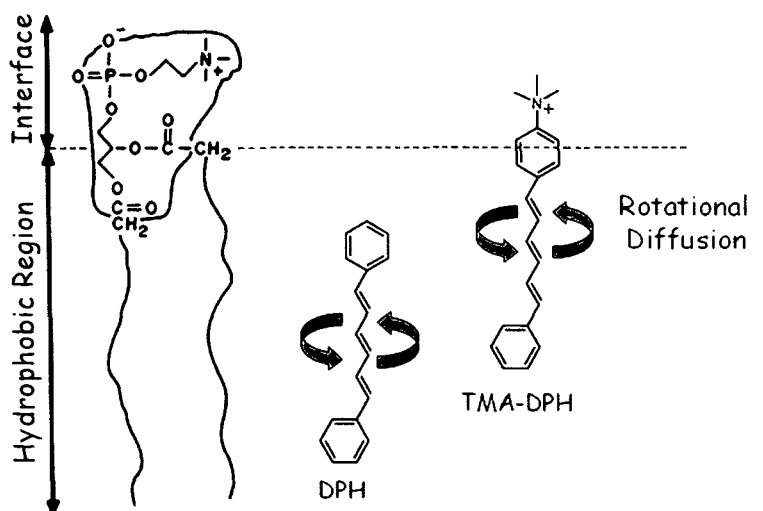


Figure 2.7. A schematic representation of half of the membrane bilayer showing the chemical structures and locations of the fluorescence probes DPH and TMA-DPH. The location of the DPH group in TMA-DPH and the average location of DPH in membranes is shown according to Kaiser and London (1998). The horizontal line at the bottom indicates the center of the bilayer. See text for other details.

popular probes for monitoring organization and dynamics in membranes (Lentz, 1989). On account of its hydrophobicity, DPH readily partitions into the membrane and localizes at the fatty acyl chain region in the membrane. TMA-DPH is a derivative of DPH with a cationic moiety attached to the para position of one of the phenyl rings (Prendergast *et al.*,

1981). The amphipathic TMA-DPH is oriented in the membrane with its positive charge localized at the membrane interface (Sojic *et al.*, 1992). The DPH moiety in TMA-DPH is localized at ~ 11 Å from the center of the membrane and reports the interfacial region of the membrane (Kaiser and London, 1998). In contrast, the average location of DPH has been shown to be ~ 8 Å from the center of the membrane (Kaiser and London, 1998).

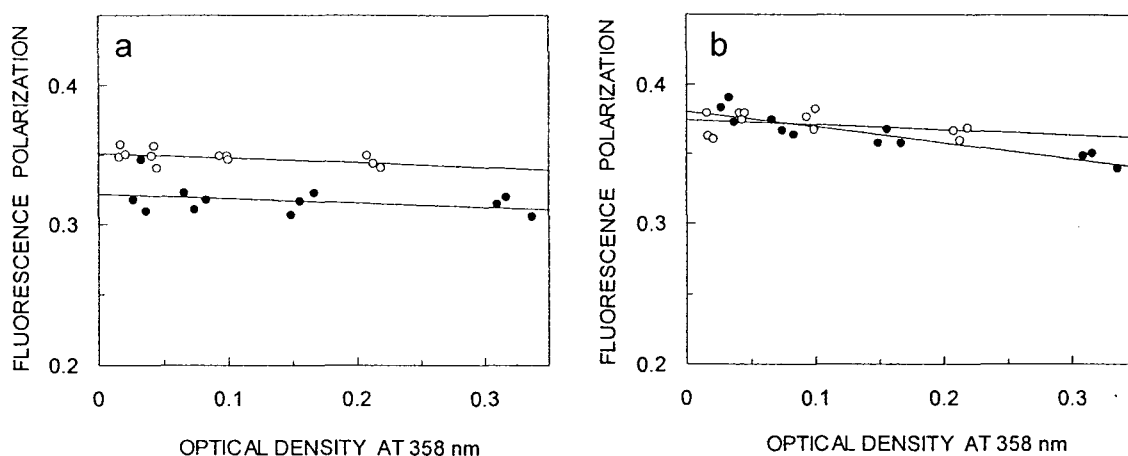


Figure 2.8. Representative plots of fluorescence polarization as a function of optical density. The plots represent the fluorescence polarization of (a) DPH and (b) TMA-DPH for native membranes (○) which serve as control and 0.6 mM digitonin-treated membranes (●) upon dilution with 50 mM Tris, pH 7.4 buffer. Fluorescence polarization was calculated as described in section 2.2. The solid lines are linear fits to the data with the intercept on the ordinate (y-axis) considered as the corrected fluorescence polarization (Lentz *et al.*, 1979). The plots are data from at least three independent experiments. See section 2.2 for other details.

We observed an increase in the optical density of samples upon increasing the concentration of digitonin which could complicate fluorescence polarization measurements using DPH and TMA-DPH. The fluorescence polarization data obtained under these conditions were corrected for scattering artifacts according to the formalism previously developed by Lentz *et al.* (Lentz *et al.*, 1979). Representative plots (at 0.6 mM digitonin) of experimentally measured fluorescence polarization as a function of optical density at the excitation wavelength are shown in Figure 2.8. The intercept on the ordinate (y-axis) from

linear fits of this data gives the corrected fluorescence polarization value (Lentz *et al.*, 1979). The correction significantly altered the polarization values of samples containing digitonin while the polarization values of control samples (without digitonin) remained unaltered.

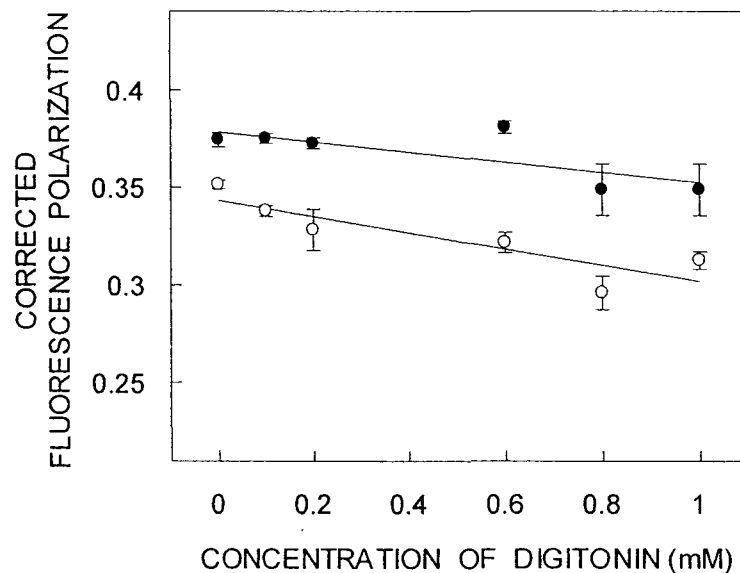


Figure 2.9. Effect of increasing concentrations of digitonin on fluorescence polarization of membrane probes DPH (○) and TMA-DPH (●) in hippocampal membranes. Fluorescence polarization experiments were carried out with membranes containing 50 nmol phospholipid at a probe to phospholipid ratio of 1:100 (mol/mol) at room temperature (23 °C). The data show corrected fluorescence polarization values (as described in section 2.2, and representative plots shown in Figure 2.8) and represent the means \pm SE of at least three independent experiments. The solid lines are linear fits of the data. See section 2.2 for other details.

Corrected fluorescence polarization values of DPH and TMA-DPH obtained this way as a function of digitonin concentration are shown in Figure 2.9. As apparent from the figure, the corrected fluorescence polarization of DPH (~0.35) in hippocampal membranes in the absence of digitonin is lower than that of TMA-DPH (~0.37). The higher polarization of TMA-DPH compared to DPH is indicative of the shallower interfacial location of TMA-DPH in the membrane (Pucadyil and Chattopadhyay, 2004a). The fluorescence

polarization of both the probes shows an overall decrease with increasing concentrations of digitonin. Interestingly, the extent of reduction in fluorescence polarization is higher for DPH (11%) compared to TMA-DPH (7%) up to 1 mM digitonin used. The presence of digitonin (at concentrations that do not deplete membrane lipids, see Figures 2.2 and 2.3) therefore induces asymmetric reduction in the membrane order in different regions of the membrane. Importantly, the relatively modest alterations in fluorescence polarization values of DPH and TMA-DPH in hippocampal membranes treated with digitonin ensure that the overall morphology of the membrane remains intact and rule out any possibility of gross changes in membrane architecture.

2.4. Discussion

Lipid-protein interactions play a crucial role in maintaining the structure and function of integral membrane proteins and receptors (Lee, 2004; Jensen and Mouritsen, 2004). A large portion of any given transmembrane receptor remains in contact with the membrane lipid environment. This raises the obvious possibility that the membrane could be an important modulator of receptor structure and function (Burger *et al.*, 2000). Monitoring lipid-receptor interactions is of particular importance because a cell has the ability of varying the lipid composition of its membrane in response to a variety of stress and stimuli, thereby changing the environment and the activity of the receptors in its membrane. In view of the importance of cholesterol in relation to membrane domains (Liscum and Underwood, 1995; Simons and Ikonen, 1997), the interaction of cholesterol with membrane receptors (Burger *et al.*, 2000; Pucadyil and Chattopadhyay, 2006) represents an important determinant in functional studies of such receptors, especially in the nervous system.

The serotonin_{1A} receptor belongs to the G-protein-coupled receptor superfamily which comprises the largest class of molecules involved in signal transduction across the plasma membrane, thus providing a mechanism of communication between the exterior and the interior of the cell (Pierce *et al.*, 2002). These receptors can be activated by ligands as chemically diverse as biogenic amines, peptides, glycoproteins, lipids, nucleotides and even photons, thus mediating diverse physiological processes such as neurotransmission, cellular metabolism, secretion, cellular differentiation and growth, and inflammatory and immune responses. As mentioned before, G-protein-coupled receptors serve as major targets for the development of novel drug candidates, and possess tremendous therapeutic potential.

These results show the complexation of cholesterol in hippocampal membranes using digitonin results in a concentration-dependent reduction in specific agonist and antagonist binding to serotonin_{1A} receptors. Complexation of membrane cholesterol with digitonin is believed to reduce the availability of free cholesterol (present data and Severs and Robenek, 1983) essential to support important membrane functions. This is supported by the observation that the presence of digitonin restores the otherwise suppressed phase transition (Estep *et al.*, 1978) of dipalmitoylphosphatidylcholine membranes containing cholesterol (Nishikawa *et al.*, 1984). In addition, cholesterol complexation by digitonin affected G-protein coupling of the receptor as monitored by the GTP- γ -S assay. The accompanying changes in membrane order were reported by corresponding changes in fluorescence polarization of membrane probes, such as DPH and TMA-DPH, which are localized at different positions (depths) in the membrane. These results point out the important role of membrane cholesterol in maintaining the function of the serotonin_{1A} receptor. This result assumes significance in the light of a tightly bound cholesterol molecule in the recently reported crystallographic structure of metarhodopsin I, an important photointermediate of rhodopsin which is a representative member of the G-protein-coupled receptor family (Ruprecht *et al.*, 2004). Interestingly, the clinical significance of membrane cholesterol levels resulting in receptor dysfunction has been aptly

exemplified in the case of cholecystokinin (CCK) receptors (Xiao *et al.*, 1999, 2000). Thus, agonist binding is reduced and G-protein coupling affected for CCK receptors isolated from muscle tissues in human gallbladders with cholesterol stones.

Our results on the inhibition of ligand binding and G-protein coupling to serotonin_{1A} receptors in presence of the cholesterol-complexing agent digitonin confirm and extend our previous observation on the requirement of membrane cholesterol for efficient serotonin_{1A} receptor function (Pucadyil and Chattopadhyay, 2004a). Importantly, since digitonin does not physically deplete cholesterol from membranes unlike agents such as methyl- β -cyclodextrin, our results serve to delineate the mechanism by which cholesterol exerts its influence on the serotonin_{1A} receptor function. We conclude that the mere non-availability of free cholesterol in the membrane is sufficient to significantly reduce the serotonin_{1A} receptor function. These results provide a comprehensive understanding of the effects of the sterol-complexing agent digitonin in particular, and the role of membrane cholesterol in general, on the serotonin_{1A} receptor function from a lipid-protein interaction perspective.

Chapter 3

Signaling by the human serotonin_{1A} receptor is impaired in cellular model of the Smith-Lemli-Opitz syndrome

3.1. Introduction

The Smith-Lemli-Opitz Syndrome (SLOS) (Smith *et al.*, 1964) is an autosomal recessive disorder characterized clinically by mental retardation, physical deformities, failure to thrive and multiple congenital anomalies (Waterham and Wanders, 2000; Yu and Patel, 2005). SLOS is caused by mutations in the gene encoding 3 β -hydroxy-steroid- Δ^7 -reductase (7-DHCR), an enzyme required in the final step of cholesterol biosynthesis (Irons *et al.*, 1993; Tint *et al.*, 1994). Till date, close to 100 different mutations in the DHCR7 gene have been identified which lead to the disease (Jira *et al.*, 2003). SLOS is ranked as one of the most serious recessive genetic conditions (Yu and Patel, 2005; Battaile and Steiner, 2000). Reduced levels of plasma cholesterol along with elevated levels of 7-dehydrocholesterol (7-DHC) (and its positional isomer 8-dehydrocholesterol, 8-DHC) and the ratio of their concentrations to that of cholesterol are representative parameters for diagnosis of SLOS (Tint *et al.*, 1995). Although SLOS has devastating effects on the nervous system, the relationship of SLOS with neuronal receptors and their membrane lipid interactions, which play a crucial role in the function of the nervous system, remains an unexplored area. Cholesterol is an important lipid in this context since it is known to regulate the function of membrane receptors (Burger *et al.*, 2000), especially neuronal receptors (Pucadyil and Chattopadhyay, 2006), thereby affecting neurotransmission. Importantly, a possible role of cholesterol in a variety of neurological disorders is well documented (Chattopadhyay and Paila, 2007).

Previous work from our laboratory has shown the requirement of membrane cholesterol in the function of an important neurotransmitter receptor, the serotonin_{1A} receptor (Pucadyil and Chattopadhyay, 2006). Keeping in mind the pharmacological relevance of the serotonin_{1A} receptor, a transmembrane protein, its interaction with the surrounding lipid environment assumes greater significance in modulating its function in healthy and diseased states.

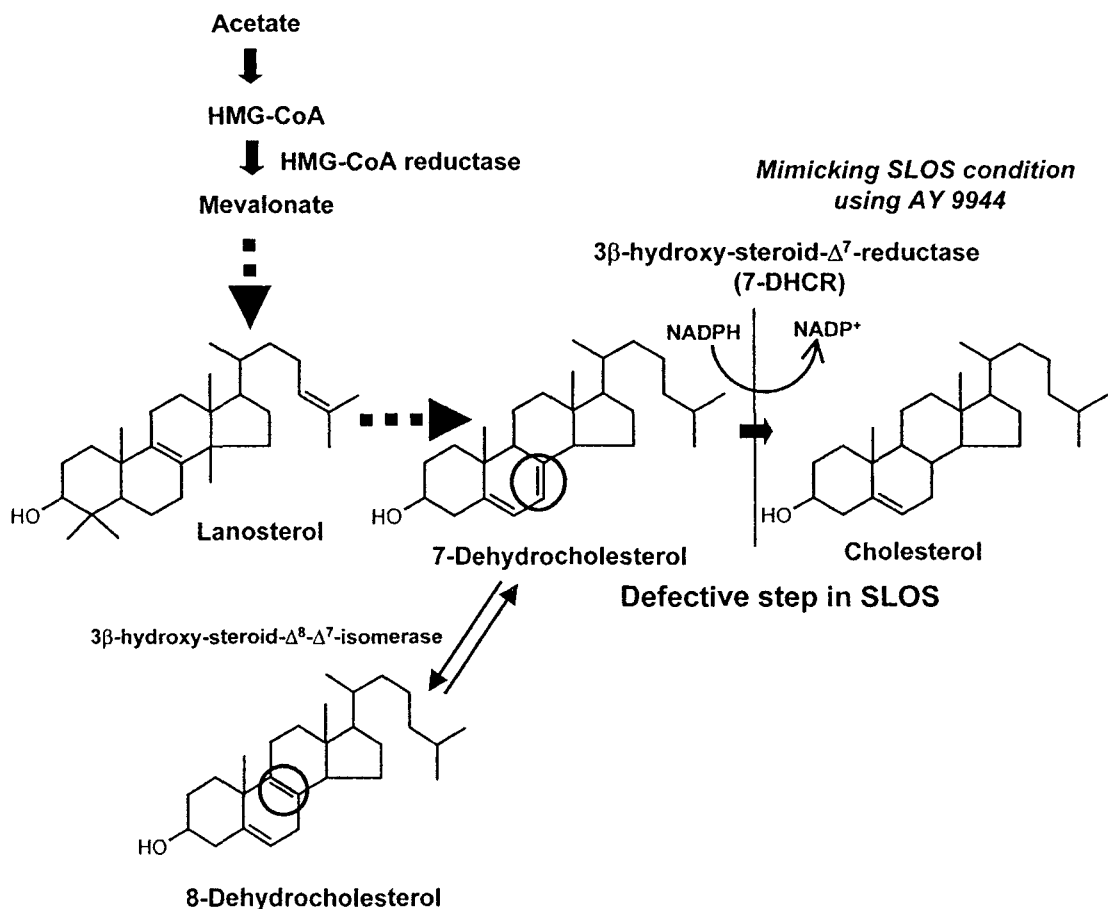


Figure 3.1. Generation of a cellular model of Smith-Lemli-Opitz syndrome. The principal route of cholesterol synthesis in humans is the Kandutsch-Russell pathway (Kandutsch and Russell, 1960). In this pathway, the immediate precursor of cholesterol is 7-DHC. The reduction of C7(8) double bond of 7-DHC to yield cholesterol is catalyzed by 3β-hydroxy-steroid-Δ⁷-reductase (7-DHCR) in an NADPH-dependent manner. Mutations in this enzyme cause SLOS, a severe developmental disorder associated with multiple congenital and morphogenic anomalies. Reduced levels of cholesterol, along with elevated levels of dehydrocholesterol (7-DHC + 8-DHC), have been characterized as a diagnostic parameter of the SLOS. 8-DHC, a positional isomer of 7-DHC, is formed due to an enzyme-catalyzed isomerization of 7-DHC. 7-DHC (and 8-DHC) differs with cholesterol only in a double bond at the 7th (or 8th) position in the sterol ring (highlighted in their chemical structures). We have generated a cellular model for SLOS by treating CHO cells stably expressing the human serotonin_{1A} receptor (CHO-5-HT_{1A}R) with AY 9944, a specific metabolic inhibitor of 7-DHCR, by altering the cholesterol and dehydrocholesterol levels, thereby mimicking the condition of mutated 7-DHCR.

A cellular model of SLOS was generated using CHO cells stably expressing the human serotonin_{1A} receptor (CHO-5-HT_{1A}R) by metabolically inhibiting the biosynthesis of cholesterol. To achieve this, AY 9944, which is a specific metabolic inhibitor of 7-DHCR, was utilized (Dvornik *et al.*, 1963). AY 9944 treatment results in reduction of cholesterol with a concomitant accumulation of 7- and 8-DHC, thereby mimicking SLOS (see Figure 3.1). We explored the function of the human serotonin_{1A} receptor under these conditions by monitoring ligand binding, G-protein coupling and downstream signaling of the receptor. Our results show that the function of the serotonin_{1A} receptor is impaired under SLOS-like condition. Importantly, metabolic replenishment of cholesterol partially restored the ligand binding activity of the serotonin_{1A} receptor. These results are significant since intake of dietary cholesterol is the recommended treatment for SLOS patients.

3.2. Materials and methods

Materials

Cholesterol, DMPC, AY 9944, EDTA, 7-DHC, coprostanol, MgCl₂, MnCl₂, 8-OH-DPAT, penicillin, streptomycin, gentamycin sulfate, polyethylenimine, PMSF, serotonin, sodium bicarbonate, and Tris were obtained from Sigma Chemical Co. (St. Louis, MO). D-MEM/F-12 [Dulbecco's modified Eagle medium:nutrient mixture F-12 (Ham) (1:1)], lipofectamine, fetal calf serum, and geneticin (G 418) were from Invitrogen Life Technologies (Carlsbad, CA). *N,O*-bis(trimethylsilyl)trifluoroacetamide (BSTFA) was obtained from Supelco (Bellefonte, PA). GTP- γ -S was from Roche Applied Science (Mannheim, Germany). BCA reagent for protein estimation was from Pierce (Rockford, IL). Forskolin and IBMX were obtained from Calbiochem (San Diego, CA). MTT was purchased from Calbiochem (La Jolla, CA). [³H]8-OH-DPAT (sp. activity = 135.0 Ci/mmol) was purchased from DuPont New England Nuclear (Boston, MA). The cyclic

[³H]AMP assay kit was purchased from Amersham Biosciences (Buckinghamshire, U.K.). GF/B glass microfiber filters were from Whatman International (Kent, U.K.). All other chemicals and solvents used were of the highest available purity. Water was purified through a Millipore (Bedford, MA) Milli-Q system and used throughout.

Methods

Cell culture and treatment with AY 9944

CHO cells stably expressing the human serotonin_{1A} receptor (termed as CHO-5-HT_{1A}R) and CHO cells stably expressing the human serotonin_{1A} receptor tagged to enhanced yellow fluorescent protein (termed as CHO-5-HT_{1A}R-EYFP) were maintained in D-MEM/F-12 (1:1) supplemented with 2.4 g/l of sodium bicarbonate, 10% fetal calf serum, 60 µg/ml penicillin, 50 µg/ml streptomycin, 50 µg/ml gentamycin sulfate, and 200 µg/ml geneticin in a humidified atmosphere with 5% CO₂ at 37 °C. Stock solution of AY 9944 was prepared in water and added to cells grown for 24 h (final concentration of AY 9944 was 1-10 µM) and incubated in 5% serum for 63-66 h. Control cells were grown under similar conditions without AY 9944 treatment.

Cell membrane preparation

Cell membranes were prepared as described earlier (Kalipatnapu *et al.*, 2004a; Paila and Chattopadhyay, 2006). Briefly, confluent cells were harvested by treatment with ice-cold buffer containing 10 mM Tris, 5 mM EDTA, 0.1 mM PMSE, pH 7.4. Cells were then homogenized at 4 °C at maximum speed with a Polytron homogenizer. The cell lysate was centrifuged at 500g for 10 min at 4 °C and the resulting post-nuclear supernatant was centrifuged at 40,000g for 30 min at 4 °C. The pellet thus obtained was suspended in 50 mM Tris buffer, pH 7.4. Total protein concentration in membranes thus isolated was determined using the BCA assay (Smith *et al.*, 1985).

Estimation of inorganic phosphate

The concentration of lipid phosphate was determined as described in section 2.2.

Estimation of cell viability

CHO-5-HT_{1A}R cells were plated at a density of ~1500 cells per well on 96-well plates and were treated with AY 9944 as described earlier in this section. Total incubation volume of each well was 200 μ l. MTT (0.5 mg/ml) was prepared in D-MEM/F-12 medium (without serum) and 200 μ l of this solution was added to each well and incubated at 37 °C for 3 h. Cells were spun down and the supernatant was removed and 100 μ l of DMSO was added to dissolve the formazan crystals into each well and absorbance was measured at 540 nm using an automatic microtiter plate reader SPECTRAMax 190 from Molecular Devices (Sunnyvale, CA). The viable cell number was directly proportional to the production of formazan.

Gas chromatography and mass spectrometry

GC-MS analysis was carried out on an Agilent 6890N gas chromatograph (Agilent Technologies, Palo Alto, CA) equipped with a model 5973i mass selective detector and 7683 series injector. For membrane sterol measurements, cellular membranes were prepared and total lipids were extracted in chloroform-methanol (Bligh and Dyer, 1959), after the addition of coprostanol as an internal recovery standard. The chloroform phase obtained was dried under nitrogen. Sterols were identified and quantitated using GC-MS as described previously (Tulenko *et al.*, 2006) with some modifications. Briefly, an aliquot of the extract was hydrolyzed in 1 M NaOH in ethanol for 1 h at 70 °C, extracted with *n*-hexane, and converted into trimethylsilyl ether derivatives followed by injection into a capillary column. This was a chemically bonded, fused silica, nonpolar CP-Sil 8CB (Varian, Middleburg, The Netherlands) capillary column (30 m \times 0.25 mm i.d., 0.25 μ m film thickness).

Chapter 3. The human serotonin_{1A} receptor function in cellular model of SLOS

oven temperature was maintained at 250 °C with a solvent delay of 5 min from the time of injection. Helium at the rate of 1.2 ml/min was used as the carrier gas under constant flow mode. The inlet and interface temperatures were kept at 250 and 280 °C, respectively. The ion source and quadrupole temperatures were kept at 230 and 150 °C, respectively. Mass spectra were scanned from 30 to 600 Da under scan mode. The ions at *m/z* 329, 351 and 370 were used under Selected Ion Monitoring (SIM) mode for the estimation of cholesterol, 7-DHC/8-DHC and coprostanol, respectively. Peak areas were obtained individually for each compound under SIM mode in the concentration range of 100-1200 ppm for cholesterol, 10-100 ppm for both 7-DHC and coprostanol, and the calibration curves were constructed. The absolute concentrations of various sterols in the samples were calculated from the calibration curves. The concentration of coprostanol is used to calculate the recovery of the sterols. Membrane sterol contents are expressed as cholesterol to total sterol ratio and cholesterol to dehydrocholesterol (7-DHC + 8-DHC) ratio.

Radioligand binding assays

Receptor binding assays were carried out with ~50 μ g of total protein as described in section 2.2.

Saturation radioligand binding assays

Saturation binding assays were carried out with increasing concentrations (0.1-7.5 nM) of the radiolabeled agonist [³H]8-OH-DPAT as described previously (Paila and Chattopadhyay, 2006). Saturation binding assays were carried out with varying concentrations (0.1-7.5 nM) of the radiolabeled agonist [³H]8-OH-DPAT and antagonist [³H]p-MPPF under conditions as described above. Non-specific binding was measured in the presence of 10 μ M serotonin for agonist and 10 μ M p-MPPI for antagonist binding. Binding data were analyzed as described previously (Pucadyil *et al.*, 2004a). The concentration of the bound radioligand (RL*) was calculated from the equation:

$$RL^* = 10^{-9} \times B / (V \times SA \times 2220) \text{ M} \quad (3)$$

where B is the bound radioactivity in disintegrations per minute (dpm) (*i.e.*, total dpm–non-specific dpm), V is the assay volume in ml, and SA is the specific activity of the radioligand. The data could be fitted best to a one site ligand binding equation. The dissociation constant (K_d) and maximum binding sites (B_{max}) were calculated by non-linear regression analysis of binding data using Graphpad Prism software version 4.00 (San Diego, CA). Data obtained after regression analysis were used to plot graphs with the GRAFIT program version 3.09b (Erithacus Software, Surrey, U.K.).

Estimation of cyclic AMP content in cells

The ability of ligands to affect the forskolin-stimulated increase in cAMP levels in cells was assessed as described below. CHO-5-HT_{1A}R cells were plated at a density of 1×10^4 cells per well of a 24-well plate and grown for 4 days in culture under conditions as described earlier. Cells were rinsed with PBS and incubated with forskolin (20 μ M) and phosphodiesterase inhibitor IBMX (50 μ M) in the presence of increasing concentrations of 8-OH-DPAT at 37 °C for 30 min in serum-free DMEM medium. The assay was terminated by adding lysis buffer (10 mM Tris, 5 mM EDTA, pH 7.4 buffer) to the cells. Cell lysates were boiled for 3 min and spun at 50,000 g for 10 min to remove precipitated protein. The amount of cAMP in an aliquot of the supernatant was estimated using the cyclic [³H]AMP assay system which is based on the protein binding method described previously (Nordstedt and Fredholm, 1990). Agonist dependent dose-response curves were analyzed according to the 4 parameter logistic function.

The ability of agonists such as 8-OH-DPAT to affect the forskolin-stimulated increase in cAMP levels in CHO-5-HT_{1A}R cells was assessed as described earlier (Paila and Chattopadhyay, 2006). The amount of cAMP in an aliquot of the supernatant was estimated using the cyclic [³H]AMP assay system which is based on the protein binding method

described previously (Norstedt and Fredholm, 1990). Agonist dependent dose-response curves were analyzed according to the four parameter logistic function using equation 1.

GTP- γ -S sensitivity assay

In experiments with GTP- γ -S, agonist binding assays were carried out as described in section 2.2.

Fluorescence anisotropy measurements

Fluorescence anisotropy experiments were carried out using the fluorescent probe DPH with membranes prepared from cells that were treated with varying concentrations of AY 9944, containing 50 nmol of total phospholipids suspended in 1.5 ml of 50 mM Tris, pH 7.4 buffer, as described earlier (Paila *et al.*, 2005) and in section 2.2. Fluorescence anisotropy (r) values were calculated from the equation (Lakowicz, 2006):

$$r = \frac{I_{VV} - GI_{VH}}{I_{VV} + 2GI_{VH}} \quad (4)$$

where I_{VV} and I_{VH} are the measured fluorescence intensities (after appropriate background subtraction) with the excitation polarizer vertically oriented and the emission polarizer vertically and horizontally oriented, respectively. G is the grating correction factor and is the ratio of the efficiencies of the detection system for vertically and horizontally polarized light and is equal to I_{HV}/I_{HH} . All experiments were done with multiple sets of samples and average values of fluorescence anisotropy are shown in Figure 3.7.

Metabolic replenishment of cholesterol with serum

After treatment with 5 μ M AY 9944, CHO-5-HT_{1A}R cells were grown for 3 days in D-MEM/F-12 (1:1) supplemented with 2.4 g/l of sodium bicarbonate, 10% fetal calf serum,

60 µg/ml penicillin, 50 µg/ml streptomycin, 50 µg/ml gentamycin sulfate, and 200 µg/ml geneticin in a humidified atmosphere with 5% CO₂ at 37 °C to achieve metabolic replenishment of cholesterol.

Western blot analysis

Cell membranes were prepared from CHO-5-HT_{1A}R-EYFP (control), AY 9944 treated and cholesterol-replenished cells as previously described earlier (Paila and Chattopadhyay, 2006) and in this section with an addition of 1:20 dilution of freshly added protease inhibitor cocktail (Roche Applied Science, Mannheim, Germany). Total protein (60 µg) from each sample was mixed with 1:4 v/v of 4x electrophoresis sample buffer and boiled for 30 min at 37 °C. Sample mixtures were loaded and separated on 10% SDS-PAGE.

After electrophoresis, gel proteins were electrophoretically transferred to a nitrocellulose membrane (Hybond ECL, Amersham Pharmacia Biotech, Little Chalfont, U.K.) using semi-dry transfer apparatus (Amersham Pharmacia Biotech, Little Chalfont, U.K.). The non specific binding sites were blocked with 10% fat-free dry milk in PBS/Tween 20, pH 7.4 for 1 h at room temperature. To monitor the expression of 5-HT_{1A}R-EYFP, blots were probed with antibodies raised against GFP (BD Biosciences, San Jose, CA; 1:10000 dilution in PBS/Tween 20), incubated overnight at 4 °C. To monitor the levels of β-actin, which acts as a loading control, membranes were probed with antibodies raised against β-actin (Chemicon International, Temecula, CA; diluted 1:800 in PBS/Tween 20), incubated overnight at 4 °C. Membranes were washed with PBS/Tween 20 (washing buffer) for 30 min and the wash buffer was changed every 10 min. Membranes were then incubated with 1:4000 dilution of a secondary antibody (horseradish peroxidase conjugated-anti-mouse antibody) in PBS/Tween 20 for 1 h at room temperature. Membranes were then washed and developed using the enhanced chemiluminescence detection reagents (Amersham Biosciences, Buckinghamshire, U.K.). 5-HT_{1A}R-EYFP and β-actin were

detected using the chemiluminescence detection system (Chemi-Smart 5000, Vilber Lourmat). 5-HT_{1A}R-EYFP and β -actin levels were quantitated using Bio-Profile (Bio-ID++, version 11.9).

Statistical analysis

Significance levels were estimated using student's two-tailed paired *t*-test using Microcal Origin software version 5.0 (OriginLab Corp., Northampton, MA).

3.3. Results

Cell viability upon AY 9944 treatment

Viability of CHO-5-HT_{1A}R cells was estimated upon treatment with increasing concentration of AY 9944 and shown in figure 3.2. The figure shows that cell viability was not affected upto 5 μ M AY 9944. At the highest concentration of AY 9944 used (10 μ M), there was ~30% reduction in cell viability.

Quantification of sterols using gas chromatography-mass spectrometry (GC-MS)

With an overall goal of addressing lipid-protein interactions in healthy and diseased states, we developed a cellular model of SLOS using AY 9944, a specific metabolic inhibitor of 7-DHCR, on CHO-5-HT_{1A}R cells (see Figure 3.1 for more details). Sterols (cholesterol, 7-DHC and 8-DHC) were separated, identified and quantitated using GC-MS (Figures 3.3 and 3.4). 7-DHC content in control cells was below the detection level. We observed an increase in 7-DHC content up to 2.5 μ M of AY 9944 (see Figure 3.4a), beyond which an additional peak appeared (Figure 3.3c). This peak was identified as 8-DHC (Figures 3.3c and d), a positional isomer of 7-DHC (see Figure 3.1).

The identities of the trimethylsilyl ethers of the compounds were established by comparison with authentic standards for cholesterol and 7-DHC. The peak for 8-DHC was identified using its mass spectra reported earlier (Lindenthal *et al.*, 2001; Wolf *et al.*, 1996). Importantly, the ratios of sterols generated using AY 9944 in these cases (see Figure 3.4) were comparable to the ratios reported in SLOS patients (Elias *et al.*, 2003; Lin *et al.*, 2005; Scalco *et al.*, 2003). It should be mentioned here that we estimated phospholipid contents under identical conditions by performing lipid phosphate assays. The change in phospholipid content was found to be negligible, even when the highest concentration of AY 9944 was used.

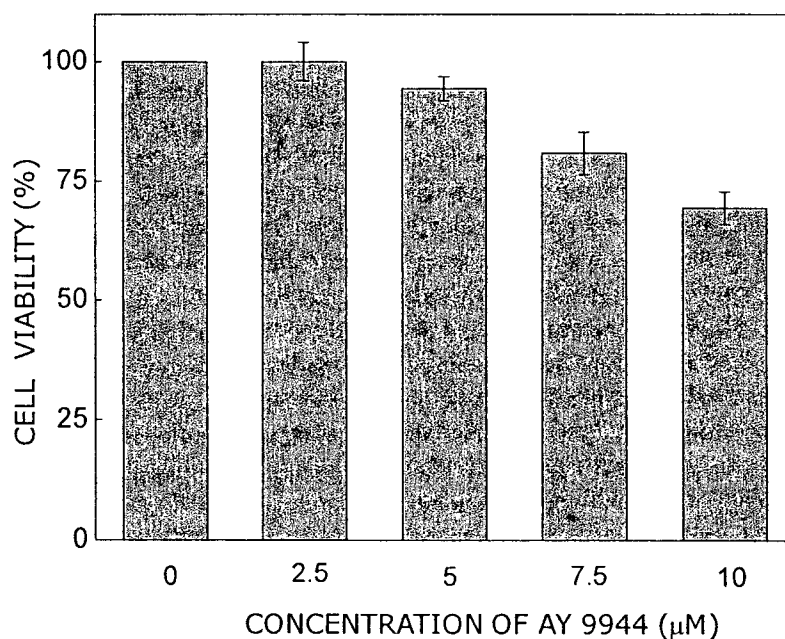


Figure 3.2. Viability of CHO-5-HT_{1A}R cells upon treatment with AY 9944. Cell viability was estimated using MTT assay. Data shown are means \pm SE of at least three independent measurements. See section 3.2 for other details.

Ligand binding activity of the human serotonin_{1A} receptor is reduced in SLOS-like condition

Since SLOS is associated with neurological deformities and malfunction, exploring the function of neuronal receptors and their membrane lipid interactions under these

conditions assumes significance. We explored the ligand binding function of the human serotonin_{1A} receptor under SLOS-like condition. Figure 3.5a shows the effect of AY 9944 treatment on specific [³H]8-OH-DPAT binding to serotonin_{1A} receptors in CHO-5-HT_{1A}R

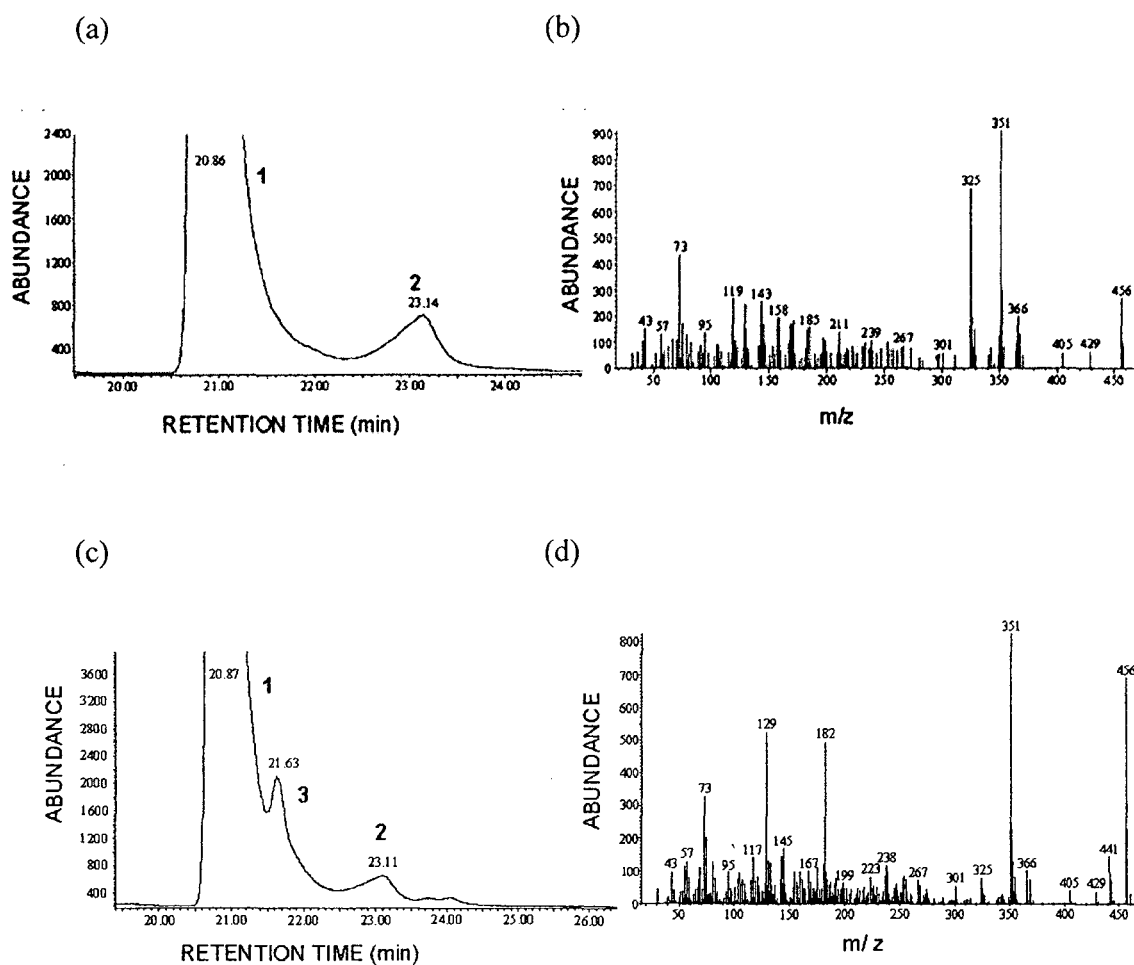


Figure 3.3. Identification of sterols. Panels (a) and (c) show representative selected ion chromatograms of sterols obtained from total lipid extracts from membranes of CHO-5-HT_{1A}R cells treated with AY 9944. An additional peak (besides 7-DHC) was observed for concentrations beyond 2.5 μ M of AY 9944. This was identified as 8-DHC, a positional isomer of 7-DHC. Peaks 1, 2 and 3 correspond to cholesterol, 7-DHC and 8-DHC, respectively. Panels (b) and (d) show the mass spectra of 7-DHC and 8-DHC. 8-DHC has a shorter retention time compared to 7-DHC. The distinctive patterns of m/z ratios of 7-DHC and 8-DHC are shown in panels (b) and (d).

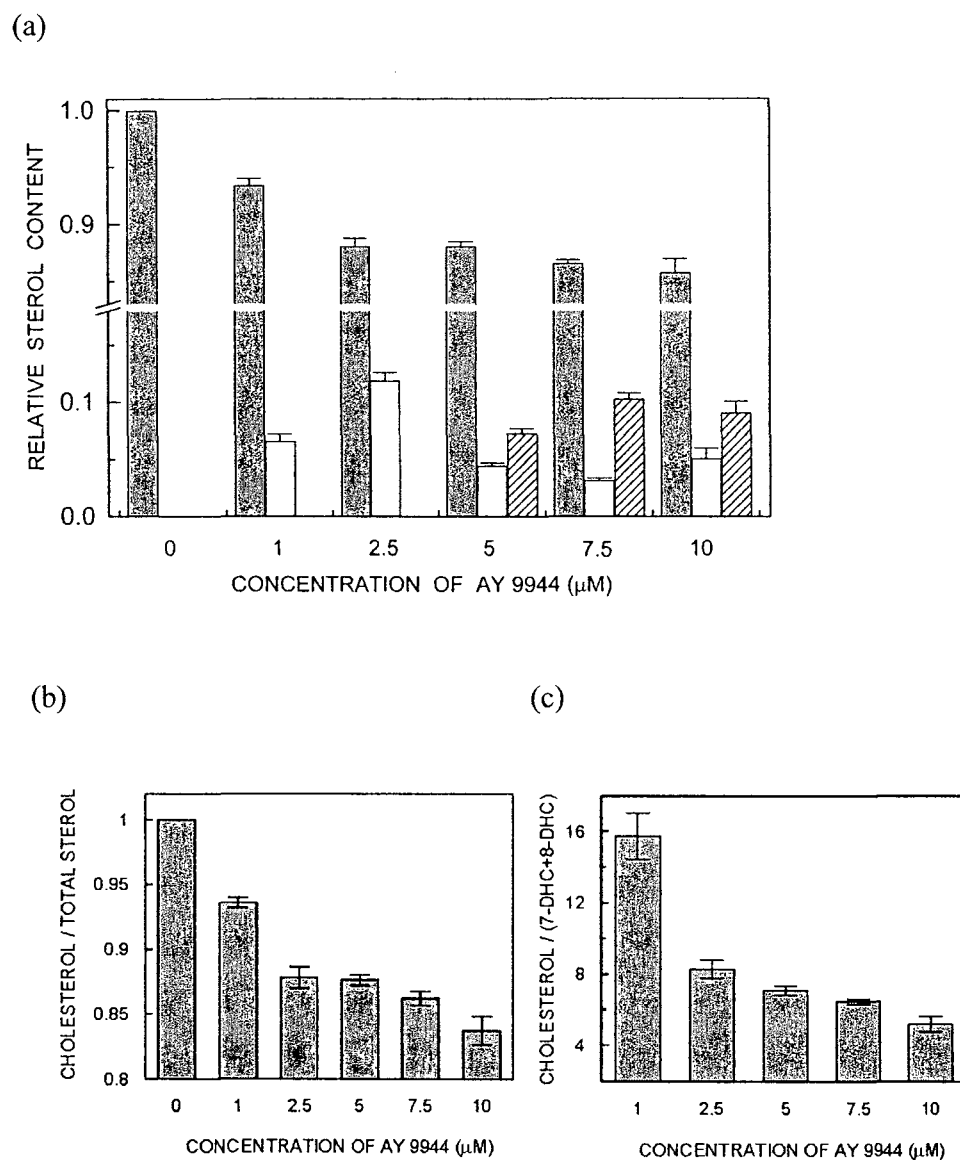


Figure 3.4. Quantitation of sterols in membranes from CHO-5-HT_{1A}R cells treated with AY 9944. Effect of increasing concentrations of AY 9944 on sterol content of membranes from CHO-5-HT_{1A}R cells. Cholesterol and 7-DHC were identified with authentic standards. 8-DHC was identified using its mass spectra reported earlier (Wolf *et al.*, 1996; Elias *et al.*, 2003). Sterols were separated and quantitated using GC-MS analysis. Panel (a) shows the relative contents of membrane cholesterol (gray bars), 7-DHC (open bars) and 8-DHC (hatched bars) from CHO-5-HT_{1A}R cells treated with increasing concentrations of AY 9944 used, and normalized to total sterol (cholesterol + 7-DHC + 8-DHC) content. The cell membrane cholesterol to total sterol ratio is shown in (b). The ratio of cholesterol to total sterol was normalized to control cells. The ratio between cholesterol and total dehydrocholesterol (7-DHC + 8-DHC) is shown in (c). Data represent means \pm SE of at least three independent experiments. See section 3.2 for other details.

cells. As shown in the figure, there is a progressive and drastic reduction in the specific [³H]8-OH-DPAT binding with increasing concentrations of AY 9944 used. The reduction in agonist binding correlates well with the reduction in ratio between cholesterol to total sterol as well as the cholesterol to dehydrocholesterol ratio (shown in Figures 3.4b and c). The agonist binding of the human serotonin_{1A} receptor is reduced to ~8% of the original value upon treatment with 10 μM AY 9944. Importantly, the reduction in agonist binding is not due to a decrease in the expression level of the human serotonin_{1A} receptor (see later, Figure 3.9). Although the requirement of membrane cholesterol in maintaining the ligand binding activity of the serotonin_{1A} receptor has previously been reported by our group (Pucadyil and Chattopadhyay, 2004a), this result represents the first observation that defective cholesterol biosynthesis could result in loss of specific agonist binding to the serotonin_{1A} receptor.

The saturation binding analysis of the specific agonist [³H]8-OH-DPAT binding to serotonin_{1A} receptors is shown in Figure 3.5b. The results of saturation binding analysis with the agonist [³H]8-OH-DPAT, carried out with membranes prepared from AY 9944 treated and control cells, revealed that the reduction in ligand binding can primarily be attributed to a reduction in the number of total binding sites with a marginal reduction in the affinity of ligand binding. There is a significant reduction (~26%, $p < 0.02$) in the maximum number of binding sites (B_{max}) when the CHO-5-HT_{1A}R cells were treated with 5 μM AY 9944.

Ligand-dependent downstream signaling efficiency of the human serotonin_{1A} receptor is reduced in SLOS-like condition

Most of the seven transmembrane domain receptors are coupled to G-proteins, and therefore guanine nucleotides are known to modulate ligand binding. The serotonin_{1A} receptor agonists such as 8-OH-DPAT are known to specifically activate the G_i/G_o class of G-proteins in CHO cells (Raymond *et al.*, 1993). Agonist binding to such receptors

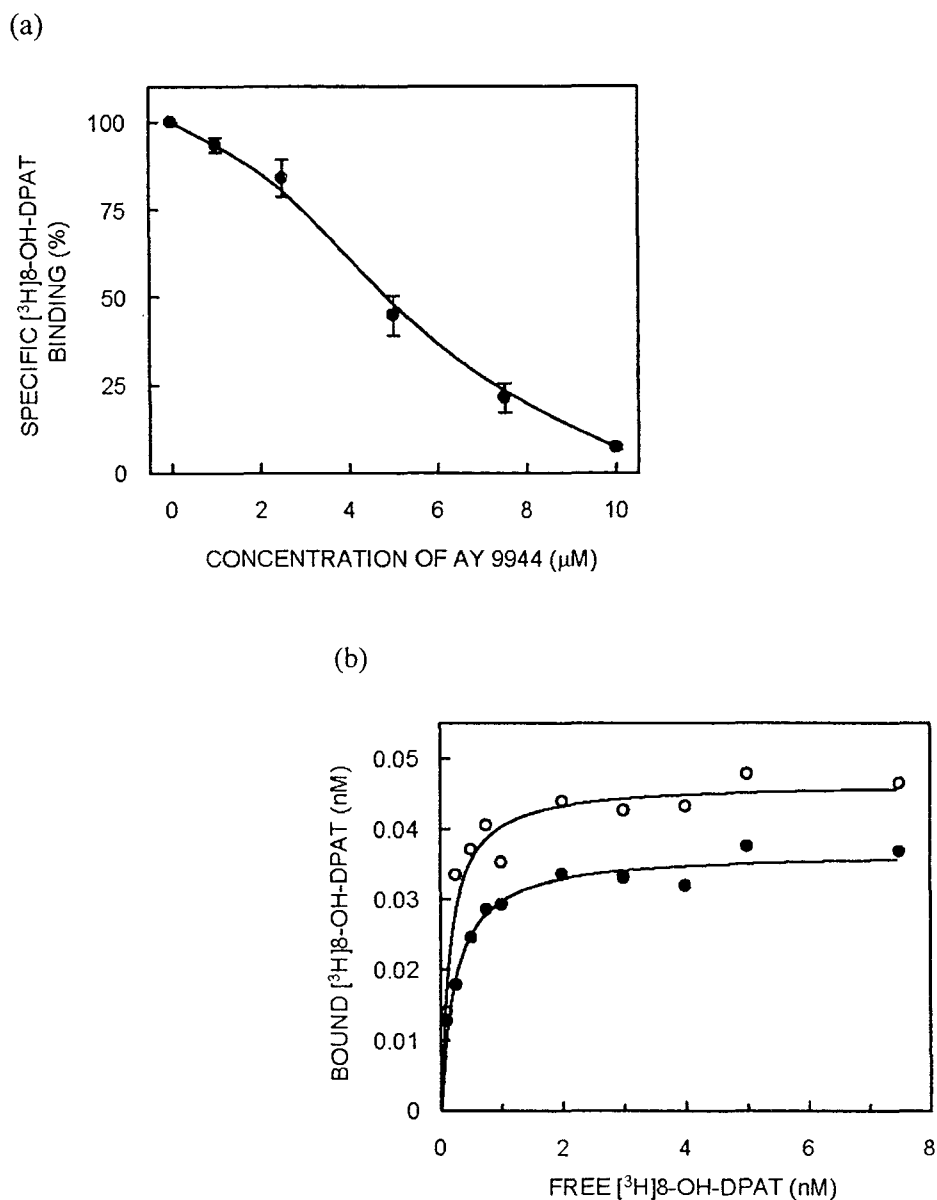


Figure 3.5. Ligand binding function of the human serotonin_{1A} receptor is inhibited in cellular model of SLOS. CHO-5-HT_{1A}R cells were treated with varying concentrations of AY 9944 and specific [³H]8-OH-DPAT binding to the serotonin_{1A} receptor was measured (shown in panel a). The concentration of [³H]8-OH-DPAT in each assay tube was 0.29 nM. Values are expressed as a percentage of specific binding for control cell membranes without AY 9944 treatment. Data shown are means ± SE of at least three independent experiments. Panel (b) shows saturation binding analysis of specific [³H]8-OH-DPAT binding to serotonin_{1A} receptors from CHO-5-HT_{1A}R cell membranes in control (O) cells and in cells treated with 5 μM AY 9944 (●). Representative plots are shown for specific [³H]8-OH-DPAT binding with increasing concentrations (0.1-7.5 nM) of [³H]8-OH-DPAT under these conditions. The curves are non-linear regression fits to the experimental data using Graphpad Prism software. See section 3.2 for other details.

Table 3.1

Parameters for [³H]8-OH-DPAT binding in control cells and cells treated with AY 9944

| | K _d (nM) | B _{max} (pmol/mg of protein) |
|-----------------|------------------------|--|
| Control | 0.26 ± 0.04 | 0.65 ± 0.03 |
| AY 9944 treated | 0.29 ± 0.02 | 0.48 ± 0.03 |

Binding parameters were calculated by analyzing saturation binding isotherms with a range (0.1-7.5 nM) of the radioligand using Graphpad Prism software. Data shown in the table represent means ± SE of three independent experiments. Concentration of AY 9944 used was 5 μM. See section 3.2 for other details.

therefore displays sensitivity to agents such as GTP-γ-S, a non-hydrolyzable analogue of GTP, that uncouple the normal cycle of guanine nucleotide exchange at the Gα subunit caused by receptor activation. We have previously shown that in the presence of GTP-γ-S, serotonin_{1A} receptors undergo an affinity transition, from a high affinity G-protein coupled to a low-affinity G-protein uncoupled state (Harikumar and Chattopadhyay, 1999). In agreement with these results, Figure 3.6a shows a characteristic reduction in binding of the agonist [³H]8-OH-DPAT in the presence of a range of concentrations of GTP-γ-S with an estimated half maximal inhibition concentration (IC₅₀) of 3.75 nM for control cells. The inhibition curve in case of cells treated with AY 9944 displays a significant (~2.5-fold, *p*<0.03) shift toward higher concentrations of GTP-γ-S with an increased IC₅₀ value of 9.92 nM. This implies that the agonist binding to the serotonin_{1A} receptor in SLOS-like condition is less sensitive to GTP-γ-S indicating that the G-protein coupling efficiency is reduced under these conditions. This suggests a possible perturbation of receptor-G-protein interaction in SLOS-like condition.

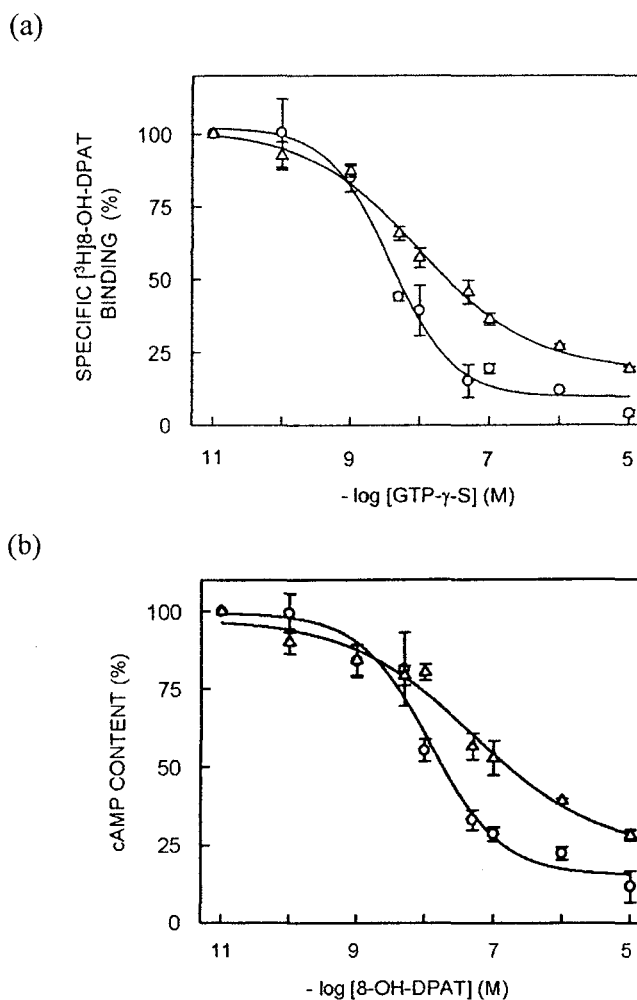


Figure 3.6. Reduced downstream signaling of the human serotonin_{1A} receptor in SLOS-like condition. The downstream signaling efficiency of the serotonin_{1A} receptor was monitored by the sensitivity of [³H]8-OH-DPAT binding to GTP-γ-S and cyclic AMP levels. Panel (a) shows the effect of increasing concentrations of GTP-γ-S on the specific binding of the agonist [³H]8-OH-DPAT to serotonin_{1A} receptors in control cells (O) and in cells treated with 5 μM AY 9944 (Δ). Values are expressed as percentages of the specific binding obtained at the lowest concentration of GTP-γ-S. The curves are non-linear regression fits to the experimental data using equation 1. The data points represent means ± SE of duplicate points from at least three independent experiments. See section 3.2 for other details. Panel (b) shows the estimation of cAMP levels in CHO-5-HT_{1A}R cells. The ability of the specific agonist (8-OH-DPAT) to reduce the forskolin-stimulated increase in cAMP levels in control cells (O) and in cells treated with 5 μM AY 9944 (Δ) was assessed. cAMP levels in cells were estimated as described in section 3.2. The curves are non-linear regression fits to the experimental data using equation 1. Data are normalized to cAMP levels present at the lowest concentration of 8-OH-DPAT used in the experiment and represent the means ± SE of duplicate points from at least three independent experiments. See section 3.2 for other details.

In addition to ligand binding properties, we monitored the function of serotonin_{1A} receptors in CHO-5-HT_{1A}R cells by measuring its ability to catalyze downstream signal transduction processes upon stimulation with the specific agonist, 8-OH-DPAT. Serotonin_{1A} receptor agonists such as 8-OH-DPAT are known to specifically activate the G_i/G_o class of G-proteins in CHO cells, which subsequently reduce cAMP levels in cells (Raymond *et al.*, 1993). As shown in Figure 3.6b, the forskolin-stimulated increase in cAMP levels is inhibited by 8-OH-DPAT with a half maximal inhibition concentration (IC₅₀) of 11.97 nM in control cells. In cells treated with AY 9944, the IC₅₀ value is increased to a considerable extent (~4-fold, $p < 0.13$) to 50.68 nM. This points out that the downstream signaling efficiency of the human serotonin_{1A} receptor is considerably reduced under this condition.

Reduction in the function of the human serotonin_{1A} receptor in SLOS-like condition is independent of the overall membrane order

In order to explore any possible change in overall membrane order upon AY 9944 treatment, we measured the fluorescence anisotropy of the fluorescent probe DPH. Fluorescence anisotropy measured using probes such as DPH is correlated to the rotational diffusion of membrane embedded probes (Lakowicz, 2006), which is sensitive to the packing of lipid fatty acyl chains. This is due to the fact that fluorescence anisotropy depends on the degree to which the probe is able to reorient after excitation, and probe reorientation is a function of local lipid packing. DPH, which is a rod-like hydrophobic molecule, partitions into the interior (fatty acyl chain region) of the bilayer. Figure 3.7 shows the effect of increasing concentrations of AY 9944 on the fluorescence anisotropy of the membrane probe DPH incorporated into CHO-5-HT_{1A}R cell membranes. The fluorescence anisotropy of DPH appears to be more or less invariant over the concentration range of AY 9944 used. These results therefore suggest that the overall (global) membrane order is not significantly altered in SLOS-like condition and changes in ligand binding activity and downstream signaling could be due to specific (local) effects (see later).

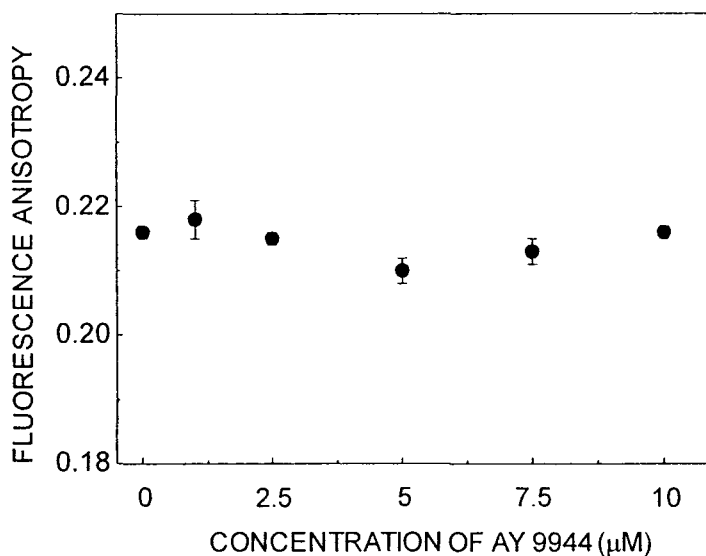


Figure 3.7. Overall membrane order is unaltered in SLOS-like condition. The overall (average) membrane order was estimated in control cell membranes and in membranes of cells treated with varying concentrations of AY 9944, using fluorescence anisotropy of the membrane probe DPH. Fluorescence anisotropy measurements were carried out with membranes containing 50 nmol phospholipid at a probe to phospholipid ratio of 1:100 (mol/mol) at room temperature (~23 °C). Data represent means \pm SE of duplicate points from at least three independent experiments. See section 3.2 for other details.

Metabolic cholesterol replenishment restores the ligand binding activity of the human serotonin_{1A} receptor

Treatment of SLOS consists of reduction of 7-DHC levels on one hand, and to supplement deficient cholesterol, on the other hand. This is generally achieved by providing supplemental cholesterol in the diet (Battaile and Steiner, 2000; Porter, 2000; Kelley and Hennekam, 2000). This is due to the fact that the supplemented dietary cholesterol would reduce cholesterol precursors by feedback inhibition of HMG-CoA reductase. In order to check the reversibility of the changes induced by AY 9944 (*i.e.*, reduction of cholesterol and accumulation of dehydrocholesterol) in SLOS-like condition in CHO-5-HT_{1A}R cells, we performed metabolic replenishment with serum cholesterol. This was carried out by incubating cells treated with AY 9944 for 3 days in serum (see section 3.2). Under these conditions, a significant ($p < 0.01$) fraction of cholesterol could be

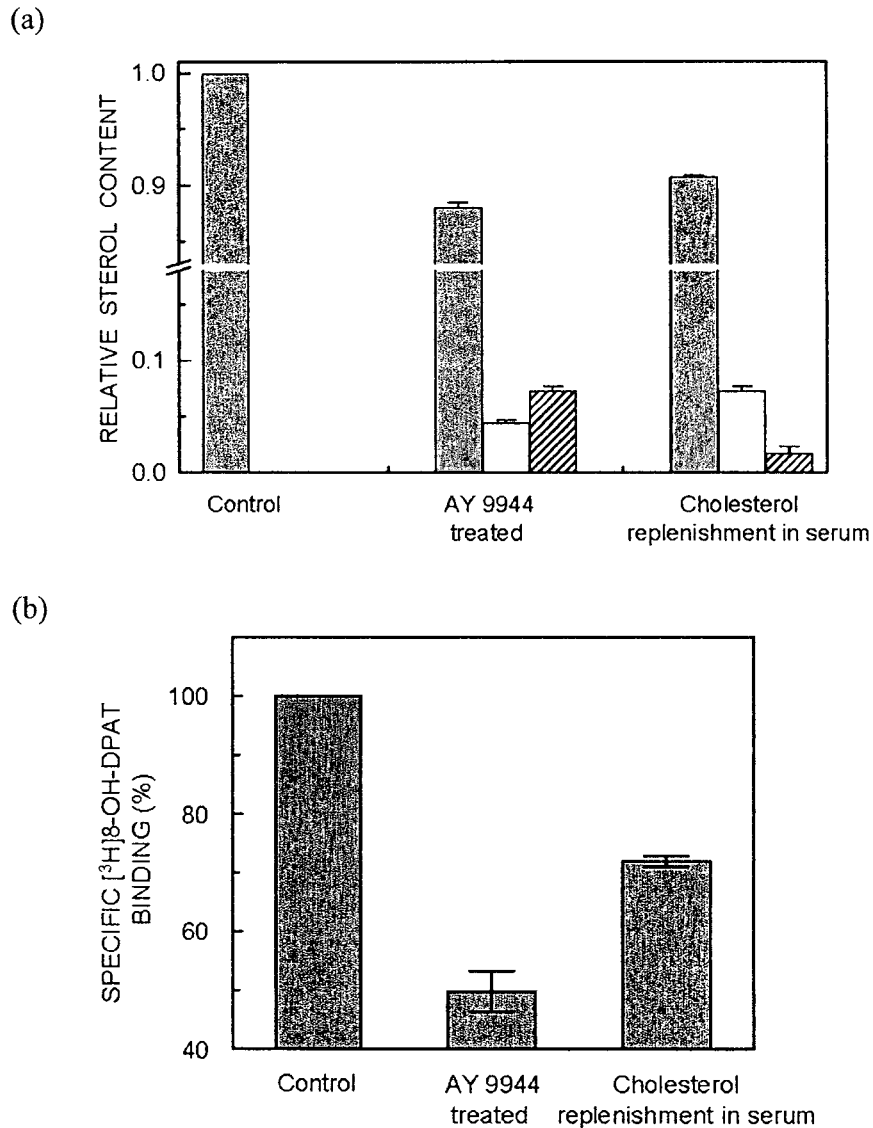


Figure 3.8. Metabolic replenishment of cholesterol with serum. After treatment with 5 μ M AY 9944, CHO-5-HT_{1A}R cells were allowed to recover by metabolic replenishment with serum cholesterol. Following AY 9944 treatment, cells were grown for 3 days in D-MEM/F-12 (1:1) medium (supplemented with 2.4 g/l of sodium bicarbonate, 10% fetal calf serum, 60 μ g/ml penicillin, 50 μ g/ml streptomycin, 50 μ g/ml gentamycin sulfate, and 200 μ g/ml geneticin) in a humidified atmosphere with 5% CO₂ at 37 °C, sterols were extracted from cell membranes and quantified using GC-MS. Panel (a) shows the relative contents of membrane cholesterol (gray bars), 7-DHC (open bars) and 8-DHC (hatched bars) in control (without AY 9944 treatment) cells, AY 9944 treated cells and cells in which cholesterol was metabolically replenished. The relative sterol contents are normalized to total sterol (cholesterol + 7-DHC + 8-DHC) content. The corresponding changes in the specific binding of the agonist [³H]8-OH-DPAT to serotonin_{1A} receptors under these conditions are shown in (b). See section 3.2 for other details.

restored, along with a concomitant reduction in 8-DHC levels, and an overall decrease in combined dehydrocholesterol levels (Figure 3.8a), resulting in significant ($p < 0.01$) recovery of the ligand binding activity (see Figure 3.8b).

The expression level of the serotonin_{1A} receptor is not reduced in SLOS-like condition

The impaired ligand binding activity and signaling of the human serotonin_{1A} receptor observed in SLOS-like condition could be due to reduced expression levels of serotonin_{1A} receptors. In order to explore this possibility, we performed Western blot analysis of 5-HT_{1A}R-EYFP in cell membranes prepared from control, AY 9944 treated and cholesterol replenished CHO-5-HT_{1A}R-EYFP cells (see Figure 3.9). For these experiments, we chose to use the receptor tagged to EYFP (5-HT_{1A}R-EYFP) since no monoclonal antibodies for the serotonin_{1A} receptor are available yet, and the polyclonal antibodies have been reported to give variable results on Western blots (Zhou *et al.*, 1999). We have earlier shown that EYFP fusion to the serotonin_{1A} receptor does not affect the ligand binding properties, G-protein coupling and signaling functions of the receptor (Pucadyil *et al.*, 2004a). Figure 3.9b shows that the levels of the serotonin_{1A} receptor in membranes are not reduced in SLOS-like condition. The receptor level is slightly increased (~1.4-fold compared to control) following AY 9944 treatment. This increase, however, was found to be not significant ($p > 0.05$). After metabolic replenishment with serum cholesterol, the receptor level increased to ~1.6-fold. It has been previously reported that serotonin_{1A} receptor levels in CHO cells could increase upon induction of stress (Singh *et al.*, 1996).

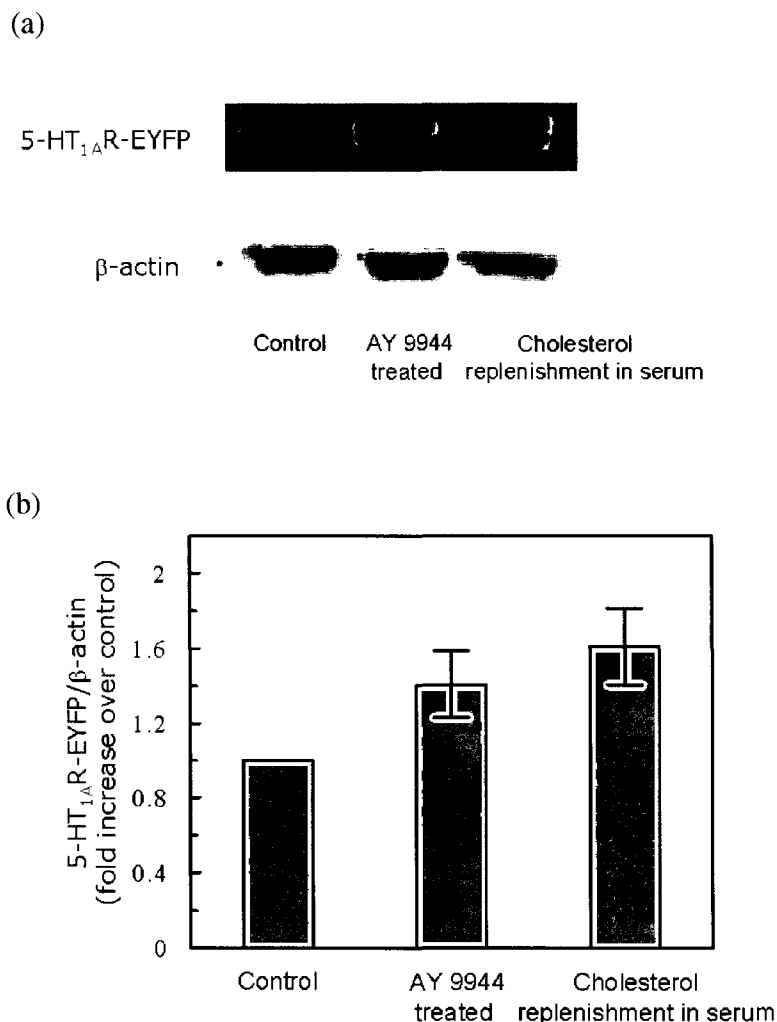


Figure 3.9. The expression level of the human serotonin_{1A} receptor is not reduced in membranes of cellular model of SLOS. Western blot analysis of 5-HT_{1A}R-EYFP in membranes prepared from CHO-5-HT_{1A}R-EYFP (control) cells, CHO-5-HT_{1A}R-EYFP cells treated with 5 μM AY 9944 and after metabolic replenishment with serum cholesterol. Panel (a) shows the human serotonin_{1A} receptor tagged to EYFP with corresponding β-actin probed with antibodies directed against GFP and β-actin. Panel (b) shows the quantitation of 5-HT_{1A}R-EYFP and β-actin levels using densitometry. 5-HT_{1A}R-EYFP levels were normalized to β-actin of the corresponding sample. Data are shown as fold increase of 5-HT_{1A}R-EYFP over control and represent means ± SE of at least four independent experiments. See section 3.2 for other details.

3.4. Discussion

SLOS is a congenital and developmental malformation syndrome associated with defective cholesterol biosynthesis. Patients diagnosed with SLOS typically show growth and mental retardation, microcephaly, cleft palate, syndactyly, urogenital abnormalities, and a variety of other anatomical defects. SLOS is clinically characterized by reduced levels of plasma cholesterol coupled with accumulation of 7- and 8-DHC. Learning disabilities and mental retardation are present in at least 95% of SLOS patients (Porter, 2000) which could be attributed to impaired neurotransmission. The relationship between clinical severity and biochemical parameters in SLOS is an ongoing area of research. It has been previously reported that reduced cholesterol levels are associated with increased clinical severity, while the correlation between 7-DHC and clinical severity is weak (Cunniff *et al.*, 1997). These results are supported using SLOS animal model, which shows that cholesterol deficit but not accumulation of precursor sterols, is the major cause of abnormal embryogenesis in SLOS (Gaoua *et al.*, 2000). Importantly, cholesterol is an essential lipid in this context since a number of neurological diseases share a common etiology of defective cholesterol metabolism in the brain (Porter, 2002). As mentioned earlier, we have previously shown the requirement of membrane cholesterol in the function of the serotonin_{1A} receptor (Pucadyil and Chattopadhyay, 2004a; 2006). Based on this evidence, it appears that reduction in cholesterol levels could contribute to the impairment of function of the serotonin_{1A} receptor under SLOS-like condition, although effects of accumulation of dehydrocholesterol may not be ruled out.

Serotonin_{1A} receptors are members of a superfamily of seven transmembrane domain receptors (Perez, 2003) that couple to and transduce signals via G-proteins (Pucadyil *et al.*, 2005a; Kalipatnapu and Chattopadhyay, 2007a). The effect of metabolic inhibition of cholesterol biosynthesis on the function of the human serotonin_{1A} receptor in CHO-5-HT_{1A}R cells was monitored. These results show that ligand binding activity, G-

protein coupling and downstream signaling of serotonin_{1A} receptors are impaired in SLOS-like condition. The potential clinical relevance of this observation stems from the fact that defective cholesterol biosynthesis constitutes a common theme for a number of genetically inherited disorders (Waterham, 2006). These results assume greater significance in the light of recent findings that symptoms of anxiety and major depression are apparent in humans upon long term administration of statins which are inhibitors of the first enzyme (HMG-CoA reductase) in the cholesterol biosynthesis pathway (Papakostas *et al.*, 2004). Interestingly, SLOS carriers have been reported to be at greater risk of suicidal behavior (Lalovic *et al.*, 2004) and a recent study has shown that serotonin_{1A} receptors play a key role in the biology of suicidal behavior (Pichot *et al.*, 2005).

Importantly, our results show that the receptor level is not reduced under this condition. This implies that the fraction of functional receptors is reduced upon AY 9944 treatment resulting in a higher fraction of non-functional receptors. Interestingly, these results could be related to an earlier report describing abnormal development of serotonergic neurons in SLOS mouse model (Waage-Baudet *et al.*, 2003). In addition, modulation of serotonergic transmission has been implicated in cholesterol-lowering therapy (Vevera *et al.*, 2005). Our results assume significance in the light of the fact that SLOS patients suffer from impaired neurotransmission. It should be mentioned here that although we have monitored the levels of membrane sterols and clinical reports from patient samples rely on plasma sterols, it has been earlier reported that modulation of membrane and plasma sterols are positively correlated (Lijnen *et al.*, 1996). Based on our results, it could be possible that the function of serotonin_{1A} receptors is reduced in SLOS patients, since the membrane sterol levels we obtained match well with reported serum sterol levels in SLOS patients (Elias *et al.*, 2003; Lin *et al.*, 2005; Scalco *et al.*, 2003). Clearly, further work is needed in this area to support this hypothesis.

The effect of cholesterol on the structure and function of integral membrane proteins has been a subject of intense investigation (see chapter 1). We have earlier shown that

oxidation of membrane cholesterol with cholesterol oxidase leads to inhibition of the ligand binding activity of the serotonin_{1A} receptor (Pucadyil *et al.*, 2005b). In the present work, we have utilized a cellular model of SLOS in order to delineate the specific and global effects of cholesterol in the function of the serotonin_{1A} receptor. SLOS serves as an appropriate condition to test this since the two aberrant sterols that get accumulated in SLOS, i.e., 7- and 8-DHC, differ with cholesterol only in a double bond. Our results show that the overall membrane order, as monitored with the fluorescent probe DPH, does not exhibit significant change in SLOS-like condition (Figure 3.7). Interestingly, we have recently shown that 7-DHC does not support the function of the serotonin_{1A} receptor without any change in overall membrane order (Singh *et al.*, 2007). We therefore conclude that the requirement for maintaining ligand binding activity is more stringent than the requirement for maintaining membrane order. Taken together, these results indicate that the molecular basis for the requirement of membrane cholesterol in maintaining the ligand binding activity of serotonin_{1A} receptors could be specific interaction, although global bilayer effects may not be ruled out (Prasad *et al.*, 2009).

Cholesterol is often found distributed non-randomly in domains in biological membranes (See chapter 1). It would be interesting to compare to what extent 7- and 8-DHC could mimic cholesterol in this regard. It has been previously reported using a number of approaches that membrane domains formed by 7-DHC differ with those formed by cholesterol in protein composition (Keller *et al.*, 2004), packing (Berring *et al.*, 2005) and stability (Wolf and Chachaty, 2000; Wolf *et al.*, 2001; Megha *et al.*, 2006). In addition, model membranes mimicking SLOS membranes have been reported to exhibit atypical membrane organization (Tulenکو *et al.*, 2006) and curvature (Gondre-Lewis *et al.*, 2006). It is therefore possible that mere replacement of cholesterol with 7-DHC may significantly affect aspects of membrane organization such as near neighbor interactions (7-DHC is more polar than cholesterol) and accessible surface area. Interestingly, it has been reported that

the activity of inward-rectifier K⁺ channels is modulated even by optical isomers of cholesterol thereby exemplifying the specificity of interaction (Romanenko *et al.*, 2002).

Dietary cholesterol has been proposed as a potential therapy in the treatment of SLOS and currently a lot of research is focused on developing a formula as food supplement for SLOS patients (Lin *et al.*, 2005). We have metabolically replenished cholesterol in cells pre-treated with AY 9944 with serum and found that the ligand binding activity of the human serotonin_{1A} receptor could be recovered to a significant extent (Figure 3.8b). Metabolic replenishment of cholesterol is relevant since the only feasible treatment for SLOS patients is regular intake of dietary cholesterol. It has been reported earlier that administration of dietary cholesterol can partially reverse some of the behavioral abnormalities (Kelley and Hennekam, 2000). It is possible that the impaired function of receptors such as the serotonin_{1A} receptor in SLOS patients could be regained to some extent after cholesterol administration. Taken together, our results could be potentially useful in understanding the molecular basis that underlie the pathophysiology of this disorder and could provide novel insight in formulating future treatment for the disease.

Chapter 4

Metabolic depletion of sphingolipids impairs
ligand binding and signaling functions of the
human serotonin_{1A} receptor

4.1. Introduction

Sphingolipids are essential and indispensable components of eukaryotic cell membranes and constitute 10-20% of the total membrane lipids (Holthius *et al.*, 2001). Sphingolipids are thought to be involved in the regulation of cell growth, differentiation, and neoplastic transformation through participation in cell-cell communication, and possible interaction with receptors and signaling systems. Sphingolipids such as sphingomyelin are regarded as reservoirs for second messengers such as sphingosine, ceramide and sphingosine 1-phosphate (Merrill *et al.*, 1996). Sphingolipids are abundant in the plasma membrane compared to intracellular membranes. Their distribution in the bilayer appears to be heterogeneous, and it has been postulated that sphingolipids and cholesterol occur in laterally segregated lipid domains (sometimes termed as 'lipid rafts') (Brown, 1998; Masserini and Ravasi, 2001; Mukherjee and Maxfield, 2004; see chapter 1).

Ceramide is at the center of sphingolipid metabolism and has been recognized as a critical second messenger (Hannun and Obeid, 2002). Ceramide levels can reach up to 10 mol% of the total phospholipids (Hannun, 1996) emphasizing its role as a signaling molecule. Furthermore, the formation of ceramide upon stimulation occurs in restricted cellular sites, and the local concentration of ceramide has been estimated to exceed 25 mol% (Holopainen *et al.*, 2000). The pool of ceramide is maintained by *de novo* synthesis. The cellular levels of ceramide and sphingomyelin can be modulated using compounds such as fumonisins. Fumonisins have been extensively used to explore functions of ceramides, sphingomyelin and complex sphingolipids (Desai *et al.*, 2002). Fumonisins are a group of naturally occurring mycotoxins, which are ubiquitous contaminants of corn and other grain products, produced by *Fusarium verticelloides* and several other *Fusarium* species (Gelderblom *et al.*, 1988; Marasas, 1996). There are at least 14 known fumonisins of which fumonisin B₁ (FB₁) is the most abundant (Dragan *et al.*, 2001). FB₁ is structurally similar to sphingoid bases such as sphinganine and sphingosine (see Figure 4.1), which are

intermediates in sphingolipid metabolism, and an important site of inhibition is the reaction catalyzed by sphinganine *N*-acetyltransferase (ceramide synthase) (Wang *et al.*, 1991). Consumption of FB₁ through contaminated corn has been reported to induce neurotoxicity (Desai *et al.*, 2002; Gelderblom *et al.*, 1992), and esophageal and liver cancer in humans (Soriano *et al.*, 2005). Although little is known about the molecular mechanism of action by which these mycotoxins induce carcinogenic effects, disruption of the sphingolipid metabolism appears to be a major factor. It has been previously demonstrated that inhibition of sphingolipid biosynthesis using FB₁ results in depletion of cellular (glyco)sphingolipids and significantly affects axonal growth, suggesting that sphingolipids may play a vital role in regulating neuronal development (Harel and Futerman, 1993). Sphingolipids have been demonstrated to regulate apoptosis, survival and regeneration of cells in the nervous system. In addition, the role of sphingolipids in the development and progression of several neurological diseases such as Alzheimer's disease is well documented (Posee de Chaves, 2006), which could be due to impaired neurotransmission. Modulating sphingolipid levels and monitoring the function of an important neurotransmitter receptor therefore assumes relevance.

The serotonin_{1A} receptor is an important neurotransmitter G-protein coupled receptor and serves as an important target in the development of therapeutic agents for neuropsychiatric disorders such as anxiety and depression. Keeping in mind the pharmacological relevance of the serotonin_{1A} receptor, its interaction with the surrounding lipid environment assumes greater significance in modulating its function in healthy and diseased states. This chapter describes about the work in which sphingolipid levels in CHO cells stably expressing the human serotonin_{1A} receptor (CHO-5-HT_{1A}R) were modulated by metabolically inhibiting the biosynthesis of sphingolipids. In order to achieve this, FB₁ (a specific metabolic inhibitor of ceramide synthase) was utilized. FB₁ treatment results in reduction of sphingomyelin levels. The function of the human serotonin_{1A} receptor under these conditions was explored by monitoring ligand binding, G-protein coupling and

downstream signaling of the receptor along with lateral mobility measurements using Fluorescence Recovery After Photobleaching (FRAP). Our results show that the function of the serotonin_{1A} receptor is impaired upon metabolic depletion of sphingomyelin. These results are significant since FB₁ induces a number of diseases (see above) and could possibly even impair neurotransmission. Importantly, our results provide evidence, that sphingolipids are necessary for ligand binding and downstream signaling of the human serotonin_{1A} receptor. In addition, our results demonstrate that the effect of sphingomyelin on the ligand binding function of the serotonin_{1A} receptor caused by metabolic depletion of sphingolipids is reversible.

4.2. Materials and methods

Materials

DMPC, fumonisin B₁, EDTA, MgCl₂, MnCl₂, 8-OH-DPAT, penicillin, streptomycin, gentamycin sulfate, polyethylenimine, PMSF, *p*-MPPI, primuline, serotonin, sphingosine, sodium bicarbonate, and Tris were obtained from Sigma Chemical Co. (St. Louis, MO). D-MEM/F-12 [Dulbecco's modified Eagle medium:nutrient mixture F-12 (Ham) (1:1)], fetal calf serum, and geneticin (G 418) were from Invitrogen Life Technologies (Carlsbad, CA). GTP- γ -S was from Roche Applied Science (Mannheim, Germany). Porcine brain sphingomyelin was purchased from Avanti Polar Lipids (Alabaster, AL). BCA reagent for protein estimation was from Pierce (Rockford, IL). Forskolin and IBMX were obtained from Calbiochem (San Diego, CA). [³H]8-OH-DPAT (sp. activity = 135.0 Ci/mmol) and [³H]*p*-MPPF (sp. activity = 70.5 Ci/mmol) were purchased from DuPont New England Nuclear (Boston, MA). The cyclic [³H]AMP assay kit was purchased from Amersham Biosciences (Buckinghamshire, U.K.). GF/B glass microfiber filters were from Whatman International (Kent, U.K.). Pre-coated silica gel 60 thin layer chromatography plates were

from Merck (Merck, Germany). All other chemicals and solvents used were of the highest available purity. Water was purified through a Millipore (Bedford, MA) Milli-Q system and used throughout.

Cell culture and FB₁ treatment

CHO cells stably expressing the human serotonin_{1A} receptor (termed as CHO-5-HT_{1A}R) and stably expressing the human serotonin_{1A} receptor tagged to enhanced yellow fluorescent protein (termed as CHO-5-HT_{1A}R-EYFP) were maintained in D-MEM/F-12 (1:1) supplemented with 2.4 g/l of sodium bicarbonate, 10% fetal calf serum, 60 µg/ml penicillin, 50 µg/ml streptomycin, 50 µg/ml gentamycin sulfate, and 200 µg/ml geneticin in a humidified atmosphere with 5% CO₂ at 37 °C. Stock solutions (1 mM) of FB₁ were prepared in water and added to cells grown for 24 h (final concentration of FB₁ was 2-6 µM) and incubated in 5% serum for 63-66 h. Control cells were grown under similar conditions without FB₁ treatment.

Cell membrane preparation

Cell membranes were prepared as described earlier (Kalipatnapu *et al.*, 2004a; Paila and Chattopadhyay, 2006) and in section 3.2. Total protein concentration in the isolated membranes was determined using the BCA assay (Smith *et al.*, 1985).

Estimation of sphingomyelin by thin layer chromatography

Total lipid extraction from membranes of control and FB₁ treated cells was carried out according to Bligh and Dyer (1959). Lipid extracts were dried under a stream of nitrogen at 45 °C. The dried extracts were resuspended in a mixture of chloroform/methanol (1:1, v/v). Total lipid extracts were resolved by thin layer chromatography (TLC) using chloroform/methanol/acetic acid/water (25:15:4:2, v/v/v/v) as the solvent system (Ito *et al.*, 2002). The separated lipids were visualized by spraying a

fluorescent stain, primuline (Skipski, 1975). Sphingomyelin standard was used to identify sphingomyelin bands on the thin layer chromatogram run with total lipid extracts obtained from membranes of control and FB₁ treated cells. The sphingomyelin bands were scraped from the TLC plates, and lipids were re-extracted with chloroform/methanol (1:1, v/v) from samples, and the phosphate contents were estimated and normalized to the phosphate content obtained from native (control) cell membranes.

Estimation of inorganic phosphate

The concentration of lipid phosphate was as described in section 2.2.

Radioligand binding assays

Receptor binding assays were carried out as described in section 2.2 with ~50 µg total protein.

GTP-γ-S sensitivity assay

In order to estimate the efficiency of G-protein coupling, GTP-γ-S sensitivity assays were carried out as described in section 2.2.

Estimation of cyclic AMP content in cells

The ability of ligands to affect the forskolin-stimulated increase in cAMP levels in CHO-5-HT_{1A}R cells was assessed as described in section 3.2.

Fluorescence anisotropy measurements

Fluorescence anisotropy experiments were carried out using the fluorescent probe DPH with membranes prepared from cells that were treated with varying concentrations of FB₁, containing 50 nmol of total phospholipids suspended in 1.5 ml of 50 mM Tris, pH 7.4 buffer, as described earlier (Paila *et al.*, 2005) and in section 3.2.

Metabolic replenishment of sphingolipids using sphingosine

After treatment with 6 μ M FB₁, CHO-5-HT_{1A}R cells were grown for 24 hs in D-MEM/F-12 (1:1) supplemented with 1 μ M sphingosine, 2.4 g/l of sodium bicarbonate, 10% fetal calf serum, 60 μ g/ml penicillin, 50 μ g/ml streptomycin, 50 μ g/ml gentamycin sulfate, and 200 μ g/ml geneticin in a humidified atmosphere with 5% CO₂ at 37 °C in order to achieve replenishment of sphingolipids.

Confocal microscopy and live cell imaging

In order to visualize the serotonin_{1A} receptor, CHO-K1 cells stably expressing the serotonin_{1A} receptor tagged to enhanced yellow fluorescent protein (referred to as CHO-5-HT_{1A}R-EYFP) were used (Pucadyil *et al.*, 2004a). CHO-5-HT_{1A}R-EYFP cells were plated at a density of 5 x 10⁴ cells on a 40 mm glass coverslip and were grown in D-MEM/F-12 medium with or without FB₁. Coverslips were washed twice with 3 ml of HEPES-Hanks, pH 7.4 buffer, and mounted on an FCS2 closed temperature controlled Bioptechs chamber (Butler, PA). The chamber was gently perfused with 10 ml of the same buffer and was allowed to attain 37 °C, which took ~10 min. Images were acquired on an inverted Zeiss LSM 510 Meta confocal microscope (Jena, Germany), with a 63x, 1.2 NA water immersion objective using the 514 nm line of an argon laser. EYFP fluorescence emission was collected using the 535-590 nm bandpass filter.

Fluorescence recovery after photobleaching (FRAP) measurements and statistical analysis

FRAP experiments were carried out at room temperature (~23 °C) on cells that were grown in D-MEM/F-12 medium containing 5% serum with or without FB₁ treatment on Lab-Tek chambered coverglass (Nunc, Denmark). Fluorescence images of cells grown on Lab-Tek chambers were acquired in the presence of PBS buffer pH 7.4, containing 0.5 mM MgCl₂ and 1 mM CaCl₂. Images were acquired on an inverted Zeiss LSM 510 Meta confocal microscope as described above, and recorded at a 225 μ m pinhole resolution,

giving an optimal z-slice thickness of 1.7 μm . A circular region of interest (ROI), with a radius of 1.4 μm was chosen as the bleach ROI. The time interval between successive scans was ~ 0.53 s. Analysis with a control ROI drawn a fair distance away from the bleach ROI indicated no significant bleach while fluorescence recovery was monitored. Data representing the mean fluorescence intensity of the bleached ROI were background subtracted using an ROI placed outside the cell boundary and were analyzed to determine the diffusion coefficient (D). FRAP recovery plots were analyzed on the basis of the equation for a uniform disk illumination condition (Soumpasis, 1983):

$$F(t) = [F(\infty) - F(0)] [\exp(-2\tau_d/t) (I_0(2\tau_d/t) + I_1(2\tau_d/t))] + F(0) \quad (5)$$

where $F(t)$ is the mean background corrected and normalized fluorescence intensity at time t in the bleached ROI, $F(\infty)$ is the recovered fluorescence at time $t = \infty$, $F(0)$ is the bleached fluorescence intensity set at time $t = 0$, and τ_d is the characteristic diffusion time. I_0 and I_1 are modified Bessel functions. Diffusion coefficient (D) is determined from the equation:

$$D = \omega^2 / 4\tau_d \quad (6)$$

where ω is the actual radius of the bleached ROI. Mobile fraction estimates of the fluorescence recovery were obtained from the equation:

$$\text{mobile fraction} = [F(\infty) - F(0)] / [1 - F(0)] \quad (7)$$

where the mean background corrected and normalized prebleach fluorescence intensity is equal to unity. Nonlinear curve fitting of the fluorescence recovery data to equation 5 was carried out using the Graphpad Prism software version 4.00 (San Diego, CA). Frequency distribution plot and statistical analysis were performed using Microcal Origin software version 5.0 (OriginLab Corp., Northampton, MA).

Western blot analysis

Cell membranes were prepared from CHO-5-HT_{1A}R-EYFP (control), FB₁ treated and FB₁ treatment followed by sphingosine-treated cells as previously described earlier (section 3.2; Paila and Chattopadhyay, 2006) with an addition of 1:20 dilution of freshly

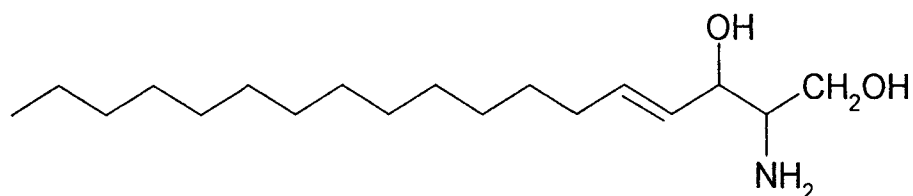
added protease inhibitor cocktail (Roche Applied Science, Mannheim, Germany). Western blot analysis was performed as described in section 3.2.

4.3. Results

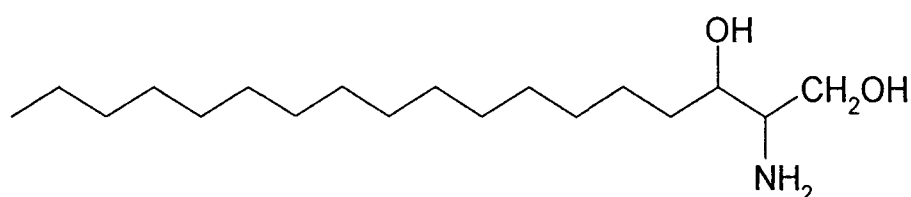
Quantification of sphingomyelin upon metabolic depletion using FB₁

CHO cells stably expressing the human serotonin_{1A} receptor (CHO-5-HT_{1A}R) were treated with FB₁, in order to achieve the metabolic depletion of sphingolipids. FB₁ is a potent and competitive inhibitor of ceramide synthase, the enzyme that catalyzes the acylation of sphinganine in *de novo* biosynthesis of sphingolipids and the reutilization of sphingosine derived from sphingolipid turnover (Merrill *et al.*, 1996). The structures of sphingosine, sphinganine and FB₁ are shown in Figure 4.1. Besides disrupting sphingolipid metabolism, FB₁ is known to induce oxidative stress leading to cytotoxicity when used at high concentrations (Kouadio *et al.*, 2005). It is therefore important to ensure that the FB₁ concentrations used are below the concentration range in which cytotoxic effects are predominant. It has previously been shown that treatment up to 50 μ M FB₁ does not result in cell death (Yu *et al.*, 2001; Sjögren and Svenningsson, 2007). We therefore chose to use low concentrations of FB₁ and the concentration of FB₁ used in the present work never exceeded 6 μ M. Total lipids were extracted from membranes prepared from control and FB₁ treated cells, and were separated on TLC plates (shown in Figure 4.2a). Sphingomyelin bands were scraped from chromatographic plates and their phosphate contents were estimated as described in section 4.2 and shown in Figure 4.2b. The sphingomyelin content shows a progressive reduction with increasing FB₁ concentration. Figure 4.2b shows that ~80% of sphingomyelin is metabolically depleted in membranes of CHO-5-HT_{1A}R following treatment with 6 μ M FB₁.

Sphingosine



Sphinganine



Fumonisin B₁

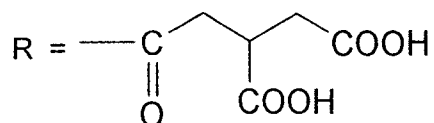
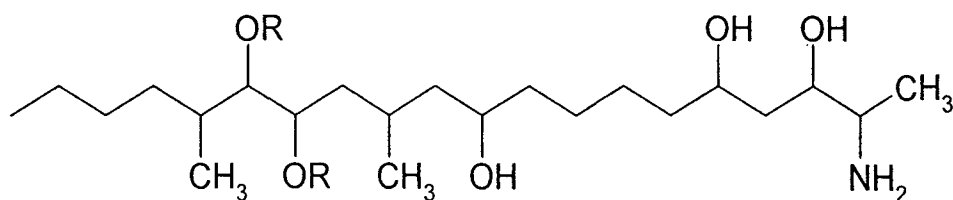


Figure 4.1. Chemical structures of sphingosine, sphinganine and fumonisin B₁. Fumonisin B₁ is a potent and competitive inhibitor of ceramide synthase (*N*-acetyltransferase), the enzyme that catalyzes the acylation of sphinganine in *de novo* biosynthesis of sphingolipids and the reutilization of sphingosine derived from sphingolipid turnover (Merrill *et al.*, 1996). See text for more details.

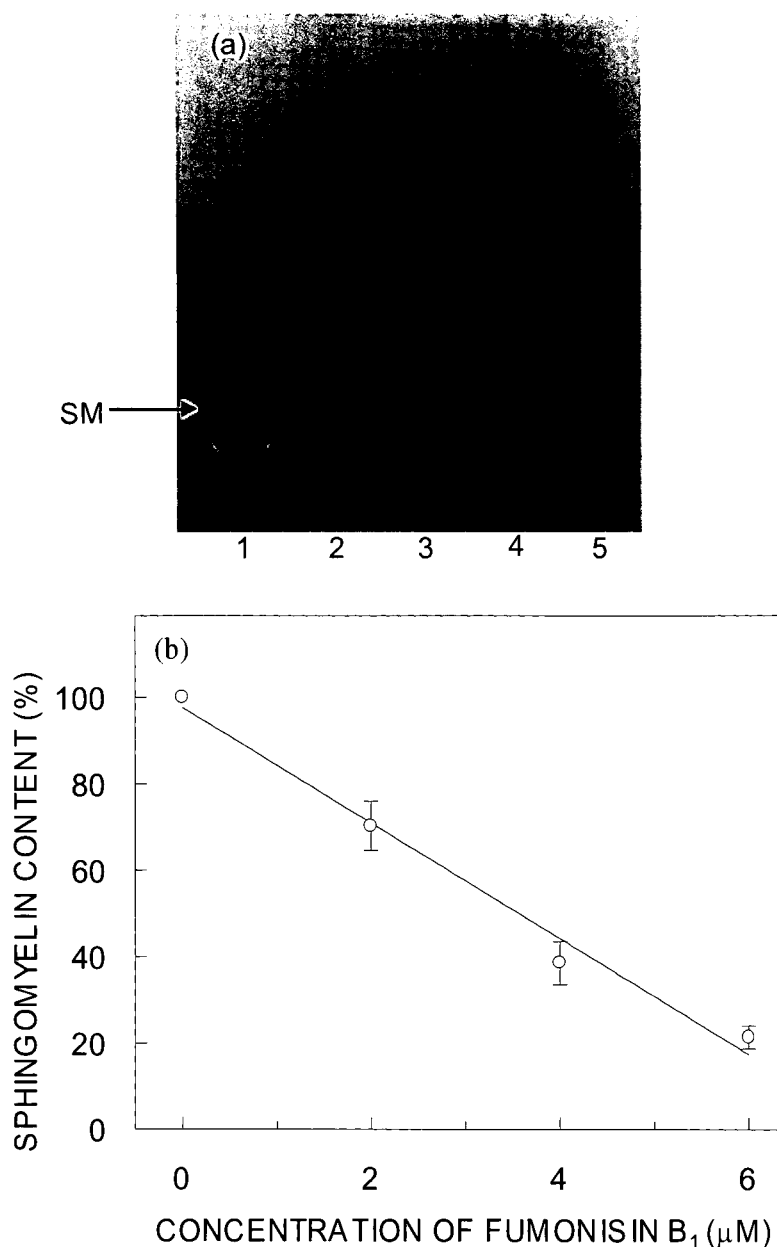


Figure 4.2. Estimation of sphingomyelin content in membranes isolated from control cells and cells treated with varying concentrations of FB₁. Total lipids were extracted from membranes of control cells and cells treated with varying concentrations of FB₁ and were separated by thin layer chromatography as shown in (a). The lanes represent lipids extracted from membranes from control cells (lane 2), and membranes isolated from cells treated with 2 (lane 3), 4 (lane 4) and 6 (lane 5) μM of FB₁. The arrow represents position of sphingomyelin on the thin layer chromatogram identified using a standard in lane 1. Sphingomyelin contents were quantified by estimation of phosphate content and are shown in (b). Values are expressed as percentages of the sphingomyelin content of membranes of control cells (without any treatment). Data represent means ± SE of at least three independent experiments. See section 4.2 for other details.

Specific ligand binding of the human serotonin_{1A} receptor is reduced upon metabolic depletion of sphingolipids

In order to monitor the effect of metabolic depletion of sphingolipids on the ligand binding activity of the serotonin_{1A} receptor, CHO-5-HT_{1A}R cells were treated with varying concentrations of FB₁ and ligand binding was measured. For this, we measured binding of the selective serotonin_{1A} receptor agonist [³H]8-OH-DPAT and antagonist [³H]*p*-MPPF to cell membranes prepared from CHO-5-HT_{1A}R cells under control (without FB₁ treatment) and FB₁ treated conditions. Figure 4.3 shows the decrease in specific binding of the selective serotonin_{1A} receptor agonist [³H]8-OH-DPAT with increasing concentrations of FB₁ (Figure 4.3a), and the accompanying reduction in membrane sphingomyelin levels (Figure 4.3b). The specific agonist binding is reduced to ~57% of the original value upon metabolic depletion of ~80% sphingomyelin. The effects of increasing concentrations of FB₁ and accompanying sphingomyelin depletion on specific [³H]*p*-MPPF binding to the serotonin_{1A} receptor are shown in panels (c) and (d), respectively. Figure 4.3c shows that specific binding of the selective antagonist [³H]*p*-MPPF is decreased with FB₁ treatment, and is reduced to ~65% of its original value upon treatment with 6 μM FB₁. Figure 4.3 shows that the reduction in ligand binding is somewhat drastic till ~30% sphingomyelin is lost (corresponding to 2 μM FB₁). Taken together, these results show that the reduction in membrane sphingomyelin content in CHO-5-HT_{1A}R cells by metabolic depletion using FB₁ results in the loss of the serotonin_{1A} receptor ligand binding ability.

Ligand-dependent downstream signaling efficiency of the human serotonin_{1A} receptor is reduced upon metabolic depletion of sphingolipids

Figure 4.4a shows a characteristic reduction in binding of the agonist [³H]8-OH-DPAT in the presence of a range of concentrations of GTP-γ-S with an estimated half maximal inhibition concentration (IC₅₀) of 3.41 nM for control cells. The inhibition curve in case of cells treated with 6 μM FB₁ displays a significant (~5-fold) shift toward higher

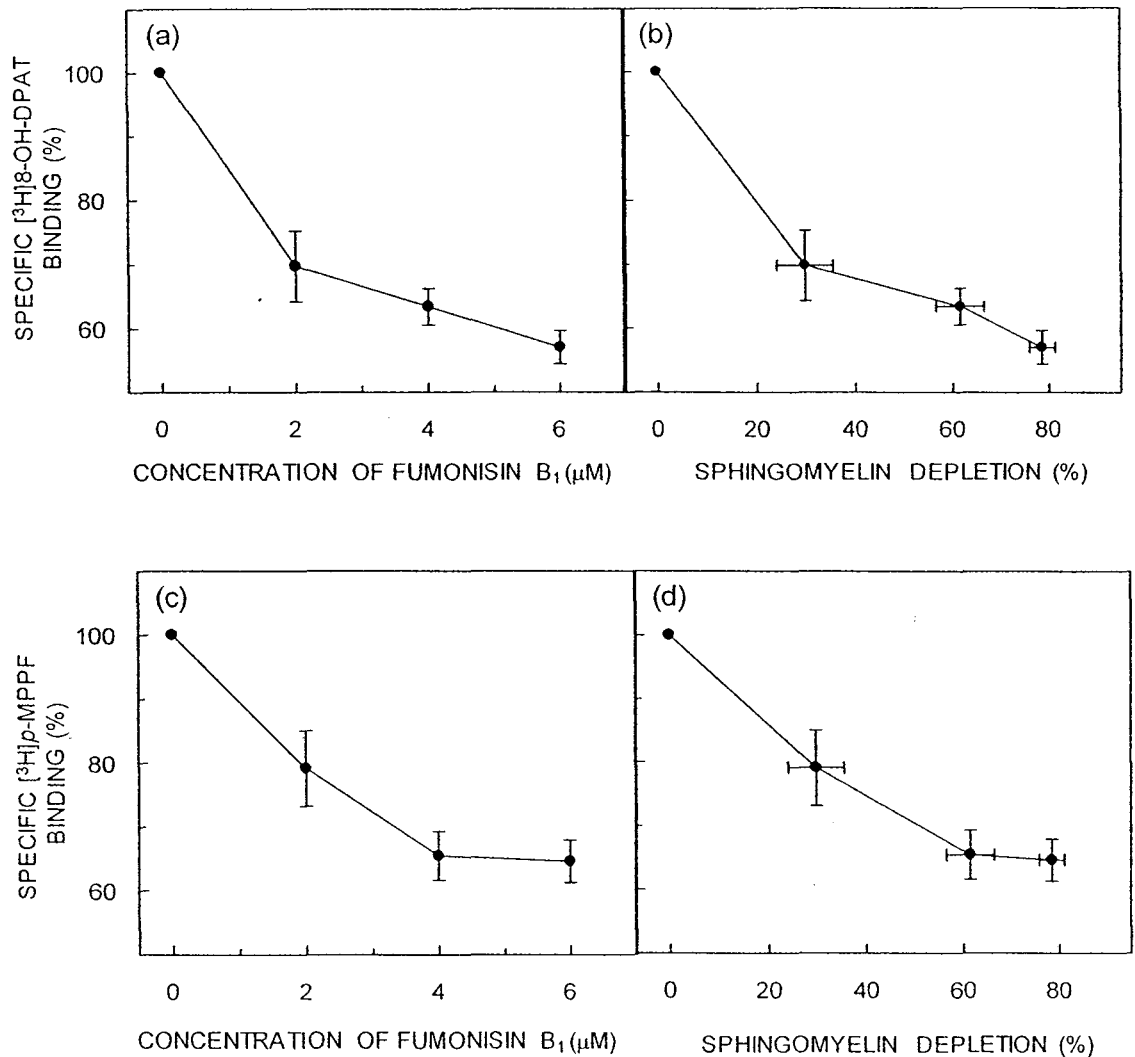


Figure 4.3. Effect of metabolic depletion of sphingolipids on specific ligand binding of the human serotonin_{1A} receptor. CHO-5-HT_{1A}R cells were treated with varying concentrations of FB₁ and specific [³H]8-OH-DPAT binding to the serotonin_{1A} receptor in membranes isolated from these cells was measured and shown in (a). The change in specific [³H]8-OH-DPAT binding is plotted with increasing sphingomyelin depletion in (b). Values are expressed as percentages of specific binding for control cell membranes without FB₁ treatment. Data shown are means ± SE of at least three independent experiments. The effects of increasing concentrations of FB₁ and accompanying sphingomyelin depletion on specific [³H]p-MPPF binding to the serotonin_{1A} receptor are shown in panels (c) and (d), respectively. Values are expressed as percentages of specific binding for control cell membranes without FB₁ treatment. Data shown are means ± SE of at least three independent experiments. Data for the extent of sphingomyelin depletion with increasing concentrations of FB₁ are taken from Figure 4.2b. See section 4.2 for other details.

concentrations of GTP- γ -S with an increased IC₅₀ value of 19.75 nM. This implies that the agonist binding to the serotonin_{1A} receptor upon metabolic depletion of sphingolipids is less sensitive to GTP- γ -S indicating that the G-protein coupling efficiency is reduced under these conditions. This indicates a possible perturbation of receptor-G-protein interaction upon metabolic depletion of sphingolipids.

In addition to ligand binding properties, we monitored the function of serotonin_{1A} receptors in CHO-5-HT_{1A}R cells by measuring its ability to catalyze downstream signal transduction processes upon stimulation with the specific agonist, 8-OH-DPAT. Serotonin_{1A} receptor agonists such as 8-OH-DPAT are known to specifically activate the G_i/G_o class of G-proteins in CHO cells, which subsequently reduce cAMP levels in cells (Raymond *et al.*, 1993). As shown in Figure 4.4b, the forskolin-stimulated increase in cAMP levels is inhibited by 8-OH-DPAT with a half maximal inhibition concentration (IC₅₀) of 9.49 nM in control cells. In cells treated with 6 μ M FB₁, the IC₅₀ value is increased to a significant extent (~2.5-fold) to 23.93 nM. This points out that the downstream signaling efficiency of the human serotonin_{1A} receptor is reduced under sphingolipid depleted condition.

The overall membrane order remains largely invariant upon metabolic depletion of sphingolipids

In order to monitor any possible change in overall membrane order upon FB₁ treatment, we measured the fluorescence anisotropy of the fluorescent probe DPH. Figure 4.5 shows the effect of increasing concentrations of FB₁ on the fluorescence anisotropy of the membrane probe DPH incorporated into CHO-5-HT_{1A}R cell membranes. The fluorescence anisotropy of DPH appears to decrease slightly (~14%) upon treatment with 6 μ M FB₁, compared to the fluorescence anisotropy value in membranes prepared from control cells (without FB₁ treatment). The slight reduction in overall membrane order could be due to disruption of ordered sphingomyelin-rich domains since sphingomyelin and

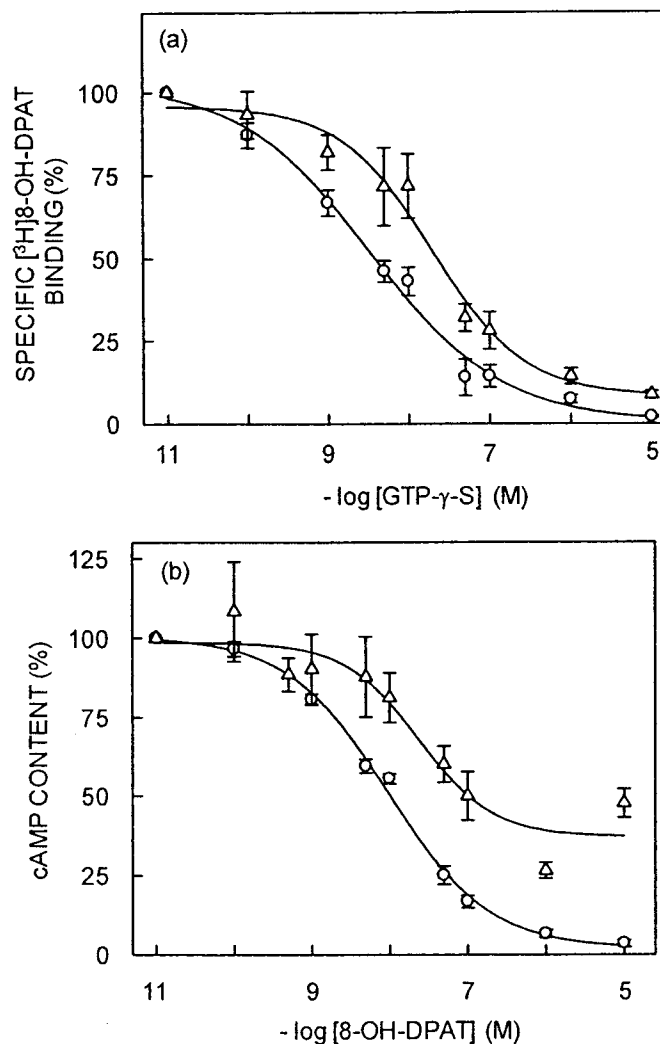


Figure 4.4. Reduced downstream signaling of the human serotonin_{1A} receptor upon metabolic depletion of sphingolipids. The downstream signaling efficiency of the serotonin_{1A} receptor was monitored by the sensitivity of [³H]8-OH-DPAT binding to GTP-γ-S and cyclic AMP levels. Panel (a) shows the effect of increasing concentrations of GTP-γ-S on specific binding of the agonist [³H]8-OH-DPAT to serotonin_{1A} receptors in control cells (O) and in cells treated with 6 μM FB₁ (Δ). Values are expressed as percentages of specific binding obtained at the lowest concentration of GTP-γ-S. The curves are non-linear regression fits to the experimental data using equation 1. The data points represent means ± SE of duplicate points from at least three independent experiments. See section 4.2 for other details. Panel (b) shows the estimation of cAMP levels in CHO-5-HT_{1A}R cells. The ability of the specific agonist (8-OH-DPAT) to reduce the forskolin-stimulated increase in cAMP levels in control cells (O) and in cells treated with 6 μM FB₁ (Δ) was assessed. cAMP levels in cells were estimated as described in section 4.2. The curves are non-linear regression fits to the experimental data using equation 1. The data are normalized to cAMP levels present in the lowest concentration of 8-OH-DPAT used in the experiment and represent the means ± SE of duplicate points from at least three independent experiments. See section 4.2 for other details.

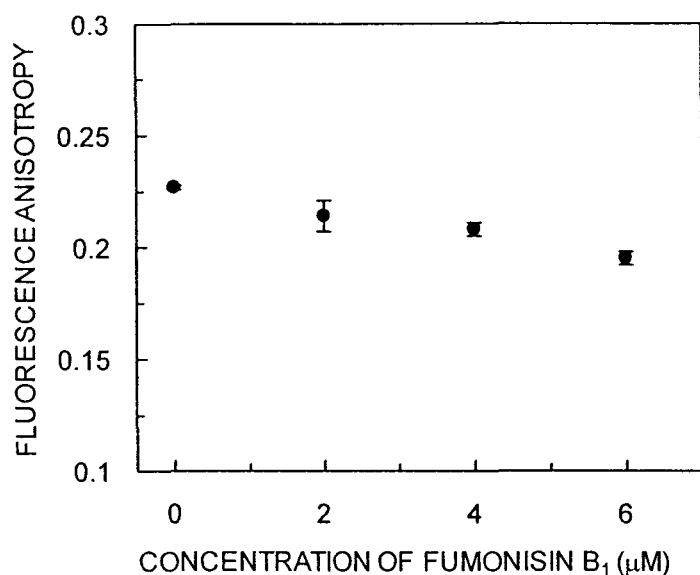


Figure 4.5. Measurement of overall membrane order upon metabolic depletion of sphingolipids. The overall (average) membrane order was estimated in control cell membranes and in membranes of cells treated with varying concentrations of FB₁, using fluorescence anisotropy of the membrane probe DPH. Fluorescence anisotropy measurements were carried out with membranes containing 50 nmol phospholipid at a probe to phospholipid ratio of 1:100 (mol/mol) at room temperature (~23 °C). The data represent means ± SE of duplicate points from at least three independent experiments. See section 4.2 for other details.

ceramide have previously been reported to partition into ordered domains (Ramstedt and Slotte, 2006). These results therefore suggest that the overall (global) membrane order does not change by a considerable extent upon metabolic depletion of sphingolipids.

Replenishment of sphingolipids using sphingosine restores the membrane sphingomyelin content and ligand binding function of the human serotonin_{1A} receptor

In order to monitor the reversibility of the effect of sphingolipids on the function of the human serotonin_{1A} receptor, CHO-5-HT_{1A}R cells were treated with sphingosine and the sphingomyelin content and ligand binding function of the receptor were measured. Figure 4.6 shows that pre-treatment of CHO-5-HT_{1A}R cells with FB₁ followed by treatment with sphingosine, results in restoration of sphingomyelin levels to normal and the corresponding

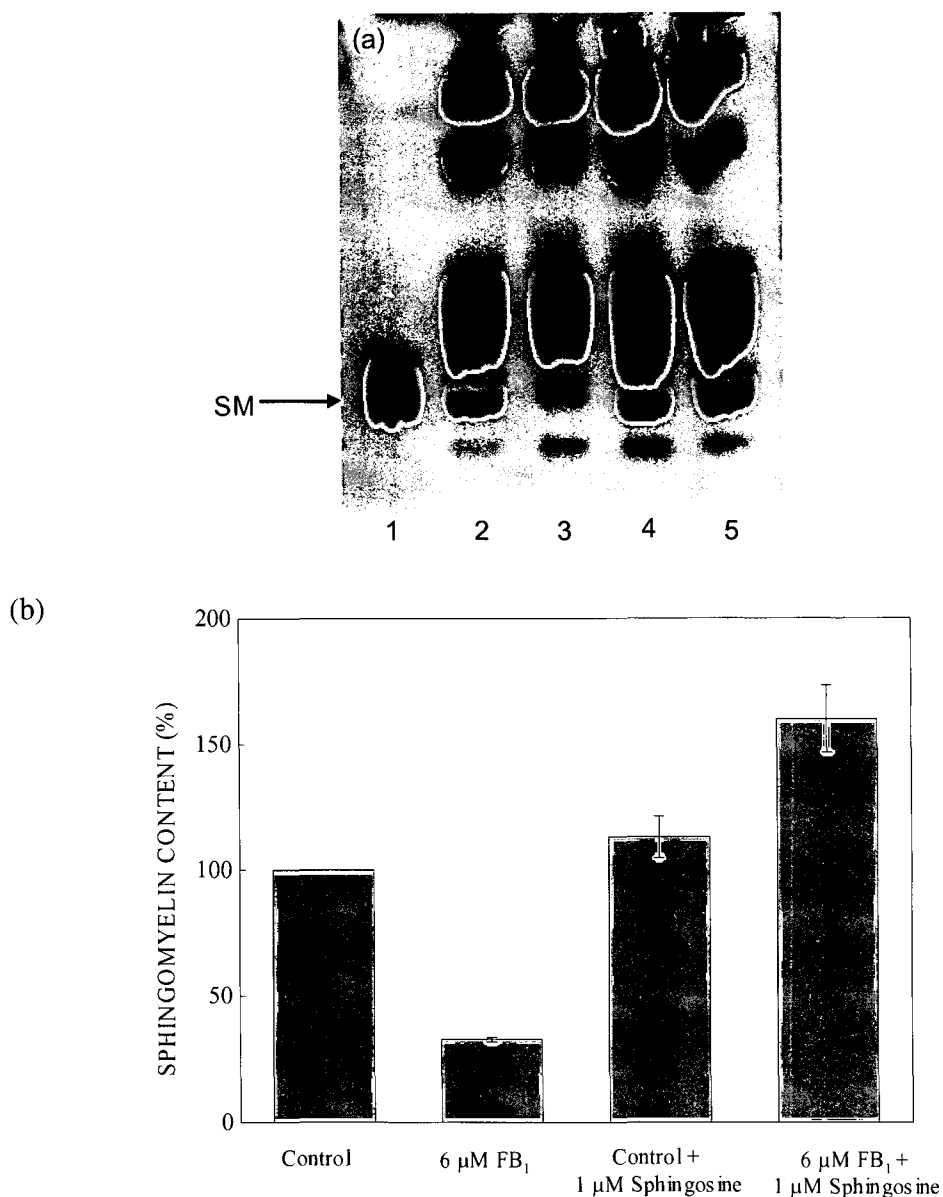


Figure 4.6. Replenishment of sphingolipids using sphingosine. After treatment with 6 μM FB₁, CHO-5-HT_{1A}R cells were grown for 24 hs with 1 μM sphingosine in D-MEM/F-12 (1:1) medium (supplemented with 2.4 g/l of sodium bicarbonate, 10% fetal calf serum, 60 $\mu\text{g/ml}$ penicillin, 50 $\mu\text{g/ml}$ streptomycin, 50 $\mu\text{g/ml}$ gentamycin sulfate, and 200 $\mu\text{g/ml}$ geneticin) in a humidified atmosphere with 5% CO₂ at 37 °C. Total lipids were extracted from cells and were separated by thin layer chromatography as shown in (a). The lanes represent lipids extracted from membranes from control cells (lane 2), and membranes isolated from cells treated with 6 μM of FB₁ (lane 3), membranes isolated from control cells incubated with 1 μM sphingosine (lane 4) and membranes isolated from cells after treatment with 6 μM of FB₁ and incubated with 1 μM sphingosine (lane 5). The arrow represents position of sphingomyelin on the thin layer chromatogram identified using a standard in lane 1. Sphingomyelin contents were quantified by estimation of phosphate content and are shown in (b). Values are expressed as percentages of the sphingomyelin content of membranes of control cells (without any treatment). Data represent means \pm SE of at least three independent experiments. See section 4.2 for other details.

changes in the ligand binding function are shown in Figure 4.7. Total lipids were extracted from membranes prepared from control, FB₁ treated and sphingosine treated cells, which were pre-treated with FB₁. Total lipids were separated on TLC plates and are shown in Figure 4.6a. Sphingomyelin bands were scraped from chromatographic plates and their phosphate contents were estimated as described in section 4.2 and shown in Figure 4.6b. This Figure shows that ~70% of sphingomyelin is metabolically depleted in membranes of CHO-5-HT_{1A}R cells following treatment with 6 μM FB₁. The membrane sphingomyelin content was increased to ~115% in control and to ~160% in FB₁ treated cells upon treatment with sphingosine (Figure 4.6).

Figure 4.7 demonstrates the restoration in specific binding of the selective serotonin_{1A} receptor agonist [³H]8-OH-DPAT upon sphingolipid replenishment. The specific agonist binding is reduced to ~60% of the original value upon FB₁ treatment and is restored to its normal level upon treatment with sphingosine. Figure 4.7 shows that the ligand binding function of the receptor is increased to ~117% upon sphingolipid replenishment. Taken together, these results show that the reduction in the ligand binding function of the serotonin_{1A} receptor by metabolic depletion using FB₁ is reversible.

The membrane expression level of the human serotonin_{1A} receptor is not reduced upon FB₁ treatment

The impaired ligand binding activity and signaling of the human serotonin_{1A} receptor observed upon FB₁ treatment could be due to reduced expression levels of serotonin_{1A} receptors. In order to explore this possibility, we performed Western blot analysis of 5-HT_{1A}R-EYFP in cell membranes prepared from control, FB₁ treated and sphingolipid replenished CHO-5-HT_{1A}R-EYFP cells (see Figure 4.8). For these experiments, we chose to use the receptor tagged to EYFP (5-HT_{1A}R-EYFP) since no monoclonal antibodies for the serotonin_{1A} receptor are available yet, and the polyclonal antibodies have been reported to give variable results on Western blots (Zhou *et al.*, 1999).

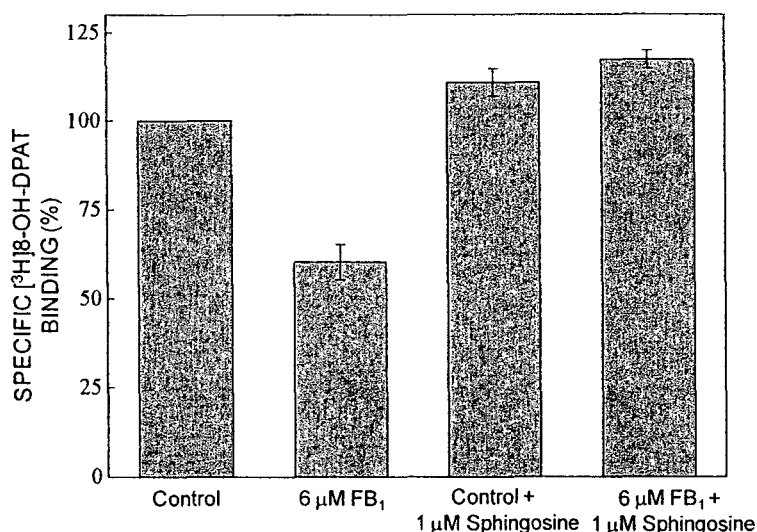


Figure 4.7. The changes in the specific binding of the agonist [³H]8-OH-DPAT to serotonin_{1A} receptors under control, 6 μ M FB₁ treated and sphingolipid replenished conditions. See section 4.2 for other details.

We have earlier shown that EYFP fusion to the serotonin_{1A} receptor does not affect the ligand binding properties, G-protein coupling and signaling functions of the receptor (Pucadyil *et al.*, 2004a). Figure 4.8b shows that the levels of the serotonin_{1A} receptor in membranes are not reduced upon FB₁ treatment. The receptor level is slightly increased (~1.2-fold compared to control) following FB₁ treatment. It has been previously reported that serotonin_{1A} receptor levels in CHO cells could increase upon induction of stress (Singh *et al.*, 1996b).

Cellular morphology and overall fluorescence distribution of EYFP tagged serotonin_{1A} receptors remain unaltered upon metabolic depletion of sphingolipids

Our group has earlier shown that EYFP fusion to the serotonin_{1A} receptor does not affect the ligand binding properties, G-protein coupling and signaling functions of the receptor (Pucadyil *et al.*, 2004a). CHO-K1 cells stably expressing the 5-HT_{1A}R-EYFP therefore represent a reliable system to explore membrane organization and dynamics of the

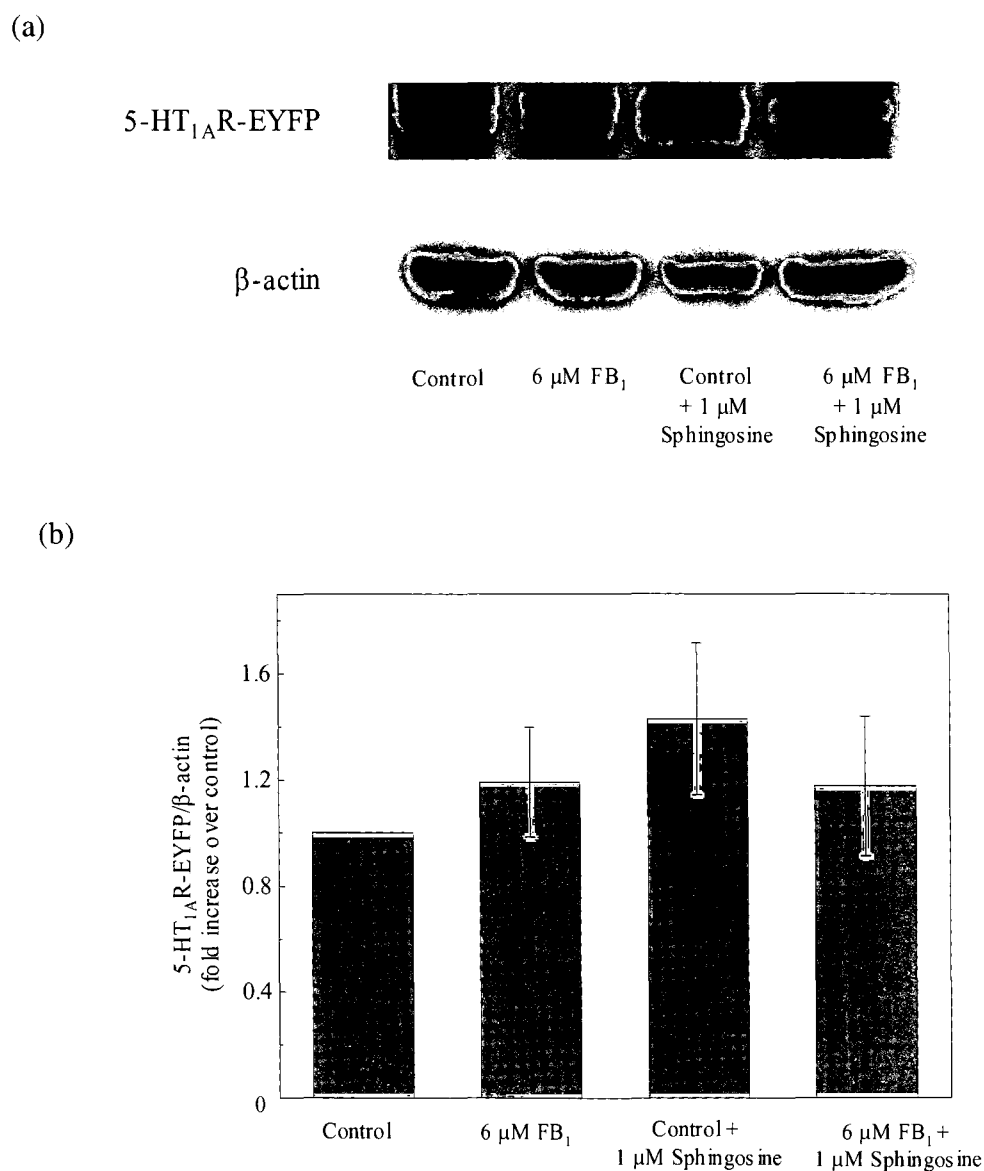
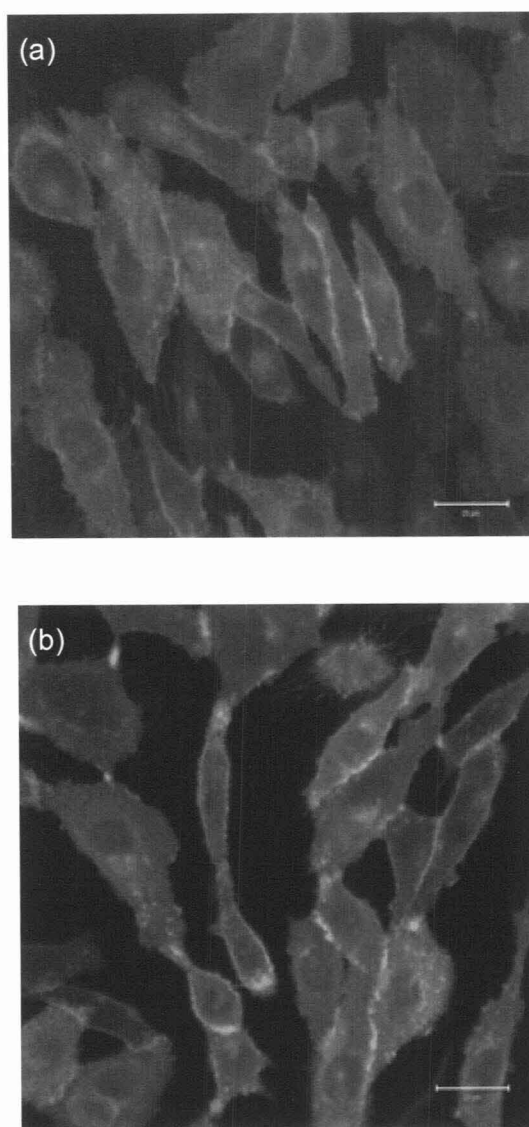


Figure 4.8. The expression level of the human serotonin_{1A} receptor is not reduced in membranes upon FB₁ treatment. Western blot analysis of 5-HT_{1A}R-EYFP in membranes prepared from CHO-5-HT_{1A}R-EYFP (control) cells, CHO-5-HT_{1A}R-EYFP cells treated with 6 μM FB₁ and after incubating with sphingosine to achieve replenishment of sphingolipids. Panel (a) shows the human serotonin_{1A} receptor tagged to EYFP with corresponding β-actin probed with antibodies directed against GFP and β-actin. Panel (b) shows the quantitation of 5-HT_{1A}R-EYFP and β-actin levels using densitometry. 5-HT_{1A}R-EYFP levels were normalized to β-actin of the corresponding sample. Data are shown as fold increase of 5-HT_{1A}R-EYFP over control and represent means ± SE of at least four independent experiments. See section 4.2 for other details.



will **Figure 4.9.** Cellular morphology and the overall distribution of 5-HT_{1A}R-EYFP remain unaltered in control and cells treated with 6 μM FB₁. Panels (a) and (b) show typical fluorescence distribution of 5-HT_{1A}R-EYFP in CHO-5-HT_{1A}R-EYFP cells under control (a) and 6 μM FB₁ treated (b) conditions. Fluorescence images of cells grown on coverslips and placed in the Biopetechs FCS2 closed chamber system were acquired at 37 °C in the presence of HEPES-Hanks buffer. The images represent mid-plane confocal sections of the cells under conditions as described in section 4.2. The scale bar represents 20 μm. See section 4.2 for other details.

serotonin_{1A} receptor. The fluorescence distribution of 5-HT_{1A}R-EYFP in CHO-5-HT_{1A}R-EYFP cells was observed in control cells and cells treated with 6 μM FB₁ (shown in Figure 4.9). Analyses of several independent images acquired with control and 6 μM FB₁ treated

CHO-5-HT_{1A}R-EYFP cells do not indicate a significant redistribution of fluorescence of the 5-HT_{1A}R-EYFP. These results set up the background for the experiments described below to assess diffusion characteristics of the receptor by FRAP as they indicate that the analysis of fluorescence recovery is not complicated by any significant alteration in the distribution of receptors due to FB₁ treatment during these experiments.

Fluorescence recovery after photobleaching analysis of 5-HT_{1A}R-EYFP

Fluorescence recovery after photobleaching involves generating a concentration gradient of fluorescent molecules by irreversibly photobleaching a fraction of fluorophores in the sample region. The dissipation of this gradient with time owing to diffusion of fluorophores into the bleached region from the unbleached regions in the membrane is an indicator of the mobility of the fluorophores in the membrane. A representative panel of images showing the recovery of fluorescence intensity after photobleaching is shown in Figure 4.10 (panels (a-d)). A representative fluorescence recovery plot with regression fits to the data is shown in Figure 4.10 (lower panel). A large data set was collected keeping in mind the inherent statistical variation in biological membranes. The frequency distribution histograms of diffusion coefficients and mobile fractions of 5-HT_{1A}R-EYFP in control cells and cells treated with 6 μ M FB₁ are shown in Figure 4.11 (panels a-d). The diffusion coefficient of 5-HT_{1A}R-EYFP did not exhibit any significant change upon FB₁ treatment (Figure 4.11, panels a and b). The distribution of diffusion coefficients remain essentially unimodal with comparable standard deviations indicating the presence of a predominantly single mobile population (at least in the time scale of FRAP measurement), which does not display any significant change upon FB₁ treatment. Interestingly, the mobile fraction of 5-HT_{1A}R-EYFP shows a significant ($\sim 7\%$, $p < 0.001$) increase in its mean value upon FB₁ treatment (see panels c and d), although the distribution remains essentially unimodal.

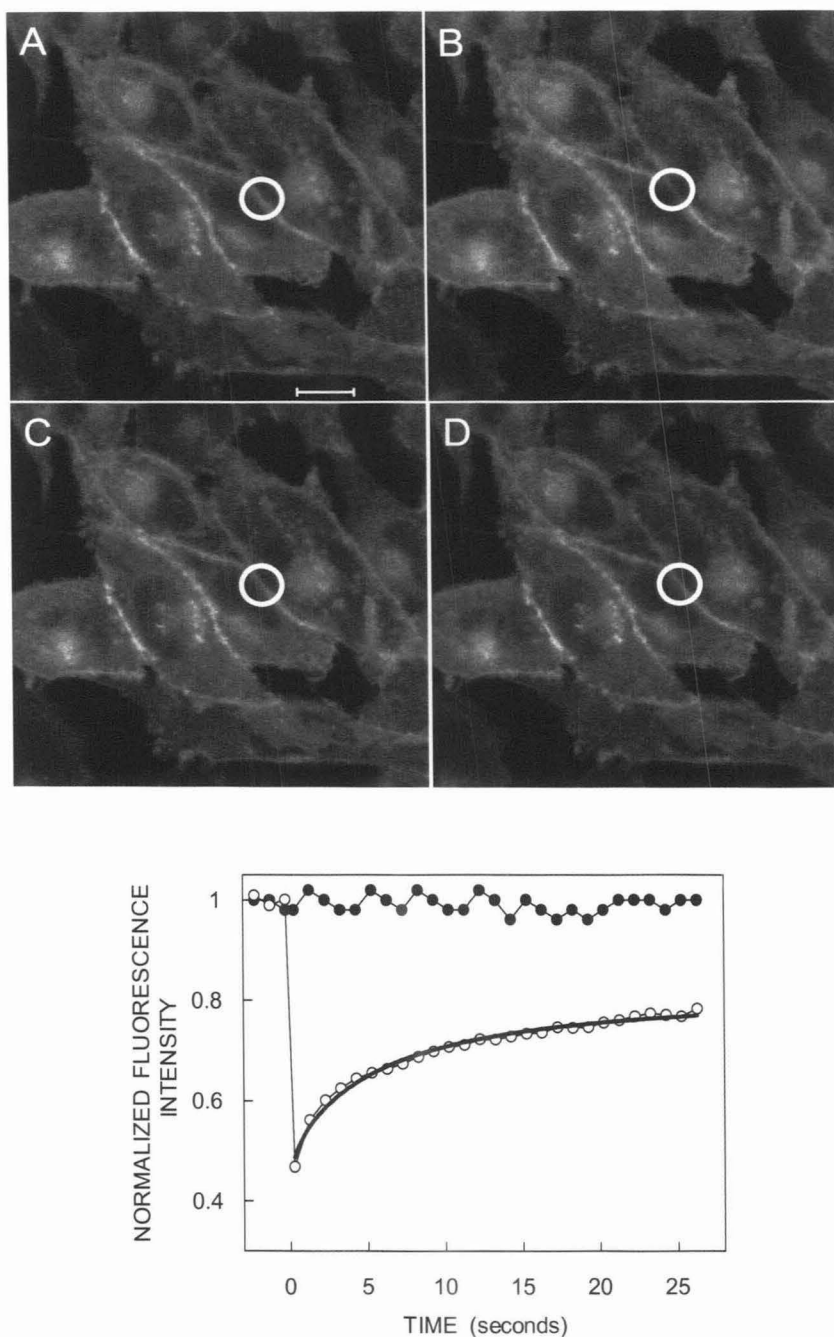


Figure 4.10. Representative images of recovery of fluorescence intensity after photobleaching of 5-HT_{1A}R-EYFP in CHO-5-HT_{1A}R-EYFP cells. Fluorescence images of cells represent confocal sections of the cell periphery and were acquired at room temperature (~23 °C). Panels A-D show fluorescence intensity monitored at various time points corresponding to prebleach, bleach, immediate postbleach and complete recovery, respectively. The scale bar represents 10 μm. The fluorescence recovery plot (see lower panel) shows a single set of normalized data, fitted to equation 5. The recovery of 5-HT_{1A}R-EYFP (○), and background (●) fluorescence intensities are shown. Note that the background fluorescence intensity (●) monitored for the same time period indicates no significant photobleaching of the field due to repeated imaging. The prebleach intensities are shown at time $t < 0$. See section 4.2 for other details.

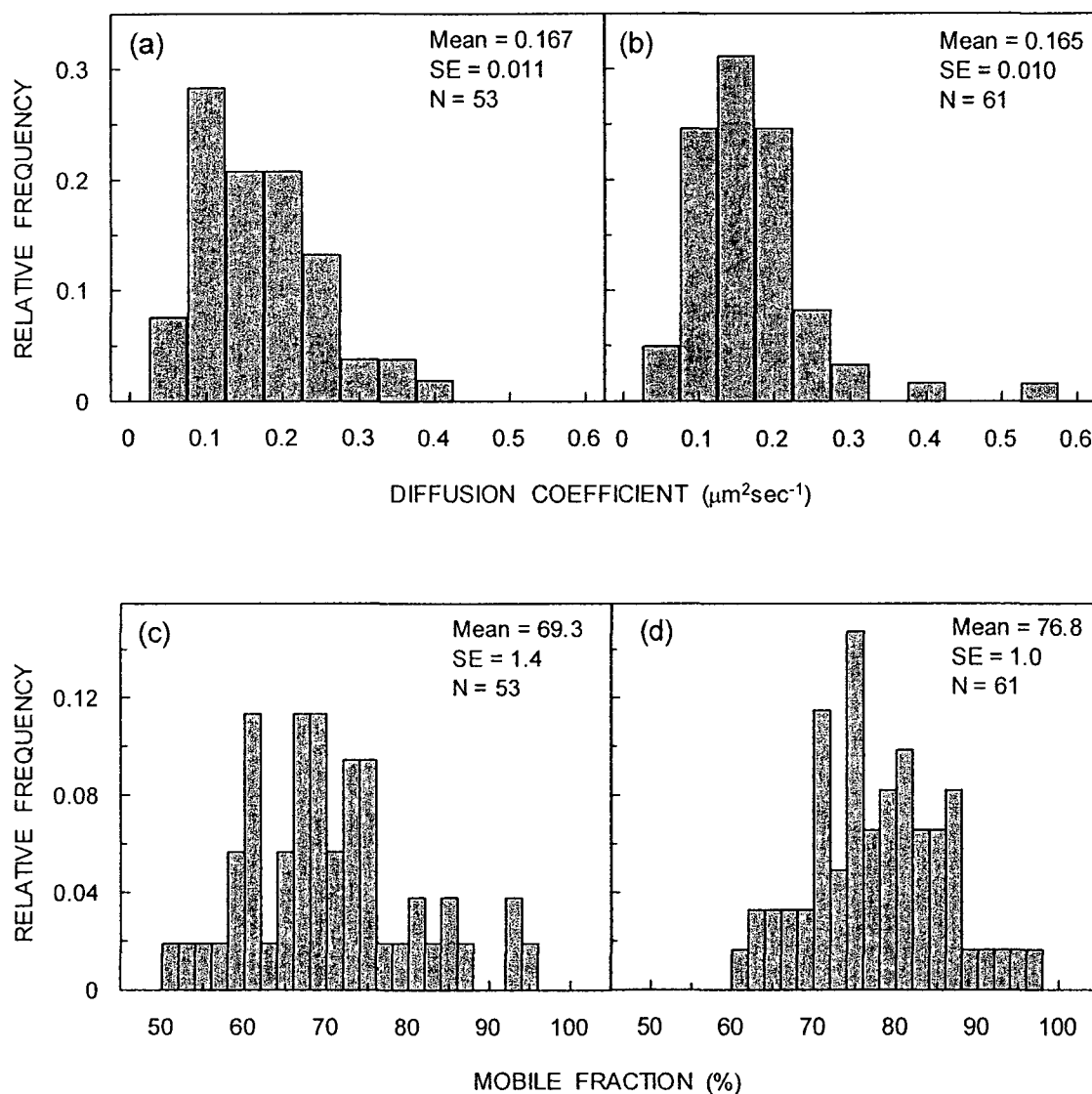


Figure 4.11. Frequency distribution histograms of the diffusion coefficient and mobile fraction of 5-HT_{1A}R-EYFP determined by FRAP. The frequency distribution histograms are obtained by fitting the normalized recovery data of individual experiments to equation 5. Panels (a) and (b) show the diffusion coefficient histograms for control (untreated) cells, and 6 μM FB₁ treated cells, respectively. Panels (c) and (d) show the mobile fraction histograms for control (untreated) cells, and 6 μM FB₁ treated cells, respectively. The means \pm SE are shown in all cases. N represents the number of independent experiments performed in each case. See section 4.2 for other details.

4.4. Discussion

Sphingomyelin typically amounts to 2-15% of the total phospholipids of mammalian cells (Koval and Pagano, 1991) and even higher levels of sphingomyelin are found in the peripheral nerve and brain tissue (Soriano *et al.*, 2005). Its subcellular localization is mainly in the plasma membrane. Metabolic turnover of sphingomyelin produces derivatives such as ceramide, sphingosine, sphingosine 1-phosphate which have crucial role in signal transduction events (Futerman and Hannun, 2004). The metabolic turnover of sphingomyelin therefore is involved in the regulation of signal transduction (Koval and Pagano, 1991). In view of the importance of sphingolipids in relation to membrane domains (Ramstedt and Slotte, 2006), the interaction of sphingolipids with membrane receptors represents an important determinant in functional studies of such receptors.

Sphingolipids are being increasingly implicated in the pathogenesis of several disorders such as cancer, metabolic and neurological disorders (Zeidan and Hannun, 2007). In this work, we have modulated sphingolipid levels in CHO-5-HT_{1A}R cells by metabolically inhibiting the biosynthesis of sphingolipids using FB₁. FB₁ acts as a competitive inhibitor to ceramide synthase, which acylates sphinganine to ceramide. Since FB₁ has been reported to induce neurodegeneration (Osuchowski *et al.*, 2005), thereby leading to changes in neurotransmission, exploring the function of an important neurotransmitter receptor under these conditions assumes relevance. We explored the function of the human serotonin_{1A} receptor under these conditions by monitoring ligand binding, G-protein coupling and downstream signaling of the receptor. Our results show that the function of the serotonin_{1A} receptor is impaired upon metabolic depletion of sphingolipids. Importantly, our results show that the receptor level is not reduced under this condition. This implies that the fraction of functional receptors is reduced upon FB₁ treatment resulting in a higher fraction of non-functional receptors. Sphingolipids were replenished using sphingosine in cells pre-treated with FB₁ and it was found that the

sphingomyelin content and ligand binding activity of the human serotonin_{1A} receptor could be recovered (Figures 4.6 and 4.7). In addition, we observe a small but significant increase in mobile fraction of the receptor upon sphingolipid depletion although the overall membrane order does not get altered significantly. It is important to mention here that the possibility that FB₁ may exert effects other than inhibition of sphingolipid metabolism must always be considered, and an earlier report has described the inhibition of protein phosphatases by FB₁ (Fukuda *et al.*, 1996). However, such effects are observed at much higher concentrations, several orders of magnitude higher than the concentrations used by us.

The implication of membrane organization on the signaling functions of G-protein coupled receptors represents an interesting aspect. The role of membrane domains in the organization and function of the serotonin_{1A} receptor assumes relevance against this backdrop. This issue was previously addressed in our laboratory by employing the biochemical criterion of detergent insolubility. Utilizing a novel green fluorescent protein-based assay, we reported that a small yet significant fraction (~26%) of the serotonin_{1A} receptor exhibits detergent (Triton X-100) insolubility (Kalipatnapu and Chattopadhyay, 2004a, 2005b). These results are further supported by previous findings from our laboratory using a detergent-free approach (Kalipatnapu and Chattopadhyay, 2007b). Importantly, the detergent (Triton X-100) insoluble fraction of the serotonin_{1A} receptor has recently been estimated to be ~30% using density gradient centrifugation (Renner *et al.*, 2007). The close agreement in the estimate of fraction of receptors in such membrane domains, using very different approaches, points out the existence of a significant population of the receptor in such domains. It is interesting to postulate the nature and composition of such putative domains. Our laboratory has previously shown that membrane cholesterol is required for ligand binding and G-protein coupling of the serotonin_{1A} receptor (Pucadyil and Chattopadhyay, 2006; Pucadyil and Chattopadhyay, 2004a). Our present results demonstrate that sphingolipids are necessary for maintaining the function of the serotonin_{1A}

receptor. Interestingly, we observe no significant alteration in membrane cholesterol levels upon metabolic depletion of sphingolipids using FB₁. However, it is difficult to correlate functional characteristics with membrane organization of the receptor in a direct fashion.

The effect of sphingolipids on the conformation and function of membrane proteins could be due to specific interaction (Fantini, 2003). For example, the nerve growth factor receptor tyrosine kinase has been shown to interact directly with gangliosides (Mutoh *et al.*, 1995). Alternatively, it could be due to modulations in the membrane physical properties induced by sphingolipids or, due to a combination of both factors. Although our results show a slight reduction in overall membrane order upon sphingolipid depletion, specific interaction of sphingolipids with the serotonin_{1A} receptor cannot be ruled out. Interestingly, our results show that the diffusion coefficient of the receptor exhibits no significant change with sphingolipid depletion, while the mobile fraction of the receptor increases by a small yet significant extent. Such a change in the mobile fraction could be attributed to the perturbation of receptor-sphingolipid assembly that preexisted in the membrane prior to sphingolipid depletion. This proposition is supported by the recently reported copatching of a fraction (~30%) of the serotonin_{1A} receptor with GM1 (Renner *et al.*, 2007). The population of receptor in such an assembly could appear immobile in the time scale of FRAP measurements, perhaps limited by the rate of diffusion of the entire assembly. Upon sphingolipid depletion, some of these receptors may be freed resulting in an increase in mobile fraction.

Taken together, these results show that sphingolipids have an important role in maintaining the function of the serotonin_{1A} receptor, and could be relevant in understanding the role of the membrane lipid environment on the activity and signal transduction of other G-protein coupled receptors.

Chapter 5

Oligomerization of the human serotonin_{1A} receptor in live cells: A time-resolved fluorescence anisotropy approach

5.1. Introduction

A number of studies have demonstrated the capability of a variety of G-protein coupled receptors (GPCRs) to interact and form functional homo-dimers or oligomers (Shanti and Chattopadhyay, 2000; Milligan, 2006). Such oligomerization has been assumed to be involved in the proper folding of receptors, thereby providing the framework for efficient and controlled signal transduction. Importantly, recent structural data available for GPCRs suggest that the surface area of a GPCR monomer facing the cytosol is too small to support simultaneous interaction of α and β/γ subunits of G-proteins (Maggio *et al.*, 2007). Based on this consideration, it was suggested that one molecule of the G-protein trimer could be interfaced with a homo-dimer in case of rhodopsin (Maggio *et al.*, 2007). In addition, it was reported that one G-protein trimer binds the homo-dimer in case of the leukotriene B₄ receptor (Baneres and Parello, 2003). Yet, there is another school of thought which envisages that the functional unit of GPCR could be a monomer. For example, it has been argued that only one receptor molecule is capable of activating its cognate G-protein in case of rhodopsin (Chabre and La Maire, 2005) and the β_2 -adrenergic receptor (Whorton *et al.*, 2007). In spite of the wealth of information accumulated for GPCR signaling and function, there appears to be no consensus on their oligomeric status. In addition, it appears that it is not clear whether the minimum signaling unit of GPCRs is a monomer or oligomer. Preformed oligomers of certain GPCRs could serve as signaling platforms and may retain its multimeric status throughout signaling. Other GPCRs could cycle through monomeric and multimeric states in a ligand-regulated process (Park *et al.*, 2004).

The serotonin_{1A} receptor is an important G-protein coupled neurotransmitter receptor which is a central player in a multitude of physiological processes, and serves as an important target in the development of therapeutic agents for neuropsychiatric disorders (Pucadyil *et al.*, 2005a; Kalipatnapu and Chattopadhyay, 2007a). Previous results from our laboratory comprehensively demonstrated the requirement of membrane cholesterol in the

function of the serotonin_{1A} receptor (Pucadyil and Chattopadhyay, 2004a; and reviewed in Pucadyil and Chattopadhyay, 2006). Importantly, we have recently generated a cellular model of the Smith-Lemli-Opitz syndrome (SLOS), using a metabolic inhibitor of cholesterol biosynthesis (AY 9944) and showed that the function of serotonin_{1A} receptors is impaired in SLOS-like condition (Paila *et al.*, 2008; see chapter 3). In addition, we have observed that the modulation of sphingomyelin levels using fumonisin B₁ (FB₁) results in the inhibition of the function of serotonin_{1A} receptors (see chapter 4). Interestingly, the oligomerization status of this receptor is beginning to be addressed (Salim *et al.*, 2002; Łukasiewicz *et al.*, 2007; Kobe *et al.*, 2008). FRET (Fluorescence Resonance Energy Transfer) is a widely used approach to address the oligomerization status of GPCRs in cells (Lohse *et al.*, 2008). HomoFRET (*i.e.*, FRET between identical fluorophores) represents a useful approach to monitor aggregation of membrane-bound molecules in general (Sharma *et al.*, 2004) and eliminates some of the limitations of heteroFRET measurements (such as the bleed-through problem). As in the case of heteroFRET, the fluorophores must be within a critical distance of each other in homoFRET and the emission spectrum of the donor should overlap with the excitation spectrum of the acceptor. In homoFRET, donor and acceptor would correspond to identical fluorophores. Fluorophores with relatively small Stokes' shift will therefore have a greater probability of homoFRET than fluorophores with larger Stokes' shift. A unique advantage of homoFRET is that it has the potential to resolve oligomers composed of more than two monomers (Runnels and Scarlata, 1995; Yeow and Clayton, 2007). HomoFRET is usually accompanied by no change in fluorescence lifetime or intensity and is monitored by a decrease in fluorescence anisotropy (Tramier *et al.*, 2003). In this chapter, the oligomerization status of the serotonin_{1A} receptor tagged to Enhanced Yellow Fluorescent Protein (EYFP) in live cells under various conditions such as ligand stimulation and membrane lipid modulation is described, utilizing time-resolved fluorescence anisotropy measurements on cells under a fluorescence microscope.

Oligomerization of the serotonin_{1A} receptor upon acute and metabolic deprivation of cholesterol and modulation of sphingolipid levels was monitored.

5.2. Materials and methods

Materials

AY 9944, fumonisin B₁, M β CD, 8-OH-DPAT, penicillin, streptomycin, gentamycin sulfate, Tris, serotonin and sodium bicarbonate were obtained from Sigma Chemical Co. (St. Louis, MO). D-MEM/F-12 [Dulbecco's modified Eagle medium:nutrient mixture F-12 (Ham) (1:1)], fetal calf serum, and geneticin (G 418) were from Invitrogen Life Technologies (Carlsbad, CA). All other chemicals used were of the highest available quality. Water was purified through a Millipore (Bedford, MA) Milli-Q system and used throughout.

Experimental setup

The time-resolved fluorescence microscope was a combination of a picoseconds time-resolved fluorescence spectrometer and an inverted epifluorescence microscope (Srivastava and Krishnamoorthy, 1997). The time-resolved fluorescence measurements described here were carried out with a Time Correlated Single Photon Counting (TCSPC) setup coupled with a picosecond laser. A titanium-sapphire picosecond laser beam (Tsunami, Spectra Physics, USA) pumped by a diode pumped CW Nd-Vanadate laser (532 nm) (Millenia X, Spectra Physics, USA) was used to excite EYFP at 460 nm. The pulse width of the excitation laser beam was typically 1-4 ps. A pulse repetition rate of 82 MHz was reduced to a repetition rate of 4 MHz by a pulse picker. The ps pulses obtained after frequency doubling were guided to the objective lens by a dichroic mirror and focused onto the cells. Time-resolved fluorescence measurements were carried out on a Nikon Diaphot

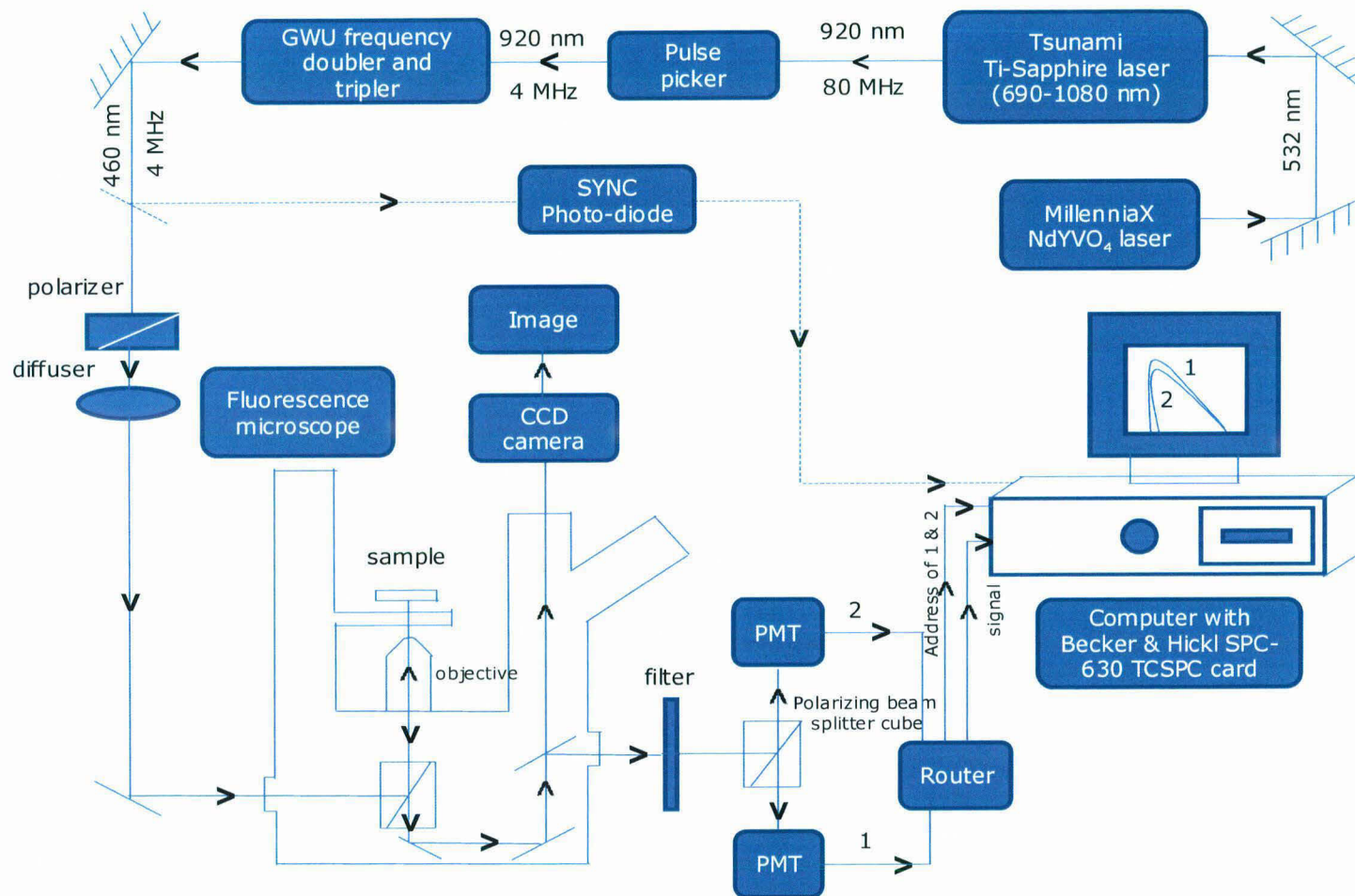


Figure 5.1. Schematic diagram of the time-resolved fluorescence microscope setup used for acquiring time-resolved fluorescence data on live cells. The main components of the setup are (i) a pico-second laser (ii) an inverted fluorescence microscope (iii) a time-resolved single photon counting (TCSPC) spectrometer.

300 microscope fitted with a 20x objective with 0.75 numerical aperture maintained at room temperature (~ 23 °C). The fluorescence emission collected by the same objective lens was passed through a cut-off filter (475 nm), a polarizer and a pinhole placed in the image plane. Time-resolution of the fluorescence signal was obtained by coupling the microscope to a TCSPC setup. The temporal resolution of the setup is ~ 50 ps and the spatial resolution is ~ 1 μm in the x-y plane. The measurements typically require ~ 100 fluorophore molecules in the observation volume. The instrument response function was estimated by the use of oxonol VI whose fluorescence lifetime is < 50 ps. The full width at half maximum height of the instrument response function estimated in this way was ~ 160 ps. All fluorescent probes were excited using the frequency doubled (460 nm) output of the Tsunami laser. Fluorescence emission was collected using the 475 nm bandpass filter. The schematic of the setup used for time-resolved fluorescence anisotropy measurements is shown in Figure 5.1.

In fluorescence lifetime measurements, the emission was monitored at the magic angle (54.7°) to eliminate the contribution from the decay of anisotropy. In time-resolved anisotropy measurements, the emission was collected at directions parallel (I_{\parallel}) and perpendicular (I_{\perp}) to the polarization of the excitation beam. The anisotropy was calculated as

$$r(t) = \frac{I_{\parallel}(t) - I_{\perp}(t)G(\lambda)}{I_{\parallel}(t) + 2I_{\perp}(t)G(\lambda)} \quad (8)$$

where $G(\lambda)$ is the geometry factor at the wavelength λ of emission. The G factor of the emission collection optics was determined in separate experiments using a standard sample (fluorescein). The fluorescence decay curves at magic angle were analyzed by deconvoluting the observed decay with the IRF to obtain the intensity decay function represented as a sum of discrete exponentials

$$I(t) = \sum_i \alpha_i \exp(-t/\tau_i) \quad (9)$$

where $I(t)$ is the fluorescence intensity at time t and α_i is the amplitude of the i^{th} lifetime τ_i such that $\sum_i \alpha_i = 1$. The time-resolved anisotropy decay was analyzed based on the model

$$I_{\parallel}(t) = I(t)[1+2r(t)]/3 \quad (10)$$

$$I_{\perp}(t) = I(t)[1-r(t)]/3 \quad (11)$$

where $I_{\parallel}(t)$ and $I_{\perp}(t)$ are the decays of the parallel (\parallel) and perpendicular (\perp) components of the emission

$$r(t) = r_0 \{ \beta_1 \exp(-t/\phi_1) + \beta_2 \exp(-t/\phi_2) \} \quad (12)$$

where r_0 is the initial anisotropy (in case of EGFP, $r_0=0.35$) and β_i is the amplitude of the i^{th} rotational correlation time ϕ_i such that $\sum_i \beta_i = 1$. The shorter component ϕ_1 representing the internal motion of the fluorophore could be modeled as a hindered rotation.

Cells and cell culture

CHO-K1 cells stably expressing the serotonin_{1A} receptor, tagged to enhanced yellow fluorescent protein (referred to as CHO-5-HT_{1A}R-EYFP), were used for all measurements. CHO-5-HT_{1A}R-EYFP cells were grown in DMEM/F-12 (1:1) supplemented with 2.4 g/l of sodium bicarbonate, 10% fetal calf serum, 60 µg/ml penicillin, 50 µg/ml streptomycin and 50 µg/ml gentamycin sulfate in a humidified atmosphere with 5% CO₂ at 37 °C. CHO-5-HT_{1A}R-EYFP cells were maintained in the above-mentioned conditions with 300 µg/ml geneticin. Cells for fluorescence microscopy and time-resolved anisotropy measurements were grown in Lab-Tek chambered coverglass (Nunc, Denmark).

Stimulation of serotonin_{1A} receptor in CHO-5-HT_{1A}R-EYFP cells

CHO-5-HT_{1A}R-EYFP cells were treated with 10 µM 8-OH-DPAT for 30 min at room temperature (~23 °C) to stimulate the serotonin_{1A} receptor.

Acute cholesterol depletion of cells in culture

Cells plated in Lab-Tek chambered coverglass were grown for 3 days followed by incubation in serum-free D-MEM/F-12 (1:1) medium for 3 h. Cholesterol depletion was carried out by treating cells with increasing concentrations of M β CD in serum-free D-MEM/F-12 (1:1) medium for 30 min at 37 °C followed by a wash with serum-free D-MEM/F-12 (1:1) medium.

Metabolic cholesterol and sphingomyelin deprivation of cells in culture

In order to achieve metabolic deprivation of cholesterol and sphingomyelin, 5 μ M AY 9944 and 6 μ M FB₁ were used, respectively. Stock solutions of AY 9944 and FB₁ were prepared in water and added to cells grown for 24 h to a final concentration of 5 μ M AY 9944 and 6 μ M FB₁, and incubated in 5% serum for 63–66 h. Control cells were grown under similar conditions without any treatment.

Statistical analysis of data

Apparent initial anisotropy (r_{in}^{app}) values were obtained by averaging the first few (typically 4-5) early anisotropy values after stabilization. The limiting (or fundamental) anisotropy is defined as r_0 and was estimated as the value of r_{in}^{app} obtained for EGFP in 80% glycerol. Amplitude of the unresolved fast correlation time (β_1) attributed to homoFRET was obtained using the calculation shown in Appendix. Frequency distribution analysis and plotting were performed using Microcal Origin software version 6.0 (OriginLab Corp., Northampton, MA, USA). Significance levels were estimated using student's two-tailed unpaired t-test using the Microcal Origin software version 6.0 (OriginLab Corp., Northampton, MA, USA).

5.3. Results and Discussion

In general, the observed fluorescence anisotropy decay (see Figure 5.2) could be attributed to two factors. (i) homo energy transfer (homoFRET) between identical fluorophores, and (ii) rotational dynamics of fluorophores in the time scale of measurements. The rotation of EYFP is slow due to its relatively large size, and therefore does not result in depolarization of fluorescence (Piston and Kremers, 2007), in case of 5-HT_{1A}R-EYFP. Under these conditions, the initial fast reduction in anisotropy could be attributed to homoFRET between EYFP tagged to the serotonin_{1A} receptor, implying that the two serotonin_{1A} receptors are in close proximity.

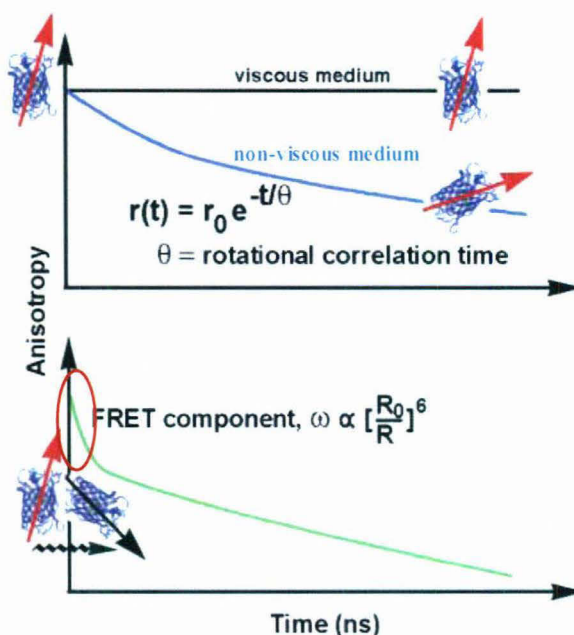


Figure 5.2. Schematic diagram showing the expected time-resolved fluorescence anisotropy decay profiles for dilute GFP-fluorophores (top) immobilized in a viscous solution (black line) or freely rotating in a non-viscous solution (blue line). From this decay profile in non-viscous medium, rotational correlation time (θ) of the fluorophore could be calculated by fitting the decay profile to a model. Interestingly, fluorophores undergoing homoFRET (green line, bottom) have an additional fast fluorescence anisotropy decay rate, ω (highlighted in the bottom panel). Careful analysis of homoFRET data could provide information on oligomerization of GFP tagged receptors. Adapted and modified from Sharma *et al.* (2004).

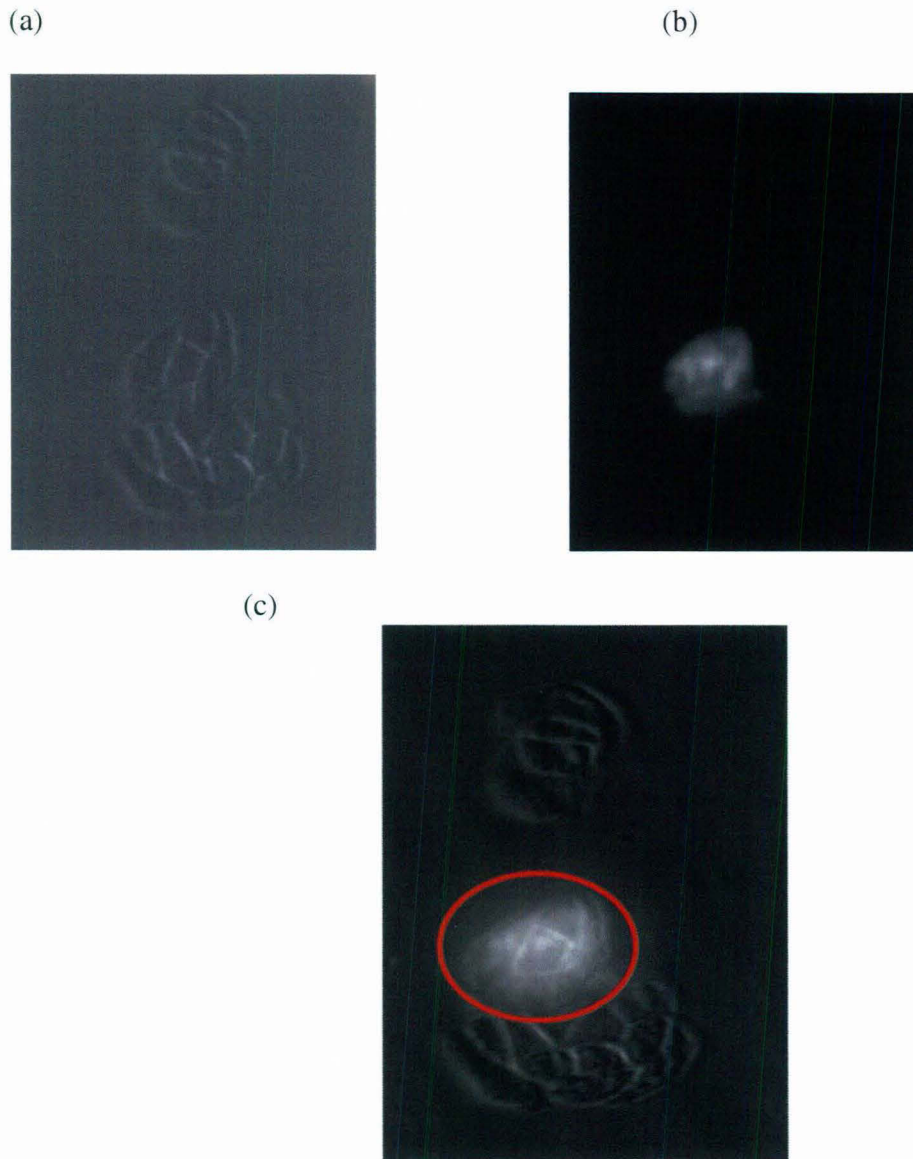


Figure 5.3. Representative images of CHO cells stably expressing the human serotonin_{1A} receptor tagged with EYFP (CHO-5-HT_{1A}R-EYFP) under (a) transmitted light, (b) laser light showing fluorescence image of CHO-5-HT_{1A}R-EYFP cells upon excitation at 460 nm. Panel (c) shows CHO-5-HT_{1A}R-EYFP cells under both laser and transmitted light. Cells that are fluorescent upon exposure to laser are highlighted. Fluorescence images of cells grown in Lab-Tek chambers were acquired in the presence of HEPES-Hanks buffer. See section 5.2 for other details.

Previous results from our laboratory have demonstrated that heterologously expressed serotonin_{1A} receptor, tagged to EYFP on its cytoplasmic end, in CHO cells is

functionally similar to the native receptor (Pucadyil *et al.*, 2004a). Figure 5.3 shows representative images of CHO-5-HT_{1A}R-EYFP cells under transmitted and laser light sources. Polarization of emitted light could be reduced by the optical setup with high

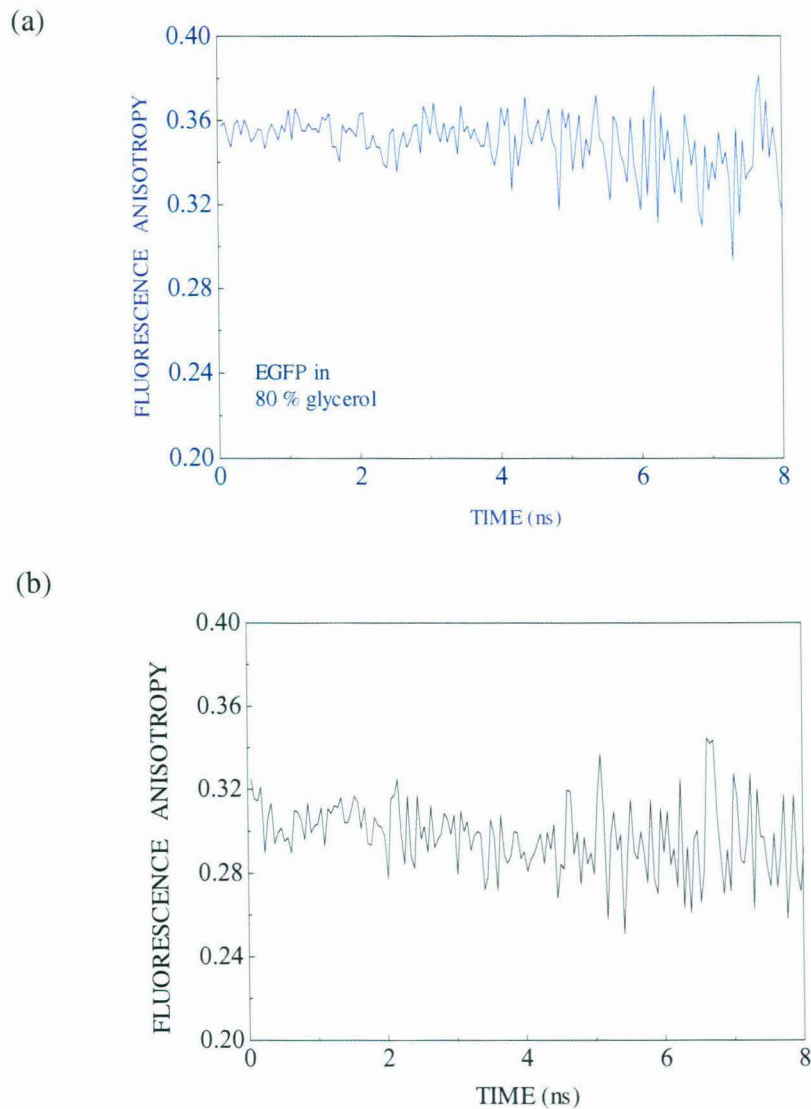


Figure 5.4. Representative time-resolved fluorescence anisotropy decays of (a) EGFP in 80% glycerol and (b) EYFP tagged to the serotonin_{1A} receptor. EGFP and EYFP was excited at 460 nm and emission was collected using a cut-off filter of 475 nm and measured with TCSPC setup.

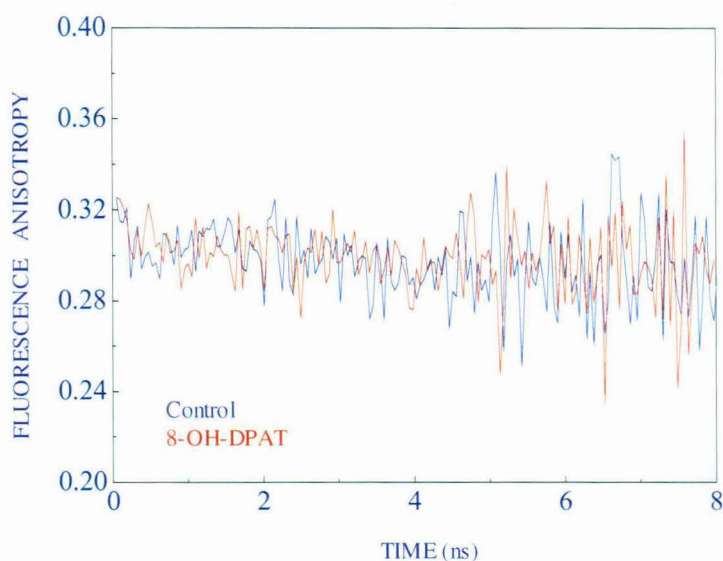


Figure 5.5. Representative fluorescence anisotropy decays of the serotonin_{1A} receptor tagged to EYFP under control condition (blue) and upon stimulation with specific agonist, 8-OH-DPAT at 10 μ M concentration (red). EYFP was excited at 460 nm and emission was collected using a cut-off filter of 475 nm and measured with TCSPC setup. Experiments were carried out on CHO-5-HT_{1A}R-EYFP cells in HEPES-Hanks buffer (pH 7.4) at room temperature (\sim 23 $^{\circ}$ C).

numerical aperture lenses. It has therefore been suggested that polarized FRET experiments should be limited to imaging with lenses with a numerical aperture of ≤ 1.0 (Piston and Kremers, 2007). Keeping this in mind, all experiments were carried out using 20x objective with 0.75 NA. Preservation of polarization in the microscope set-up was confirmed by the recovery of anisotropy decay kinetics of fluorescein and EGFP wherein the observed initial anisotropy was 0.35-0.36 (Figure 5.4a).

Constitutive oligomerization of the serotonin_{1A} receptor

Enhanced Green Fluorescent Protein (EGFP) in 80% glycerol shows a limiting or fundamental anisotropy (r_0) of \sim 0.35 (see Figure 5.4), in agreement with the value reported earlier (Saxena *et al.*, 2005). Limiting anisotropy is a fundamental property of a

fluorophore and depends only on the angle between the absorption and emission dipoles (transition moments) and is measured in the absence of any rotational diffusion. We have provided apparent initial anisotropy (r_{in}^{app}) values (see section 5.2) in a given condition and control condition in each figure for comparison. Table 5.2 shows representative values of r_{in}^{app} under these conditions. These values in the table 5.2 should not be used for comparison of r_{in}^{app} between a given condition and control due to unavoidable day-to-day variations in r_{in}^{app} . Our results show an apparent initial anisotropy (r_{in}^{app}) of ~ 0.30 in cells under control conditions (Figure 5.4). This value is significantly lower compared to the corresponding value of EYFP in glycerol (~ 0.38 , Borst *et al.*, 2005). This reduction in r_{in}^{app} could be attributed to rapid and unresolved homoFRET. A possible interpretation for this could be homoFRET in pre-existing oligomers of the receptor. Interestingly, such constitutive oligomerization, a relatively new paradigm in GPCRs, has been demonstrated in case of the neuropeptide Y receptor 1 (Harding *et al.*, 2009) and angiotensin II type 2 (AT₂) receptors (Miura *et al.*, 2005). For example, in case of AT₂ receptors, constitutively active homo-oligomers have been reported to be translocated to the cell membrane and induce cell signaling, independent of receptor conformation and ligand stimulation (Miura *et al.*, 2005). There could be another possibility where the oligomerization could be constitutive, yet ligand-dependent, such as in case of the thyrotropin-releasing hormone receptor (Kroeger *et al.*, 2001). Interestingly, the β_2 -adrenergic receptor, a closely related GPCR to the serotonin_{1A} receptor, exhibits constitutive activity (Rasmussen *et al.*, 2007). Sequence analysis of the serotonin_{1A} receptor gene shows considerable ($\sim 43\%$) amino acid similarity with the β_2 -adrenergic receptor in the transmembrane domain (Kalipatnapu and Chattopadhyay, 2007a). Rasmussen and coworkers attributed the constitutive activity of the β_2 -adrenergic receptor to its structurally flexible conformation. Interestingly, when coexpressed with G_z in Sf9 cells, the serotonin_{1A} receptor exhibits agonist-independent activation (Barr and Manning, 1997). Whether constitutive oligomerization could be related to constitutive activity of the receptor represents an intriguing possibility.

Oligomerization of the serotonin_{1A} receptor upon stimulation with agonist

Ligand-dependent homo- and hetero-oligomerization of dopamine (D₂) and adenosine (A_{2A}) receptors in living neuronal cells was recently reported using Bimolecular Fluorescence Complementation (Vidi *et al.*, 2008). In order to explore the oligomerization status of the human serotonin_{1A} receptor upon ligand stimulation, CHO-5-HT_{1A}R-EYFP cells were treated with 8-OH-DPAT (10 μM). Figure 5.5 shows representative fluorescence anisotropy decay profiles of control and ligand-stimulated CHO-5-HT_{1A}R-EYFP cells. 8-OH-DPAT acts as a specific agonist of the serotonin_{1A} receptor and displays high affinity ($K_d \sim 1$ nM) for the receptor (Pucadyil *et al.*, 2004a). The apparent initial anisotropy (r_{in}^{app}) in CHO-5-HT_{1A}R-EYFP cells under control conditions was ~ 0.29 and the corresponding value upon ligand stimulation is ~ 0.27 . Our results show that there is no significant change in r_{in}^{app} upon stimulation of serotonin_{1A} receptors with its specific agonist 8-OH-DPAT (see Figure 5.6). This indicates that there is no significant change in oligomerization status of the receptor upon ligand stimulation.

Acute but not metabolic deprivation of cholesterol affects the oligomerization of the serotonin_{1A} receptor

The modulatory role of membrane cholesterol on ligand binding activity and G-protein coupling of the hippocampal serotonin_{1A} receptor was previously shown by depleting cholesterol from native membranes using methyl-β-cyclodextrin (MβCD) (Pucadyil and Chattopadhyay, 2004a). We have recently proposed that membrane cholesterol requirement for receptor function could be specific and cholesterol may occupy nonannular binding sites on the receptor (Paila *et al.*, 2009; see chapter 1). We treated CHO-5-HT_{1A}R-EYFP cells with 10 mM MβCD to achieve acute depletion of cholesterol and with 5 μM AY 9944 for metabolic deprivation of cholesterol. AY 9944 is a specific metabolic inhibitor of 7-dehydrocholesterol reductase (7-DHCR) in the biosynthetic pathway of cholesterol (Dvornik *et al.*, 1963). Therefore, treatment of CHO-5-HT_{1A}R-

EYFP cells with AY 9944 results in reduction of cholesterol with a concomitant accumulation of 7-DHC (and its isomer, 8-DHC), giving rise to conditions mimicking SLOS (see chapter 3). SLOS serves as an appropriate condition to delineate the specific and global effects of cholesterol in the function of the serotonin_{1A} receptor, since the two aberrant sterols that get accumulated in SLOS, *i.e.*, 7- and 8-DHC, differ with cholesterol only in a double bond.

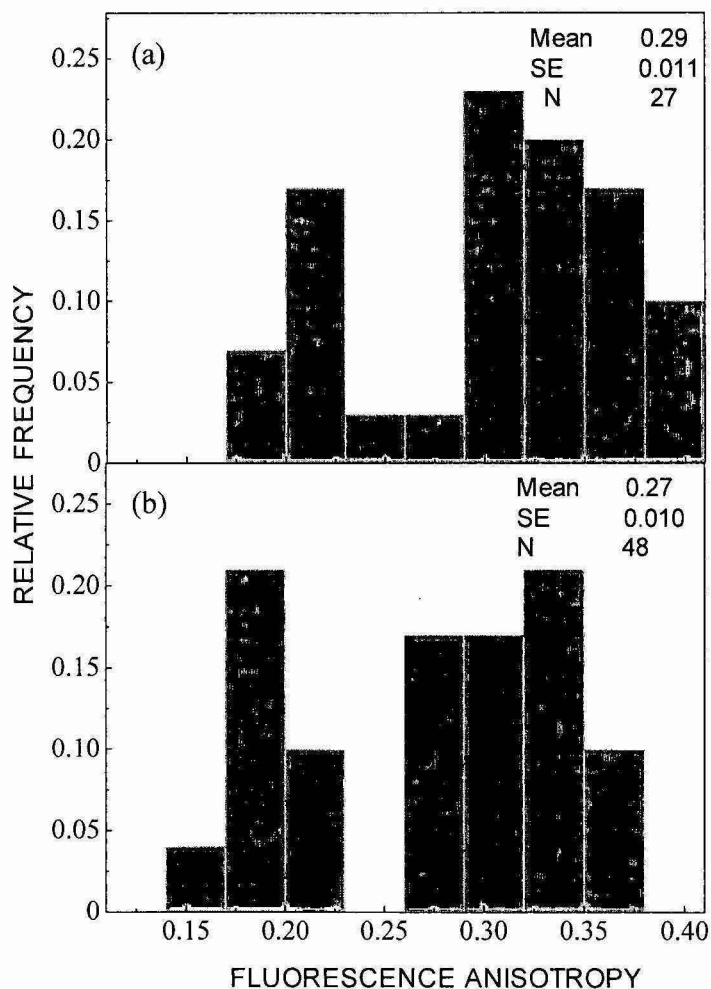


Figure 5.6. Frequency distribution histograms of the fluorescence anisotropy of 5-HT_{1A}R-EYFP. Panels a and b show the fluorescence anisotropy histograms for control (untreated) cells, and upon ligand stimulation with 8-OH-DPAT, respectively. The means \pm SE are shown in all cases. N represents the number of independent measurements performed in each case. See section 5.2 for other details.

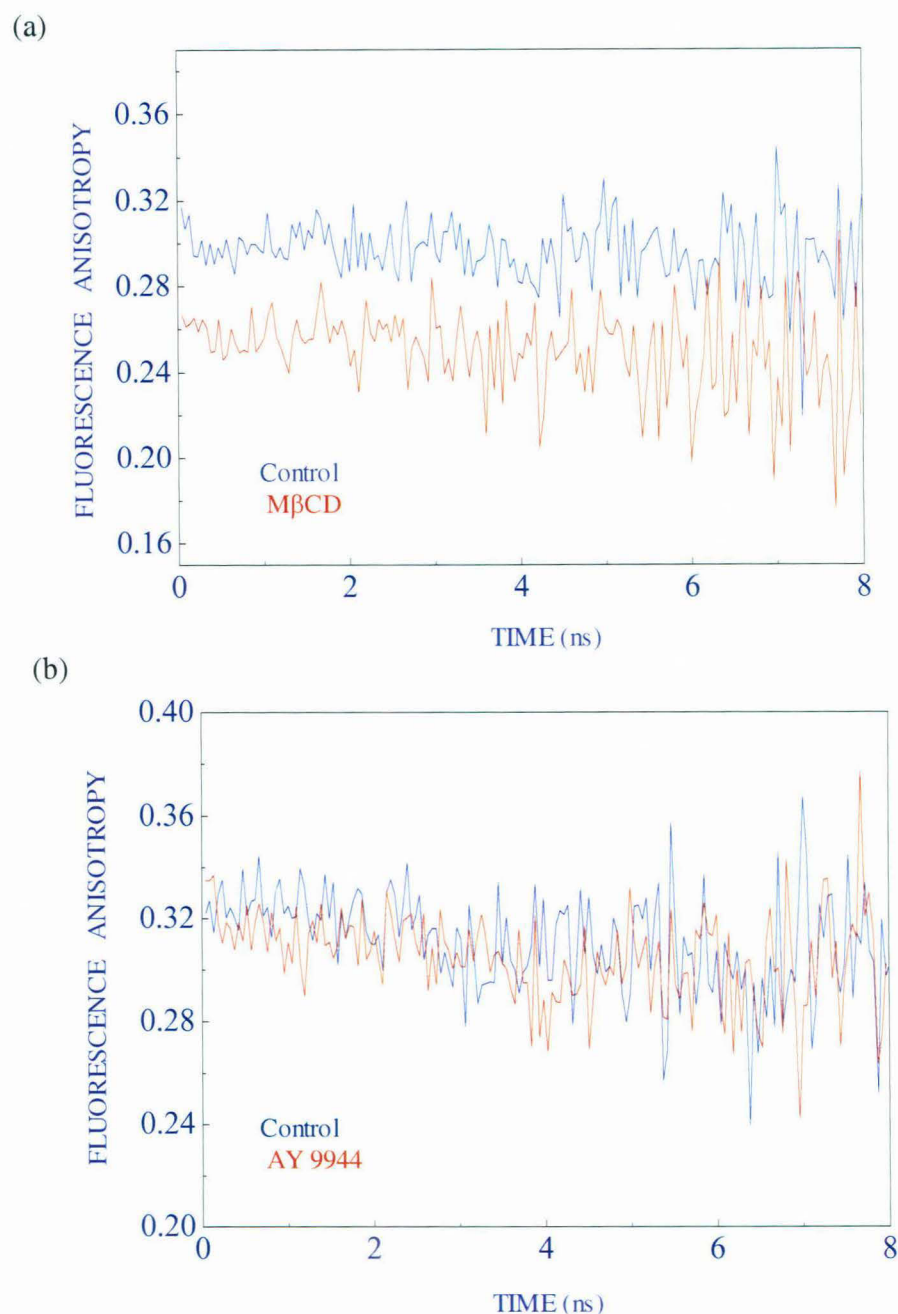


Figure 5.7. Representative fluorescence anisotropy decays of the serotonin_{1A} receptor tagged to EYFP upon acute and metabolic cholesterol deprivation. Panel (a) shows anisotropy decays of CHO-5-HT_{1A}-EYFP cells under control (blue) and acute cholesterol depleted (red) conditions. Acute depletion of cholesterol was achieved using 10 mM M β CD. Panel (b) shows anisotropy decays of CHO-5-HT_{1A}-EYFP cells under control (blue) and metabolic cholesterol deprived (red) conditions. Metabolic deprivation of cholesterol was achieved using 5 μ M AY 9944. EYFP was excited at 460 nm and emission was collected using a cut-off filter of 475 nm and measured with TCSPC setup. Experiments were carried out on cells in HEPES-Hanks buffer (pH 7.4) at room temperature (\sim 23 $^{\circ}$ C).

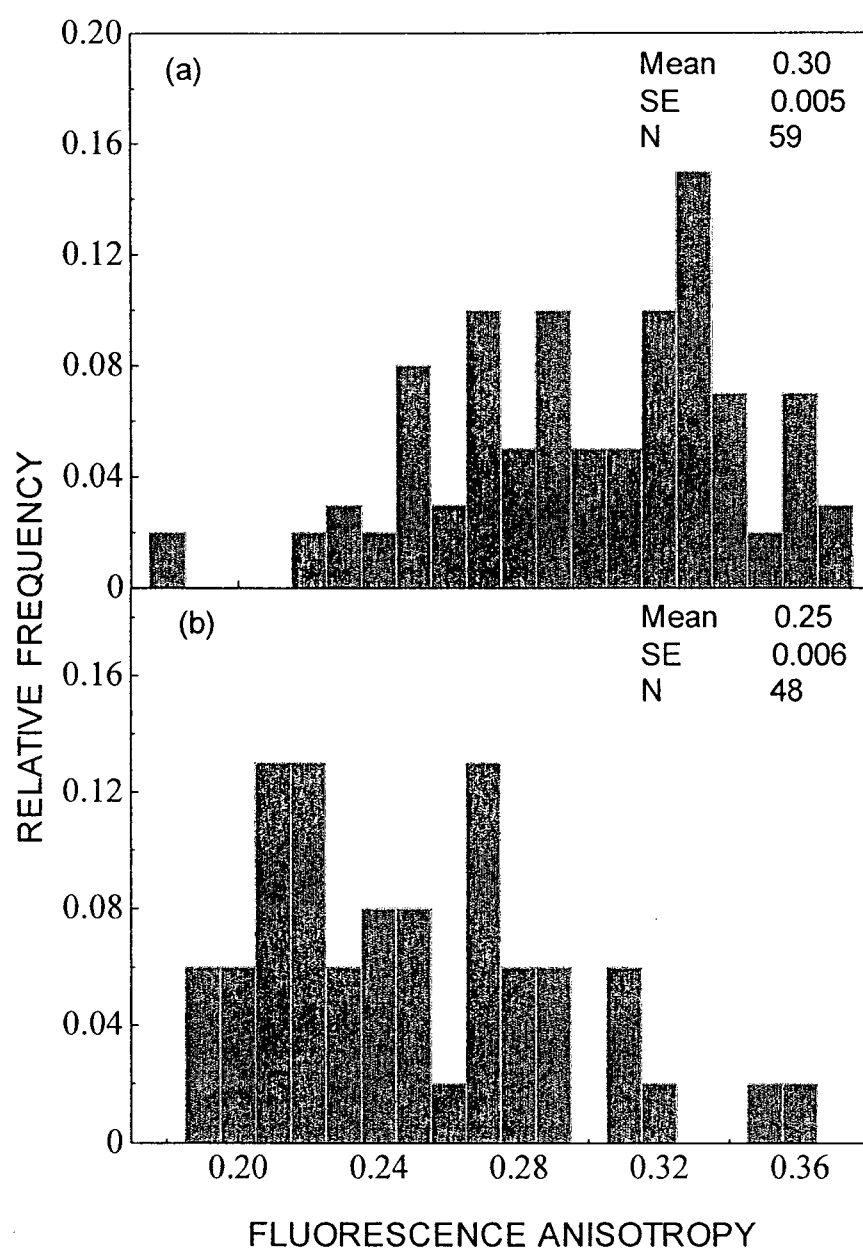


Figure 5.8. Frequency distribution histograms of the fluorescence anisotropy of 5-HT_{1A}R-EYFP. Panels a and b show the fluorescence anisotropy histograms for control (untreated) cells, and acute cholesterol depleted cells, respectively. Acute cholesterol depletion was achieved using 10 mM M β CD. The means \pm SE are shown in all cases. N represents the number of independent measurements performed in each case. See section 5.2 for other details.

Table 5.1

Representative fluorescence anisotropy decay parameters of the serotonin_{1A} receptor tagged to EYFP under control and acute cholesterol-depleted conditions using M β CD*

| | ϕ_1 (ns) | β_1 | ϕ_2 (ns) | β_2 | r_0 | r_{ss} |
|--|---------------|-----------|---------------|-----------|-------|----------|
| Control | 0.21 | 0.24 | 155 | 0.76 | 0.388 | 0.298 |
| Acute cholesterol depletion (using M β CD) | 0.14 | 0.35 | 105 | 0.65 | 0.390 | 0.254 |

* EYFP was excited at 460 nm and emission was collected using a cut-off filter of 475 nm and measured with TCSPC setup.

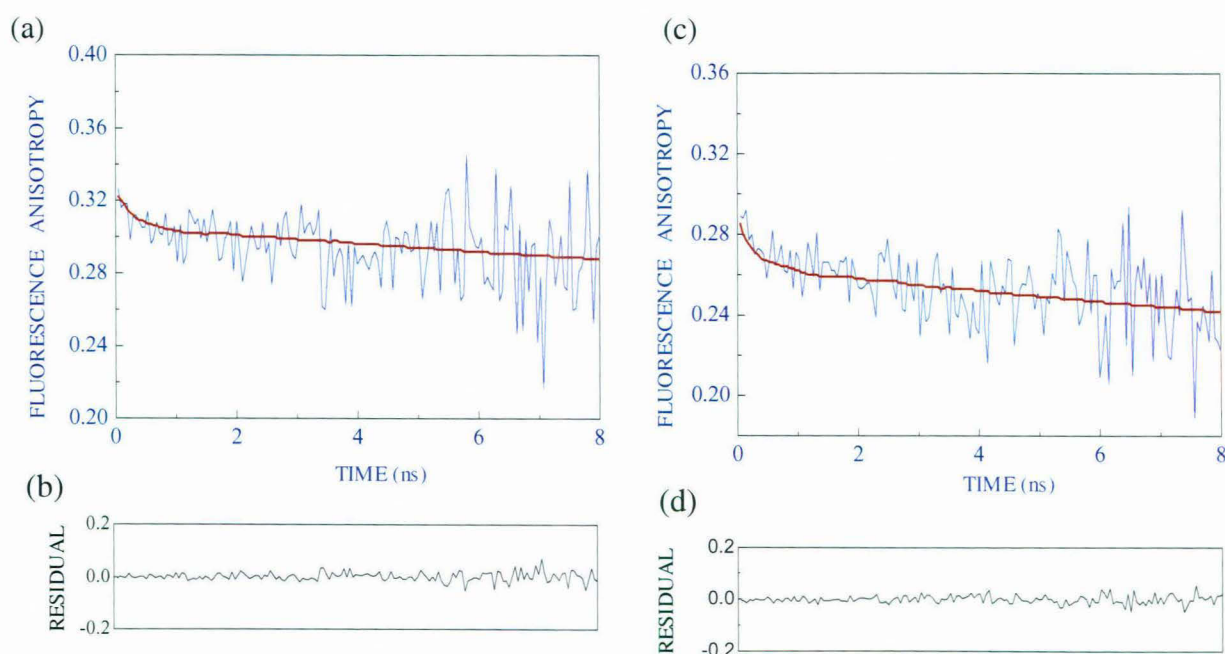


Figure 5.10. Representative time resolved fluorescence anisotropy decays (experimental and calculated) of serotonin_{1A} receptor tagged to EYFP under (a) control and (c) acute cholesterol-depleted conditions. Acute cholesterol depletion was achieved using M β CD. Fits to biexponential anisotropy decay model are shown. Panels (b) and (d) show the autocorrelation function of the weighted residuals. EYFP was excited at 460 nm and emission was collected using a cut-off filter of 475 nm and measured with the TCSPC setup. Experiments were carried out on CHO-5-HT_{1A}R-EYFP cells in HEPES-Hanks buffer (pH 7.4) at room temperature (~ 23 °C). See section 5.2 for other details.

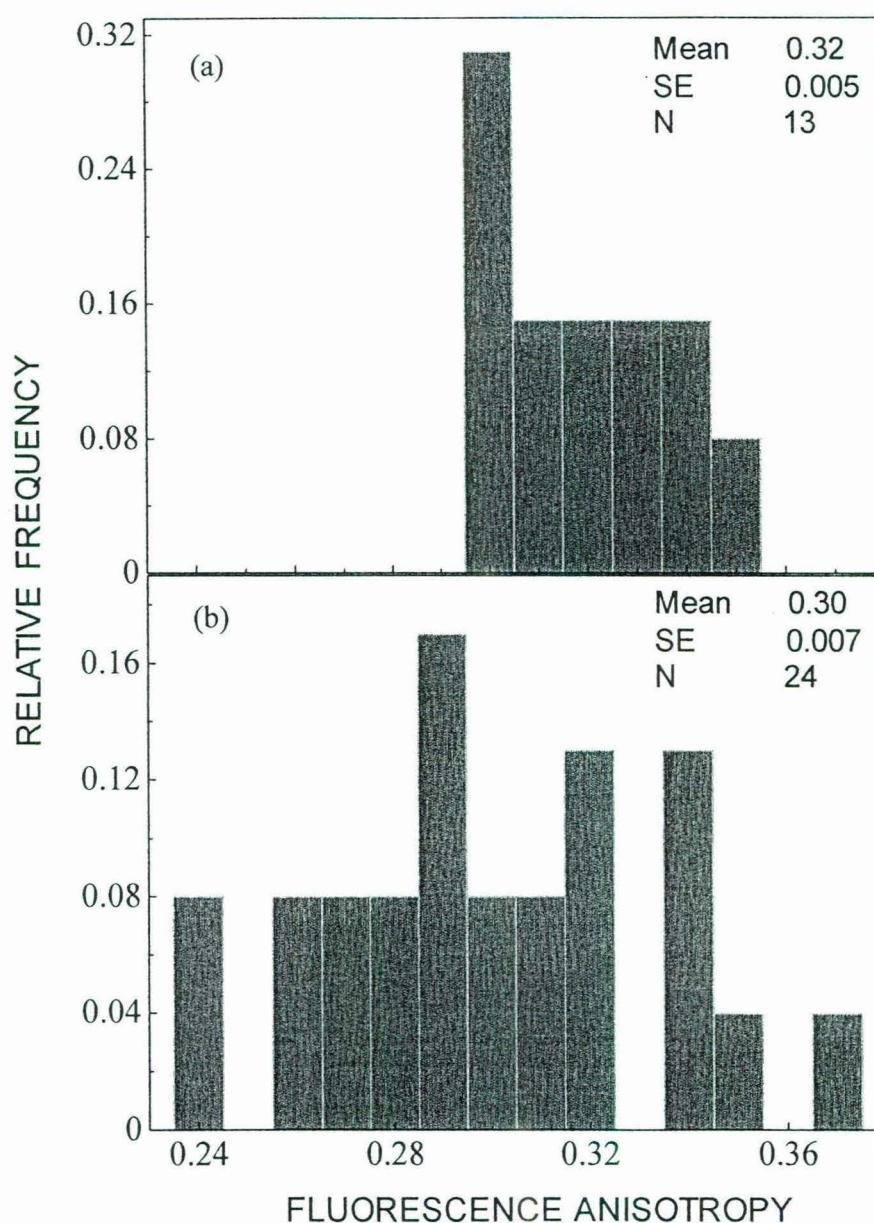


Figure 5.10. Frequency distribution histograms of the fluorescence anisotropy of 5-HT_{1A}R-EYFP. Panels a and b show the fluorescence anisotropy histograms for control (untreated) cells, and metabolic cholesterol depleted cells, respectively. Metabolic cholesterol depletion was achieved using 5 μ M AY 9944, which is a biosynthetic inhibitor of 7-DHCR. The means \pm SE are shown in all cases. N represents the number of independent measurements performed in each case. See section 5.2 for other details.

Representative anisotropy decays of control and cholesterol depleted CHO-5-HT_{1A}R-EYFP cells are depicted in Figure 5.7. The apparent initial anisotropy (r_{in}^{app}) is

decreased upon treatment with M β CD to ~ 0.25 (Figure 5.8). This reduction is significant ($p < 0.001$), implying that serotonin_{1A} receptors reorganize into higher oligomers upon acute cholesterol depletion. These results assume relevance in the light of previous results from our laboratory (Kalipatnapu and Chattopadhyay, 2005; Pucadyil and Chattopadhyay, 2007b). It was earlier shown using detergent insolubility using Triton X-100 that the serotonin_{1A} receptor expressed in CHO cells is predominantly detergent-soluble (Kalipatnapu and Chattopadhyay, 2004a). These results showed that a small yet significant fraction of the serotonin_{1A} receptor exhibits detergent insolubility, which increases upon depletion of membrane cholesterol using M β CD (Kalipatnapu and Chattopadhyay, 2005b). An independent study employing Fluorescence Recovery After Photobleaching (FRAP) with varying bleach spot radii showed that lateral diffusion parameters are altered in a manner that is consistent with dynamic confinement of serotonin_{1A} receptors in the plasma membrane upon acute cholesterol depletion (Pucadyil and Chattopadhyay, 2007b). These results, along with the present results showing change in oligomerization status upon acute cholesterol depletion, suggest a reorganization of serotonin_{1A} receptors in cholesterol-depleted cells with oligomerized receptors occupying larger domains.

On the other hand, metabolic depletion of cholesterol using AY 9944 results in a significant ($p < 0.06$) reduction in r_{in}^{app} to ~ 0.30 (see Figure 5.10). The reduction in r_{in}^{app} , however, is considerably less than the corresponding reduction obtained in case of acute cholesterol depletion using M β CD. The reduction in r_{in}^{app} could be attributed to the oligomerization of the receptor. However, reduction in r_{in}^{app} due to change in membrane lipid environment, arising due to the presence of 7- and 8-DHC cannot be ruled out. Interestingly, we have recently shown that the immediate biosynthetic precursors of cholesterol could not support the function of the serotonin_{1A} receptor (Singh *et al.*, 2007; Paila *et al.*, 2008) and leads to change in membrane organization and dynamics (Shrivastava *et al.*, 2008).

Modulation of sphingolipid levels of CHO-5-HT_{1A}R-EYFP cells does not alter the oligomerization of the serotonin_{1A} receptor

Sphingolipids are essential components of eukaryotic cell membranes and are thought to be involved in a variety of cellular functions which include cellular growth, differentiation, and signaling. Mycotoxins such as fumonisins can disrupt sphingolipid metabolism and treatment with fumonisins represents an efficient approach to modulate cellular sphingolipid levels. We modulated sphingolipid levels in CHO-5-HT_{1A}R-EYFP cells, by metabolically inhibiting the biosynthesis of sphingolipids using FB₁. It was estimated that ~80% of sphingomyelin is metabolically depleted in CHO-5-HT_{1A}R-EYFP cells with 6 μ M FB₁ (see chapter 4).

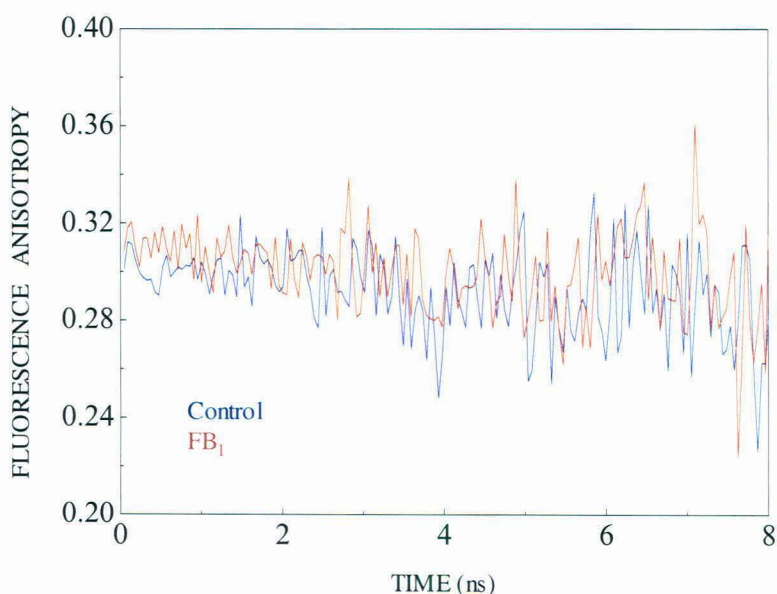


Figure 5.11. Representative fluorescence anisotropy decays of the serotonin_{1A} receptor tagged to EYFP under control (blue) and sphigomyelin-depleted conditions (red). FB₁ (6 μ M) was used to modulate sphingomyelin levels of CHO-5-HT_{1A}R-EYFP cells. All other conditions are as described in Figure 5.5.

Figure 5.11 shows representative anisotropy decays of EYFP tagged to serotonin_{1A} receptor under control and metabolic sphingolipid deprived conditions. Our results show that

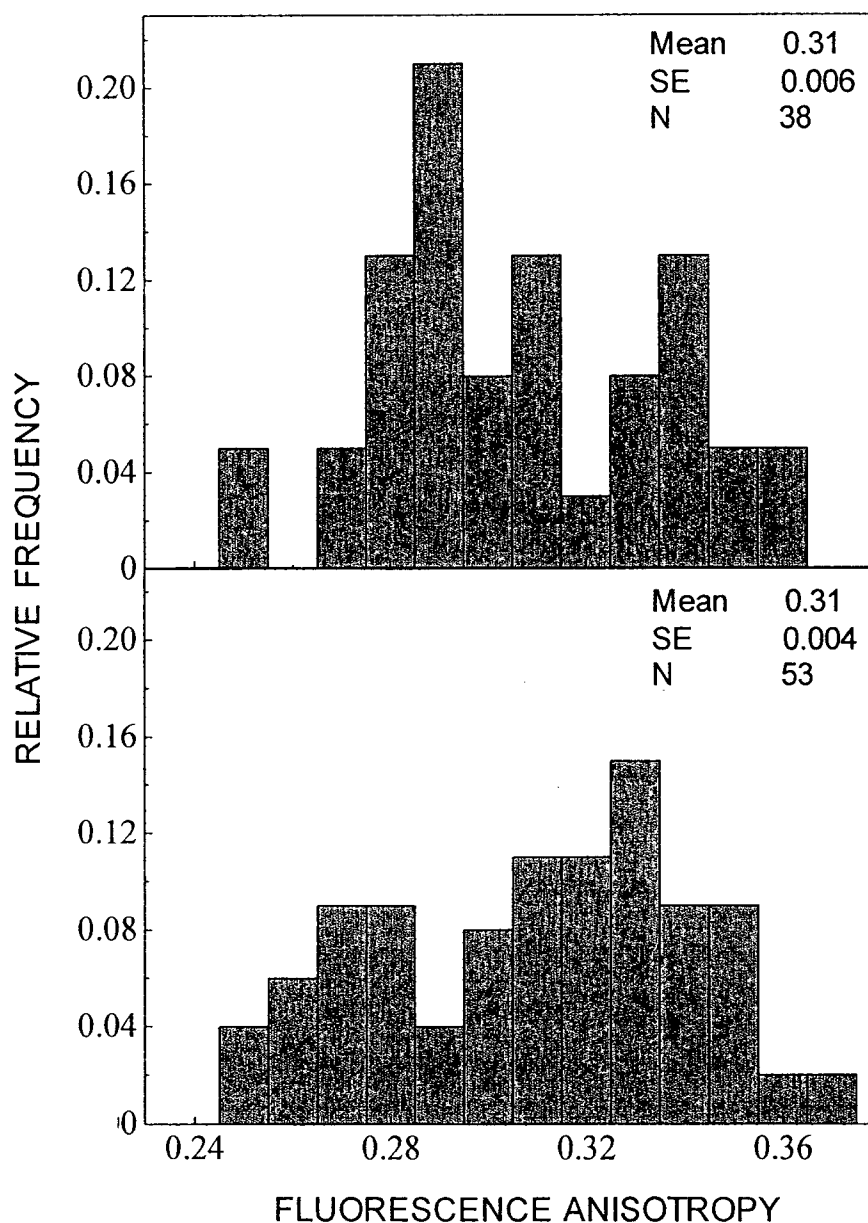


Figure 5.12. Frequency distribution histograms of the fluorescence anisotropy of 5-HT_{1A}R-EYFP. Panels a and b show the fluorescence anisotropy histograms for control (untreated) cells, and FB₁ treated cells, respectively. The means \pm SE are shown in all cases. N represents the number of independent measurements performed in each case. See section 5.2 for other details.

r_{in}^{app} value remains unaltered upon metabolic sphingolipid depletion (see Figure 5.12).

These results suggest that the oligomerization status of the serotonin_{1A} receptor is unaffected upon metabolic sphingolipid depletion.

Fluorescence anisotropy is independent of the intensity from CHO-5-HT_{1A}R-EYFP cells

The oligomerization status of membrane receptors could be influenced by receptor expression levels as was recently shown in the case of neurokinin-1 receptor (Meyer *et al.*, 2006). In order to examine any systematic change in the apparent initial anisotropy with fluorescence intensity, anisotropy decays obtained from cells at varying fluorescence intensities were monitored and plotted in Figure 5.13. Negative correlation between the intensity and r_{in}^{app} could imply that higher brightness would correspond to higher levels of constitutive clustering of receptors resulting in lower values of r_{in}^{app} . Figure 5.13 shows that r_{in}^{app} values do not exhibit any dependence (trend) on fluorescence intensity of CHO-5-HT_{1A}R-EYFP cells, reinforcing that the present results on oligomerization of the serotonin_{1A} receptor are independent of receptor expression levels.

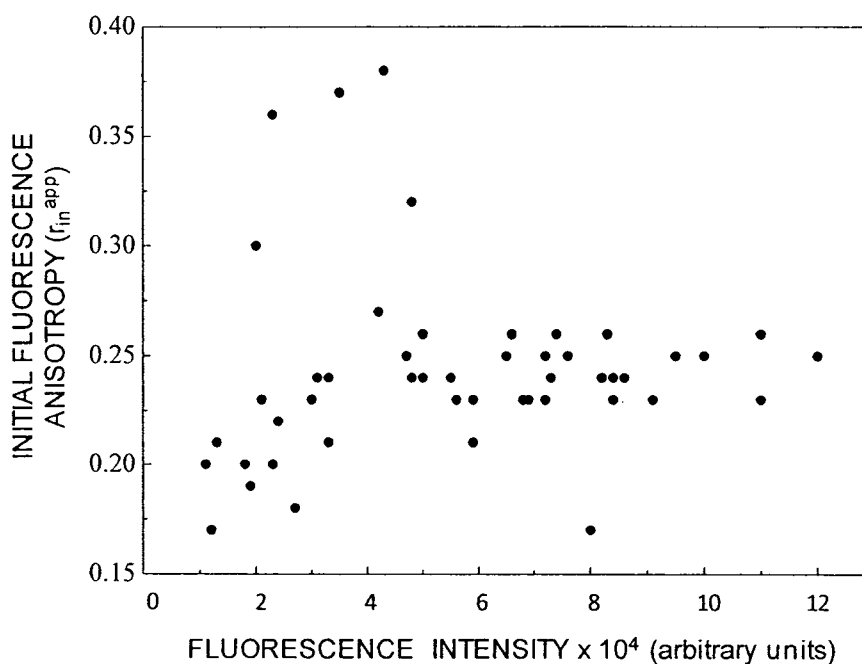


Figure 5.13. Apparent initial anisotropy values of the serotonin_{1A} receptor tagged to EYFP are independent of the fluorescence intensity from CHO-5-HT_{1A}R-EYFP cells. Excitation wavelength was 460 nm. These measurements are done by moving the focused laser beam to different locations within a cell or different cells showing different brightness. All other conditions are as in Figure 5.5.

Several studies showed that oligomerization occurs early after biosynthesis of GPCRs, suggesting that it has a primary role in receptor maturation (Terrillon and Bouvier, 2004) and oligomerization might be a prerequisite for transport of GPCRs to the cell surface.

Table 5.2

Apparent initial time-resolved fluorescence anisotropy of CHO-5-HT_{1A}R-EYFP cells under various conditions

| CHO-5-HT _{1A} R-EYFP cells | Apparent initial fluorescence anisotropy (r_{in}^{app}) | β_1^b |
|--|---|--------------|
| Control ^a | 0.29 ± 0.011 | 0.24 ± 0.030 |
| Ligand (8-OH-DPAT) treated | 0.27 ± 0.010 | 0.29 ± 0.026 |
| Control ^a | 0.30 ± 0.005 | 0.21 ± 0.014 |
| MβCD treated (acute depletion) | 0.25 ± 0.006 | 0.34 ± 0.016 |
| Control ^a | 0.32 ± 0.005 | 0.16 ± 0.013 |
| AY 9944 treated (metabolic depletion) | 0.30 ± 0.007 | 0.21 ± 0.018 |
| Control ^a | 0.31 ± 0.006 | 0.19 ± 0.012 |
| Sphingolipid-depleted (using FB ₁) | 0.31 ± 0.004 | 0.18 ± 0.011 |

^aFor each condition, corresponding control experiment was performed due to unavoidable day-to-day variations in r_{in}^{app} . In our data analysis, we compared r_{in}^{app} under a specific condition and the same value from the corresponding control.

^bAmplitude of the unresolved fast correlation time (β_1) attributed to homoFRET (see Appendix).

For example, it has been reported using mutants of the β_2 -adrenergic receptor (Salahpour *et al.*, 2004), V2 vasopressin receptor (Zhu and Wess, 1998) and the D₂ dopamine receptor (Lee *et al.*, 2000) that these mutants could inhibit the transport of respective wild-type receptors to the cell surface. This is due to the ability of the mutants to disrupt the homodimerization process, necessary for transport. For example, disruption of

oligomerization by mutating the residues in the β_2 -adrenergic receptor resulted in reduction in the cell surface expression of this receptor (Salahpour *et al.*, 2004). Our present results, however, do not provide any information on the biogenesis of constitutive oligomers of the serotonin_{1A} receptor. However, it is not clear whether oligomerization during biosynthesis is a generally followed pathway in all GPCRs (Park *et al.*, 2004).

There are a few reports in the literature on the oligomerization of other serotonin receptors. Serotonin_{2C} receptors are previously shown to function as homo-dimers expressed on plasma membranes of live cells (Herrick-Davis *et al.*, 2004). In order to explore the ligand/receptor/G-protein stoichiometry, Herrick-Davis and coworkers coexpressed mutated/inactive serotonin_{2C} receptors with wild-type/functional serotonin_{2C} receptors. Interestingly, the results showed that inactive serotonin_{2C} receptors inhibit wild-type serotonin_{2C} receptor function by forming nonfunctional heterodimers expressed on the plasma membrane. These results are consistent with the model in which a GPCR dimer binds two molecules of ligand and a G-protein, and indicate that dimerization is essential for the serotonin_{2C} receptor function (Herrick-Davis *et al.*, 2005). One of the earlier observations that serotonin receptors could form oligomers was provided from the studies of Xie *et al.* (1999) where the authors demonstrated that serotonin_{1B} and serotonin_{1D} receptors exist as monomers and homo-dimers when expressed alone and as monomers and heterodimers when coexpressed.

These results have potential implications in future drug design and development in pathophysiological conditions in which serotonin_{1A} receptors are implicated. Homo- and heterooligomerization of GPCRs assumes greater significance in the pharmacology of GPCRs since oligomerization gives rise to pharmacological diversity (Terrillon and Bouvier, 2004), opening new avenues for therapeutics (Shanti and Chattopadhyay, 2000). This would also offer an attractive mechanism for increasing the diversity of cellular responses to extracellular signals or stimuli.

Chapter 6

The human serotonin_{1A} receptor expressed
in neuronal cells: Toward a native ^{28.}
environment for neuronal receptors.

6.1. Introduction

Mammalian cells in culture heterologously expressing membrane receptors represent convenient systems to address problems in receptor biology due to higher expression levels of the receptors (Tate and Grisshammer, 1996). An important consideration in such expression systems is selecting a cell type which is derived from the tissue of natural occurrence of the receptor. This is particularly true for receptors of neural origin since the membrane lipid composition of cells in the nervous system is unique. This unique membrane lipid composition has been correlated with increased complexity in the organization of the nervous system during evolution (Sastry, 1985). Organization and dynamics of cellular membranes in the nervous system therefore play a crucial role in the function of neuronal membrane receptors. Lipids found in neuronal membranes are often necessary for maintaining the structure and function of neuronal receptors. For example, it has previously been shown that gangliosides specifically interact with proteins localized in the exoplasmic leaflet of neuronal plasma membranes (Prioni *et al.*, 2004). Moreover, spatiotemporal signaling in neuronal membranes is believed to be stringently controlled by membrane domains (such as 'lipid rafts') formed by specific lipids and through lipid-protein interactions (Tsui-Pierchala *et al.*, 2002; Fivaz and Meyer, 2003; Golub *et al.*, 2004; Gielen *et al.*, 2006). Keeping this in mind, the pharmacological and functional characterization of the human serotonin_{1A} receptor stably expressed in HN2 cells, which are a hybrid cell line between hippocampal cells and mouse neuroblastoma (Lee *et al.*, 1990), are described in this chapter. Further, it is demonstrated that agonist and antagonist binding to the receptor exhibit differential sensitivity to the non-hydrolyzable GTP analogue, GTP- γ -S, as was observed earlier with the native receptor from bovine hippocampus. In addition, the serotonin_{1A} receptor expressed in these cells displays typical downstream signaling of the receptor as monitored by ligand-dependent changes in cAMP levels. These results show that the human serotonin_{1A} receptor expressed in HN2 cells displays characteristic features

found in the native receptor isolated from bovine hippocampus and represents a realistic model system for the receptor.

6.2. Materials and methods

Materials

EDTA, fetal calf serum, MgCl₂, MnCl₂, 8-OH-DPAT, *p*-MPPI, penicillin, streptomycin, gentamycin sulfate, polyethylenimine, PMSF, serotonin, sodium bicarbonate, and Tris were obtained from Sigma Chemical Co. (St. Louis, MO). DMEM and G-418 were from Life Technologies (Grand Island, NY). GTP- γ -S was from Roche Applied Science (Mannheim, Germany). BCA reagent for protein estimation was from Pierce (Rockford, IL). [³H]8-OH-DPAT (sp. activity = 135.0 Ci/mmol) and [³H]*p*-MPPF (sp. activity = 70.5 Ci/mmol) were purchased from DuPont New England Nuclear (Boston, MA). The cyclic [³H]AMP (TRK 432) assay kit was purchased from Amersham Biosciences (Buckinghamshire, U.K.). GF/B glass microfiber filters were from Whatman International (Kent, U.K.). All other chemicals used were of the highest purity available. Water was purified through a Millipore (Bedford, MA) Milli-Q system and used throughout.

Cells and cell culture

The intronless human genomic clone G-21 (Fargin *et al.*, 1988) which encodes the human serotonin_{1A} receptor was used to generate stable transfectants in HN2 cells which is a hybrid cell line between hippocampal cells and mouse neuroblastoma (Lee *et al.*, 1990). These cells expressing the human serotonin_{1A} receptor, originally referred to as HN2-5 (Banerjee *et al.*, 1993), were a generous gift from Dr. Probal Banerjee (College of Staten Island, City University of New York, U.S.A.). These cells are referred to as HN2-5-HT_{1A}R

in this chapter. Cells were grown in DMEM supplemented with 3.7 g/l of sodium bicarbonate, 10% fetal calf serum, 60 µg/ml penicillin, 50 µg/ml streptomycin, 50 µg/ml gentamycin sulfate, and 200 µg/ml geneticin in a humidified atmosphere with 5% CO₂ at 37 °C.

Preparation of cell membranes

Cell membranes were prepared as described earlier (Chattopadhyay *et al.*, 2004; Kalipatnapu *et al.*, 2004a; Paila and Chattopadhyay, 2006) and in section 3.2. and total protein concentration in membranes thus isolated was determined using the BCA assay (Smith *et al.*, 1985).

Radioligand binding assays

Receptor binding assays were carried out as described in section 2.2 with ~60 µg total protein.

GTP-γ-S sensitivity assay

GTP-γ-S binding assays were carried out as described in section 2.2.

Saturation radioligand binding assays

Saturation radioligand binding assays were carried out as described in section 3.2.

Competition binding assays

Competition binding assays against the radiolabeled agonist [³H]8-OH-DPAT (0.29 nM) and antagonist [³H]p-MPPF (0.5 nM) were carried out in presence of a range of concentrations (typically from 10⁻¹¹ to 10⁻⁶ M) of the unlabeled competitor. The concentration of the bound radiolabeled ligand was calculated from equation 1 (section 2.2).

Data for the competition assays were analyzed using equation 1 to obtain the IC₅₀ concentrations of the unlabeled competitor ligand. Binding parameters, namely dissociation constant (K_d) and maximum binding sites (B_{max}), were calculated from the following equations as previously described (Akera and Cheng, 1977; DeBlasi *et al.*, 1989):

$$K_d = IC_{50} - L \quad (13)$$

$$B_{max} = B \times (IC_{50}/L) \quad (14)$$

where L is the concentration of the radiolabeled ligand, (0.29 nM for the agonist and 0.5 nM for the antagonist) used in the assay and B is the concentration of the bound ligand in the absence of the competitor. The affinity of the displacing ligands is expressed as the apparent dissociation constant (K_i) for the competing ligands, where K_i is calculated using the Cheng-Prusoff equation (Cheng and Prusoff, 1973):

$$K_i = IC_{50} / [1 + (L / K_d)] \quad (15)$$

where IC₅₀ is the concentration of the competing ligand leading to 50% inhibition of specific binding and L and K_d are the concentration and dissociation constant of the labeled ligand. K_d values are those determined from saturation binding assays for the respective radioligand.

Estimation of cAMP levels in cells

cAMP levels in cells were estimated as described in section 3.2.

6.3. Results

Linearity of radioligand binding with increasing concentrations of total protein

The specific binding of the serotonin_{1A} receptor agonist [³H]8-OH-DPAT and antagonist [³H]p-MPPF to membranes prepared from HN2 cells that stably express

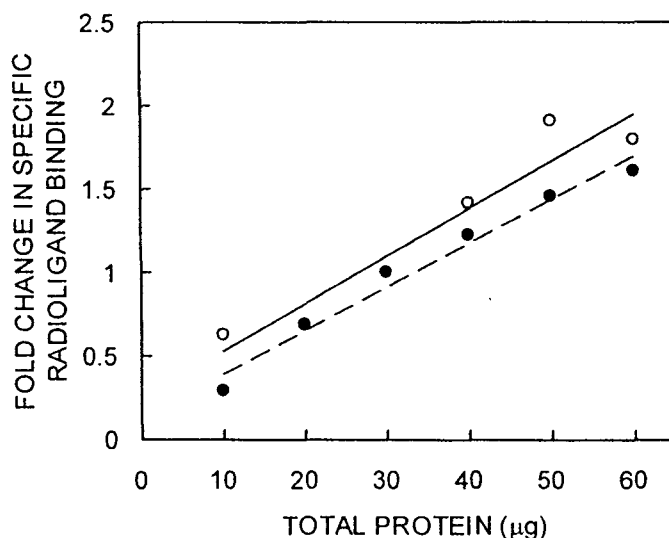


Figure 6.1. Fold change in specific binding of the agonist [³H]8-OH-DPAT (—○—) and antagonist [³H]p-MPPF (----●----) to serotonin_{1A} receptors from HN2-5-HT_{1A}R cell membranes with increasing amounts of total membrane protein. Values are normalized with respect to specific binding obtained with 30 µg total protein in the assay. Concentrations of [³H]8-OH-DPAT (0.29 nM) and [³H]p-MPPF (0.5 nM) were kept constant in the assay. Data shown are means of duplicate points from a representative experiment. See section 6.2 for other details.

serotonin_{1A} receptors (termed as HN2-5-HT_{1A}R cells) was characterized. Figure 6.1 shows that the binding of the radiolabeled ligands is linear over a broad range of protein concentrations. Non-specific binding defined with 10 µM serotonin for agonist binding and 10 µM p-MPPI for antagonist binding was ~10% or less than the total binding. These results suggest that under the conditions of the assay (*i.e.*, with 0.29 nM of [³H]8-OH-DPAT or 0.5 nM of [³H]p-MPPF, and using 60 µg total protein), there is no significant depletion of the radiolabel during the course of the assay. In other words, these conditions are appropriate for analyzing binding parameters of the receptor using the radiolabeled agonist and antagonist (Hulme, 1990). In addition, these results suggest that the incubation time of 1 h for the assay is sufficient for radioligand binding to have reached equilibrium conditions.

Saturation binding analysis of radiolabeled agonist and antagonist

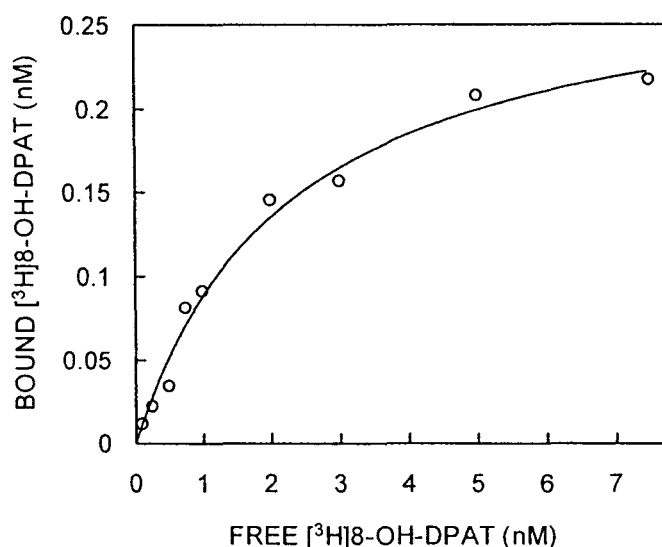


Figure 6.2. Saturation binding analysis of specific [³H]8-OH-DPAT binding to serotonin_{1A} receptors from HN2-5-HT_{1A}R cell membranes. A representative plot is shown for specific [³H]8-OH-DPAT binding with increasing concentrations (0.1-7.5 nM) of free [³H]8-OH-DPAT. The curve is a non-linear regression fit to the experimental data using Graphpad Prism software version 4.00 program. See section 6.2 and Table 6.1 for other details.

The saturation binding analyses of the specific agonist [³H]8-OH-DPAT and antagonist [³H]*p*-MPPF binding to serotonin_{1A} receptors from HN2-5-HT_{1A}R membranes were carried out using a range of concentration (0.1-7.5 nM) of the radiolabeled ligands and the binding plots are shown in Figures 6.2 and 6.3. Data for saturation binding were analyzed using Graphpad Prism software version 4.0 program and the binding parameters are shown in Table 6.1. The estimated K_d value (~2.20 nM) for [³H]8-OH-DPAT binding to serotonin_{1A} receptors in HN2-5-HT_{1A}R membranes is in excellent agreement with the K_d value reported earlier for the native rat (Milligan *et al.*, 2001), and bovine (Harikumar and Chattopadhyay, 1998, 1999) hippocampal serotonin_{1A} receptor. Table 6.1 also shows that the serotonin_{1A} receptors expressed in HN2-5-HT_{1A}R cells bind to [³H]*p*-MPPF with a K_d of ~2.70 nM, in good agreement with the affinity displayed by the native hippocampal receptor (Harikumar and Chattopadhyay, 2001).

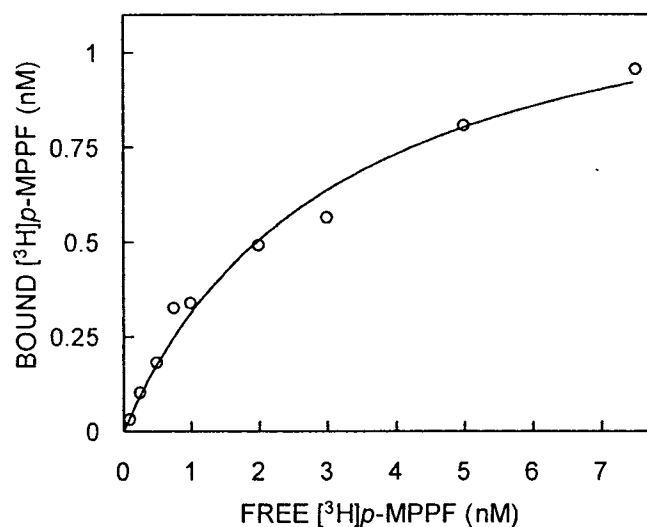


Figure 6.3. Saturation binding analysis of specific [³H]p-MPPF binding to serotonin_{1A} receptors from HN2-5-HT_{1A}R cell membranes. A representative plot is shown for specific [³H]p-MPPF binding with increasing concentrations (0.1-7.5 nM) of free [³H]p-MPPF. The curve is a non-linear regression fit to the experimental data using Graphpad Prism software version 4.00 program. See section 6.2 and Table 6.1 for other details.

Table 6.1

Binding parameters^a of the agonist [³H]8-OH-DPAT and antagonist [³H]p-MPPF binding to serotonin_{1A} receptors from HN2-5-HT_{1A}R cells

| Ligand | K _d (nM) | B _{max} (pmol/mg of protein) |
|----------------------------|------------------------|--|
| [³ H]8-OH-DPAT | 2.20 ± 0.05 | 2.08 ± 0.30 |
| [³ H]p-MPPF | 2.70 ± 0.39 | 9.20 ± 1.88 |

^aBinding parameters were calculated by analyzing saturation binding isotherms with a range (0.1-7.5 nM) of both radioligands using Graphpad Prism software version 4.00 program. Data shown in the table represent the means ± SE of three independent experiments. See section 6.2 for other details.

Competition binding analysis of radiolabeled agonist and antagonist

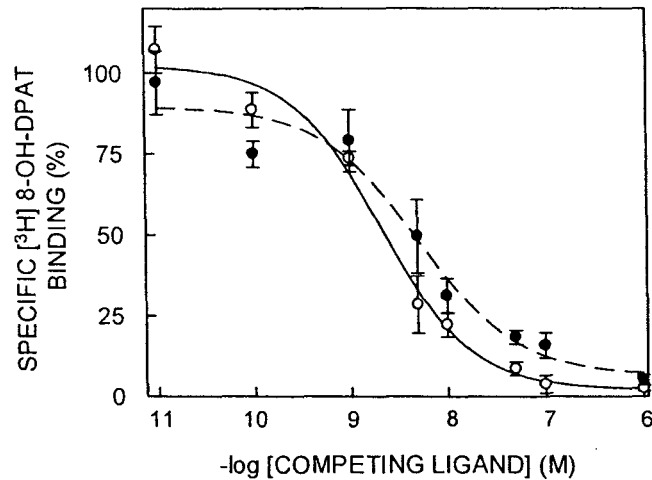


Figure 6.4. Competition binding analysis of specific [³H]8-OH-DPAT binding to serotonin_{1A} receptors from HN2-5-HT_{1A}R cell membranes. Values are expressed as percentages of specific binding obtained in the absence of the competing ligand. Radioligand binding assays were carried out with [³H]8-OH-DPAT in the presence of a range of 8-OH-DPAT (—○—) and serotonin (----●----) concentrations. The curves are non-linear regression fits to the experimental data using equation 1 (section 2.2). Data points represent means ± SE of duplicate points from three independent experiments. See section 6.2 and Table 6.2 for other details.

Further pharmacological characterization of the specific agonist and antagonist binding was carried out by performing competition binding experiments in presence of unlabeled ligands which act as competitors. Figures 6.4 and 6.5 show the competition displacement curves of specific agonist [³H]8-OH-DPAT by the competing ligands 8-OH-DPAT and serotonin, and of the antagonist [³H]*p*-MPPF by *p*-MPPI for serotonin_{1A} receptors from HN2-5-HT_{1A}R membranes. The half maximal inhibition concentrations (IC₅₀) and the inhibition constants (K_i) for the competing ligands are shown in Table 6.2.

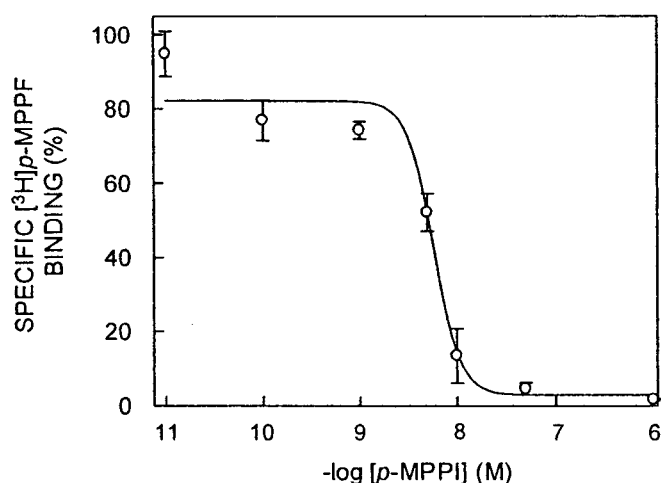


Figure 6.5. Competition binding analysis of specific [³H]p-MPPF binding to serotonin_{1A} receptors from HN2-5-HT_{1A}R cell membranes. Values are expressed as percentages of specific binding obtained in the absence of the competing ligand. Radioligand binding assay was carried out with 0.5 nM [³H]p-MPPF in the presence of a range of p-MPPI concentrations. The curve is a non-linear regression fit to the experimental data using equation 1 (section 2.2). Data points represent means ± SE of duplicate points from three independent experiments. See section 6.2 and Table 6.2 for other details.

Based on the formalism developed previously (Akera and Cheng, 1977; DeBlasi *et al.*, 1989), binding parameters obtained from saturation binding analysis (see Table 6.1) were compared with those obtained from competition binding analysis with similar ligands but in their unlabeled form acting as competitors. The binding parameters, namely K_d and B_{max} , thus obtained are shown in Table 6.3. As shown in the table, these values are in good agreement with values in Table 6.1.

Sensitivity of ligand binding to GTP- γ S

Most of the seven transmembrane domain receptors are coupled to G-proteins (Clapham, 1996), and guanine nucleotides are known to regulate ligand binding. The 5-HT_{1A} receptor agonists such as 5-HT or 8-OH-DPAT are known to specifically activate the G_i/G_o class of G-proteins (Emerit *et al.*, 1990; Clawges *et al.*, 1997). In contrast,

Table 6.2

Competition binding analysis^b of [³H]8-OH-DPAT and [³H]*p*-MPPF binding to serotonin_{1A} receptors from HN2-5-HT_{1A}R cells

| Competing ligand | [³ H]8-OH-DPAT | | [³ H] <i>p</i> -MPPF | |
|------------------|----------------------------|---------------------|----------------------------------|---------------------|
| | IC ₅₀ (nM) | K _i (nM) | IC ₅₀ (nM) | K _i (nM) |
| 8-OH-DPAT | 2.08 ± 0.40 | 1.65 ± 0.35 | - | - |
| serotonin | 5.10 ± 0.50 | 1.74 ± 0.46 | - | - |
| <i>p</i> -MPPI | - | - | 5.77 ± 0.09 | 4.47 ± 0.63 |

^bCompetition binding data were analyzed using equation 1 (section 2.2) to determine IC₅₀ values. The K_i values were obtained using equation 15 for which the K_d values were obtained from Table 6.1. Binding of [³H]8-OH-DPAT (0.29 nM) and [³H]*p*-MPPF (0.5 nM) was competed out with a range of concentrations of the unlabeled ligands. Data represent the means ± SE of three independent experiments. See section 6.2 for other details.

antagonists do not catalyze the activation of G-proteins (Kung *et al.*, 1995). Therefore, agonist binding to such receptors displays sensitivity to agents that uncouple the normal cycle of guanine nucleotide exchange at the G-protein alpha subunit caused by activation of the receptor. Sensitivity of agonist binding to guanine nucleotides can be monitored by performing ligand binding assays in the presence of GTP-γ-S, a non-hydrolyzable analogue of GTP. We have previously shown that the specific binding of the agonist [³H]8-OH-DPAT to bovine hippocampal serotonin_{1A} receptors is sensitive to guanine nucleotides and is inhibited with increasing concentrations of GTP-γ-S (Harikumar and Chattopadhyay, 1999; Javadekar-Subhedar and Chattopadhyay, 2004). Our results showed that in presence of GTP-γ-S, the serotonin_{1A} receptor undergoes an affinity transition, from a high affinity

Table 6.3

Binding parameters^c for [³H]8-OH-DPAT and [³H]*p*-MPPF obtained from competition binding experiments

| Competing ligand | [³ H]8-OH-DPAT | | [³ H] <i>p</i> -MPPF | |
|------------------|----------------------------|------------------------------------|----------------------------------|------------------------------------|
| | K _d (nM) | B _{max} (pmol/mg protein) | K _d (nM) | B _{max} (pmol/mg protein) |
| 8-OH-DPAT | 1.57 ± 0.40 | 4.02 ± 0.80 | - | - |
| <i>p</i> -MPPI | - | - | 4.80 ± 0.74 | 9.72 ± 0.58 |

^cCompetition binding data were analyzed with a range of concentrations of unlabeled 8-OH-DPAT against [³H]8-OH-DPAT (0.29 nM) and with unlabeled *p*-MPPI against [³H]*p*-MPPF (0.5 nM). Binding parameters were calculated using equations 13 and 14 from the IC₅₀ values in Table 6.2. Data represent the means ± SE of three independent experiments. See section 6.2 for other details.

G-protein coupled to a low affinity G-protein uncoupled state (Harikumar and Chattopadhyay, 1999). In agreement with these results, Figure 6.6 shows a characteristic reduction in binding of the agonist [³H]8-OH-DPAT in presence of a range of concentration of GTP-γ-S with an estimated IC₅₀ of 90.44 ± 1.80 nM which is in excellent agreement with our earlier results with the receptor from native hippocampal source (Kalipatnapu and Chattopadhyay, 2004b; Pucadyil and Chattopadhyay, 2004a). This indicates that the human serotonin_{1A} receptor is coupled to G-proteins when expressed in HN2 cells and exhibits typical sensitivity to GTP-γ-S, a characteristic feature of the native hippocampal receptor.

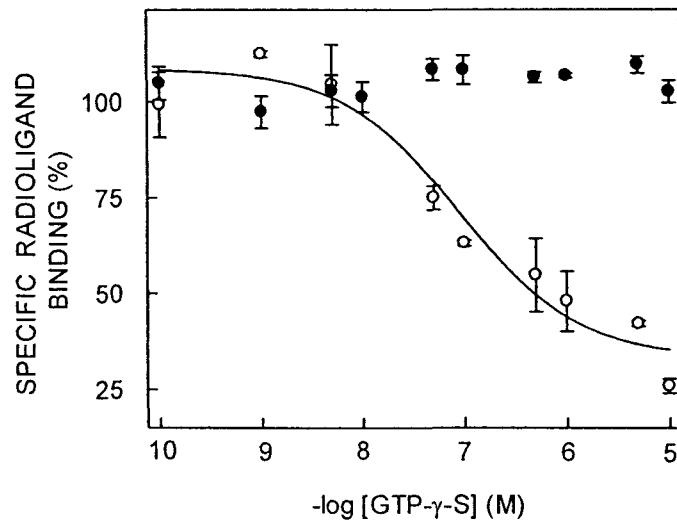


Figure 6.6. Effect of increasing concentrations of GTP- γ -S on the specific binding of the agonist [³H]8-OH-DPAT (O) and antagonist [³H]*p*-MPPF (●) to serotonin_{1A} receptors from HN2-5-HT_{1A}R cell membranes. Values are expressed as percentages of the specific binding obtained in the absence of GTP- γ -S. The curve associated with [³H]8-OH-DPAT binding is a non-linear regression fit to the experimental data using equation 1 (section 2.2). Data points represent means \pm SE of duplicate points from three independent experiments. See section 6.2 for other details.

In contrast to agonist binding, antagonist [³H]*p*-MPPF binding to serotonin_{1A} receptors from the bovine hippocampus has previously been shown to be insensitive to GTP- γ -S (Harikumar and Chattopadhyay, 1999; Javadekar-Subhedhar and Chattopadhyay, 2004; Kalipatnapu *et al.*, 2004b). Figure 6.6 shows that the specific [³H]*p*-MPPF binding to serotonin_{1A} receptors from HN2-5-HT_{1A}R cells remains invariant over a large range of concentrations of GTP- γ -S, in a manner analogous to what is observed with the native receptor from bovine hippocampus. This implies that the agonist 8-OH-DPAT and the antagonist *p*-MPPF binding can be used to differentially discriminate G-protein coupling of the serotonin_{1A} receptor in HN2-5-HT_{1A}R cells. Interestingly, the B_{\max} values in Table 6.1 for serotonin_{1A} receptors using the antagonist [³H]*p*-MPPF are far greater (~4 fold higher) than that obtained using agonist [³H]8-OH-DPAT. This has been previously shown for native systems such as rat hippocampus (Kung *et al.*, 1995) and bovine hippocampus

(Harikumar and Chattopadhyay, 1999). Since the binding of the antagonist [³H]p-MPPF is unaffected by GTP- γ -S (Figure 6.6) it indicates that [³H]p-MPPF binds to all available populations of the receptor, those coupled to G-proteins and free (not coupled to G-proteins) receptors. The B_{max} value for the antagonist [³H]p-MPPF therefore is greater than the corresponding value for the agonist [³H]8-OH-DPAT, which would predominantly bind to G-protein coupled form of the receptor. Since endogenous G-proteins could be in limiting amounts compared to heterologously expressed receptors in such expression systems (Kenakin, 1997), the B_{max} values of the agonist and antagonist may tend to display greater differences in such systems compared to native systems. However, the ligand binding affinities of the serotonin_{1A} receptor from HN2-5-HT_{1A}R cells and native systems are in good agreement and therefore the pharmacological characteristics of the receptor appear to be preserved in HN2-5-HT_{1A}R cells.

Ligand-dependent downstream signaling: measurement of cAMP levels

The primary function of serotonin_{1A} receptors is to inhibit adenylate cyclase thereby reducing the levels of cAMP. While in some systems this reduction can be observed in the basal level of cAMP itself, in others the effect is made more dramatic by spiking the cAMP levels using forskolin, which independently stimulates adenylate cyclase (Pucadyil *et al.*, 2005a; Kalipatnapu and Chattopadhyay, 2007a). We examined the signaling function of the serotonin_{1A} receptor expressed in HN2 cells by monitoring its ability to catalyze downstream signal transduction processes upon stimulation with serotonin_{1A} receptor ligands. The serotonin_{1A} receptor agonists such as serotonin and 8-OH-DPAT are known to specifically activate the G_i/G_o class of G-proteins (Raymond *et al.*, 1993) which

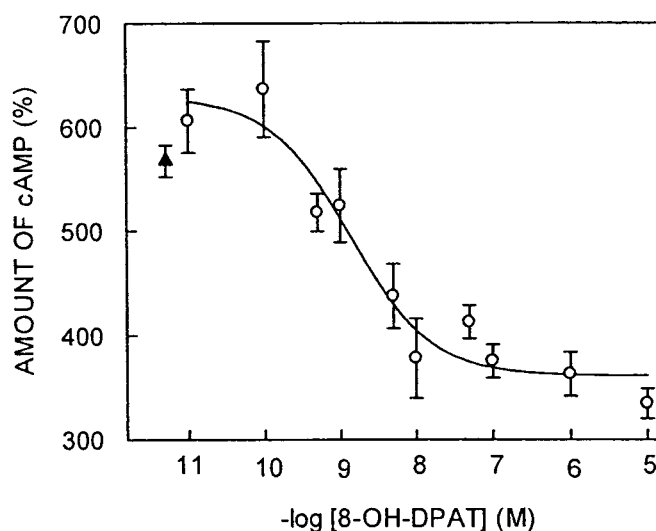


Figure 6.7. Effect of increasing concentrations of 8-OH-DPAT on downstream signaling of serotonin_{1A} receptors in HN2-5-HT_{1A}R cells. The ability of the specific serotonin_{1A} receptor agonist 8-OH-DPAT to inhibit the forskolin-stimulated cAMP levels was assayed in HN2-5-HT_{1A}R cells. Data points are expressed as percentages of the cAMP levels in cells in the absence of forskolin and 8-OH-DPAT. Data for the increase in cAMP levels in the presence of forskolin in untreated (▲) cells is shown for comparison. Inhibition curves were analyzed by the 4 parameter logistic function (equation 1; section 2.2). Data points represent means \pm SE of at least three independent experiments. See section 6.2 for other details.

subsequently reduce the cAMP levels. As shown in Figure 6.7, the forskolin-stimulated increase in cAMP levels is efficiently inhibited by 8-OH-DPAT in a characteristic concentration-dependent manner with an IC₅₀ value of 1.35 ± 0.07 nM in good agreement with earlier reported value (Kellett *et al.*, 1999). This indicates that the normal function of these receptors to transduce signals via G-proteins which inhibit adenylate cyclase is maintained in HN2-5-HT_{1A}R cells. Interestingly, cAMP is known to regulate immune responses, and modifications in cAMP signaling are involved in the pathophysiology and treatment of depression. For example, patients suffering from depression have been reported to show lower adenylate cyclase activity due to altered serotonergic signaling (Mizrahi *et al.*, 2004).

6.4. Discussion

A useful approach for performing pharmacological studies on GPCRs is to use a functional receptor system that converts receptor-ligand interaction into a cellular signal which allows to monitor the relationship between concentration and response (Kenakin, 1997). With the advent of molecular biology, there have been an increasing number of genetically engineered recombinant receptor systems for the study of drug-receptor interactions. This has led to a corresponding increase in the testing of new drugs in recombinant receptor systems. However, differences in host membrane lipid composition often complicate interpretation of drug testing results in such systems, and can lead to receptors with characteristics different from native receptors. For example, it has earlier been reported that although the rat cortical serotonin_{1A} receptor exists only in the high affinity state in its native environment, it displays both high and low affinity when expressed in HEK293 cells (Watson *et al.*, 2000). It is therefore judicious to develop recombinant expression systems in which the membrane lipid composition closely mimics the native lipid environment. Although serotonin_{1A} receptors have previously been expressed in non-neuronal cell lines such as CHO (Newman-Tancredi *et al.*, 1997) and HEK293 (Kellett *et al.*, 1999), there have been very few attempts to express and characterize the receptor in neuronal cells. Our choice of HN2 cells as an expression system for characterizing serotonin_{1A} receptors is based on the observation that cell lines of neural origin represent realistic models for understanding signal transduction in neuronal cells (Lee *et al.*, 1990).

In this chapter, the pharmacological and functional characterization of the human serotonin_{1A} receptor stably expressed in HN2 cells is described. Our results show that serotonin_{1A} receptors expressed in HN2 cells display ligand binding properties that are in good agreement to what is observed with native receptors such as rat and bovine hippocampal serotonin_{1A} receptors. In addition, it is demonstrated that the differential

discrimination of G-protein coupling by the agonist 8-OH-DPAT and the antagonist *p*-MPPF, a hallmark of the native receptor, is preserved for the receptor expressed in HN2 cells. More importantly, serotonin_{1A} receptors in HN2-5-HT_{1A}R cells can efficiently catalyze downstream signal transduction by reducing cAMP levels.

Cholesterol organization, traffic, and dynamics in the brain are stringently controlled since the input of cholesterol into the central nervous system is almost exclusively from *in situ* synthesis as there is no evidence for the transfer of cholesterol from blood plasma to brain (Dietschy and Turley, 2001). As a result, a number of neurological diseases share a common etiology of defective cholesterol metabolism in the brain (Porter, 2002). In the Smith-Lemli-Opitz syndrome, for example, the marked abnormalities in brain development and function leading to serious neurological and mental dysfunctions have their origin in the fact that the major input of brain cholesterol comes from *in situ* synthesis and such synthesis is defective in this syndrome (Waterham and Wanders, 2000). Interestingly, it was previously shown using a variety of approaches that the function of hippocampal serotonin_{1A} receptor displays a great degree of sensitivity to membrane cholesterol (Pucadyil and Chattopadhyay, 2004a, 2005; Pucadyil *et al.*, 2004a; Pucadyil *et al.*, 2005b; Paila *et al.*, 2005). Expression of this receptor in a cell line of neuronal origin therefore assumes greater relevance in this context, and provides a convenient cellular system to address these issues.

Since native tissues (of neuronal origin in particular) often have very low quantities of a specific type of receptor, solubilization and purification of neuronal receptors from native sources continue to be challenging issues in contemporary membrane biology (Kalipatnapu and Chattopadhyay, 2005a). It is in this context that membrane receptors expressed in a cell line with native-like membrane lipid environment gains significance. The levels of receptors expressed this way are often much higher than found in native tissues making these systems amenable to solubilization and purification of the given receptor. Effective solubilization and purification of membrane receptors with optimum

ligand binding activity and intact signal transduction components represent important steps in understanding structure-function relationship and pharmacological characterization of a specific receptor, and may constitute the first step in the detailed molecular characterization of GPCRs.

Chapter 7

Conclusion and future perspectives

7.1. Conclusion

The serotonin_{1A} receptor: a representative member of the GPCR superfamily in the context of membrane cholesterol dependence of receptor function

The modulatory role of cholesterol on the ligand binding activity and G-protein coupling of the hippocampal serotonin_{1A} receptor has been shown in our laboratory using various approaches which include treatment with (i) M β CD, which physically depletes cholesterol from membranes (Pucadyil and Chattopadhyay, 2004a, 2005) (ii) the sterol-complexing agent digitonin (chapter 2; Paila *et al.*, 2005), and (iii) the sterol-binding antifungal polyene antibiotic nystatin (Pucadyil *et al.*, 2004b). While treatment with M β CD physically depletes cholesterol from membranes, treatment with other agents modulates the availability of membrane cholesterol without physical depletion. In addition, metabolic depletion of cholesterol using cholesterol lowering agents such as statins resulted in the reduction of the ligand binding of serotonin_{1A} receptors (Shrivastava, S., Pucadyil, T.J., Chattopadhyay, A., unpublished observations). The underlying tenet brought out by these data implies that it is the *non-availability of cholesterol*, rather than the manner in which its availability is modulated, is crucial for ligand binding of the serotonin_{1A} receptor. Importantly, replenishment of membranes with cholesterol using M β CD-cholesterol complex led to recovery of ligand binding activity to a considerable extent. In order to test the stringency of the requirement of cholesterol for the function of the serotonin_{1A} receptor, membranes were treated with cholesterol oxidase which catalyzes the oxidation of cholesterol to cholestenone. The results showed that oxidation of membrane cholesterol led to inhibition of the ligand binding activity of the serotonin_{1A} receptor without altering overall membrane order (Pucadyil *et al.*, 2005b). To further explore the specificity of cholesterol requirement, a cellular model of the Smith-Lemli-Opitz Syndrome (SLOS) was recently generated, using cells stably expressing the human serotonin_{1A} receptor (chapter 3; Paila *et al.*, 2008). The cellular model of SLOS was generated by metabolically inhibiting the biosynthesis of cholesterol, utilizing a specific inhibitor (AY 9944) of the enzyme

required in the final step of cholesterol biosynthesis. SLOS serves as an appropriate condition to delineate the specific and global effects of cholesterol in the function of the serotonin_{1A} receptor, since the two aberrant sterols that get accumulated in SLOS, *i.e.*, 7- and 8-DHC, differ with cholesterol only in a double bond. Importantly, metabolic replenishment of cholesterol using serum partially restored the ligand binding activity of the serotonin_{1A} receptor (see chapter 3). Interestingly, we have recently shown that 7-DHC does not support the function of the serotonin_{1A} receptor without any change in overall membrane order (Singh *et al.*, 2007; Chattopadhyay *et al.*, 2007). Cholesterol depletion from native hippocampal membranes followed by replenishment with 7-DHC, did not result in restoration of the ligand binding to the serotonin_{1A} receptor, in spite of recovery of membrane order (Singh *et al.*, 2007). In addition, solubilization of the hippocampal serotonin_{1A} receptor is accompanied by loss of membrane cholesterol, which results in a reduction in specific ligand binding activity and overall membrane order (Chattopadhyay *et al.*, 2007). Replenishment of cholesterol to solubilized membranes restores the cholesterol content of the membrane and significantly enhances specific ligand binding activity and overall membrane order. Importantly, replenishment of solubilized hippocampal membranes with 7-DHC does not restore ligand binding activity of the serotonin_{1A} receptor, in spite of recovery of membrane order. Interestingly, it has been recently shown that the effects of 7-DHC and cholesterol on membrane organization and dynamics are considerably different (Shrivastava *et al.*, 2008). We therefore conclude that the requirement for maintaining ligand binding activity is more stringent than the requirement for maintaining membrane order. Taken together, these results indicate that the molecular basis for the requirement of membrane cholesterol in maintaining the ligand binding activity of serotonin_{1A} receptors could be specific interaction, although global bilayer effects may not be ruled out (Prasad *et al.*, 2009).

Cholesterol binding motif(s) in serotonin_{1A} receptors ?

In the overall context of the presence of CCM in the recently reported crystal structure of the β_2 -adrenergic receptor (Hanson *et al.*, 2008), it is an appropriate time now to consider whether there is similar CCM(s) present in the serotonin_{1A} receptor and if present, whether it is conserved during the evolution of the receptor. This is particularly relevant in view of the similarity between the serotonin_{1A} and β_2 -adrenergic receptors (~43% amino acid similarity in the transmembrane domain) (Kalipatnapu and Chattopadhyay, 2007), and the reported cholesterol dependence of serotonin_{1A} receptor function (Pucadyil and Chattopadhyay, 2006). In order to examine the evolution of specific cholesterol binding site(s) of the serotonin_{1A} receptor over various phyla, we analyzed amino acid sequences of the serotonin_{1A} receptor from available databases (see Figure 7.1). Partial, duplicate and other non-specific sequences were removed from the set of sequences obtained. The amino acid sequences used for the analysis belong to diverse taxons that include insects, fish and other marine species, amphibians and extending up to mammals. Initial alignment was carried out using ClustalW. It is apparent from this alignment that the cholesterol binding motif, which includes Tyr73 in the putative transmembrane helix II and Arg151, Ile157 and Trp161 in the putative transmembrane helix IV (see Figure 1.3, chapter 1), is conserved in most species. Realignment with ClustalW (after eliminating the relatively divergent parts of the receptor) resulted in conservation of the motif across all phyla analyzed, except in organisms such as *T. adhaerens* and *S. purpuratus*. Interestingly, pairwise alignment of the human serotonin_{1A} receptor with the human β_2 -adrenergic receptor and rhodopsin exhibited conservation of the motif in all sequences (data not shown). It therefore appears that cholesterol binding sites represent an inherent characteristic feature of serotonin_{1A} receptors which is conserved during the course of evolution. It is interesting to note here that cholesterol binding sites appear to be present even in organisms which are not capable of biosynthesis of cholesterol. Organisms which lack cholesterol biosynthesis could, however,

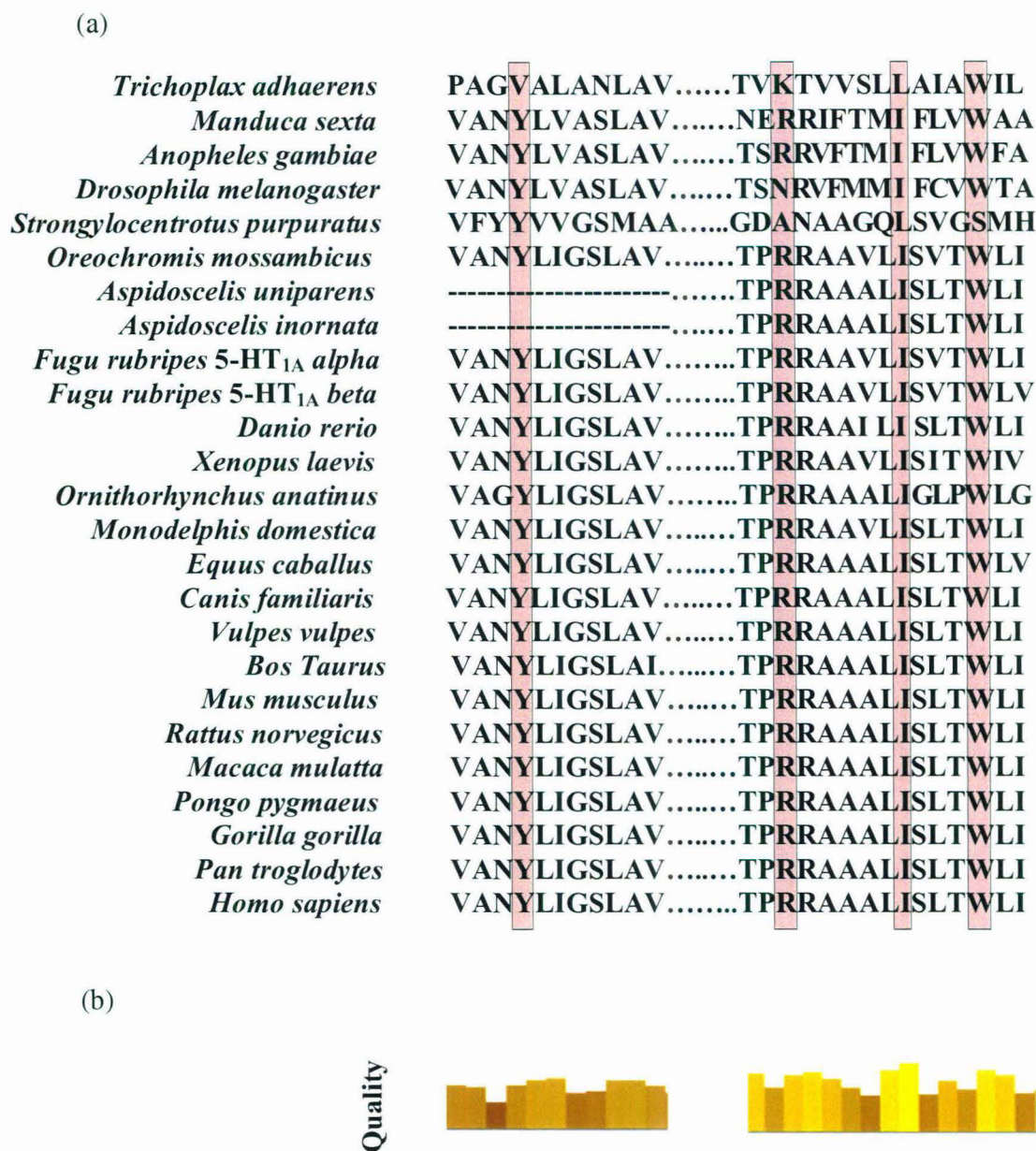


Figure 7.1. Multiple alignment of the serotonin_{1A} receptor around the CCM of interest with the conserved residues highlighted. As evident from the panel (a), Trp161 is the most conserved residue, except in *S. purpuratus*. The sequences of *T. adhaerens*, *M. sexta* and *A. gambiae* are putative serotonin_{1A} receptors whereas those of *S. purpuratus*, *B. taurus*, *O. anatinus*, *D. rerio*, *M. domestica* and *M. mulatta* are predicted by homology. Panel (b) is a graphical representation displaying the quality of alignment, with lighter shades representing higher quality. Amino acid sequences of serotonin_{1A} receptors are from NCBI and ExPasy databases.

acquire cholesterol through diet (Bloch, 1983). Organisms such as insects possess sterols that are different from cholesterol which have diverged from cholesterol during the sterol evolution pathway (Clark and Bloch, 1959). The presence of CCM in these organisms could be due to binding of closely related sterols or dietary cholesterol to CCM.

Future Perspectives

Mutations in CCM motif: functional consequences

Previous work from our laboratory has demonstrated that membrane cholesterol is required for the function of the serotonin_{1A} receptor, which could be due to specific interaction of the receptor with cholesterol. Based on these results, we envisage that there could be specific/nonannular cholesterol binding site(s) (see chapter 1) in the serotonin_{1A} receptor. Our future work will focus on mutating some of the putative amino acid residues (Tyr73, Arg151, Ile157 and Trp161) that could be involved in the cholesterol binding site of the serotonin_{1A} receptor followed by stable expression in cells of interest. We plan to carry out functional and organizational (in the context of membrane localization and domains) analyses of the mutated receptor, in order to gain further insight into membrane cholesterol dependence of receptor function.

Effects of different sterols on properties of membrane with varying phases

Cholesterol is the most representative sterol present in vertebrate membranes and is the end product of the long and multistep sterol biosynthetic pathway. 7-Dehydrocholesterol (7-DHC), and lathosterol are the immediate biosynthetic precursors of cholesterol in the Kandutsch-Russell pathway. Desmosterol is the immediate biosynthetic precursor in the Bloch pathway. Konrad Bloch speculated that the sterol biosynthetic pathway parallels sterol evolution (the 'Bloch hypothesis'). According to this hypothesis, cholesterol has been

selected over a very long time scale of natural evolution for its ability to optimize certain physical properties of eukaryotic cell membranes with regard to biological functions (Bloch, 1983). Cholesterol precursors should therefore have properties that gradually support the cellular function of higher organisms as they progress along the pathway toward cholesterol. Defects in the cholesterol biosynthetic pathway have been identified with several inherited metabolic disorders (Waterham, 2006). Comparative studies of the effects of cholesterol and its evolutionary precursors on membranes therefore assume significance. Desmosterol and 7-DHC differ with cholesterol only in a double bond at 24th and 7th positions, respectively. Lathosterol, unlike 7-DHC and desmosterol, has only a double bond in its chemical structure, which differs with cholesterol in its position. We have previously shown that although both 7-DHC and desmosterol differ with cholesterol in one double bond, they exhibit differential effects on membrane organization and dynamics (Shrivastava *et al.*, 2008). Importantly, we showed earlier that the effect of cholesterol and desmosterol on membrane organization and dynamics is similar in most cases, while 7-DHC has a considerably different effect. This demonstrates that the position of the double bond in sterols is an important determinant in maintaining membrane order and dynamics (Shrivastava *et al.*, 2008).

Our future plan includes monitoring the effect of cholesterol and its immediate biosynthetic precursors on biophysical and dynamic properties of fluid (disordered) and gel (ordered) phase membranes. Toward this goal, we plan to utilize fluorescence, Differential Scanning Calorimetry (DSC), Electron Spin Resonance (ESR) approaches. These measurements assume relevance since the accumulation of cholesterol precursors have been reported to result in severe pathological conditions (Waterham, 2006).

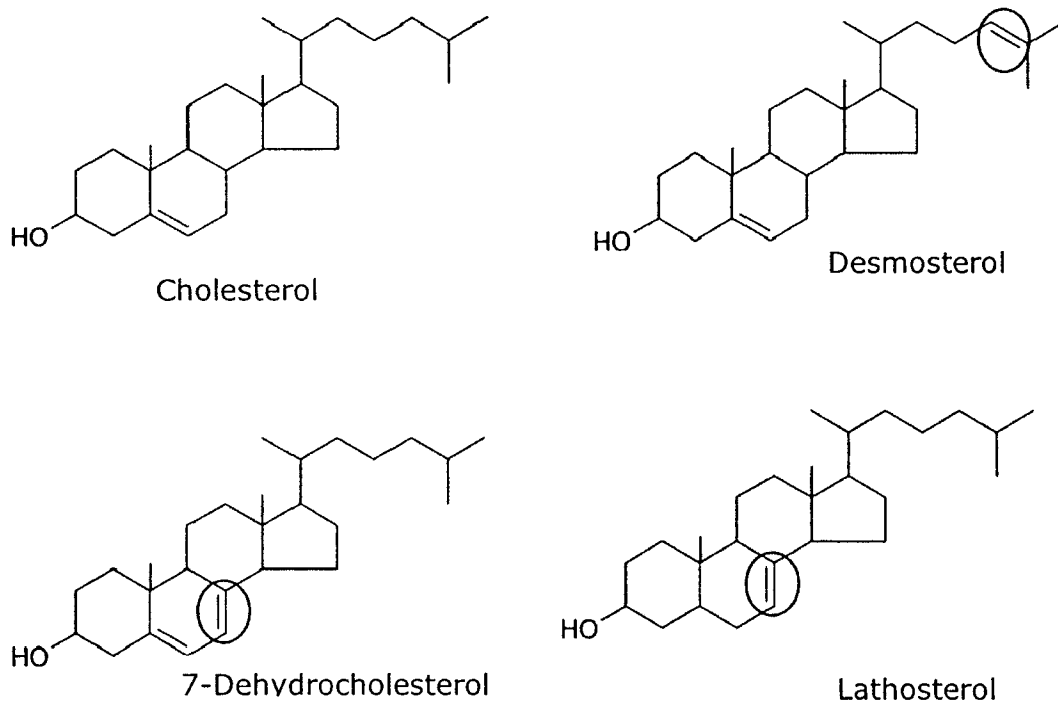


Figure 7.2. Chemical structures of immediate biosynthetic precursors of cholesterol. 7-Dehydrocholesterol and lathosterol are biosynthetic precursors of cholesterol in the Kandutsch-Russell (Kandutsch and Russell, 1960) and desmosterol is the precursor of cholesterol in Bloch (Bloch, 1983) pathway. 7-Dehydrocholesterol differs with cholesterol only in a double bond at the 7th position in the sterol ring, and desmosterol differs with cholesterol only in a double bond at the 24th position in the flexible alkyl side chain. Both lathosterol and cholesterol have one double bond which differs in its position in these sterols (highlighted in their chemical structures).

Exploring the physical properties of membranes from SLOS patient fibroblasts and their matched controls

SLOS is clinically diagnosed by reduced plasma levels of cholesterol along with elevated levels of 7-dehydrocholesterol (and its positional isomer 8-dehydrocholesterol) and the ratio of their concentrations to that of cholesterol. Considering the importance of cholesterol in maintaining the membrane physical properties, it would be interesting to compare to what extent 7- and 8- DHC could mimic cholesterol in this regard. It has been previously reported using a number of approaches that membrane domains formed by 7-

DHC differ with those formed by cholesterol in protein composition (Keller *et al.*, 2004), packing (Berring *et al.*, 2005) and stability (Wolf and Chachaty, 2000; Wolf *et al.*, 2001; Megha *et al.*, 2006). Interestingly, model membranes mimicking SLOS membranes have been reported to exhibit atypical membrane organization (Tulenکو *et al.*, 2006) and curvature (Gondre-Lewis *et al.*, 2006). It is therefore possible that mere replacement of cholesterol with 7-DHC may significantly affect aspects of membrane organization such as near neighbor interactions (7-DHC is more polar than cholesterol) and accessible surface area. We plan to obtain skin fibroblasts from SLOS patients and matched healthy controls, and monitor the organization and dynamics of membranes derived from total lipids extracted from SLOS and control fibroblasts, using fluorescence-based approaches. The results of these experiments could potentially provide novel insight regarding the organization of membranes in SLOS.

Functional solubilization and purification of the serotonin_{1A} receptor

Membrane protein purification represents an area of considerable challenge in contemporary membrane biology. Studies carried out on purified and reconstituted membrane receptors have considerably advanced our knowledge of the molecular aspects of receptor function (Gether 2000). It is noteworthy that none of the subtypes of G-protein coupled serotonin receptors has yet been purified to homogeneity from natural sources. An essential criterion for purification of an integral membrane protein is that the protein must be carefully removed from the native membrane and individually dispersed in solution. This process is known as solubilization and is most effectively accomplished using amphiphilic detergents (Garavito and Ferguson-Miller 2001; Kalipatnapu and Chattopadhyay 2005a). Solubilization of a membrane protein is a process in which the proteins and lipids that are held together in the native membrane are suitably dissociated in a buffered detergent solution. Effective solubilization and purification of G-protein coupled

receptors in a functionally active form represent important steps in understanding structure-function relationship and pharmacological characterization of a specific receptor.

As in the case of other membrane proteins, low expression levels of the serotonin_{1A} receptor in natural membranes, and inherent difficulties in purifying membrane proteins have posed considerable challenges in addressing various issues related to membrane biology of the serotonin_{1A} receptor. It is for this reason that none of the subtypes of G-protein coupled serotonin receptors has yet been purified to homogeneity from native sources. Nonetheless, natural membranes and cultured cells heterologously expressing the serotonin_{1A} receptor together have made it possible to address important aspects related to membrane organization and function of the serotonin_{1A} receptor. It has recently been possible to purify the heterologously expressed serotonin_{1A} receptor from *Xenopus laevis* employing a novel strategy (Zhang *et al.*, 2005). A comprehensive understanding of the serotonin_{1A} receptor function in relation to its membrane lipid environment is important in view of the enormous implications of the serotonin_{1A} receptor function in human health (Julius, 1998), and the observation that several diagnosed brain diseases are attributed to altered lipid-protein interactions (Chattopadhyay and Paila, 2007). The serotonin_{1A} receptor could be expressed in baculovirus expression system and could be solubilized and purified. Following the purification of the receptor, the proposed nonannular lipid binding sites in the receptor could be validated. Depending on the yield of the purified receptor, the serotonin_{1A} receptor could be crystallized using some of the recently developed crystallization strategies, such as crystallizing the membrane protein from cubic phase (Caffrey, 2009).

GPCRs are involved in a multitude of physiological functions and represent important drug targets (Schlyer and Horuk, 2006; Jacoby *et al.*, 2006; Insel *et al.*, 2007). Although the pharmacological and signaling features of GPCRs have been studied widely, aspects related to their interaction with membrane lipids have been addressed in relatively few cases. In this context, the realization that lipids such as cholesterol could influence the

function of GPCRs has remarkably transformed our idea regarding the function of this important class of membrane proteins. With progress in deciphering molecular details on the nature of this interaction, our overall understanding of GPCR function in health and disease would improve significantly, thereby enhancing our ability to design better therapeutic strategies to combat diseases related to malfunctioning of these receptors.

References

- Akera, T. and Cheng, V.-J. K. (1977) *Biochim. Biophys. Acta* 470, 412-423.
- Akiyama, T., Takagi, S., Sankawa, U., Inari, S. and Saitô, H. (1980) *Biochemistry* 19, 1904-1911.
- Albert, A.D. and Boesze-Battaglia, K. (2005) *Prog. Lipid Res.* 44, 99-124.
- Albert, A.D., Young, J.E. and Yeagle, P.L. (1996) *Biochim. Biophys. Acta* 1285, 47-55.
- Albert, P.R., Zhou, Q.-Y., Van Tol H.H.M., Bunzow, J.R. and Civelli, O. (1990) *J. Biol. Chem.* 265, 5825-5832.
- Amundson, D.M. and Zhou, M. (1999) *J. Biochem. Biophys. Methods* 38, 43-52.
- Arvidsson, L. E., Hacksell, U., Nilsson, J. L., Hjorth, S., Carlsson, A., Lindberg, P., Sanchez, D. and Wikstrom, H. (1981) *J. Med. Chem.* 24, 921-923.
- Azmitia, E. C. (2001) *Brain and Dev.* 23, S1-S10 (Suppl.1).
- Bahouth, S.W. and Malbon, C.C. (1987) *Biochem. J.* 248, 557-566.
- Baldwin, J.M. (1994) *Curr. Opin. Cell Biol.* 6, 180-190.
- Ballesteros, J.A. and Weinstein, H. (1995) *Methods Neurosci.* 25, 366-428.
- Banères, J.L. and Parello, J. (2003) *J. Mol. Biol.* 329, 815-829.
- Banerjee P., Berry-Kravis E., Bonafede-Chhabra D. and Dawson G. (1993) *Biochem. Biophys. Res. Commun.* 192, 104-110.
- Bari, M., Battista, N., Fezza, F., Finazzi-Agrò, A. and Maccarrone, M. (2005a) *J. Biol. Chem.* 280, 12212-12220.
- Bari, M., Paradisi, A., Pasquariello, N. and Maccarrone, M. (2005b) *J. Neurosci. Res.* 81, 275-283.
- Barr, A.J. and Manning, D.R. (1997) *J. Biol. Chem.* 272, 32979-32987.
- Battaile, K.P. and Steiner, R.D. (2000) *Mol. Genet. Metab.* 71, 154-162.
- Ben-Arie, N., Gileadi, C. and Schramm, M. (1988) *Eur. J. Biochem.* 176, 649-654.
- Bennet, M.P. and Mitchell, D.C. (2008) *Biophys. J.* 95, 1206-1216.
- Berring, E.E., Borrenpohl, K., Fliesler, S.J. and Serfis, A.B. (2005) *Chem. Phys. Lipids* 136, 1-12.

- Bhatnagar, A., Sheffler, D.J., Kroeze, W.K., Compton-Toth, B. and Roth, B.L. (2004) *J. Biol. Chem.* 279, 34614-34623.
- Bligh, E.G. and Dyer, W.J. (1959) *Can. J. Biochem. Physiol.* 37, 911-917.
- Bloch, K.E. (1983) *CRC Crit. Rev. Biochem.* 14, 47-92.
- Borst, J.W., Hink, M.A., van Hoek, A. and Visser, A.J. (2005) *J. Fluoresc.* 15, 153-160.
- Brown, R.E. (1998) *J. Cell Sci.* 111, 1-9.
- Bruns, R.F., Lawson-Wendling, K. and Pugsley, T.A. (1983) *Anal. Biochem.* 132, 74-81.
- Burger, K., Gimpl, G. and Fahrenholz, F. (2000) *Cell. Mol. Life Sci.* 57, 1577-1592.
- Cabrera-Vera, T.M, Vanhauwe, J., Thomas, T.O., Medkova, M., Preininger, A., Mazzoni, M.R. and Hamm, H.E. (2003) *Endocr. Rev.* 24, 765-781.
- Caffrey, M. (2009) *Annu. Rev. Biophys.* (in press)
- Chabre, M. and le Maire, M. (2005) *Biochemistry* 44, 9395-9403.
- Charest, A., Wainer, B.H. and Albert, P.R. (1993) *J. Neurosci.* 13, 5164-5171.
- Chattopadhyay, A. (1992) Membrane penetration depth analysis using fluorescence quenching: a critical review. in: *Biomembrane Structure and Function: The State of The Art* (Gaber, B.P. and Easwaran, K.R.K., Eds), pp. 153-163. Adenine Press, Schenectady, NY.
- Chattopadhyay, A. (2003) *Chem. Phys. Lipids* 122, 3-17.
- Chattopadhyay, A. and Kalipatnapu, S. (2004) *J. Biosci.* 29, 101-102.
- Chattopadhyay, A. and London, E. (1984) *Anal. Biochem.* 139, 408-412.
- Chattopadhyay, A. and Paila, Y.D. (2007) *Biochem. Biophys. Res. Commun.* 354, 627-633.
- Chattopadhyay, A., Harikumar, K.G. and Kalipatnapu, S. (2002) *Mol. Membr. Biol.* 19, 211-220.
- Chattopadhyay, A., Jafurulla, M.D., Kalipatnapu, S., Pucadyil, T.J. and Harikumar, K.G. (2005) *Biochem. Biophys. Res. Commun.* 327, 1036-1041.
- Chattopadhyay, A., Jafurulla, Md. and Kalipatnapu, S. (2004) *Cell. Mol. Neurobiol.* 24,

293-300.

Cheng, Y.-C. and Prusoff, W. H. (1973) *Biochem. Pharmacol.* 22, 3099-3108.

Cherezov, V., Rosenbaum, D.M., Hanson, M.A., Rasmussen, S.G.F., Thian, F.S., Kobilka, T.S., Choi, H.-J., Kuhn, P., Weis, W.I., Kobilka, B.K. and Stevens, R.C. (2007) *Science* 318, 1258-1265.

Clapham, D. E. (1996) *Nature* 379, 297-299.

Clark, A.J. and Bloch, K. (1959) *J. Biol. Chem.* 234, 2578-2582.

Clawges, H. M., Depree, K. M., Parker, E. M. and Graber, S. G. (1997) *Biochemistry* 36, 12930-12938.

Colozo, A.T., Park, P.S.-H., Sum, C.S., Pisterzi, L.F. and Wells, J.W. (2007) *Biochem. Pharmacol.* 74, 236-255.

Cunniff, C., Kratz, L.E., Moser, A., Natowicz, M.R. and Kelley, R.I. (1997) *Am. J. Med. Genet.* 68, 263-269.

Cuthbertson, J.M., Doyle, D.A. and Sansom, M.S.P. (2005) *Protein Eng. Des. Sel.* 18, 295-308.

DeBlasi, A., O'Reilly, K. and Motulsky, H. J. (1989) *Trends Pharmacol. Sci.* 10, 227- 229.

DeDecker, B.S., O'Brien, R., Fleming, P.J., Geiger, J.H., Jackson, S.P. and Sigler, P.B. (1996) *J. Mol. Biol.* 264, 1072-1084.

del Olmo, E., López-Giménez, J.F., Vilaró, M.T., Mengod, G., Palacios, J.M. and Pazos, A. (1998) *Mol. Brain. Res.* 60, 123-126.

Desai, K., Sullards, C., Allegood, J., Wang, E., Schmelz, E.M., Hartl, M., Humpf, H.-U., Liotta, D.C., Peng, Q. and Merrill, A.H., Jr. (2002) *Biochim. Biophys. Acta* 1585, 188-192.

Devaux, P.F. and Seigneuret, M. (1985) *Biochim. Biophys. Acta* 822, 63-125.

Dietschy, J. M. and Turley, S. D. (2001) *Curr. Opin. Lipidol.* 12, 105-112.

Dontchev, V., Ichev, K., Ovtscharoff, W. and Surchev, L. (1994) *Acta Histochem.* 96, 165-174.

- Dragan, Y.P., Bidlack, W.R., Cohen, S.M., Goldsworthy, T.L., Hard, G.C., Howard, P.C., Riley, R.T. and Voss, K.A. (2001) *Toxicol. Sci.* 61, 6-17.
- Dreja, K., Voldstedlund, M., Vinten, J., Trantum-Jensen, J., Hellstrand, P. and Swärd, K. (2002) *Arterioscler. Thromb. Vasc. Biol.* 22, 1267-1272.
- Dvornik, D., Kraml, M., Dubuc, J., Givner, M. and Gaudry, R. (1963) *J. Am. Chem. Soc.* 85, 3309.
- East, J.M., Melville, D. and Lee, A.G. (1985) *Biochemistry* 24, 2615-2623.
- Elias, E.R., Hansen, R.M., Irons, M., Quinn, N.B. and Fulton, A.B. (2003) *Arch. Ophthalmol.* 121, 1738-1743.
- Elias, P.M., Goerke, J., Friend, D.S. and Brown, B.E. (1978) *J. Cell Biol.* 78, 577-596.
- Ellena, J.F., Blazing, M.A. and McNamee, M.G. (1983) *Biochemistry* 22, 5523-5535.
- Emerit, M. B., El Mestikawy, S., Gozlan, H., Rouot, B. and Hamon, M. (1990) *Biochem. Pharmacol.* 39, 7-18.
- Epand, R.F., Thomas, A., Brasseur, R., Vishwanathan, S.A., Hunter, E. and Epand, R.M. (2006) *Biochemistry* 45, 6105-6114.
- Eroglu, C., Brugger, B., Wieland, F. and Sinning, I. (2003) *Proc. Natl. Acad. Sci. USA* 100, 10219-10224.
- Eroglu, C., Cronet, P., Panneels, V., Beaufile, P. and Sinning, I. (2002) *EMBO Rep.* 3, 491-496.
- Esmann, M., Watts, A. and Marsh, D. (1985) *Biochemistry* 24, 1386-1393.
- Estep, T.N., Mountcastle, D.B., Biltonen, R.L. and Thompson, T.E. (1978) *Biochemistry* 17, 1984-1989.
- Fahrenholz, F., Klein, U. and Gimpl, G. (1995) *Adv. Exp. Med. Biol.* 395, 311-319.
- Fantini, J. (2003) *Cell. Mol. Life Sci.* 60, 1027-1032.
- Fargin A., Raymond J. R., Lohse M. J., Kobilka B. K. and Lefkowitz R. J. (1988) *Nature* 335, 358-360.
- Fivaz, M. and Meyer, T. (2003) *Neuron* 40, 319-330.

- Frank, M., Thumer, L., Lohse, M.J. and Bunemann, M. (2005) *J. Biol. Chem.* 280, 24584-24590.
- Fredriksson, R. and Schiöth, H.B. (2005) *Mol. Pharmacol.* 67, 1414-1425.
- Fukuda, H., Shima, H., Vesonder, R.F., Tokuda, H., Nishino, H., Katoh, S., Tamura, S., Sugimura, T. and Nagao, M. (1996) *Biochem. Biophys. Res. Commun.* 220, 160-165.
- Futerman, A.H. and Hannun, Y.A. (2004) *EMBO Rep.* 5, 777-782.
- Gaoua, W., Wolf, C., Chevy, F., Ilien, F. and Roux, C. (2000) *J. Lipid Res.* 41, 637-646.
- Garavito, R.M. and Ferguson-Miller, S. (2001) *J. Biol. Chem.* 276, 32403-32406.
- Gaspar, P., Cases, O. and Maroteaux, L. (2003) *Nat. Rev. Neurosci.* 4, 1002-1012.
- Gelderblom, W.C., Jaskiewicz, K., Marasas, W.F., Thiel, P.G., Horak, R.M., Vleggaar, R. and Kriek, N.P. (1988) *Appl. Environ. Microbiol.* 54, 1806-1811.
- Gelderblom, W.C., Semple, E., Marasas, W.F. and Farber, E. (1992) *Carcinogenesis* 13, 433-437.
- Gether, U. (2000) *Endocr. Rev.* 21, 90-113.
- Gether, U. and Kobilka, B.K. (1998) *J. Biol. Chem.* 273, 17979-17982.
- Gielen, E., Baron, W., Vandeven, M., Steels, P., Hoekstra, D. and Ameloot, M. (2006) *Glia* 54, 499-512.
- Gimpl, G. and Fahrenholz, F. (2002) *Biochim. Biophys. Acta* 1564, 384-392.
- Gimpl, G., Burger, K. and Fahrenholz, F. (1997) *Biochemistry* 36, 10959-10974.
- Gimpl, G., Burger, K. and Fahrenholz, F. (2002a) *Trends Biochem. Sci.* 27, 596-599.
- Gimpl, G., Klein, U., Reiländer, H. and Fahrenholz, F. (1995) *Biochemistry* 34, 13794-13801.
- Gimpl, G., Wiegand, V., Burger, K. and Fahrenholz, F. (2002b) *Prog. Brain. Res.* 139, 43-55.
- Gingrich, J.A. and Hen, R. (2001) *Psychopharmacology* 155, 1-10.
- Golub, T., Wacha, S. and Caroni, P. (2004) *Curr. Opin. Neurobiol.* 14, 542-550.

- Gondre-Lewis, M.C., Petrache, H.I., Wassif, C.A., Harries, D., Parsegian, A., Porter, F.D. and Loh, Y.P. (2006) *J. Cell Sci.* 119, 1876-1885.
- Gozlan, H., El Mestikawy, S., Pichat, L., Glowinski, J. and Hamon, M. (1983) *Nature* 305, 140-142.
- Hall, R.A., Premont, R.T. and Lefkowitz, R.J. (1999) *J. Cell Biol.* 145, 927-932.
- Hamm, H.E. (2001) *Proc. Natl. Acad. Sci. USA* 98, 4819-4821.
- Hannun, Y.A. (1996) *Science* 274, 1855-1859.
- Hannun, Y.A. and Obeid, L.M. (2002) *J. Biol. Chem.* 277, 25847-25850.
- Hanson, M.A., Cherezov, V., Griffith, M.T., Roth, C.B., Jaakola, V.-P., Chien, E.Y.T., Velasquez, J., Kuhn, P. and Stevens, R.C. (2008) *Structure* 16, 897-905.
- Harding, P.J., Attrill, H., Boehringer, J., Ross, S., Wadhams, G.H., Smith, E., Armitage, J.P., Watts, A. (2009) *Biophys. J.* 96, 964-973.
- Harel, R. and Futerman, A.H. (1993) *J. Biol. Chem.* 268, 14476-14481.
- Harikumar, K. G. and Chattopadhyay, A. (2001) *Cell. Mol. Neurobiol.* 21, 453-464.
- Harikumar, K.G. and Chattopadhyay, A. (1999) *FEBS Lett.* 457, 389-392.
- Harikumar, K.G. and Chattopadhyay, A. (1998) *Cell. Mol. Neurobiol.* 18, 535-553.
- Harikumar, K.G., Puri, V., Singh, R.D., Hanada, K., Pagano, R.E. and Miller, L.J. (2005) *J. Biol. Chem.* 280, 2176-2185.
- Harris, J.S., Epps, D.E., Davio, S.R. and Kezdy, F.J. (1995) *Biochemistry* 34, 3851-3857.
- Herrick-Davis, K., Grinde, E. and Mazurkiewicz, J.E. (2004) *Biochemistry* 43, 13963-13971.
- Herrick-Davis, K., Grinde, E., Harrigan, T.J. and Mazurkiewicz, J.E. (2005) *J. Biol. Chem.* 280, 40144-40151.
- Higashijima, T., Ferguson, K.M., Sternweis, P.C., Smigel, M.D. and Gilman, A.G. (1987) *J. Biol. Chem.* 262, 762-766.
- Hite, R.K., Gonen, T., Harrison, S.C. and Walz, T. (2008) *Pflugers Arch.* 456, 651-661.
- Holopainen, J.M., Angelova, M.I. and Kinnunen, P.K. (2000) *Biophys. J.* 78, 830-838.

- Holthius, J.C., Pomorski, T., Riggers, R.J., Sprong, H. and van Meer, G. (2001) *Physiol. Rev.* 81, 1689-1723.
- Hoyer, D., Hannon, J.P. and Martin, G.R. (2002) *Pharmacol. Biochem. Behav.* 71, 533-554.
- Huang, P., Xu, W., Yoon, S.-I., Chen, C., Chong, P.L.-G. and Liu-Chen, L.-Y. (2007) *Biochem. Pharmacol.* 73, 534-549.
- Huber, T., Menon, S. and Sakmar, T.P. (2008) *Biochemistry* 47, 11013-11023.
- Hulme, E. C. (1990) Receptor binding studies, a brief outline. In Hulme, E. C. (ed.), *Receptor-Effector Coupling: A Practical Approach*, IRL Press, New York, pp. 203-215.
- Insel, P.A., Tang, C.M., Hahntow, I. and Michel, M.C. (2007) *Biochim. Biophys. Acta* 1768, 994-1005.
- Irons, M., Elias, E.R., Salen, G., Tint, G.S. and Batta, A.K. (1993) *Lancet* 341, 1414.
- Ito, J., Nagayasu, Y., Kato, K., Sato, R. and Yokoyama, S. (2002) *J. Biol. Chem.* 277, 7929-7935.
- Jacoby, E., Bouhelal, R., Gerspacher, M. and Seuwen, K. (2006) *Chem. Med. Chem.* 1, 760-782.
- Jamin, N., Neumann, J.M., Ostuni, M.A., Vu, T.K., Yao, Z.X., Murail, S., Robert, J.C., Giatzakis, C., Papadopoulos, V. and Lacapere, J.J. (2005) *Mol. Endocrinol.* 19, 588-594.
- Javadekar-Subhedar, V. and Chattopadhyay, A. (2004) *Mol. Membr. Biol.* 21, 119-123.
- Jensen, M.Ø. and Mouritsen, O.G. (2004) *Biochim. Biophys. Acta* 1666, 205-226.
- Ji, T.H., Grossmann, M. and Ji, I. (1998) *J. Biol. Chem.* 273, 17299-17302.
- Jira, P.E., Waterham, H.R., Wanders, R.J.A., Smeitink, J.A.M., Sengers, R.C.A. and Wevers, R.A. (2003) *Ann. Hum. Genet.* 67, 269-280.
- Jones, O.T. and McNamee, M.G. (1988) *Biochemistry* 27, 2364-2374.

- Jones, O.T., Eubanks, J.H., Earnest, J.P. and McNamee, M.G. (1988) *Biochemistry* 27, 3733-3742.
- Jost, P.C., Griffith, O.H., Capaldi, R.A. and Vanderkooi, G. (1973) *Proc. Natl. Acad. Sci. USA* 70, 480-484.
- Julius, D. (1998) *Proc. Natl. Acad. Sci. USA* 95, 15153-15154.
- Kabara, J.J. (1973) *Prog. Brain Res.* 40, 363-382.
- Kaiser, R.D. and London, E. (1998) *Biochemistry* 37, 8180-8190.
- Kalipatnapu, S. and Chattopadhyay, A. (2004a) *FEBS Lett.* 576, 455-460.
- Kalipatnapu, S. and Chattopadhyay, A. (2004b) *Cell. Mol. Neurobiol.* 24, 403-422.
- Kalipatnapu, S. and Chattopadhyay, A. (2005a) *IUBMB Life* 57, 505-512.
- Kalipatnapu, S. and Chattopadhyay, A. (2005b) *Mol. Membr. Biol.* 22, 539-547.
- Kalipatnapu, S. and Chattopadhyay, A. (2007a) *Cell. Mol. Neurobiol.* 27, 1097-1116.
- Kalipatnapu, S. and Chattopadhyay, A. (2007b) *Cell. Mol. Neurobiol.* 27, 463-474.
- Kalipatnapu, S., Jafurulla, Md., Chandrasekaran, N. and Chattopadhyay, A. (2004b) *Biochem. Biophys. Res. Commun.* 323, 372-376.
- Kalipatnapu, S., Pucadyil, T.J., Harikumar, K.G. and Chattopadhyay, A. (2004a) *Biosci. Rep.* 24, 101-115.
- Kandutsch, A.A. and Russell, A.E. (1960) *J. Biol. Chem.* 235, 2256-2261.
- Karnik, S. S., Gogonea, S., Patil, S., Saad, Y. and Takezako, T. (2003) *Trends Endocrinol. Metab.* 14, 431-437.
- Keller, R.K., Arnold, T.P. and Fliesler, S.J. (2004) *J. Lipid Res.* 45, 347-355.
- Kellett, E., Carr, I. C. and Milligan, G. (1999) *Mol. Pharmacol.* 56, 684-692.
- Kelley, R.I. and Hennekam, R.C.M. (2000) *J. Med. Genet.* 37, 321-335.
- Kenakin, T. (1997) *Trends Pharmacol. Sci.* 18, 456-464.
- Kirilovsky, J. and Schramm, M. (1983) *J. Biol. Chem.* 258, 6841-6849.
- Kirilovsky, J., Eimerl, S., Steiner-Mordoch, S. and Schramm, M. (1987) *Eur. J. Biochem.* 166, 221-228.

- Klein, U., Gimpl, G. and Fahrenholz, F. (1995) *Biochemistry* 34, 13784-13793.
- Knowles, P.F., Watts, A. and Marsh, D. (1979) *Biochemistry* 18, 4480-4487.
- Kobe, F., Renner, U., Woehler, A., Wlodarczyk, J., Papusheva, E., Bao, G., Zeug, A., Richter, D.W., Neher, E. and Ponimaskin, E. (2008) *Biochim. Biophys. Acta* 1783, 1503-1516.
- Kobilka, B.K., Frielle, T., Collins, S., Yang-Feng, T., Kobilka, T.S., Francke, U., Lefkowitz, R.J. and Caron, M.G. (1987) *Nature* 329, 75-79.
- Kolakowski, Jr. L.F. (1994) *Receptors Channels* 2, 1-7.
- Kóta, Z., Páli, T. and Marsh, D. (2004) *Biophys. J.* 86, 1521-1531.
- Koval, M. and Pagano, R.E. (1991) *Biochim. Biophys. Acta* 1082, 113-125.
- Kroeger, K.M., Hanyaloglu, A.C., Seeber, R.M., Miles, L.E. and Eidne, K.A. (2001) *J. Biol. Chem.* 276, 12736-12743.
- Kroeze, W.K., Sheffler, D.J. and Roth, B.L. (2003) *J. Cell Sci.* 116, 4867-4869.
- Kung, M.-P., Frederick, D., Mu, M., Zhuang, Z.-P. and Kung, H. F. (1995) *J. Pharmacol. Exp. Ther.* 272, 429-437.
- Lagane, B., Gaibelet, G., Meilhoc, E., Masson, J.-M., Cézanne, L. and Lopez, A. (2000) *J. Biol. Chem.* 275, 33197-33200.
- Lakowicz, J.R. Principles of fluorescence spectroscopy, 3rd ed. New York: Kluwer-Plenum Press; 2006.
- Lalovic, A., Merkens, L., Russell, L., Arsenaull-Lapierre, G., Nowaczyk, M.J.M., Porter, F.D., Steiner, R.D. and Turecki, G. (2004) *Am. J. Psychiatry* 161, 2123-2125.
- Lange, C., Nett, J.H., Trumpower, B.L. and Hunte, C. (2001) *EMBO J.* 20, 6591-6600.
- Lee, A.G. (2003) *Biochim. Biophys. Acta* 1612, 1-40.
- Lee, A.G. (2004) *Biochim. Biophys. Acta* 1666, 62-87.
- Lee, A.G. (2005) *Mol. Biosyst.* 1, 203-212.
- Lee, A.G., East, J.M., Jones, O.T., McWhirter, J., Rooney, E.K. and Simmonds, A.C. (1982) *Biochemistry* 21, 6441-6446.

- Lee, D., Huang, W. and Lim, A.T. (2000) *Mol. Psychiatry* 5, 39-48.
- Lee, H. J., Hammond, D. N., Large, T. H., Roback, J. D., Sim, J. A., Brown, D. A., Otten, U. H. and Wainer, B. H. (1990) *J. Neurosci.* 10, 1779-1787.
- Lemonde, S., Turecki, G., Bakish, D., Du, L., Hrdina, P.D., Bown, C.D., Sequeira, A., Kushwaha, N., Morris, S.J., Basak, A., Ou, X.-M. and Albert, P.R. (2003) *J. Neurosci.* 23, 8788-8799.
- Lentz, B.R. (1989) *Chem. Phys. Lipids* 50, 171-190.
- Lentz, B.R., Moore, B.M. and Barrow, D.A. (1979) *Biophys. J.* 25, 489-494.
- Lijnen, P., Echevaría-Vázquez, D. and Petrov, V. (1996) *Methods Find. Exp. Clin. Pharmacol.* 18, 123-136.
- Lin, D.S., Steiner, R.D., Flavell, D.P. and Connor, W.E. (2005) *Pediatr. Res.* 57, 765-770.
- Lin, S.H. and Civelli, O. (2004) *Ann. Med.* 36, 204-214.
- Lindenthal, B., Aldaghlis, T.A., Kelleher, J.K., Henkel, S.M., Tolba, R., Haidl, G. and von Bergmann, K. (2001) *J. Lipid Res.* 42, 1089-1095.
- Liscum, L. and Underwood, K.W. (1995) *J. Biol. Chem.* 270, 15443-15446.
- Lohse, M.J., Hein, P., Hoffmann, C., Nikolaev, V.O., Vilardaga, J.P. and Bünemann, M. (2008) *Br. J. Pharmacol.* 153 (Suppl 1), S125-S132.
- Loura, L.M. and Prieto, M. (1997) *Biophys. J.* 72, 2226-2236.
- Lukasiewicz, S., Błasiak, E., Faron-Górecka, A., Polit, A., Tworzydło, M., Górecki, A., Wasylewski, Z., Dziedzicka-Wasylewska, M. (2007) *Pharmacol. Rep.* 59, 379-392.
- Maggio, R., Innamorati, G. and Parenti, M. (2007) *J. Neurochem.* 103, 1741-1752.
- Marasas, F.W. (1996) *Adv. Exp. Med. Biol.* 392, 1-17.
- Marius, P., Alvis, S.J., East, J.M. and Lee, A.G. (2005) *Biophys. J.* 89, 4081-4089.
- Marius, P., Zagnoni, M., Sandison, M.E., East, J.M., Morgan, H. and Lee, A.G. (2008) *Biophys. J.* 94, 1689-1698.

- Marsh, D. (1990) *FEBS Lett.* 268, 371-375.
- Mason, R.P., Tulenko, T.N. and Jacob, R.F. (2003) *Biochim. Biophys. Acta* 1610, 198-207.
- Masserini, M. and Ravasi, D. (2001) *Biochim. Biophys. Acta* 1532, 149-161.
- Mauch, D.H., Nägler, K., Schumacher, S., Göritz, C., Müller, E.C., Otto, A. and Pfrieder, F.W. (2001) *Science* 294, 1354-3157.
- McClare, C.W.F. (1971) *Anal. Biochem.* 39, 527-530.
- Megha, Bakht, O. and London, E. (2006) *J. Biol. Chem.* 281, 21903-21913.
- Merrill, A.H., Jr., Liotta, D.C. and Riley, R.T. (1996) *Trends Cell Biol.* 6, 218-223.
- Meyer, B.H., Segura, J.-M., Martinez, K.L., Hovius, R., George, N., Johnsson, K. and Vogel, H. (2006) *Proc. Natl. Acad. Sci. USA* 103, 2138-2143.
- Meyer, B.H., Segura, J.M., Martinez, K.L., Hovius, R., George, N., Johnsson, K. and Vogel, H. (2006) *Proc. Natl. Acad. Sci. USA* 103, 2138-2143.
- Milligan G. (2006) *Drug Discov Today* 11, 541-549.
- Milligan, G. (2007) *Biochim. Biophys. Acta* 1768, 825-835.
- Milligan, G., Kellet, E., Dacquet, C., Dubreuil, V., Jacoby, E., Millan, M. J., Lavielle, G. and Spedding, M. (2001) *Neuropharmacology* 40, 334-344.
- Milligan, G., Parenti, M. and Magee, A.I. (1995) *Trends Biochem. Sci.* 20, 181-187.
- Mitchell, D.C., Straume, M., Miller, J.L. and Litman, B.J. (1990) *Biochemistry* 29, 9143-9149.
- Miura, S.-i., Karnik, S.S. and Saku, K. (2005) *J. Biol. Chem.* 280, 18237-18244.
- Mizrahi, C., Stojanovic, A., Urbina, M., Carreira, I. and Lima, L. (2004) *Int. Immunopharmacol.* 4, 1125-1133.
- Monastyrskaya, K., Hostettler, A., Buergi, S. and Draeger, A. (2005) *J. Biol. Chem.* 280, 7135-7146.
- Mukherjee, S. and Chattopadhyay, A. (1996) *Biochemistry* 35, 1311-1322.
- Mukherjee, S. and Maxfield, F.R. (2004) *Annu. Rev. Cell Dev. Biol.* 20, 839-866.

- Mutoh, T., Tokuda, A., Miyadai, T., Hamaguchi, M. and Fujiki, N. (1995) *Proc. Natl. Acad. Sci. USA* 92, 5087-5091.
- Neer, E.J. (1995) *Cell* 80, 249-257.
- Newman-Tancredi, A., Conte, C., Chaput, C., Verrièle, L. and Millan, M. J. (1997) *Neuropharmacology* 36, 451-459.
- Nguyen, D.H. and Taub, D. (2002a) *J. Immunol.* 168, 4121-4126.
- Nguyen, D.H. and Taub, D. (2002b) *Blood* 99, 4298-4306.
- Nguyen, D.H. and Taub, D.D. (2003) *Exp. Cell Res.* 291, 36-45.
- Nishikawa, M., Nojima, S., Akiyama, T., Sankawa, U. and Inoue, K. (1984) *J. Biochem.* 96, 1231-1239.
- Nogi, T., Fathir, I., Kobayashi, M., Nozawa, T. and Miki, K. (2000) *Proc. Natl. Acad. Sci. USA* 97, 13561-13566.
- Norstedt, C. and Fredholm, B.B. (1990) *Anal. Biochem.* 189, 231-234.
- Ohvo-Rekila, H., Ramstedt, B., Leppimaki, P. and Slotte, J.P. (2002) *Prog. Lipid Res.* 41, 66-97.
- Ostrom, R.S. (2002) *Mol. Pharmacol.* 61, 473-476.
- Ostrom, R.S. and Insel, P.A. (2004) *Br. J. Pharmacol.* 143, 235-245.
- Ostrom, R.S., Post, S.R. and Insel, P.A. (2000) *J. Pharmacol. Exp. Ther.* 294, 407-412.
- Osuchowski, M.F., Edwards, G.L. and Sharma, R.P. (2005) *Neurotoxicology* 26, 211-221.
- Paila, Y.D. and Chattopadhyay, A. (2006) *Cell. Mol. Neurobiol.* 26, 925-942.
- Paila, Y.D. and Chattopadhyay, A. (2009) *Glycoconj. J.* (in press).
- Paila, Y.D., Murty, M.R.V.S., Vairamani, M. and Chattopadhyay, A. (2008) *Biochim. Biophys. Acta* 1778, 1508-1516.
- Paila, Y.D., Pucadyil, T.J. and Chattopadhyay, A. (2005) *Mol. Membr. Biol.* 22, 241-249.
- Paila, Y.D., Tiwari, S. and Chattopadhyay, A. (2009) *Biochim. Biophys. Acta* 1788, 295-302.

- Palsdottir, H. and Hunte, C. (2004) *Biochim. Biophys. Acta* 1666, 2-18.
- Pang, L., Graziano, M. and Wang, S. (1999) *Biochemistry* 38, 12003-12011.
- Papakostas, G.I., Öngür, D., Iosifescu, D.V., Mischoulon, D. and Fava, M. (2004) *Eur. Neuropsychopharmacol.* 14, 135-142.
- Papoucheva, E., Dumuis, A., Sebben, M., Richter, D.W. and Ponimaskin, E.G. (2004) *J. Biol. Chem.* 279, 3280-3291.
- Park, P.S., Filipek, S., Wells, J.W. and Palczewski, K. (2004) *Biochemistry* 43, 15643-15656.
- Perez, D.M. (2003) *Mol. Pharmacol.* 63, 1202-1205.
- Peroutka, S.J. and Howell, T.A. (1994) *Neuropharmacology* 33, 319-324.
- Pichot, W., Hansenne, M., Pinto, E., Reggers, J., Fuchs, S. and Ansseau, M. (2005) *Biol. Psychiatry* 58, 854-858.
- Pierce, K.L., Premont, R.T. and Lefkowitz, R.J. (2002) *Nat. Rev. Mol. Cell Biol.* 3, 639-650.
- Piston, D.W. and Kremers, G.J. (2007) *Trends Biochem. Sci.* 32, 407-414.
- Politowska, E., Kaźmierkiewicz, R., Wiegand, V., Fahrenholz, F. and Ciarkowski, J. (2001) *Acta Biochim. Pol.* 48, 83-93.
- Porter, F.D. (2000) *Mol. Genet. Metab.* 71, 163-174.
- Porter, F.D. (2002) *J. Clin. Invest.* 110, 715-724.
- Pose de Chaves, E. I. (2006) *Biochim. Biophys. Acta* 1758, 1995-2015.
- Powl, A.M., East, J.M. and Lee, A.G. (2007) *Biophys. J.* 93, 113-122.
- Prasad, R., Singh, P. and Chattopadhyay, A. (2009) *Glycoconj. J.* (doi: 10.1007/s10719-008-9185-x)
- Prendergast, F.G., Haugland, R.P. and Callahan, P.J. (1981) *Biochemistry* 20, 7333-7338.
- Prioni, S., Mauri, L., Loberto, N., Casellato, R., Chigorno, V., Karagogeos, D., Prinetti, A. and Sonnino, S. (2004) *Glycoconj. J.* 21, 461-470.
- Pucadyil, T. J. and Chattopadhyay, A. (2005) *Biochim. Biophys. Acta* 1714, 35-42.

- Pucadyil, T. J., Kalipatnapu, S., Harikumar, K. G., Rangaraj, N., Karnik, S. S. and Chattopadhyay, A. (2004a) *Biochemistry* 43, 15852-15862.
- Pucadyil, T. J., Shrivastava, S. and Chattopadhyay, A. (2004b) *Biochem. Biophys. Res. Commun.* 320, 557-562.
- Pucadyil, T.J. and Chattopadhyay, A. (2004a) *Biochim. Biophys. Acta* 1663, 188-200.
- Pucadyil, T.J. and Chattopadhyay, A. (2004b) *Biochim. Biophys. Acta* 1661, 9-17.
- Pucadyil, T.J. and Chattopadhyay, A. (2006) *Prog. Lipid Res.* 45, 295-333.
- Pucadyil, T.J. and Chattopadhyay, A. (2007a) *Trends Parasitol.* 23, 49-53.
- Pucadyil, T.J. and Chattopadhyay, A. (2007b) *Biochim. Biophys. Acta* 1768, 655-668.
- Pucadyil, T.J., Kalipatnapu, S. and Chattopadhyay, A. (2005a) *Cell. Mol. Neurobiol.* 25, 553-580.
- Pucadyil, T.J., Shrivastava, S. and Chattopadhyay, A. (2005b) *Biochem. Biophys. Res. Commun.* 331, 422-427.
- Ramstedt, B. and Slotte, J. P. (2006) *Biochim. Biophys. Acta* 1758, 1945-1956.
- Rasmussen, S.G., Choi, H.J., Rosenbaum, D.M., Kobilka, T.S., Thian, F.S., Edwards, P.C., Burghammer, M., Ratnala, V.R., Sanishvili, R., Fischetti, R.F., Schertler, G.F., Weis, W.I. and Kobilka, B.K. (2007) *Nature* 450, 383-387.
- Raymond, J.R., Mukhin, Y.V., Gettys, T.W. and Garnovskaya, M.N. (1999) *Br. J. Pharmacol.* 127, 1751-1764.
- Raymond, J.R., Olsen, C.L. and Gettys, T.W. (1993) *Biochemistry* 32, 11064-11073.
- Renner, U., Glebov, K., Lang, T., Papusheva, E., Balakrishnan, S., Keller, B., Richter D.W., Jahn, R. and Ponimaskin, E. (2007) *Mol. Pharmacol.* 72, 502-513.
- Romanenko, V.G., Rothblat, G.H. and Levitan, I. (2002) *Biophys. J.* 83, 3211-3222.
- Rukmini, R., Rawat, S.S., Biswas, S.C. and Chattopadhyay, A. (2001) *Biophys. J.* 81, 2122-2134.
- Runnels, L.W. and Scarlata, S.F. (1995) *Biophys. J.* 69, 1569-1583.

- Ruprecht, J.J., Mielke, T., Vogel, R., Villa, C. and Schertler, G.F. (2004) *EMBO J.* 23, 3609-3620.
- Salahpour, A., Angers, S., Mercier, J.F., Lagacé, M., Marullo, S. and Bouvier, M. (2004) *J. Biol. Chem.* 279, 33390-33397.
- Salim, K., Fenton, T., Bacha, J., Urien-Rodriguez, H., Bonnert, T., Skynner, H.A., Watts, E., Kerby, J., Heald, A., Beer, M., McAllister, G. and Guest, P.C. (2002) *J. Biol. Chem.* 277, 15482-15485.
- Sastry, P. S. (1985) *Prog. Lipid Res.* 24, 69-176.
- Saxena, A.M., Udgaonkar, J.B. and Krishnamoorthy, G. *Protein Sci.* 14, 1787-1799.
- Scalco, F.B., Cruzes, V.M., Vendramini, R.C., Brunetti, I.L. and Moretti-Ferreira, D. (2003) *Braz. J. Med. Biol. Res.* 36, 1327-1332.
- Schlyer, S. and Horuk, R. (2006) *Drug Discov. Today* 11, 481-493.
- Schroeder, F., Woodford, J.K., Kavecansky, J., Wood, W.G. and Joiner, C. (1995) *Mol. Membr. Biol.* 12, 113-119.
- Severs, N.J. and Robenek, H. (1983) *Biochim. Biophys. Acta* 737, 373-408.
- Shanti, K. and Chattopadhyay, A. (2000) *Curr. Sci.* 79, 402-403.
- Sharma, P., Varma, R., Sarasij, R.C., Ira, Gousset, K., Krishnamoorthy, G., Rao, M., Mayor, S. (2004) *Cell* 116, 577-589.
- Shrivastava, S., Paila, Y.D., Dutta, A. and Chattopadhyay, A. (2008) *Biochemistry* 47, 5668-2677.
- Simmonds, A.C., East, J.M., Jones, O.T., Rooney, E.K., McWhirter, J. and Lee, A.G. (1982) *Biochim. Biophys. Acta* 693, 398-406.
- Simons, K. and Eehalt, R. (2002) *J. Clin. Invest.* 110, 597-603.
- Simons, K. and Ikonen, E. (1997) *Nature* 387, 569-572.
- Simons, K. and Ikonen, E. (2000) *Science* 290, 1721-1726.
- Simons, K. and Toomre, D. (2000) *Nat. Rev. Mol. Cell Biol.* 1, 31-39.
- Simons, K. and van Meer, G. (1988) *Biochemistry* 27, 6197-6202.

- Singh, J. K., Chromy, B. A., Boyers, M. J., Dawson, G. and Banerjee, P. (1996a) *J. Neurochem.* 66, 2361-2372.
- Singh, J.K., Yan, Q., Dawson, G. and Banerjee, P. (1996b) *Biochim. Biophys. Acta* 1310, 201-211.
- Singh, P., Paila, Y.D. and Chattopadhyay, A. (2007) *Biochem. Biophys. Res. Commun.* 358, 495-499.
- Sjögren, B. and Svenningsson, P. (2007) *Acta Physiol.* 190, 47-53.
- Sjögren, B., Hamblin, M.W. and Svenningsson, P. (2006) *Eur. J. Pharmacol.* 552, 1-10.
- Skipski, V.P. (1975) *Meth. Enzymol.* 35, 396-425.
- Smith, D.W., Lemli, L. and Opitz, J.M. (1964) *J. Pediatr.* 64, 210-217.
- Smith, P.K., Krohn, R.I., Hermanson, G.T., Mallia, A.K., Gartner, F.H., Provenzano, M.D., Fujimoto, E.K., Goeke, N.M., Olson, B.J. and Klenk, D.C. (1985) *Anal. Biochem.* 150, 76-85.
- Sojicic, Z., Toplak, H., Zuehlke, R., Honegger, U.E., Buhlmann, R. and Wiesmann, U.N. (1992) *Biochim. Biophys. Acta* 1104, 31-37.
- Soriano, J.M., González, L. and Catalá, A.I. (2005) *Prog. Lipid Res.* 44, 345-356.
- Soumpasis, D.M. (1983) *Biophys. J.* 41, 95-97.
- Srivastava, A. and Krishnamoorthy, G. (1997) *Arch. Bioch. Biophys.* 340, 159-167.
- Straume, M. and Litman, B.J. (1988) *Biochemistry* 27, 7723-7733.
- Tate, C. G. and Grisshammer, R. (1996) *Trends Biotechnol.* 14, 426-430.
- Terrillon, S. and Bouvier, M. (2004) *EMBO Rep.* 5, 30-34.
- Thielen, R.J. and Frazer, A. (1995) *Life Sci.* 56, 163-168.
- Tint, G.S., Irons, M., Elias, E.R., Batta, A.K., Frieden, R., Chen, T.S. and Salen, G. (1994) *N. Engl. J. Med.* 330, 107-113.
- Tint, G.S., Seller, M., Hughes-Benzie, H., Batta, A.K., Shefer, S., Genest, D., Irons, M., Elias, E. and Salen, G. (1995) *J. Lipid Res.* 36, 89-95.
- Toth, M. (2003) *Eur. J. Pharmacol.* 463, 177-184.

- Tramier, M., Piolot, T., Gautier, I., Mignotte, V., Coppey, J., Kemnitz, K., Durieux, C., Coppey-Moisan, M. (2003) *Methods Enzymol.* 360, 580-597.
- Tsui-Pierchala, B. A., Encinas, M., Milbrandt, J. and Johnson, E. M. (2002) *Trends Neurosci.* 25, 412-417.
- Tulenko, T.N., Chen, M., Mason, P.E. and Mason, R.P. (1998) *J. Lipid Res.* 39, 947-956.
- Tulenko, T.N., Boeze-Battaglia, K., Mason, R.P., Tint, G.S., Steiner, R.D., Connor, W.E. and Labelle, E.F. (2006) *J. Lipid Res.* 47, 134-143.
- Turley, S.D., Bruns, D.K. and Dietschy, J.M. (1998) *Am. J. Physiol.* 274, E1099-E1105.
- Vance, J.E., Hayashi, H. and Karten, B. (2005) *Semin. Cell Dev. Biol.* 16, 192-212.
- Vevera, J., Fisar, Z., Kvasnicka, T., Zdenek, H., Stárková, L., Ceska, R. and Papezová, H. (2005) *Psychiatry Res.* 133, 197-203.
- Vidi, P.A., Chemel, B.R., Hu, C.D. and Watts, V.J. (2008) *Mol. Pharmacol.* 74, 544-551.
- Waage-Baudet, H., Lauder, J.M., Dehart, D.B., Kluckman, K., Hiller, S., Tint, G.S. and Sulik, K.K. (2003) *Int. J. Dev. Neurosci.* 21, 451-459.
- Wang, E., Norred, W.P., Bacon, C.W., Riley, R.T. and Merrill, A.H., Jr. (1991) *J. Biol. Chem.* 266, 14486-14490.
- Waterham, H.R. (2006) *FEBS Lett.* 580, 5442-5449.
- Waterham, H.R. and Wanders, R.J.A. (2000) *Biochim. Biophys. Acta* 1529, 340-356.
- Watson, J., Collin, L., Ho, M., Riley, G., Scott, C., Selkirk, J. V. and Price, G. W. (2000) *Br. J. Pharmacol.* 130, 1108-1114.
- Watts, A., Volovski, I.D. and Marsh, D. (1979) *Biochemistry* 18, 5006-5013.
- Whorton, M.R., Bokoch, M.P., Rasmussen, S.G., Huang, B., Zare, R.N., Kobilka, B. and Sunahara, R.K. (2007) *Proc. Natl. Acad. Sci. USA* 104, 7682-7687.
- Winter, C.G. (1974) *Ann. N.Y. Acad. Sci.* 242, 149-157.
- Wolf, C. and Chachaty, C. (2000) *Biophys. Chem.* 84, 269-279.
- Wolf, C., Chevy, F., Pham, J., Kolf-Clauw, M., Citadelle, D., Mulliez, N. and Roux, C. (1996) *J. Lipid Res.* 37, 1325-1333.

- Wolf, C., Koumanov, K., Tenchov, B. and Quinn, P.J. (2001) *Biophys. Chem.* 89, 163-172.
- Wood, W.G., Schroeder, F., Avdulov, N.A., Chochina, S.V., Igbavboa, U. (1999) *Lipids* 34, 225-234.
- Xiao, Z.-L., Chen, Q., Amaral, J., Biancani, P. and Behar, J. (2000) *Am. J. Physiol. Gastrointest. Liver Physiol.* 278, G251-G258.
- Xiao, Z.-L., Chen, Q., Amaral, J., Biancani, P., Jensen, R.T. and Behar, J. (1999) *Am. J. Physiol.* 276, G1401-G1407.
- Xie, Z., Lee, S.P., O'Dowd, B.F. and George, S.R. (1999) *FEBS Lett.* 456, 63-67.
- Xu, W., Yoon, S.-I., Huang, P., Wang, Y., Chen, C., Chong, P.L.-G. and Liu-Chen, L.-Y. (2006) *J. Pharmacol. Exp. Ther.* 317, 1295-1306.
- Xu, X. and London, E. (2000) *Biochemistry* 39, 843-849.
- Yankovskaya, V., Horsefield, R., Törnroth, S., Luna-Chavez, C., Miyoshi, H., Léger, C., Byrne, B., Cecchini, G. and Iwata, S. (2003) *Science* 299, 700-704.
- Yao, Z. and Kobilka, B. (2005) *Anal. Biochem.* 343, 344-346.
- Yeagle, P.L. (1982) *Biophys. J.* 37, 227-239.
- Yeow, E.K. and Clayton, A.H. (2007) *Biophys. J.* 92, 3098-3104.
- Yu, C. H., Lee, Y. M., Yun, Y. P. and Yoo, H. S. (2001) *Arch. Pharm. Res.* 24, 136-143.
- Yu, H. and Patel, S.B. (2005) *Clin. Genet.* 68, 383-391.
- Zeidan, Y.H. and Hannun, Y.A. (2007) *Trends Mol. Med.* 13, 327-336.
- Zhou, F.C., Patel, T.D., Swartz, D., Xu, Y. and Kelley, M.R. (1999) *Mol. Brain Res.* 69, 186-201.
- Zhu, X. and Wess, J. (1998) *Biochemistry* 37, 15773-15784.
- Zhuang, Z.-P., Kung, M.-P. and Kung, H.F. (1994) *J. Med. Chem.* 37, 1406-1407.

Appendix

We start with equation 12 (p. 109) in which the time-resolved fluorescence anisotropy is described by a biexponential anisotropy decay model

$$r(t) = r_0 \{ \beta_1 \exp(-t/\phi_1) + \beta_2 \exp(-t/\phi_2) \} \quad (A1)$$

where r_0 is the initial anisotropy (in case of EYFP, $r_0 = 0.38$) and β_i is the amplitude of the i^{th} rotational correlation time ϕ_i such that $\sum_i \beta_i = 1$

When the correlation time ϕ_1 (ascribed to homoFRET in the present situation) is too fast to be resolved, we can assume that $\phi_1 \ll t$ (the first observable time-point), the first term in the right-hand side becomes negligible and we obtain

$$r(t) = r_0 \beta_2 \exp(-t/\phi_2)$$

Thus $r_0 \beta_2$ corresponds to $r_{\text{in}}^{\text{app}}$ estimated from the first few data points of r vs. t curves.

At $t = 0$, $r(t) = r(0) = r_0$, and equation (A1) under this condition can be written as

$$r_0 = r_0 \{ \beta_1 \exp(-0/\phi_1) + \beta_2 \exp(-0/\phi_2) \} \quad (A2)$$

Since $\exp(-0/\phi_1) = 1$ and $\exp(-0/\phi_2) = 1$, equation (A2) becomes

$$r_0 = r_0 \{ \beta_1 + \beta_2 \}$$

$$r_0 = r_0 \beta_1 + r_0 \beta_2 \quad (A3)$$

Since $r_0 \beta_2$ corresponds to $r_{\text{in}}^{\text{app}}$, equation (A3) can be written as

$$r_0 = r_0 \beta_1 + r_{\text{in}}^{\text{app}}, \text{ which upon rearrangement yields}$$

$$\beta_1 = (r_0 - r_{\text{in}}^{\text{app}} / r_0) \quad (A4)$$

The values of β_1 shown in Table 5.2 are obtained using this equation